THE UNIVERSITY OF NEW SOUTH WALES
KENSINGTON, NSW AUSTRALIA 2033

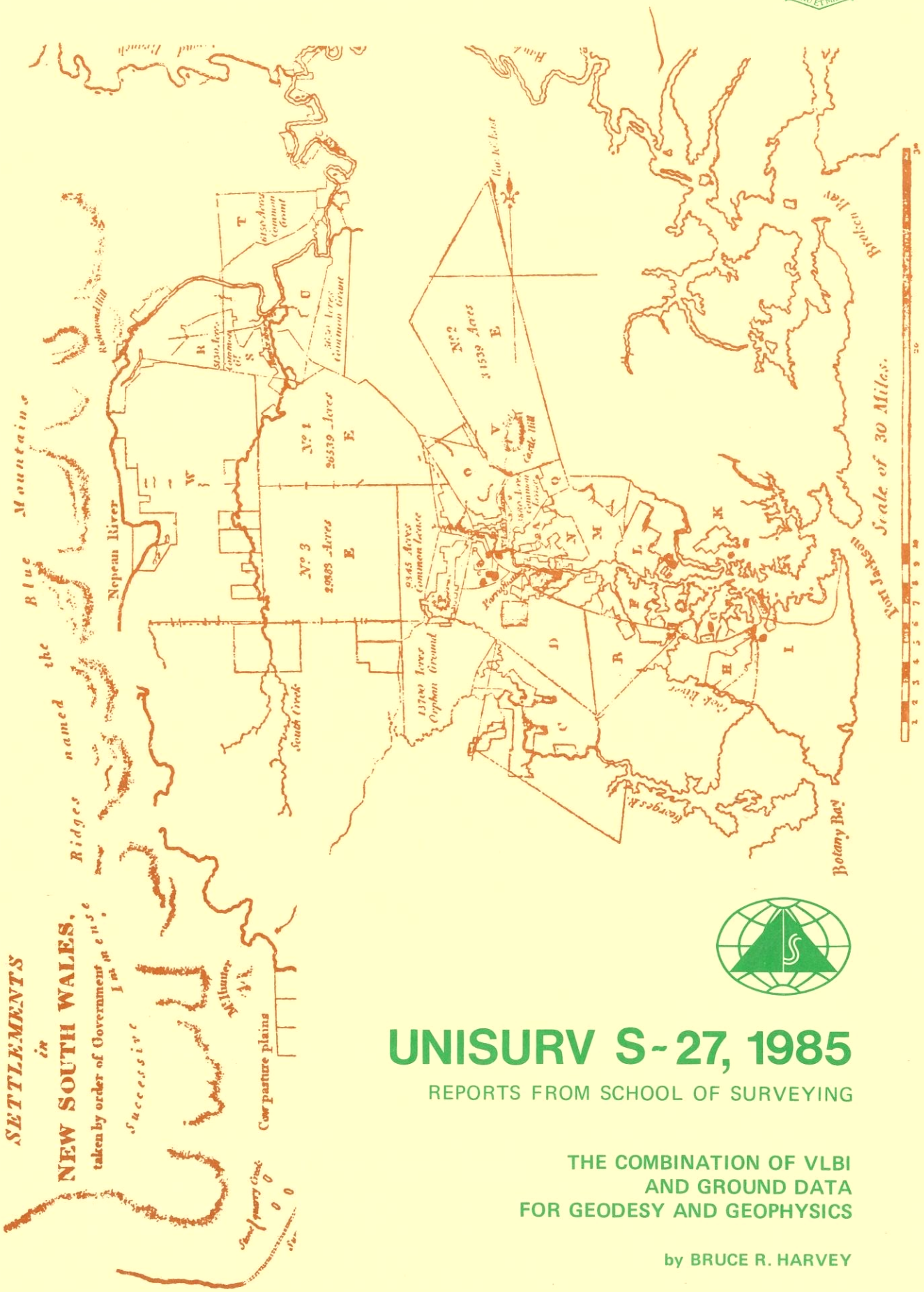

UNISURV S-27, 1985

REPORTS FROM SCHOOL OF SURVEYING

THE COMBINATION OF VLBI AND GROUND DATA FOR GEODESY AND GEOPHYSICS

by BRUCE R. HARVEY

UNISURV REPORT S27, 1985

THE COMBINATION OF VLBI AND GROUND DATA FOR GEODESY AND GEOPHYSICS

by

Bruce R. Harvey

Received February, 1985.

SCHOOL OF SURVEYING
THE UNIVERSITY OF NEW SOUTH WALES
P.O. BOX 1
KENSINGTON, N.S.W. 2033
AUSTRALIA

National Library of Australia
CARD NO. and ISBN 0 85839 041 8

ABSTRACT

A thorough analytical procedure for the combination of VLBI and geodetic survey measurements and their evaluation and comparison is developed and presented. Crustal deformation analysis, comparisons between space techniques, and the strengthening of geodetic networks are the main applications. VLBI analysis is reviewed and the variance covariance matrix of the observables is investigated. The effects of systematic errors, particularly biases in the tropospheric corrections, on VLBI results are investigated and classified.

The results of the first geodetic VLBI experiment within Australia are presented and their accuracies estimated. These results are combined with the corresponding ground measurements of the Australian Geodetic Network. Ground measurements and their adjustment are briefly reviewed and systematic errors considered. The survey connection to VLBI reference points is also considered.

A method which combines VLBI and ground data by estimating the transformation parameters relating the preadjusted coordinates of the points of each network is recommended. Several models and appropriate statistical tests are investigated. Additional parameters are included in the combination models to account for systematic biases affecting the observations. Rigorous procedures are given for the application of these results.

Methods for studying regional strain are discussed. Several models for 2D and 3D strain are examined. The recommended approach to strain analysis is to initially compute the 3D strain parameters from the adjusted coordinates of the points in each network. If statistical tests indicate that the vertical components of strain are insignificant then, strain should be computed with a 2D model which includes parameters for 3D rotations. The best 2D models are the 2D ellipsoidal model and the 3D topocentric model, with vertical strain fixed at zero. The presence of systematic errors in the data should be checked because they may corrupt the estimated strain. It is recommended that VLBI and ground data be combined at each epoch. Any strain detected is not due to crustal movements. If no significant strain is detected, then the geophysical strain between these epochs can be determined.

AUSTRALIAN VLBI GEODESY NETWORK 1982


ALICE SPRINGS

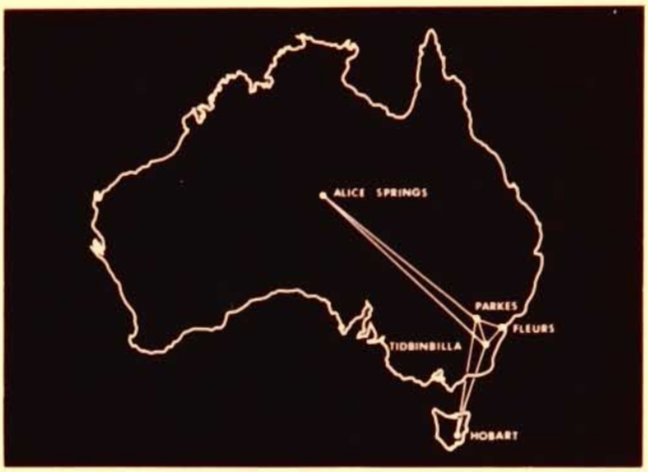


PARKES


FLEURS


TIDBINBILLA


HOBART

CORRECTIONS TO UNISURV S-27

THE COMBINATION OF VLBI AND GROUND DATA FOR GEODESY AND GEOPHYSICS

by Bruce R. Harvey

Page v reads -

APPENDIX B TAS PROGRAM LISTING 239

It should be -
APPENDIX B TAS PROGRAM 239

Page 43 Para 3 Line 2 reads -

fixed axis, an error in source position due to refracltive

It should be -
fixed axis, an error in source position due to refractive

Page 98 reads -

Figure 6.1 Cardan Rotations. (Rx(k) Ry(θ) Rz(ω)).

It should be -
Figure 6.1 Cardan Rotations. (Rz(k) Ry(θ) Rx(ω)).

Page 109 para 2 Line 1 reads -

The stochastic model be correct as well as the mathematical

It should be -
The stochastic model must be correct as well as the mathematical

Page 116 para 2 line 9 reads -

may also reveal magnitude of the effects of these errors.

It should be -
may also reveal the magnitude of the effects of these errors.

Page 117 para 2 Line 4 reads -

is necessary to check that the residuals normally are

It should be -
is necessary to check that the residuals are normally

Page 144 Line 3 reads -

$$= \sigma^2_{Lt} \,/\, Lf^2 \;+\; Lt^2\, \sigma^2_{Lf} \,/\, LfR$$

It should be -

$$= \sigma^2_{Lt} \,/\, Lf^2 \;+\; Lt^2\, \sigma^2_{Lf} \,/\, Lf^4$$

Page 157, the equations read -

$$\begin{bmatrix} AX \\ \Delta Y \\ \Delta Z \end{bmatrix} = s \begin{bmatrix} 1 & k & -\theta \\ -k & 1 & \omega \\ \theta & -\omega & 1 \end{bmatrix} \begin{bmatrix} \Delta x \\ \Delta y \\ \Delta z \end{bmatrix}$$

then the

$$VCV_{\Delta X \Delta Y \Delta Z} = J \begin{bmatrix} VCV_{\Delta x \Delta y \Delta z} & 0 \\ 0 & VCV_{s\omega\theta k} \end{bmatrix} J^T$$

where $J = \begin{bmatrix} s & sk & -s\theta & \Delta x + k\Delta y - \theta\Delta z & -s\Delta z & s\Delta y & 0 \\ -sk & s & s\omega & \Delta y - k\Delta x + \omega\Delta z & 0 & -s\Delta x & s\Delta z \\ s\theta & -s\omega & s & \theta\Delta x - \omega\Delta y + \Delta z & s\Delta x & 0 & -s\Delta y \end{bmatrix}$

They should be -

$$\begin{bmatrix} \Delta X \\ \Delta Y \\ \Delta Z \end{bmatrix} = s \begin{bmatrix} 1 & k & -\theta \\ -k & 1 & \omega \\ \theta & -\omega & 1 \end{bmatrix} \begin{bmatrix} \Delta x \\ \Delta y \\ \Delta z \end{bmatrix}$$

then the

$$VCV_{\Delta X \Delta Y \Delta Z} = J \begin{bmatrix} VCV_{\Delta x \Delta y \Delta z} & 0 \\ 0 & VCV_{s\omega\theta k} \end{bmatrix} J^T$$

where $J = \begin{bmatrix} s & sk & -s\theta & \Delta x + k\Delta y - \theta\Delta z & 0 & -s\Delta z & s\Delta y \\ -sk & s & s\omega & \Delta y - k\Delta x + \omega\Delta z & s\Delta z & 0 & -s\Delta x \\ s\theta & -s\omega & s & \theta\Delta x - \omega\Delta y + \Delta z & -s\Delta y & s\Delta x & 0 \end{bmatrix}$

Page 167 last 3 lines read -

$$\omega_{13} = \theta = (\partial\Delta x/\partial x - \partial\Delta z/\partial z)/2$$
$$\omega_{12} = k = (\partial\Delta x/\partial x - \partial\Delta y/\partial y)/2$$
$$\omega_{23} = \omega = (\partial\Delta y/\partial y - \partial\Delta z/\partial z)/2$$

They should be -

$$\omega_{13} = \theta = (\partial\Delta x/\partial z - \partial\Delta z/\partial x)/2$$
$$\omega_{12} = k = (\partial\Delta x/\partial y - \partial\Delta y/\partial x)/2$$
$$\omega_{23} = \omega = (\partial\Delta y/\partial z - \partial\Delta z/\partial y)/2$$

CONTENTS.

ACKNOWLEDGEMENTS.

I am most grateful to Prof. Art Stolz, my supervisor. We have had many useful discussions and his help has been invaluable. I appreciate his efforts to provide me with the opportunity to meet, and have discussions with, prominent people working in the fields of this research. Thank you Art for all that you have done.

Special thanks also go to Dr David Jauncey (CSIRO) and Dr Peter Morgan (CCAE) for their assistance, especially during my stay in the USA.

Among the many people whose help has been appreciated are: David Close, Dr Ewan Masters, Bernie Hirsch, and Prof. John Allman (UNSW); Dr Arthur Neill, David Morabito, and Dr Bob Preston (JPL); Prof. Irwin Shapiro, Dr Tom Herring, Dr Michael Ratner, and Dr Bob King (MIT); Prof. Kurt Lambeck (ANU), Dr Hugh Bibby (DSIR, NZ), and Dr Richard Coleman (Sydney Uni.). I thank them all for their useful discussions and for taking an interest in my work.

During this research I was supported initially by a University of NSW Postgraduate Scholarship and then by a Commonwealth Postgraduate Research Scholarship. The School of Surveying generously provided funds for my travel and accommodation overseas.

Finally I wish to thank all my friends and relatives who have encouraged and supported me.

CHAPTER 1.

INTRODUCTION

Why combine VLBI data with ground survey data?

There are three main reasons for combining VLBI (Very Long Baseline Interferometry) and ground data. These are:
1) To obtain improved values of strain and crustal deformation for geophysical applications.
2) To facilitate comparisons between VLBI, SLR (Satellite Laser Ranging) and GPS (Global Positioning System) measurements. These techniques cannot be observed from the same sites, thus ground measurements are required to connect the sites.
3) To strengthen ground survey networks and to check for, and control, systematic errors in ground observations.

In the past geodetic networks were established primarily for mapping purposes. Now, they are also required as control for local and regional surveys such as engineering surveys. If the control network is less accurate than a Surveyor's measurements, then he will have to establish his own control to guard against systematic and other error accumulation. This would be expensive and inefficient. It also violates the basic surveying dictum of "working from the whole to the part". If accurate surveys are adjusted to agree with less accurate control, the quality of the survey is degraded. With the accurate instruments now available the old control may not be sufficiently accurate in some regions of Australia. Therefore improving the ground network by including data from high precision space techniques such as VLBI is very desirable. An accurate geodetic network could also be used as control for determining GPS satellite orbits.

Accurate geodetic measurements are needed for a better understanding of earthquakes and the plate tectonics hypothesis, and to select very stable areas of the earth's

crust. For these purposes a combined network of ground and VLBI data may be more useful than either measurement technique on its own. This is because VLBI measurements are generally more accurate than ground measurements. Moreover, they can be obtained in a day rather than months. However ground networks are much more dense than VLBI networks. A dense network is particularly useful because it enables studies of regional and local deformations that may compensate and therefore not be detected over longer distances. Moreover the ground data usually spans many years compared to the few years of VLBI data. Another consideration is that over long distances repeat measurements by the space techniques may cost less than repeat measurements by conventional geodetic techniques.

Geophysicists have a number of basic questions that they wish answered (eg. Lambeck, 1980 and Shapiro, 1983). Among these are:
How is strain distributed as a function of time and position along, near, and within plate boundaries?
Do plate motions accelerate after earthquakes?
Does slow and extensive deformation occur prior to sudden failure?
Is crustal uplift a precursor of earthquakes?
What is the nature of the current movement of the plates?
Are plates moving at similar rates and directions as they have done over periods of millions of years as determined by geological and geophysical evidence?
How does an individual plate move?
Does it move as a rigid body or do episodic strain waves propagate across the plate?
What is the relation between horizontal and vertical motions, particularly along plate boundaries?

These and other questions are important in the understanding of earthquakes and deformations, and their possible prediction. To answer them requires determination of position, or rate of change of position, in seismic zones and at places separated by hundreds or thousands of

kilometres. Measurement accuracies of the order of a few centimetres are required, and the measurements should be obtained from dense networks remeasured at frequent intervals.

Deformations that are of interest range from world wide plate tectonic motions to crustal movements in seismic zones. Determining that a point on a plate is moving or that a baseline between two plates is changing does not describe the whole plate motion. We need to know about the stability of the plate and whether large scale deformations of a magnitude comparable with the interplate motion are occurring. Hence a network of observing sites on each plate is necessary to determine relative plate motion. On a smaller scale, of a few kilometres, it is possible that there is local movement at each site. Thus a local network is also needed to account for this movement before estimating plate motions. By combining ground and space techniques, an important combination of accuracy and spatial coverage can be achieved.

For distances less than 10km, it is expected that ground techniques will remain the primary measurements for monitoring crustal motions (Panel on Crustal Movement Measurements, 1981). These techniques are quite suitable over short distances. However errors accumulate over longer distances. Moreover the measurements are expensive and time consuming, especially for distances greater than about 100km, so they cannot be repeated frequently. For distances greater than 10km but less than several hundred kilometres a combination of ground and space data will probably give the best results. Accordingly, the combination of data from networks spanning regions from ten to several hundred kilometres is studied in this thesis. For longer distances space techniques are the most accurate. Moreover, worldwide geodetic measurements can only be carried out by space techniques.

Earthquakes are a very serious hazard. Their reliable

prediction is not yet possible (Kisslinger, 1984). However an understanding of crustal strain accumulation and crustal movements may help to eventually predict earthquakes. Earthquakes are caused by failure to resist tectonic stress which accumulates over a period of time. Strain rate is a key factor in determining the frequency of earthquake occurrence and accumulated strain is a key factor in determining the magnitude of earthquakes. However the temporal and spatial extent and the magnitude of the strain changes preceding earthquakes are not thoroughly understood (Kisslinger, 1984). The distribution of strain depends on geological factors but generally it diminishes with distance from the fault. For major earthquakes the strain may extend tens of kilometers, or more.

Although most crustal movement occurs at plate boundaries, earthquakes, regional uplift, and subsidence do occur within plate interiors. The existence of these deformations well within plates is not explained by the present plate tectonics model. Deformation also results from human activity such as the extraction of minerals, water, oil and gas, the creation of reservoirs, and ground loading by cities. This deformation also causes economic losses.

Reliable knowledge of which portions of plates are stable is important for the siting of major dams, nuclear power generating facilities, and the disposal of nuclear and other man-made waste. It is not sufficient to know where the hazardous areas are and to avoid them. We need to know with confidence where these facilities can be put. When choosing sites, decisions should be based on estimates of the present stability obtained from geodetic data as well as evidence of stability on the geological time scale. Currently the future tectonic stability of a site is predicted from geological considerations. If the site has been stable in the past then it is often presumed that it will be stable in the future. However new geological processes may have recently begun and may have altered the stability of the site. High quality geodetic data is needed

to test this possibility.

Australia is thought to be within one large plate (see Fig. 1.1) moving fairly rapidly north east. Figure 1.2 shows that the continent is relatively aseismic. Though small earthquakes do occur and there are regions of activity that indicate stress accumulation. There is no evidence of active major fault zones but the plate as a whole may be subject to deformation (Denham et al, 1979). Measurements between points in Australia and points in Indonesia, New Guinea, New Zealand, Fiji and Antartica could detect relative plate motion. Non-tectonic ground motion in this region must also be studied.

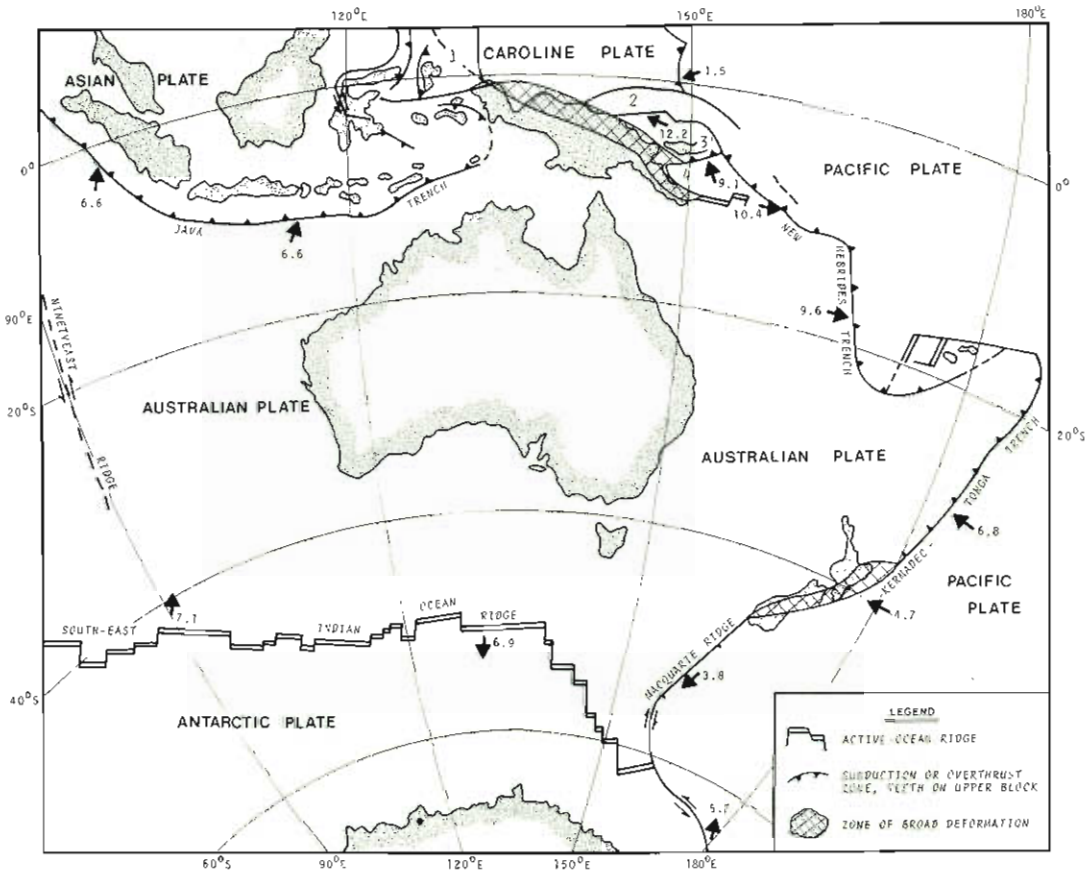

Figure 1.1 Generalised Plate Tectonics of the Australian Region.

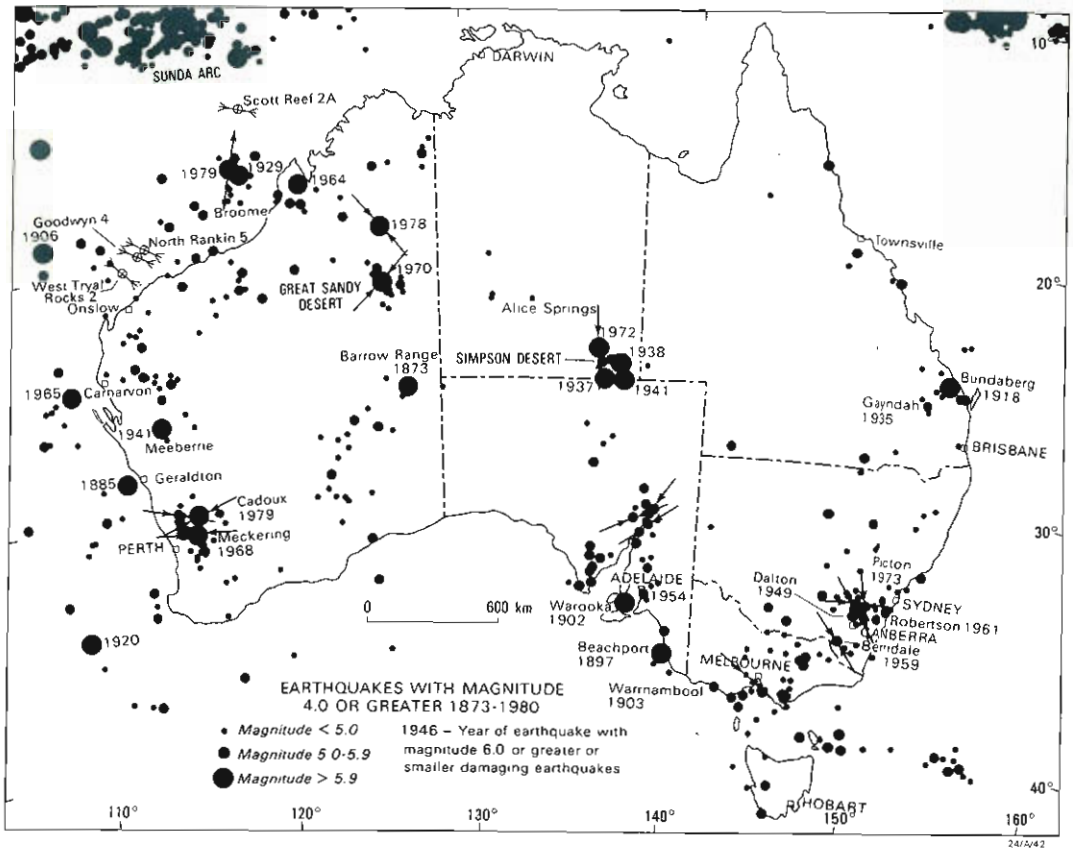

Figure 1.2 Earthquakes with magnitude 4.0 or greater in Australia, 1873 - 1980. (From BMR 82, Yearbook of the Bureau of Mineral Resources, Geology and Geophysics, Australian Government Publishing Service Canberra, 1983.)

Improved information on the accuracies, not just precisions, that can be achieved by ground and space techniques is needed. The Panel on Crustal Movement Measurements (1981) states that "Measurements must be made outside of regions where crustal motions are likely to be large or erratic to obtain an understanding of measurement errors. Studies should be undertaken to recommend analytical procedures for evaluating and intercomparing the different techniques". This thesis aims to investigate and recommend the required analytical procedures.

It is well known that the error sources of the ground, VLBI, SLR, and GPS techniques are almost independent. Continual comparisons are therefore useful to independently evaluate the accuracies of each technique. Ideally, all measurements to be compared should be observed at the same

time. Otherwise any movements in the interval spanned by the observations could corrupt the comparison. Since it is often difficult to make all measurements at the same time, and because the ground measurements are not observed instantaneously, it is better to observe in regions where the ground is not deforming significantly over the time spans covered. Moreover, to obtain the most benefit, these comparisons should be between measurements of the highest quality attainable. Unfortunately the geodetic observations are not always of the highest quality.

The Panel on Crustal Movement Measurements (1981) recommended that "Theoretical studies and analysis of existing data should be given much higher priority than they currently enjoy". It is important to analyse data thoroughly to make suggestions for the planning of new experiments. The data may also contain information about deformation or systematic measurement errors which is not initially apparent.

The effects of systematic errors should be considered and resolved before apparent geodetic changes are interpreted as having tectonic causes. The Panel on Crustal Movement Measurements (1981) recommended that "The techniques of acquisition and analysis of geodetic data used for monitoring tectonic motions should be thoroughly investigated for validity. Intercomparisons of space- and ground- based geodetic techniques should be given a high priority". An aim of this thesis is to investigate these problems.

From the above discussion it can be seen that there are at least three good reasons for investigating the optimal combination of VLBI and ground measurements. The question of how to correctly combine the two data types is the subject of the remainder of this thesis.

Chapter 2 describes and reviews the fundamentals of VLBI and includes a discussion on the estimates of the

accuracies of delay and delay rate observations, and the correlations between them. The reference frames used and experiment schedule design are described because they are an important basis for discussions of the combination of different data types and VLBI error sources.

Chapter 3 discusses systematic modelling errors of VLBI. Particular attention is given to the way errors propagate into the baseline results. There are two types of systematic errors: 1) those whose propagation into the baseline results depends on the observation schedule, and 2) those that are independent of the schedule. The effect of some errors on baseline results can be represented as uniform scale factors, as simple rotations of the baselines about some axis, or as a shift of the baselines. However the effect of some errors cannot be represented so simply. This classification is convenient when combining VLBI data either with other VLBI data from different epochs or with ground data.

The results of the first geodetic VLBI experiment within Australia are presented in Chapter 4. Estimates of the accuracies obtained and possible error sources are discussed. The results are compared with those obtained by conventional geodetic measurements. This data is then used in subsequent chapters to test and compare the various models for combining data and for strain analysis.

A brief review of conventional geodetic surveys and their error sources is given in Chapter 5. Even though well documented elsewhere, this review is justifiably presented here because it is necessary to understand the error sources of both data types before they can be combined properly. The survey connection of the VLBI reference point to the geodetic survey is also discussed. This connection is as important as any of the measurements in either network.

Chapter 6 deals with the theory of combining two sets of

data. The peculiarities of different data sets, the importance of accurate variance covariance (VCV) matrices, and the theory of transformations are discussed. Analysis procedures are developed and appropriate statistical tests are presented. An understanding of scale factors and rotation matrices is developed. The geometry of the network of points common to both data sets, least squares adjustment applied to this problem (and its associated computational errors), and the inclusion of additional parameters are also studied.

In Chapter 7 models that could be used to combine the data sets are compared. While most of these models have been described by other authors, they are discussed here in terms of a full least squares adjustment. Numerical examples with real and simulated data are given. These models are then expanded to include additional parameters to absorb possible systematic errors in the data. A new parameter which is discussed is a bias error in the tropospheric corrections to the VLBI data. A computer program was written to do the necessary calculations and it is listed in Appendix B. Comments are also made on the correct use of the results obtained from adjustments with these models.

A brief review of strain theory and deformation analysis is given in Chapter 8. Models for 3D strain analysis are presented. These models refer the strain to a geocentric frame, a local topocentric plane, and an ellipsoidal surface. The models are compared and contrasted using examples from real and simulated data. A number of possible models for studying 2D strain are then presented with examples, again using real and simulated data, and preferences given. Comments on the applications of strain analysis and the effects of systematic errors in the data are given. Rigorous analysis procedures are developed.

CHAPTER 2.

VLBI.

The basic theory of VLBI is well documented by, Whitney (1974), Robertson (1975), Ma (1978), Shapiro (1976, 1978, and 1983), and Bock (1980). Consequently only those aspects of the theory which are essential to the research in this thesis, are briefly presented here.

In the geodetic analysis of VLBI data we use 'observations' which are themselves estimates from complex instrumental and analysis procedures. While requiring an understanding of these processes, we are more concerned with optimal experiment design, improving mathematical models, devising sound computational and statistical procedures, and the application of the results. This chapter therefore concentrates on the geodetic rather than the instrumental aspects of VLBI.

OBSERVABLES.

Natural radio sources emit electromagnetic radiation over a wide range of frequencies. A radio telescope selects a particular narrow range of these frequencies (bandwidth) and ignores signals at all other frequencies. The selected signal is then amplified and recorded as described below.

Generally, a particular portion of the radio signal from the source will arrive at one site before it arrives at another (Fig. 2.1). This time delay is the basic observable of VLBI. If the observed radio source is outside the solar system, the wavefront received at each site can be regarded as a plane wave and the direction to the source from each site as parallel (Cannon, 1978). The delay, τ, can be related to the source direction, $\hat{s}$, and the baseline vector, B, by the formula -

$$\tau \cong B \cdot \hat{s} \ / c \qquad (2.1)$$

where c is the velocity of light. An expanded form of the

above formula is (Whitney, 1974) -

$$\tau = [B_x \cos(\alpha_g - \alpha_s) - B_y \cos\delta_s \sin(\alpha_g - \alpha_s) + B_z \sin\delta_s]/c \qquad (2.2)$$

where B_X, B_y, B_Z are the components of the baseline, δ_s and α_s are the declination and right ascension of the source, and α_g is the right ascension of the Greenwich meridian. These simple expressions do not allow for instrumental effects, refraction of the signal through the atmosphere or the effect of the earth's rotation. If τ is measured, s is known and various corrections are made, then the components of B can be determined. The magnitude of τ is always less than about 0.02 seconds for any baseline connecting sites on the earth's surface. The most common measure of τ is the group delay (eg. Rogers, 1970).

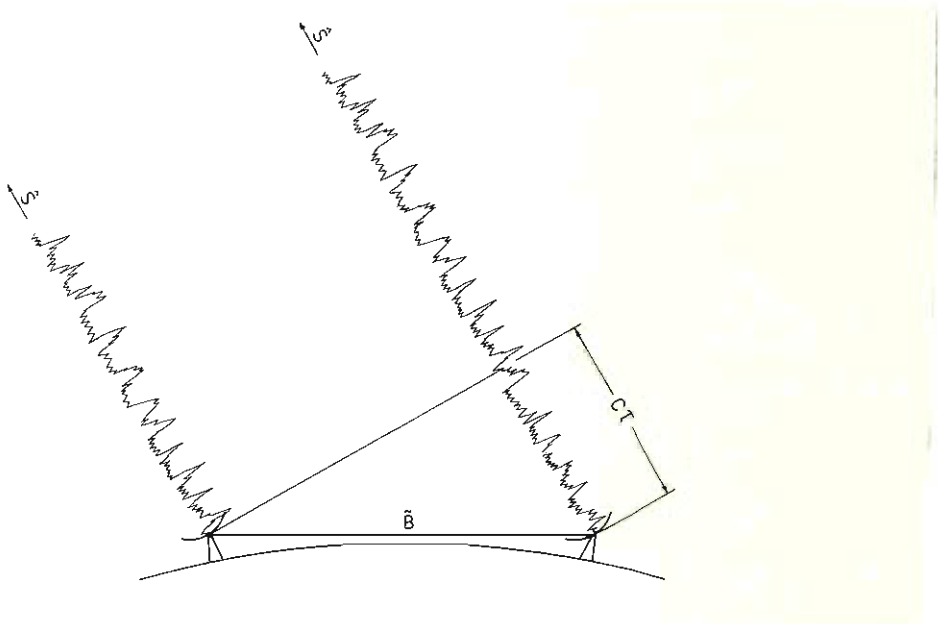

Figure 2.1 Group delay.

The second VLBI observable is delay rate (Fig. 2.2). This is the time rate of change of delay. It is caused by the earth's rotation with respect to the source. As the earth rotates on its axis, the time delay exhibits a diurnal sinusoidal variation because the angle between the baseline and the source direction changes. The observation of delay rate requires simpler instrumentation than that required for the observation of delay. However the use of delay rate observations alone gives poor determinations of the Z component of baselines because the angle between the source

direction and the Z component does not change with time.

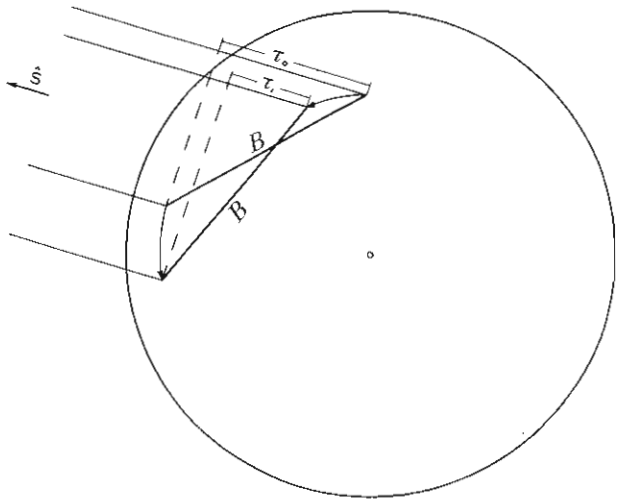

Figure 2.2 Delay rate.
(Looking down on the earth's rotation axis.)

The third observable is phase delay ϕ, which is related to delay by -

$$\phi = \omega\tau \qquad (2.3)$$

where ω is the angular frequency ($2\pi f$) of the received radio signal. The phase delay is the difference in phase of the signals received at each site (Fig. 2.3). It also has a diurnal sinusoidal variation. The phase difference at the two sites will contain a number of complete rotations of phase or whole wavelengths, as well as a fraction of one rotation of phase or part of a wavelength. While the fractional part can be measured, it is difficult to determine the number of complete rotations, n. This is because n changes as the earth rotates and as the atmosphere changes. In order to determine n and therefore ϕ, the baseline, the atmosphere and its fluctuations, and various other systematic effects have to be modelled to an accuracy of about 1cm.

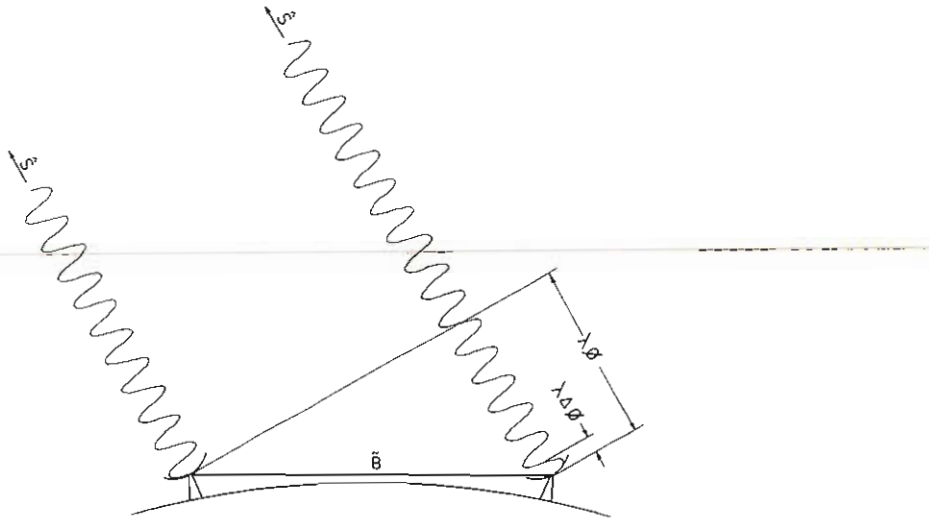

Figure 2.3 Phase delay.
(λ = wavelength, ΔØ = phase difference)

The uncertainties presently being obtained are about 20ps for (ambiguous) phase delays, 50ps (1.5cm) for group delays, and 0.1ps/s (0.003cm/s) for phase delay rates (Rogers et al, 1983). The accuracies of these measurements, and therefore of the baseline, are almost independent of baseline length. However, the signal received at each end of a short baseline (say, 1km) will pass through virtually the same atmosphere, so the effects will tend to cancel. While on a long baseline (say, 1000km), the atmospheric effect at each site may be significantly different and may not necessarily cancel.

RECORDING AND CORRELATION.

There are a number of VLBI recording systems. The Mark II system (Clark, 1973) was used in the Australian experiment described in Chapter 4. This system has a larger bandwidth and consumes less tape than the older Mark I system. The Mark III system (Hinteregger, 1980), which can be regarded as 28 Mark II systems working simultaneously, is the most advanced system yet developed. While the Mark I and Mark II systems were merely designed for recording data, the Mark III system was designed as a complete VLBI unit. It controls observing schedules, equipment, recording of

signals, recording of other data, correlation and subsequent analysis for geodetic and astronomic results. The Mark II systems are more widely available. However, they require more operator control and provide results of a slightly lower accuracy.

The received radio signals are at too high a frequency to be directly recorded on magnetic tape, so an oscillator in the radio telescope produces a frequency close to the frequency of the radio signal. This oscillator signal is combined, or heterodyned, with the natural signal and a beat signal is produced. The frequency of this beat signal is equal to the difference between the frequencies of the natural and oscillator signals. The beat frequency is of the order of a few MHz and is typically recorded on video tape.

In the system used in the Australian experiment (see Chapter 4), the beat signal was sampled once every 250ns for a 2MHz bandwidth system. If the amplitude of the beat signal at the sample point is positive, a one is recorded; if negative, a zero is recorded. So the recorded signal is merely a series of zeros and ones. This binary system, into which timing codes are periodically inserted, is very suitable for computer analysis.

In the tape correlation stage of VLBI processing, the tapes from each site are brought together and the recorded binary patterns from each tape are compared. The delay, delay rate and phase observables are then computed (see Thomas (1973, 1980) for details).

The received signal is contaminated by background noise. Thus a single observation may not give a good value of the observables. The adverse effects of background noise are, in practice, reduced by compressing the data. For example, eight minutes of observations contain about 2×10^9 bits per telescope site. These are compressed to obtain one value of each of the observables.

Two special techniques to improve accuracy will be mentioned here, namely Bandwidth Synthesis (BWS) and dual frequency observations. To make delay measurements more accurate, it is necessary to increase the recorded bandwidth. Since the bandwidth is restricted by the tape, to 2MHz for the Mark II system, BWS was devised (Rogers, 1970). Preselected frequency bands, each of 2MHz bandwidth, are sequentially recorded over a total bandwidth of 40MHz or more. The sampled bands that are observed can be used to obtain results similar to those that would be obtained if the full band had been recorded. In the Mark II system each band is recorded sequentially for a short time (eg 1s). In the Mark III system they are recorded simultaneously.

The second technique to improve accuracy is to observe at two widely separated frequencies. Refraction in the ionosphere is a function of the observed frequency. By observing at two frequencies, it is possible to calculate the effect of the ionosphere on each of the signals and to correct for it. Observations are typically made at 2.3GHz (S band) and 8.4GHz (X band). These S/X observations provide the simplest and most accurate method of eliminating ionospheric errors.

GEODETIC PARAMETERS.

Several distinct types of model are required in order to analyse the VLBI observables for geodetic information. They can be classified as those related to: the rotation of the earth in space, the displacement of individual stations, the atmospheric retardation of the wavefront, and relativistic effects. The rotation models include precession, nutation, sidereal time, and polar motion.

Shapiro (1978), Bock (1980), and Dermanis and Grafarend (1980) show which VLBI parameters are estimable. Estimable parameters are those that can be uniquely determined from error free observations. Of the geodetic parameters only

baseline lengths and source declinations are estimable. The remaining geodetic parameters (site coordinates and baseline components) are determined relative to the orientations of the inertial and terrestrial frames. Thus only their variations, or changes, are estimable. Geocentric site coordinates are not estimable because the observations are primarily a function of the differences of these coordinates for each baseline. Thus one site's coordinates cannot be determined unless the other site's coordinates are known.

Changes in polar motion and universal time (UT1) are estimable but their values at some initial epoch are not. The initial values must therefore be held fixed at a priori values derived from an independent technique. For a single baseline, VLBI data are sensitive to only two of the three parameters for polar motion and UT1. Rotation of a baseline about an axis parallel to the baseline results in a parallel shift of the baseline components. This shift cannot be detected from observations of sources which are virtually at infinity. For example, a north-south baseline is not sensitive to a rotation about the spin axis, ie UT1. Similarly, an east-west baseline is not sensitive to the components of polar motion perpendicular to the baseline. Thus at least two baselines (preferably perpendicular) are needed to detect all three components of polar motion and UT1. Moreover any common epoch errors of the station clocks will be indistinguishable from corresponding variations in earth rotation. Long period changes of the orientation of the earth's spin axis in space (precession and nutation) can be detected from changes in the source coordinates. However, estimates obtained from VLBI are currently less accurate than the presently accepted values determined from many years of optical observations.

VCV MATRIX OF THE OBSERVATIONS.

VLBI analysis is typically done in two stages. In the first stage the observables, delay and delay rate, are estimated.

In the second stage the various parameters such as baseline and source coordinates are estimated from these observables. This two stage procedure is valid only if the full variance covariance matrix (VCV) of the observables is used. However the full VCV is rarely used.

Precisions.

Estimates of the precision of the delay and delay rate measurements can be obtained from the signal to noise ratio (SNR) of the observation and the recorded bandwidth (Whitney, 1974). The SNR is a function of the antenna diameters, system noise temperatures, antenna efficiencies, and source strength. However these values may not be known with sufficient accuracy. Moreover these estimates of the precisions of the observables do not allow for errors due to the propagation media and instrumental effects. The precisions of the observables can also be estimated from the scatter of phase within an observation scan. This is the method generally adopted. The precision of τ estimated by this method does account for fluctuations in the clocks and atmosphere during the few minutes that each observation is recorded.

A least squares analysis of the VLBI data using the above estimates of precision does not usually satisfy a posteriori statistical tests. So the estimates of precision, the stochastic models, or the functional models are incorrect. The error estimates are usually too small. Accordingly they are, conventionally, increased by adding what some VLBI analysts call 'sigcons'. In this technique a constant term is quadratically added to each precision estimate for delays and another constant term is added to the precision estimates of the delay rates. The details are given by Robertson (1975), Thomas et al. (1976), and Musman (1982). The procedure, which is standard in VLBI analysis, is iterated until the a posteriori variance factor ($\tilde{\sigma}_0^2$) approximately equals the a priori variance factor (conventionally unity). The a posteriori variance factor

can be tested against its a priori value by the variance factor test (see Chapter 6). If the test is satisfied at some selected confidence level then it is probable, at that level of confidence, that the sample of observations are from the same population as the a priori variances.

Errors in atmospheric corrections or instrumental errors such as fluctuations of the frequency standard are approximately constant for all observations and are not dependent on the SNR of the observation. So the use of sigcons is a better approach than multiplying the original error estimates by a factor. The scaling of observation formal errors or the use of sigcons tends to compensate for unmodelled systematic effects, neglected correlations between observations, and poor estimates of the precisions of other effects.

Alternatively, it should be possible to estimate a typical precision of a delay or delay rate observation from the data of a number of experiments. These values could then be used in future adjustments without the need to force $\tilde{\sigma}_0^2$ to its a priori value. Forcing the variance factor to its a priori value is poor statistical practice because it uses only the particular observations in an experiment rather than the overall experience of the population from all experiments. However the analyst must be sure that all past experiments used to estimate precisions are part of the same population, that is, they must have the same instrument quality (especially frequency standard) and similar atmospheric errors. For example, it is better to combine the data from two very similar experiments and find precision estimates that make $\tilde{\sigma}_0^2$ equal one, than to do separate solutions for each experiment, making $\tilde{\sigma}_0^2$ equal one for each solution with probably different sigcons. If a separate solution is required for each experiment then each solution should use the same values of sigcons as determined from the overall solution. The resultant $\tilde{\sigma}_0^2$ for each solution can then be statistically tested. However this approach is not recommended if there is good reason to

believe that the sigcons are different for each experiment.

Simulation studies were performed to illustrate the above procedure. Theoretical delays and rates were generated, using the schedule of the May 2-3, 1982 experiment between Tidbinbilla and Parkes (see Chapter 4). A random number generator was applied to add random noise with zero mean and a standard deviation of 150ps to the theoretical delays and similarly zero mean and standard deviation of 0.1ps/s to the delay rates. The delays and delay rates were assigned precisions of 150ps and 0.1ps/s respectively, that is equal to the induced scatter in the observations. Thirty different data sets were generated and each data set was individually adjusted. Figure 2.4 shows the resultant $\tilde{\sigma}_o^2$ of each solution. Clearly the $\tilde{\sigma}_o^2$ does not always equal unity even with "perfect" observations. In fact, it varied up to 1.3 in this example. The variation from unity was caused by the limited number of observations in each experiment.

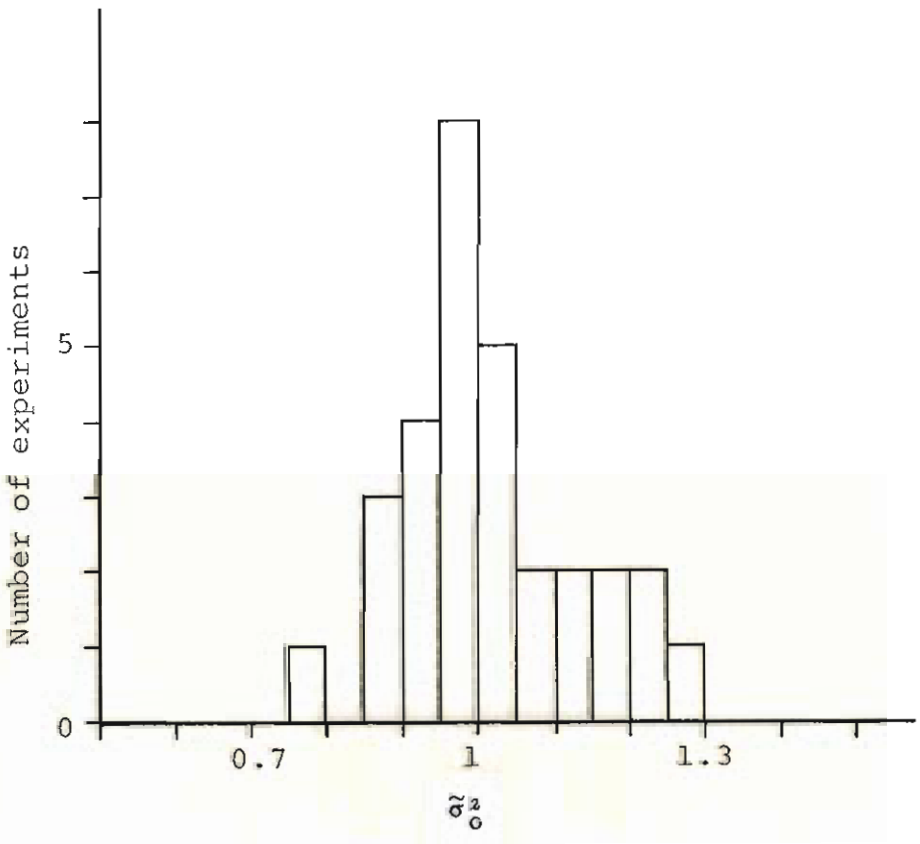

Figure 2.4 Variance factor ($\tilde{\sigma}_o^2$) simulations.

Errors in $\tilde{\sigma}_0^2$ can give optimistic or pessimistic estimates of the quality of the results if it is used to scale the precisions of the adjusted parameters. If $\tilde{\sigma}_0^2$ is at the limit of acceptability of the 95% variance factor test (see page 118) then the error in the estimated standard deviations will be more than 10%. Unless the degrees of freedom of the adjustment are greater than about 120. When the number of redundancies in the adjustment is not large, when it is not certain that all systematic errors have been eliminated, and when the variance factor test has been satisfied, it is better to use the a priori variances than the variances estimated from the adjustment.

Correlations.

The phases are computed for each section of an observation scan. These phases, of each section and of each frequency channel, are then used to determine group delay and phase delay rate and their precisions. The phase rates of each channel are about the same and because of atmospheric and oscillator instabilities, the non linear phase excursions are highly correlated (~0.9). This affects the calculation of the group delay and its precision. The values of group delay and phase delay rate at S band and at X band are then combined. The S/X corrected group delay and phase delay rate are then each assigned formal errors with zero correlation. However, if any of the observations are correlated and these correlations are ignored, then the estimates of the final formal errors will be incorrect.

There are a number of possible causes of correlations between the observables. Among the most important of these are:

1) Correlations between group delay and phase delay rate.

If all phases in a scan are of equal precision and are uncorrelated, and the observables are referred to the mid-point of the scan then the estimates of delay and rate will have zero correlation. Strictly, the mid-point of the scan

is the weighted mid-point which could be different to the centre of the time interval. Though generally the mid-time is satisfactory because each section within an observation has approximately the same weight.

Some VLBI programs use two phase delay values as input data. The delay rate is then calculated from these. The error estimates ($\sigma_\tau\sqrt{2}$ / t) of the derived rates will only be correct if the two phase delays are uncorrelated. If the two phases are positively correlated then the precision of the rate will be smaller than if the correlation had been ignored. A posteriori analysis usually indicates that the standard deviations of delay rates are far too small. It is unlikely that the phases would be negatively correlated. Hence this source of correlation can safely be ignored.

The correlation between a particular phase and the next phase should also be considered in the calculation of group delay. Currently it is assumed to be zero (Bock, 1983).

2) Correlations between S and X band observations.

In the calculation of precisions of S/X delay, and delay rate, it is assumed that the S band delay (τ_s), the X band delay (τ_x), the S band rate ($\dot{\phi}_S$), and the X band rate ($\dot{\phi}_X$) are all uncorrelated. These assumptions will now be investigated. The S/X corrected delay (and rate) are calculated independently of their precisions and correlations using -

$$\tau sx = \frac{R\tau x - \tau s}{R - 1} \qquad \dot{\phi}sx = \frac{R\dot{\phi}x - \dot{\phi}s}{R - 1} \qquad (2.5)$$

where $R = (fx/fs)^2 \cong 13$

It can easily be shown that -

$$\sigma^2_{\tau sx} = \frac{R^2\ \sigma^2_{\tau x} - 2\ R\ \sigma_{\tau x \tau s} + \sigma^2_{\tau s}}{(R - 1)^2} \qquad (2.6)$$

Now $$\rho_{\tau x \tau s} = \sigma_{\tau s \tau x} / \sigma_{\tau x}\ \sigma_{\tau s} \qquad (2.7)$$

If $\rho_{\tau x \tau s} = 0$ then

$$\sigma^2_{\tau sx} = (R\ \sigma^2_{\tau x} + \sigma^2_{\tau s}) / (R-1)^2 \qquad (2.8)$$

which is the commonly used formula. However if the correlation is not zero then the corresponding error in $\sigma^2_{\tau sx}$ is -

$$\Delta\sigma^2_{\tau sx} = 2R\rho_{\tau x\tau s}\sigma_{\tau x}\sigma_{\tau s} / (R^2\sigma^2_{\tau x} + \sigma^2_{\tau s}) \qquad (2.9)$$

If $\sigma_{\tau x} = \sigma_{\tau s}$ then $\Delta\sigma^2_{\tau sx} \cong 15\rho\%$ now $|\rho| \leqslant 1$ so $\Delta\sigma_{\tau sx} \leqslant 4\%$
The above error analysis also applies to $\sigma^2_{\dot{\phi} sx}$.

It can be seen that correlations will not affect the value of the corrected delay or delay rate. However, correlations will affect the derived precisions of the delay and rate, though by less than 4% if the S and X delays (and rates) have similar precisions. Even if τ_x were an order of magnitude more precise than τ_s the error in $\sigma_{\tau sx}$ would still be less than 10%.

3) Correlations between delay (or rate) of one scan and delay (or rate) of a later scan.

Delays (and rates) at different epochs are assumed to be uncorrelated. This could be tested by the MINQUE technique (see eg Welsch, 1981, Grafarend and Schaffrin, 1980, and Schaffrin, 1981) or some other procedure for estimating the VCV of observations. However these methods are time consuming.

4) Correlations between delays (or rates) on various co-observing baselines.

The correlation between any two of the time delays, measured around a triangle at any one time, has a maximum of 0.5. However the correlation will be much smaller in practice because the time delays are determined by a digital correlation of signals from possibly extended sources (Bock, 1983). With a very good SNR, the correlation may reach 0.1, but will usually be much less and hence can safely be ignored.

Except for source structure effects, at any given epoch, the sum of group delays around a triangle should equal zero

because instrumental and environmental effects cancel out. This provides a check on data processing. The triangular sum also checks the estimates of the VCV of the delays because the results of a number of such triangle sums and their precision estimates can be statistically tested.

The effect of atmosphere on the VCV.

When corrections are applied to the delay and delay rate data before being input to a VLBI program, or similarly are applied within the VLBI program, the VCV of the observables should also be corrected. The atmospheric corrections, the axis offset correction and other corrections whose propagation depend on the schedule all affect the VCV of the observables. Other corrections that do not depend on the schedule (eg precession and nutation constants, polar motion terms, and UT1) do not affect the VCV of the data (see Chapter 3). Since clock term corrections are not applied a priori to correct the delays and rates, the VCV of the observables does not have to be corrected for clock errors.

On short baselines the atmospheric correction is usually applied, as determined from surface meteorological data, Water Vapour Radiometer (WVR) data, if available, and refraction models. These corrections are applied as though they were error free. The correlator value of τ is corrected for atmospheric delay as follows.

$$\tau_{obs} = \tau_{geom} + \tau_{atmo} + \text{clock terms} + \ldots \quad (2.10)$$

$$\text{so } \tau_{correlator} - \tau_{atmo} = \tau_{geom} + \text{clock terms} + \ldots \quad (2.11)$$

$$\text{where} \qquad \tau_{atmo} = \tau_{atmo\ site\ 2} - \tau_{atmo\ site\ 1} \quad (2.12)$$

If the atmospheric corrections are error free then the VCV of the delays and rates does not need to be changed. However in practice the corrections for the atmospheric delay are subject to error, so the σ of the corrected τ should be increased as follows.

$$\sigma = \sqrt{\sigma^2_{\tau\ \text{correlator}} + \sigma^2_{\tau\ \text{atmo}}} \qquad (2.13)$$

where $\sigma^2_{\tau\ \text{atmo}} = \sigma^2_{\tau a\ 1} + \sigma^2_{\tau a\ 2}$ (2.14)

Note that while the atmospheric correction to a delay is the difference between the effect at each site, the variance of the correction is the sum of the variance of the effect at each site. Typically $\sigma_{\tau\ \text{correlator}}$ is about 100ps or less, and $\sigma_{\tau\ \text{atmo}}$ is about 280ps. So σ is really about 300ps, which is significantly different to $\sigma_{\tau\ \text{correlator}}$.

Consider two observations τ_i and τ_j are made on one baseline. If τ_c is the correlator delay and τ_a is the atmospheric correction to this delay, then the corrected delays are -

$$\tau_i = \tau_{ci} - \tau_{ai} \quad \text{and} \quad \tau_j = \tau_{cj} - \tau_{aj}$$

The VCV of the two corrected delays can be determined from the law of propagation of variances. If the $\sigma_{\tau c}$ are assumed equal and uncorrelated and $\sigma_{\tau a}$ is constant then the VCV of the corrected delays is -

$$\begin{bmatrix} \sigma^2_{\tau i} & \sigma_{\tau i \tau j} \\ \sigma_{\tau i \tau j} & \sigma^2_{\tau j} \end{bmatrix} = \begin{bmatrix} \sigma^2_{\tau c} + \sigma^2_{\tau a} & \sigma_{\tau a i \tau a j} \\ \sigma_{\tau a i \tau a j} & \sigma^2_{\tau c} + \sigma^2_{\tau a} \end{bmatrix} \qquad (2.15)$$

It can be seen that $\sigma_{\tau i \tau j}$ equals $\sigma_{\tau a i \tau a j}$ and that τ_i and τ_j are less correlated than τ_{ai} and τ_{aj}. What remains then, is to determine $\sigma_{\tau a i \tau a j}$. This is a difficult but necessary task because it may be significant. There are two problems when estimating the VCV of the atmospheric corrections: (1) to determine the variances or precisions of the corrections, and (2) to determine the correlations between various corrections.

The accuracies of the atmospheric corrections can be estimated from the accuracies of the meteorological observations and the models used. These are obtained by comparing the results with independent measurements of the corrections (by for example radiosonde measurements), and by comparing the results of VLBI analyses obtained when different estimates of the atmospheric corrections are

used.

A constant variance for the atmospheric delay corrections assumes that the meteorological instruments and atmospheric models perform equally well at all times. However it is possible that some models may be more accurate at night than during the day or vice versa.

The off-diagonal terms of the VCV of atmospheric corrections may not be negligible. They are not the same as the correlations between the atmospheric corrections. By using the well known crosscovariance and autocovariance methods it is possible to determine the correlation between the atmospheric corrections at different times on any one baseline, and between the corrections on various baselines. While this gives the correlations between the atmospheric corrections it does not necessarily indicate the correlations associated with the variances of these corrections.

The effects on the variances and correlations of delays (and rates) co-observed by a network of baselines also have to considered. Take, as an example, a triangle with points 1, 2 and 3. Let τ_{cij} be the delay obtained from the correlator for the baseline i-j, and Ai be the atmospheric correction at site i for the particular observation. The corrected delays for a single observation are then -

$$\begin{aligned} \tau_{12} &= \tau_{c12} + A_2 - A_1 \\ \tau_{13} &= \tau_{c13} + A_3 - A_1 \\ \tau_{23} &= \tau_{c23} + A_3 - A_2 \end{aligned} \qquad (2.16)$$

If it can be assumed that all the $\sigma_{\tau cij}$ are equal, that all the σ_{Ai} are equal, and that all correlations are zero, then the VCV of the corrected delays is -

$$\begin{bmatrix} \sigma^2_{\tau 12} & \sigma_{\tau 12\tau 13} & \sigma_{\tau 12\tau 23} \\ \sigma_{\tau 12\tau 13} & \sigma^2_{\tau 13} & \sigma_{\tau 13\tau 23} \\ \sigma_{\tau 12\tau 23} & \sigma_{\tau 13\tau 23} & \sigma^2_{\tau 23} \end{bmatrix} = \begin{bmatrix} \sigma^2_{\tau c}+2\sigma^2_A & \sigma^2_A & -\sigma^2_A \\ \sigma^2_A & \sigma^2_{\tau c}+2\sigma^2_A & \sigma^2_A \\ -\sigma^2_A & \sigma^2_A & \sigma^2_{\tau c}+2\sigma^2_A \end{bmatrix} \qquad (2.17)$$

Obviously these corrected delays are correlated by -

$$| \rho | = \sigma^2_A \; / \; (\sigma^2_{\tau c} + 2\sigma^2_A) \qquad (2.18)$$

Substituting typical values of 100ps (3cm) for $\sigma_{\tau c}$ and 100ps for σ_A yields a $|\rho|$ equal to 0.3. One limit of $|\rho|$ is 0.5 which occurs when σ_A is much larger than $\sigma_{\tau c}$. This will probably occur when good SNR is obtained to sources at low elevations. However, $|\rho|$ also depends on the instrumentation quality and on whether WVRs are employed. The other limit of $|\rho|$ is zero. This occurs when the atmospheric correction is error free.

This source of correlation between the observables is currently, and incorrectly, ignored when atmospheric corrections are applied. It is recommended that the VCV of the observables be corrected to allow for errors in the atmospheric corrections. Note that correlations will be introduced. These corrections to the VCV could be made within or prior to the VLBI adjustment. If they are made prior to the adjustment the inverse of the VCV should be input. In this case the fact that the VCV will probably be block diagonal could simplify the computations.

On baselines less than a few kilometres long the atmospheric correction would be expected to be negligible, and none of the above modifications to the VCV of the observables would be necessary. On long baselines (>1000km) the atmospheric corrections can be estimated from the observables. If this is done then the VCV of the observables does not need to be modified.

Determination of the VCV and its effects on results.

The VCV can be determined from (1) the law of propagation of variances, (2) the MINQUE technique, where assumptions about groups of precisions and correlations are made, or (3) estimating various components of the VCV and examining the resultant $\tilde{\sigma}_0^2$. A procedure which estimates and uses a full VCV is distinct from the 'sigcons' method which does not introduce correlations, account for the different elevations of various observations, or allow for the possibility of variations in the accuracy of the

atmospheric corrections. However, the variance factor test may still fail even when correctly allowing for atmospheric and other effects. This failure could be due to short period (less than the interval between 'clock breaks') clock and other instrumental errors.

The effect of errors in the VCV of the observables on the baseline results is most readily determined by comparing results obtained from solutions with different estimates of the VCV. Bock (1980) compares the results of several solutions of a triangle of baselines with only a diagonal VCV as input. The results from separate solutions for each independent baseline were compared with those from a solution which solved for the three baselines simultaneously. He reports that the baseline lengths were well behaved but the baseline components were not. Similar studies need to be done using realistic estimates for the full VCV of the observables.

EXPERIMENT SCHEDULING.

There are a number of constraints and considerations that have to be taken into account when planning a VLBI schedule. They are:

a) On short baselines, observations made at low elevation give good geometric strength in the horizontal components of the baseline vectors. A mix of high and low elevation observations give good geometric strength in the vertical components.

b) Low elevation observations are seriously affected by refraction errors.

c) Clock instability can be examined by observing each source many times during the experiment.

d) Antennas with 'azel' mounts cannot observe sources at or close to the zenith and have 'cable wrap' constraints.

e) Different antennas move at different speeds between the same two points in the sky.

f) Polar sources are seen for much longer than equatorial sources.

g) Strong sources and sources with known positions are not evenly spread in Right Ascension (RA) and declination.
h) Observing many sources gives a better geometric strength to the solution and errors in a priori position and source structure are reduced.
i) Observing only a few sources means that each source is observed more often. This gives a better solution for source position and a better indication of clock behaviour.
j) Depending on the effective bandwidth of the recording system different sources are available. Mark III can see much fainter sources than Mark II and therefore has a wider range of sources to select from.

The preparation of a schedule can be divided into three parts-

1) Choose which sources to observe.
After selecting candidate sources the arclengths between neighbouring sources should be calculated. If the arclengths are all similar and are greater than about 15o, then the sources are probably well spread in RA and declination. The distribution of various selections of sources can be compared using arclengths, RA spread and declination spread.

2) Calculate position of sources at observation times, slew times between observations (ie how long it takes the antennas to move from one direction to another), minimum scan time, and rise and fall times of sources.

3) Choose which order to observe the sources.
The optimisation of this step is difficult and has not yet been accomplished. Currently choices are based on analyst experience and by simulating the results of various schedules. By following a pattern in the sky, such as a figure eight, it is possible to choose the order in which to observe sources. But it is not advisable to make observations in clusters. For example if one group of sources were observed for a few hours and then a different

group of sources were observed it would not be possible to determine if any step in residuals between the two periods was due to clock behaviour, source position errors or some other reason.

If a schedule has been designed for a particular set of baselines on a particular day, then it can also be used on other days by simply shifting all observation times by a constant (about 4 minutes per day) to allow for the difference between sidereal and universal time rates. If the schedule is designed as a 24 hour cycle starting and finishing at the same source and same time of day then the observations can commence at virtually any time.

Existing scheduling programs are generally structured as follows. Input consists of: site coordinates, sources to be observed and their coordinates, type of antenna at each site and their slew rates and cable wrap, and the minimum elevation to be observed. Some also calculate the scan time, for which additional input are required, such as source flux, and antenna diameter, efficiency, and system temperatures. All sources names and their positions in the sky are then displayed together with the time it would take the various antennas to slew to each source. Additional information such as the number of times each source has been observed, the time since rising and before setting, and a summary of the schedule so far, may also be provided. The analyst then decides which source to observe next. Necessary increments are made, the next sky distribution is displayed. This process continues until the schedule is complete.

The optimisation of the third part of schedule design could be based on the importance, or weight, of each possible option. This weight could be determined by considering the partial derivatives, systematic error sources, and the time spent slewing to the source direction. However determining the weight is not a simple problem. Assuming it can be done, there are at least two possibilities in designing the

optimum schedule.

1) After each observation, the next observation is chosen to be that with the highest weight. However it is unlikely that any method of scheduling which selects observations one at a time, will give the optimum schedule. This is because the optimum schedule does not necessarily consist of all the maximum weighted observations.

2) Given a starting observation, all possible schedules are then generated assuming that a source is observed as soon as all antennas are pointing to it. However the number of possible schedules that arise is enormous. Moreover the schedule with the maximum weight determined as the sum of the weights of the options is not necessarily the optimum one.

A more realistic approach is carefully and independently design several possible schedules for a particular experiment. Then simulations are computed with each schedule and their results compared. The schedule which is most desirable in terms of the precisions of certain parameters and least susceptible to systematic error, is then chosen. If several schedules appear similarly useful then different schedules could be used for different experiments, thus reducing even further the effect of systematic errors in the parameters.

REFERENCE FRAMES.

The nearly inertial reference frame commonly used in VLBI has its origin at the solar system barycentre. The Z axis is perpendicular to the mean equator of some epoch eg. 1950.0 or 2000.0. The X axis points to the intersection of the mean equator and ecliptic of that epoch and the Y axis completes a right handed Cartesian system. This frame will be referred to as the conventional inertial system (CIS).

A better inertial reference frame would be defined by the

positions of certain stable sources. However conventional models for precession and nutation are used to reduce the source positions to the 1950 or 2000 system. Consequently the positions of sources will drift due to errors in these models.

The conventional terrestrial reference system (CTS) is defined with the X axis pointing towards the Greenwich meridian as defined by the Bureau Internationale de l'Heure (BIH). The Z axis points to the CIO (Conventional International Origin) pole and the Y axis completes the right handed Cartesian system. The origin may be the geocentre though in practice it is usually defined by adopting approximate geocentric coordinates of one VLBI site. This is because the geocentre cannot be determined by VLBI observations.

The conventional transformation between coordinates of the inertial frame (CIS) and those in the terrestrial frame is

$$(\mathrm{CTS}) = WSNP\ (\mathrm{CIS})$$

where W is the polar motion matrix, S is the spin (sidereal time) matrix, N is the nutation matrix and P is the precession matrix (eg. Ma, 1978).

The reference frame of the catalogue radio sources is defined by their mean coordinates referred to some standard epoch. The uncertainties of the positions of radio sources are currently of the order a few milli-arcseconds (Rogers et al, 1983).

The poles of the International Polar Motion Service (IPMS) and BIH are close to the CIO but they may not coincide. The uncertainties of the pole position and UT1, as determined by the BIH, is estimated to be about 0.01" and 1ms respectively, for five day averages (Guinot, 1978). These estimates do not include the biases in the definition of the pole and systematic drifts (Guinot, 1980). Carter et al. (1984), Carter and Robertson (1984) and Dickey et al. (1984) report on more accurate determinations of pole

position and UT1. The accuracies of pole position and UT1 are continually improving.

Comparison of, and links between, optical and radio catalogues can be made by optical observations of a few radio sources. The two types of catalogue can also be linked by VLBI observations of a few stars and planets. However these comparisons are currently limited by the uncertainties of optical measurements of position to about 0.05" (de Vegt and Gehlich, 1978). A quasar reference frame is more stable than any optical frame based on objects within the galaxy. Also there are a number of different radio source catalogues which need to be compared. The values of the precession, nutation, and earth rotation parameters are not yet known as potentially determinable by VLBI. Errors in these parameters will cause rotations of the right ascension and declination axes of the various catalogues. Assuming an error in the precession constant of 0.01"/year and a difference in observation epoch of 5 years, Johnston et al. (1982) estimate the maximum amplitude of this error in declination to be about 0.2". Such an error has a large effect on baseline results.

CHAPTER 3.

SYSTEMATIC ERRORS IN VLBI

When combining two data sets the two sets should not contain significant systematic errors. If they do then the propagation of these systematic errors on the coordinates should be known. This chapter will discuss a number of the systematic errors which affect VLBI results. Some of these will be shown to have an insignificant effect on the VLBI results compared to current measurement accuracies. The nature of the propagation of errors which have significant effects on the baseline results, will be given. In later chapters it will be shown that correct allowance for a systematic error can be made in the combined adjustment if the nature of the propagation of the error source into the baseline results is known.

When VLBI results are used for the applications discussed in Chapter 1 their VCV matrix also needs to be reliably known. The VCV of the results depends on the errors in the observations and models. If the models are inaccurate or do not allow for all effects, the estimated VCV of the results will also be inaccurate. Generally the variance terms will be too small because not all error sources will have been considered.

There are a number of ways of improving the VCV. One method is to quadratically add error terms to the estimated variances. These error terms are estimates of the effects of each systematic error. However this over simplified approach does not alter the covariance terms so the correlations between the baseline parameters are changed. Generally the absolute values of the correlations are reduced. Another approach is to multiply the VCV by some factor, or portions of the VCV by a number of factors. This approach leaves the correlations unaltered but does not necessarily give correct results. A more rigorous approach is to determine the functional relationships between the

systematic errors and the baseline parameters. The law of propagation of variances and covariances (eg Mikhail, 1976) as presented in Appendix A could then be applied.

The approach adopted here is not to alter the VCV estimated by the VLBI program. However when applying the VLBI baseline data, with its VCV, it must be remembered that the baseline parameters and their VCV are subject to bias effects. They are not, for example, the true length and its accuracy but rather an estimate of the length that is in error by some bias due to the sum of a number of systematic errors. Moreover, the precision of the length estimate is not necessarily its accuracy. So when combining VLBI data with other data, instead of using the VLBI results and an inflated VCV; the VLBI results, their estimated VCV, estimates of the effects of the various biases, and the accuracies of the bias estimates should all be included in the adjustment model. Of course, if the sum of all biases is negligible when compared to the precision of the baseline parameter, then the parameter estimates and their VCV need not be altered or bias terms considered. This matter is further discussed in Chapters 6 and 7.

The systematic errors in VLBI measurements can be classified into two basic types, those that propagate into the baseline results in a way dependent on the observation sequence (schedule), and those that are independent of the schedule. The main errors are discussed below.

SCHEDULE-INDEPENDENT ERRORS.

Error in Right Ascension origin.

If there is a constant error (offset) in the RA of all sources which have their RA fixed or constrained, then there will be an error in the baseline results. Source positions are given in a quasi inertial reference frame (eg B1950 or J2000) and calculations are done with the baseline components transformed to this system, as follows-

$$B_{CIS} = P\ N\ S\ W\ B_{CTS}$$

So
$$B_{CTS} = W^T\ S^T\ N^T\ P^T\ B_{CIS}$$

A constant error in RA rotates the baseline about the Z axis of the inertial frame as follows -

$$\Delta B_{CIS} = Rz(-\theta)\ B_{CIS}$$

where ΔB are the errors in the baseline components and θ is the error in the RA origin. (Rotation matrices such as $Rz(\theta)$ are discussed in detail on pages 97-102.) Now -

$$\begin{aligned}\Delta B_{CTS} &= W^T\ S^T\ N^T\ P^T\ \Delta B_{CIS} \\ &= W^T\ S^T\ N^T\ P^T\ Rz(-\theta)\ B_{CIS}\end{aligned}$$

Of W, S, N, and P the largest rotation is generally S which is a rotation about the Z axis. The combined effect of the other matrices do not change the orientation of the Z axis by more than about 10'. So, with only small errors -

$$\begin{aligned}\Delta B_{CTS} &\simeq Rz(-\theta)\ W^T\ S^T\ N^T\ P^T\ B_{CIS} \\ &= Rz(-\theta)\ B_{CTS}\end{aligned}$$

Therefore an error in the RA origin will only rotate the baseline about the Z axis and does not affect the scale of the baseline results. If θ is small the errors in the baseline components can be approximated by-

$$\begin{aligned}\Delta Bx &= -By\ \theta \\ \Delta By &= Bx\ \theta \quad \text{with } \theta \text{ in radians} \\ \Delta Bz &= 0\end{aligned} \qquad (3.1)$$

Thus the Z component and baseline length are not affected. E-W baselines are generally more affected than N-S baselines, because of larger Bx and By components. The error in the baseline components increases almost linearly with the length of the E-W component of the baseline. A typical value of the error in RA is about 0.05". An error of 0.05" in RA origin causes about 7cm error in the baseline orientation for a baseline with an E-W component of 300km.

Error in source declinations.

If the pole defined by the declinations in the source

catalogue, or any of the models used to transform the instantaneous spin pole to the reference pole are in error then there will be errors in the baseline and source position results. An error in the direction of the pole can be considered as a rotation about a line in the equatorial plane. The total rotation can be resolved into its component rotations about the X and Y axes. If the rotations about the X and Y axes are x and y respectively and if these rotations are small then the error in declination of a source will be -

$$\Delta\delta = y \cos\alpha - x \sin\alpha$$

The error in declination due to an inclination of the pole is less than or equal to the magnitude of the total inclination and depends on the RA of the source and the RA of the erroneous pole. So there will not be a constant error in declination. If i ($= \sqrt{(x^2 + y^2)}$) is the inclination of the pole and A is the difference in RA between the source and the erroneous pole then the error in declination is -

$$\Delta\delta = i \cos A$$

and the corresponding error in RA is -

$$\Delta\alpha = i \tan\delta \sin A$$

Since this effect corresponds to a rotation of the reference frame it will change baseline orientation but not length.

Errors in Earth Rotation.

Polar motion and UT values are typically interpolated from a table of results obtained from an independent source such as the BIH or independent VLBI measurements. The errors discussed here are the constant biases in these tables over the length of time of the experiment. Other, non-constant, errors in the tabulated values will be reflected in the VCV of the baseline results. Even if changes in polar motion and UT are solved for initial values from some independent source still have to be adopted. In either case, whether the changes in polar motion and UT values are estimated or independent data is adopted, biases may exist.

The error in baseline components due to errors in adopted values of polar motion are -

$$\begin{bmatrix} \Delta Bx \\ \Delta By \\ \Delta Bz \end{bmatrix} = Rx(-\Delta y)\ Ry(\Delta x) \begin{bmatrix} Bx \\ By \\ Bz \end{bmatrix}$$

(Note Δy here has opposite sign to the BIH definition.)

$$\begin{aligned} \Delta Bx &= -\ Bz\ x \\ \Delta By &= Bz\ \Delta y \qquad \text{where } \Delta x, \Delta y \text{ are in radians} \\ \Delta Bz &= Bx\ \Delta x - By\ \Delta y \end{aligned} \tag{3.2}$$

The error in baseline components due to errors in the adopted values of UT are -

$$\begin{bmatrix} \Delta Bx \\ \Delta By \\ \Delta Bz \end{bmatrix} = Rz(\Delta UT) \begin{bmatrix} Bx \\ By \\ Bz \end{bmatrix}$$

$$\begin{aligned} \Delta Bx &= By\ \omega_e\ \Delta UT \qquad \omega_e \cong 7.29 \text{ rads/sec} \\ \Delta By &= -Bx\ \omega_e\ \Delta UT \qquad \Delta UT \text{ in secs.} \\ \Delta Bz &= 0 \end{aligned} \tag{3.3}$$

Both these errors rotate the baselines.

Errors in the primary precession and nutation constants can also be shown to cause errors in the network coordinates which are pure rotations.

Reference clock errors.

VLBI can determine the difference between clock epoch settings but the epoch of one clock has to be held fixed. Any common errors in the epoch settings of the clocks are indistinguishable from corresponding changes in UT. An error in the epoch of the fixed clock will rotate the baseline about the Z axis (as in eqn. 3.3 above). The Z component and the baseline length are not affected.

If the error in clock epoch is less than about 1.4μsecs the error in any component of any baseline, will be less than 1mm. Clock epoch errors are reduced by regular comparison of the station clocks with international time standards. After a clock has been synchronised, by for example a

'clock visit', it will gradually drift off. Depending on the type and quality of the clock the error in clock epoch may be up to a few hundred nanoseconds a week after synchronisation. Therefore, if proper care is taken there should be negligible error in the orientation of a baseline due to clock epoch error.

Dermanis and Grafarend (1980) have shown that an error in the rate of the fixed clock cannot be separated from a scale error in the baseline results. The drift rates of H-masers and Rubidium clocks are generally less than a few parts in 10^{11}. This would cause a corresponding scale error of a few parts in 10^{11} in the baseline results. However this is insignificant when compared to the measuring precisions currently achieved by VLBI.

Effect of holding the coordinates of one site fixed.

An error in the coordinates of the fixed site will have an insignificant effect on the length and orientation of the baselines, unless the coordinates are extremely poor. Such an error causes a translation of the net.

Most of the errors that do not depend on the schedule cause a rotation of the baselines. It needs to be emphasised that the baselines are rotated with respect to the fixed point of the network. The whole network is not rotated with respect to the CTS frame. Rotations are about the axes parallel to the reference axes and passing through the fixed point. As an example let -

$$Bx = X_2 - X_1$$
$$By = Y_2 - Y_1$$
$$Bz = Z_2 - Z_1$$

be the original baseline components between points 1 and 2. Let the rotated points be 1' and 2', and $Rz(\theta)$ be the rotation matrix. If point 1 has been held fixed,
ie. $X1' = X1$, then

$$\begin{bmatrix} X_2' \\ Y_2' \\ Z_2' \end{bmatrix} = \begin{bmatrix} X_1 \\ Y_1 \\ Z_1 \end{bmatrix} + Rz(\Theta) \begin{bmatrix} Bx \\ By \\ Bz \end{bmatrix} \not\in Rz(\Theta) \begin{bmatrix} X_2 \\ Y_2 \\ Z_2 \end{bmatrix}$$

Other errors.

The scale of VLBI baseline vectors is determined by the speed of light, a common drift of the clocks used, atmospheric refraction and constraints on source positions. Until 1975 the speed of light (c) was 299 792 500 m/s. In 1983 it was decided that c would be held fixed at 299 792 458 m/s, the difference represents 0.14 ppm. The metre was redefined as the length of the path travelled by light in a vacuum during the time interval of 1/299792458 of a second. A change in the numerical value of the speed of light affects all baseline components equally.

Thus it can be seen that each of the above error sources can be represented by scale, rotation and translation parameters.

COVARIANCE ANALYSIS OF THE EFFECTS OF SYSTEMATIC ERRORS.

One method of determining the effects of a systematic error (or bias) on the baseline results is to recompute the VLBI solution with the bias parameter held fixed at various values, and compare the results of the numerous solutions. If this procedure is undesirable, because of computing costs, then covariance analysis should be performed instead. This method uses the estimated covariance matrix of the parameters to determine the effect of a bias.

The change in parameter a, Δa, (eg. a coordinate of one site) due to a change in parameter b, Δb, (eg. the tropospheric delay at one site) is calculated from -

$$\Delta a = \sigma_a \rho_{ab} \Delta b / \sigma_b = \sigma_{ab} \Delta b / \sigma^2_b \qquad (3.4)$$

Equation 3.4 is derived from the formula for least squares prediction or filtering (Mikhail, 1976) which calculates the changes in parameters a, b, c, ... n due to changes in

other parameters α, β, γ, ... ω as follows -

$$\begin{bmatrix} \Delta a \\ \Delta b \\ .. \\ \Delta n \end{bmatrix} = \begin{bmatrix} \sigma_{a\alpha} & \sigma_{a\beta} & \sigma_{a\gamma} & \cdots & \sigma_{a\omega} \\ \sigma_{b\alpha} & \sigma_{b\beta} & \sigma_{b\gamma} & \cdots & \sigma_{b\omega} \\ . & . & . & & . \\ \sigma_{n\alpha} & \sigma_{n\beta} & \sigma_{n\gamma} & \cdots & \sigma_{n\omega} \end{bmatrix} \begin{bmatrix} \sigma_\alpha^2 & \sigma_{\alpha\beta} & \sigma_{\alpha\gamma} & \cdots & \sigma_{\alpha\omega} \\ & \sigma_\beta^2 & \sigma_{\beta\gamma} & \cdots & \sigma_{\beta\omega} \\ & & & \cdots & \\ \text{sym} & & & & \sigma_\omega^2 \end{bmatrix}^{-1} \begin{bmatrix} \Delta\alpha \\ \Delta\beta \\ . \\ \Delta\omega \end{bmatrix} \quad (3.5)$$

Or, using the correlation matrix -

$$\begin{bmatrix} \Delta a/\sigma_a \\ \Delta b/\sigma_b \\ . \end{bmatrix} = \begin{bmatrix} \rho_{a\alpha} & \rho_{a\beta} & \rho_{a\gamma} & \cdots \\ \rho_{b\alpha} & \rho_{b\beta} & \rho_{b\gamma} & \cdots \\ . & . & . & \end{bmatrix} \begin{bmatrix} \sigma^2\alpha & \sigma_{\alpha\beta} & \sigma_{\alpha\gamma} & \cdots \\ \sigma_{\alpha\beta} & \sigma^2\beta & \sigma_{\beta\gamma} & \cdots \\ . & . & . & \end{bmatrix}^{-1} \begin{bmatrix} \Delta\alpha/\sigma_\alpha \\ \Delta\beta/\sigma_\beta \\ \Delta\gamma/\sigma_\gamma \end{bmatrix} \quad (3.6)$$

An adjustment of the VLBI data is calculated with the bias terms included as 'solve-for' parameters to generate the required covariance or correlation terms. The matrix to be inverted is that portion of the total VCV matrix of the adjusted parameters representing the bias parameters α to ω. In these calculations it is important to avoid rounding errors that could occur if only the printed output of each of the covariances (or correlations) were used.

SCHEDULE-DEPENDENT ERRORS.

The systematic error sources considered in this section propagate into the baseline results in a manner that depends on the schedule. For example, one experiment may use a schedule designed so that the lowest observed elevation is 10°. Another experiment may use a schedule designed with a minimum elevation of 20°. Obviously any error source that depends on the elevation of observations, such as refraction modelling biases, will have more effect on the results of one of these experiments than on the other. A lower elevation cut off produces better geometric strength and this will be reflected in the VCV of the results. However, the results may be more susceptible to systematic error. The local vertical is the coordinate most sensitive to systematic error, especially those which are elevation angle dependent.

Axis Offset Corrections.

There are three types of antennas: those with a fixed vertical axis (AZEL); those with a fixed axis pointing to the celestial pole (HADEC); and those with a fixed horizontal axis (X-Y). Whilst antennas are of various types their collecting areas (dish) are all symmetric around an axis. On this axis is a point (X in fig. 3.1) near the feed where the phase calibration is injected. This point may be called the electrical centre and it is the point to which the observed delay and rate refer. The electrical centre is not suitable as a reference point because the dish axis moves as the antenna observes in different directions.

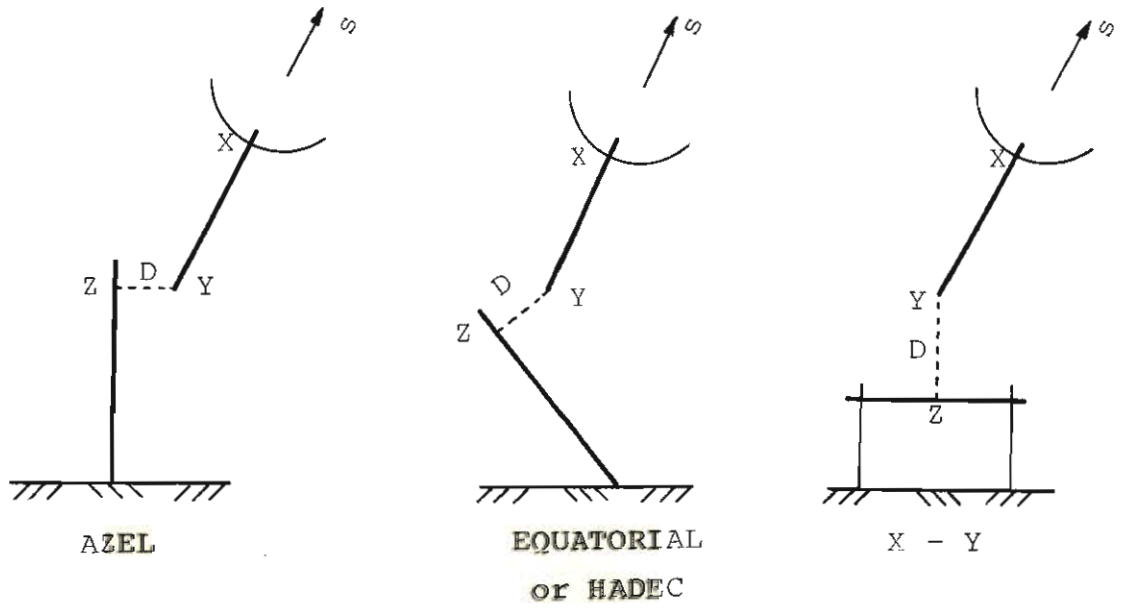

Figure 3.1. Axis Offset Diagrams.

Any point on the fixed axis would be suitable as the reference point. The difference between the direct path to the pivot of the dish axis (Y in fig. 3.1) and the reflected path to the electrical centre will be constant provided instrumental delays are independent of antenna orientation. This difference will be indistinguishable from a clock offset.

If the dish axis and the fixed axis intersect then the

reference point is the point of intersection and no corrections need to be applied to the observables. If the axes do not intersect, the reference point (Z in fig. 3.1) is defined as the intersection of the fixed axis with the plane perpendicular to the fixed axis which contains the moving axis. Some antennas have axis offsets as large as 15m, though offsets larger than about 7m are rare. The path length from Y to Z, at each site, is the correction to delay, given by -

$$A = D \sin\theta$$

where D is the axis offset and θ is the angle between the source direction and the fixed axis. The correction to delay rates is the time derivative of the delay correction -

$$\dot{A} = D \cos\theta \, d\theta/dt$$

It is possible to solve for the axis offset in a VLBI adjustment but θ must be modelled correctly. Since ground measurements of D can be sufficiently accurate it is better to adopt them, thus reducing the number of parameters to be estimated. This in turn leads to an improved solution because extra parameters tend to absorb systematic errors and affect the estimates of parameters with similar signatures.

The elevation angle of the source is corrected for atmospheric bending but the azimuth is assumed to be unaffected by refraction. In any case an error in azimuth has only a second order effect on A and $\dot{A}$.

Errors in A and $\dot{A}$ will be caused by errors in D or in θ, as follows -

$$\Delta A = \sin\theta \, \Delta D + D \cos\theta \, \Delta\theta \quad \text{and}$$

$$\Delta\dot{A} = \cos\theta \, d\theta/dt \, \Delta D - D \sin\theta \, d\theta/dt \, \Delta\theta$$

It is fortunate that errors in θ will have most effect when errors in D have least effect and vice versa.

Since $\sin\theta$ is less than or equal to one, an error of 1mm in D will always cause an error of not more than 1mm (3ps) in A. It will have most effect when θ equals 90°. That is for

horizontal observations with AZEL antennas, observations of equatorial sources for HADEC antennas, and zenith observations for X-Y antennas.

Since $\cos\theta$ is less than or equal to one, and $d\theta/dt$ is less than about 73 μrads/s, an error of 1mm in D will always cause an error of less than 0.0003 ps/s in $\dot{A}$. It will have most effect when θ equals 0^{o}. That is, for observations of polar sources with HADEC antennas, zenith observations for AZEL antennas, and horizontal observations for X-Y antennas. The error in $\dot{A}$ due to errors in D are negligible for X-Y antennas with the fixed axis aligned in the meridian, and for HADEC antennas at low latitudes, because $d\theta/dt$ is very small. Therefore errors of the order of 1mm in D have negligible effect on delays and rates.

Figure 3.2 gives the maximum error in delay due to an error in θ. Clearly, for antennas with offsets of several metres a 10' error in θ, which is about the maximum expected, could cause a 2cm error in A. Errors in θ will have most effect on A when the observed source is parallel to the fixed axis. Errors in θ will have most effect on $\dot{A}$ when the source is perpendicular to the fixed axis.

Errors in θ are caused by an error in inclination of the fixed axis, an error in source position due to refracltive bending, or an inconsistency in the reference frames of the source and fixed axis directions.

If the inclination of the fixed axis is measured to a few arcseconds and entered into the calculations then there will not be a significant error in axis offset corrections. However errors could result if the axis inclination is not measured and assumed to be in its nominal position or the measured inclination is not entered into the adjustment. As shown in Figure 3.2, this inclination needs to be known to better than 40" for antennas with offsets of more than 5m, if the correction to delay is desired to 1mm. For antennas with offsets less than one metre the inclination of the

fixed axis needs to be known to about 3.5'. Accurate measurement of the inclination of the fixed axis is most important for transportable antennas with non-intersecting axes.

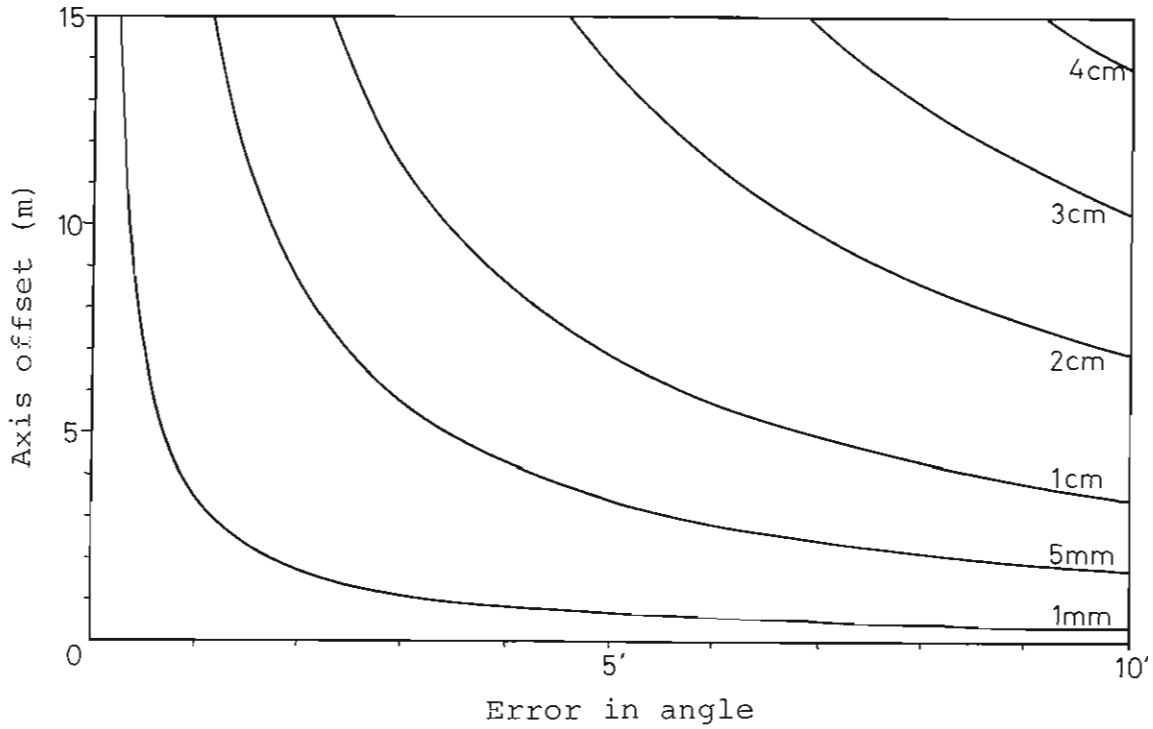

Figure 3.2 Maximum effect of error in angle between source direction and fixed axis.

The magnitude of refractive bending is about 10' at 5° elevation, 5' at 10°, 2.5' at 20°, and 1' at 50°. Most of the bending occurs within the first 10km above the ground, especially in the first kilometre. Thus surface meteorological data is useful in calculating the necessary corrections.

Bending due to the ionosphere is less than 1% of that due to troposphere for signals greater than 2GHz (Crane, 1976) and can be ignored. Current VLBI software either does not correct for refractive bending or, if it does, then does not allow for local atmospheric conditions. Numerous formulae exist for calculating the correction due to atmospheric bending at elevations greater than about 15° (eg. Saastamoinen, 1972). However at elevations below about

10^{o} the magnitude of the bending is very difficult to predict accurately. Comparison of different methods of estimating the bending show that it can be predicted to better than ±20" for elevations above 15^{o}, provided variations in atmospheric conditions are taken into account.

Refractive bending affects low elevation observations the most and therefore must be given special consideration when X-Y antennas and HADEC antennas at low latitudes are involved. Ignoring refractive bending could produce a 4 or 5cm error in delay (at 5^{o} elevation). Ignoring local atmospheric conditions at a site could cause up to 1cm error in delay. Delays measured by HADEC antennas located at high latitudes and AZEL antennas are not significantly affected by errors in refractive bending. For axis offsets less than about 3.4m the maximum error in A is 1mm, and in A is 0.003 ps/s for elevations greater than 5^{o}, and can safely be ignored.

Some radio telescopes cannot be pointed very accurately. However inaccurate pointing will not cause errors in the calculation of the axis offset correction provided the calculations use the direction normal to the wavefronts rather than the direction that the telescope was actually pointed.

Either the astronomic or geodetic site coordinates can be used in the calculation of θ, provided the direction of the fixed axis is given in the same system. Otherwise the deflections of the vertical would have to be taken into account. Depending on the latitude of the site the difference between geocentric and geodetic latitude can be as much as 11'. Since the axis offset corrections use the a priori site coordinates it is necessary that they be reasonably accurate (say a few tens of metres), especially at polar latitudes. If geodetic coordinates are used then the geodetic datum should be aligned to within a few arcseconds of the CTS.

Finally, the errors in delay and delay rate will be a combination of the errors at each site and will vary between the sum and the difference of the errors in the corrections at each site. If observations are well distributed in elevation, then the errors in the baseline components will be less than the maximum error in delay due to offset correction errors. Also, errors in the offset correction will only affect some of the observations which might have large residuals and thus be rejected.

Source position catalogue errors.

If no source positions, other than the obligatory single RA, are constrained then no systematic errors are introduced, apart from the RA origin error discussed above. However, it is often desirable to constrain source positions to independently determined values because the baseline results so determined are more precise and the redundancy of the adjustment improves. Moreover, constraining source positions to reliable values may reveal other systematic errors. On the other hand, if many source positions are estimated they may absorb some other systematic errors.

Several possible systematic errors may exist in source catalogues. Two have already been discussed, namely RA origin and declination pole errors. A constant error in RA or an error in the declination pole does not affect the scale of the baseline results. However if more than one source position is constrained then the scale of the network will be affected by errors in these positions.

Examples of other errors in the source positions are individual errors in individual source positions, errors that arise during the conversion of catalogues from one epoch to another, and errors in the variances of and correlations between the source positions. Errors may also be introduced by using different catalogues for some of the

observed sources. For example all sources above a certain declination may come from one catalogue and all those below it from another. If the two catalogues are not correctly aligned then the differences between the catalogues will distort the results. However as the accuracies of catalogues improves this error source will become less important.

It is now possible to estimate source positions with an uncertainty of a few milli-arcseconds. A 0.001" error in a source position causes about a 2cm error in a 4000km baseline and 2mm on 400km if the source is observed at about 45° elevation. Both the length and direction of the baseline are affected. A covariance analysis should be performed to determine the overall effect of errors in one or more of the constrained source positions.

Correlations between the estimates of source positions are generally ignored when constraining source positions in a VLBI adjustment. If the positions are determined from different experiments and from different networks, then the correlations are likely to be small. Even if the positions are determined from only a few observations in a single experiment, they are unlikely to be correlated by more than 0.5. If the correlations are small they have little effect on the baseline results.

Effects of source structure.

Compact and symmetrically structured extragalactic radio sources are ideal for geodetic measurements. However many sources are large and have a significantly asymmetric structure. The structure of a source can also depend on the wavelength of observation. Therefore dual-wavelength observations, used to correct the effects of ionospheric refraction, may be incorrect. There also appear to be motions of the components within some sources, and changes in the brightness of various components. Both of these effects move the centroid of the source. For example,

Kellerman (1982) shows that the centroid of 3C273, at 10GHz, has moved about 0.003" in the period 1972 to 1980. The apparent shift in the position of the centroid of 3C273 between S and X bands is about 0.004" (Kellerman, 1982). However the alignment of S band and X band structure maps is difficult.

There may be a small apparent change in source position due to source structure. This arises because the observed position will depend on the interferometer resolution if the source has an asymmetric structure. A source is considered to be a point source, ie unresolved, if its angular size is much less than λ/Dt (where λ is the shortest wavelength observed and Dt is the component of the baseline normal to the source direction). The resolution changes because Dt changes as the earth rotates, unless the baseline is parallel to the earth's spin axis. Almost all the sources that have been observed exhibit structure at at least the milli-arcsecond level.

It is generally not possible to observe only unresolved radio sources, particularly on long baselines. So source structure maps are needed to enable corrections to be made to the observations. Unfortunately for many of the sources currently used in geodetic VLBI there are no structure maps at the desired scales, and frequencies over a long time span, or even at any one epoch. The maps can only be obtained by astronomic observations using arrays of radio telescopes. Maps of southern hemisphere sources are particularly rare. The use of Mark III, which is more sensitive and therefore can observe weaker sources, allows a wider choice of sources and therefore the possibility of less structure problems.

Since geodetic measurements involve observations of a number of sources the effect of structure on the final results will be somewhat diluted.

Refraction.

The systematic errors due to refraction and their effect on the baseline results are considered here. This discussion should not be confused with the discussion in Chapter 2 where the effect of errors in the variances of the refraction corrections on the VCV matrix of the corrected delay and delay rate observations was considered.

Errors in scale due to atmospheric refraction are caused by observing at only one frequency band and by systematic errors in the estimate of the tropospheric delay at each site. However neither of these errors produce a uniform scale error and the effect on the baseline components depends on the length of the baseline. The effect is predominantly on the vertical coordinate at each site. Therefore on a short baseline (<1000km) the horizontal components of the baseline are only slightly affected but the vertical component is significantly affected. For example on a 300km baseline a 2cm error in the tropospheric delays (due, say, to a zero error in a barometer) would cause about 0.006 ppm on the horizontal components and 0.15ppm in the vertical component. On long baselines the length is also affected.

Troposphere.

To determine the tropospheric delay, current practice is to determine the dry and wet components separately. The dry zenith component is determined from surface pressure measurements and 'mapped' to the observed elevation. The wet component is determined either 1) by using meteorological models and surface measurements of humidity and temperature to determine the zenith component and then mapped to the observed elevation; or 2) water vapour radiometer measurements are used to determine the wet delay directly. Thus there are a number of sources of error in the determination of the tropospheric delay.

Alternatively, the VLBI data can be used to solve for the tropospheric delays. However this approach is better suited to long baselines measurements. If the sites are only a few hundred kilometres apart only the difference in atmospheric delay between two sites can be reliably estimated. But even then, this estimate may be less accurate than that obtained from surface data and models. Also, for this approach to work well it is necessary that the atmospheric refraction remain constant for long periods of time thus allowing many observations to be used to estimate the atmospheric delay. To help reduce correlations between the parameters and to improve the precision of the baseline length estimate it is necessary to include some observations made at low elevation angles. While observations at low elevation angles reduce the formal errors of the baseline length they also increase the solution's sensitivity to systematic errors in the zenith delay.

The error in a delay measurement due to an error in the estimated zenith delay is approximately equal to the zenith error divided by the sine of the elevation. If the troposphere zenith delay is overestimated, then all delay measurements will be too large and the station position will be depressed from its true position. In a VLBI adjustment it is always necessary to solve for at least one clock offset and one clock rate difference. These parameters will absorb some of the error in the troposphere delay. Accordingly, the residuals, even if plotted as a function of elevation, may not reveal any systematic trends due to a zenith delay bias.

Errors in surface meteorological measurements cause zenith delay errors, as follows: 1) An error of 2-3°C in temperature causes only 1mm error in zenith delay, 2) an error of 1mb in pressure causes 2mm error in zenith delay, and 3) an error of 1mb in partial pressure causes 10mm error in zenith delay. An aspiration psychrometer can measure the partial vapour pressure at a site to about $\pm$ 0.3mb. This is better than can be achieved with

hygrometers. If the barometer is not at the same height as the antenna axis then a correction needs to be applied to the pressure readings. An error in the height difference of 1m would cause an error of about 0.1mb, which is negligible. However if the height difference is large and the measured pressures are not corrected, then the error is significant.

Errors are also caused by inaccuracies in the atmospheric models and the elevation mapping function, especially those representing the wet component. They will probably have most effect on lower elevation observations. These errors are presently being investigated by Herring and Davis (priv. comm. 1984) and Lanyi (1984).

Propagation of troposphere bias error.

When the tropospheric correction is determined from surface meteorology and water vapour radiometers, an error in the zenith delay will manifest as an error in the vertical component of the baseline and will be amplified by a factor. However the effect of errors in the troposphere delay on baseline components depends on the length of the baseline being considered. On baselines a few 100km long this amplification factor is about 2.5 when the minimum observed elevation angle is 15^{o}, and about 2 when the minimum elevation angle is 30^{o}. If the observations are symmetrically distributed in azimuth there will be no significant effect on the baseline length or azimuth. If the observations are not symmetrically distributed in azimuth then the length of a baseline will also be in error. So, on long baselines where the observations are not symmetrically distributed in azimuth because of the restrictions of mutual visibility, both the baseline length and direction are in error.

The propagation of troposphere bias error into baseline results varies from one experiment schedule to the next. The effect of errors at each of the various sites, on all

the baselines have to be considered. So the notion that lengths and transverse baseline components are barely affected and that heights are affected by about twice the bias is an approximation that may not be adequate. A more rigorous approach is to use covariance analysis to determine the true propagation characteristics for each particular experiment. In this case it is necessary to include tropospheric bias terms as solve-for parameters in the VLBI adjustment. Alternatively, a reliable estimate of the effect of a zenith delay bias can be obtained by recomputing the VLBI solution with the input atmospheric data perturbed by known amounts and examining the effect on the results.

It is expected that a single bias per site per experiment would be used, though more terms could be included if desired. Fluctuations in the error in the troposphere corrections would affect the residuals and would thus be reflected in the VCV of the results. A single bias would not affect the VCV of the results.

An example of the effect of tropospheric biases on site coordinates for a simulated Tidbinbilla - Parkes - Fleurs experiment follows.

$$\begin{bmatrix} \Delta Xp \\ \Delta Yp \\ \Delta Zp \\ \Delta Xf \\ \Delta Yf \\ \Delta Zf \end{bmatrix} = K \begin{bmatrix} TBt \\ TBp \\ TBf \end{bmatrix} \quad (3.8) \qquad \text{and} \qquad \begin{bmatrix} \Delta \emptyset p \\ \Delta \lambda p \\ \Delta hp \\ \Delta \emptyset f \\ \Delta \lambda f \\ \Delta hf \end{bmatrix} = L \begin{bmatrix} TBt \\ TBp \\ TBf \end{bmatrix} \quad (3.9)$$

$$\text{Where } K = \begin{bmatrix} -1.33 & 1.36 & 0 \\ 0.79 & -0.83 & 0 \\ -1.12 & 1.05 & 0 \\ -1.33 & 0 & 1.39 \\ 0.79 & 0 & -0.76 \\ -1.12 & 0 & 1.08 \end{bmatrix} \quad \text{and } L = \begin{bmatrix} -1.6E\text{-}8 & 1.9E\text{-}9 & 0 \\ 5.1E\text{-}9 & -9.E\text{-}10 & 0 \\ 1.91 & -1.91 & 0 \\ -1.2E\text{-}8 & 0 & 2.2E\text{-}9 \\ -7.7E\text{-}9 & 0 & -4.1E\text{-}9 \\ 1.91 & 0 & -1.92 \end{bmatrix}$$

where TBi are the tropospheric biases at each site and ΔX are the corresponding changes in the site coordinates. Note

that the site coordinates need not be in a Cartesian frame. If there are n sites each with one bias term, then ΔX will have 3n-3 terms, K or L will be (3n-3,n), and TB will have n terms.

Naturally the coordinates of the fixed site are not affected but a tropospheric bias at the fixed site will affect the coordinates of all other sites and the components of all baselines from the fixed site. A tropospheric bias at a non-fixed site changes only the coordinates of that site and the components of all baselines radiating from it. The terms in K or L refer to a particular experiment, though they should not vary much from one experiment to another provided the same sites and similar schedules are used. The terms in K are usually needed to only three or four significant figures and some of them will equal zero.

Equations 3.8 and 3.9 are linear approximations that are valid only when the TBi are small, that is when the a priori atmospheric corrections are reliable. Though it is difficult to quantify how small the TBi need to be as the validity depends on the sensitivity of the VLBI solution to tropospheric bias error. Moreover, this method assumes that an accurate elevation mapping function has been applied in the VLBI program. The application of this procedure to the combination of VLBI results with either independent data or other VLBI data will be elaborated in Chapter 7.

Ionosphere.

Measurements made at S and X bands each generate delays and rates. The ionosphere corrected delays and rates are calculated from these S and X observations and no other information is required. Shapiro (1983) reports on an experiment designed to test the dual frequency (S/X) ionosphere correction. Both phase and group delays were obtained at each frequency, so the ionospheric correction could be determined from both the phase and the group

delays. However, the two estimates showed systematic differences, of the order of one centimetre, which have not yet been explained. This error source will not be considered in this thesis because it is smaller than other error sources.

Unfortunately, VLBI measurements are sometimes made at only one frequency. This can produce large errors in the results, especially on long E-W baselines. Observations not corrected for ionospheric refraction produce baseline lengths which are too long. To minimise the effect of the ionosphere when observing at only one frequency, it is better to observe only at night because the ionospheric effect is much smaller then. However this reduces the number of observations. X band observations are less affected than S band observations, but some antennas are not able to observe at frequencies higher than S band. Attempts to estimate the ionospheric correction to observations of one band only with ionosonde or Faraday rotation data and appropriate models have, so far, been unsuccessful. Moreover, the correction to baseline length as determined for one baseline cannot be applied as a correction to other baselines because of the different orientations of the baselines and the different ionospheric conditions above each site.

Examples of the effects of ionosphere error on baseline results are given in Chapter 4. Generally the vertical component is most affected. This is similar, but not identical, to tropospheric errors. Thus estimates of one may be corrupted by the effects of the other. But the effects of ionospheric error are usually larger than those due to tropospheric bias. If the effect of the ionospheric error on the baseline results is small compared to the precision of the baseline components and the uncertainties of the ground data, then this effect can be ignored and the two data sets combined. Otherwise only results based on dual frequency data should be combined with ground data.

Other errors.

Earth Tides and Ocean loading.

The Earth is subject to the gravitational forces of the Sun and Moon which produce the tides of the oceans and the earth tides. The Earth's crust is also deformed by the load of the varying ocean tide. Scherneck (1983) has computed the displacements due to ocean loading at three sites, including Tidbinbilla. He claims the displacements range between 1cm and 3cm and, with appropriate procedures, can be estimated with millimetre uncertainty. In Chapter 4 an example is given which shows the error in the baseline results due to errors in the earth tide parameters to be less than a few millimetres.

Subjective bias.

The propagation of subjective biases into the baseline results depends on the schedule, the analyst, and the data quality and quantity. A discussion of the effects of subjective biases on the baseline results of the Australian VLBI experiment is given in Chapter 4. Robertson (1975) also discusses the effect. Apart from attempting to minimise the effects of subjective bias little can be done to actually model its effect, or to suitably enlarge the terms of the VCV of the geodetic results.

CHAPTER 4.

RESULTS OF THE AUSTRALIAN GEODETIC VLBI EXPERIMENT.

VLBI IN AUSTRALIA.

VLBI experiments between Tidbinbilla, near Canberra, and Island Lagoon, near Woomera South Australia, commenced in 1967 (Robertson et al., 1967). Further experiments followed including Goldstone, California and Hartebeesthoek, South Africa. In 1971 JPL commenced VLBI experiments to establish the baselines between Tidbinbilla, Goldstone and Madrid, Spain, for astrometry, and for studies of the earth's motion (Fanselow et al., 1984). The Island Lagoon site ceased VLBI observations in 1972 and was subsequently dismantled (Gubbay, 1977). In these experiments only a single narrow S band channel was recorded. Consequently the Z components of baselines were determined to an accuracy of only about 30m (Gubbay, 1978). Since 1977 experiments between Tidbinbilla and Goldstone have continued using the Mark II BWS S/X system. Since 1980 there have been a few single channel S band experiments involving Parkes, Tidbinbilla and Hartebeesthoek. The experiment reported below was conducted in early 1982 and has been the only VLBI experiment to directly observe baselines within Australia for geodetic purposes.

In the Australian Geodetic VLBI Experiment the 250-2500km baseline vectors between five radio telescopes were determined from observations made on April 26, April 28 and May 3, 1982. The telescopes were sited at the NASA Deep Space tracking facility at Tidbinbilla (DSS43), the CSIRO Radio Observatory at Parkes, the University of Tasmania's Radio Observatory near Hobart, the University of Sydney's Fleurs Observatory near Sydney (X3), and the LANDSAT tracking station at Alice Springs (Fig. 4.1). The Tidbinbilla and Parkes telescopes have 64m diameter dishes, Fleurs and Hobart have 13.7m diameter dishes, and Alice Springs has a 9.1m diameter dish.

Figure 4.1 Locations of antennas used in the Australian Geodetic VLBI Experiment.

The experiment was designed principally to provide high-resolution maps of distant quasars and galaxies. However, it also provided a means of making accurate geodetic measurements. The goals of the geodesy part of the experiment were: (1) to measure the Parkes-Tidbinbilla baseline with an accuracy of 10cm for the horizontal components of position and 15cm for the vertical component, (2) to measure the baselines from Parkes and Tidbinbilla to Fleurs with accuracies of 15cm for the horizontal components and 30cm for the vertical component, and (3) to measure the Tidbinbilla - Hobart and Tidbinbilla - Alice Springs baselines with an accuracy of 1-2m for all three components. The results obtained indicate that the first two goals were achieved. The estimated accuracies of the measured baseline lengths and components range from 7cm to 5m. The higher accuracies were achieved for the better instrumented sites of Tidbinbilla and Parkes.

EXPERIMENT DESCRIPTION.

The antennas at Fleurs, Hobart and Alice Springs observed at S band, while those at Tidbinbilla and Parkes observed at both X and S band. The Tidbinbilla station was equipped with a Hydrogen maser frequency standard and one was installed at Parkes especially for the experiment. All other sites were equipped with Rubidium frequency standards. Water Vapour Radiometers were not available at any of the sites and phase calibration could only be carried out at Tidbinbilla. Tidbinbilla, Parkes and Fleurs were instrumented with BWS equipment to improve the accuracy of the VLBI observables. The Mark II recording system was used. In this system a spanned bandwidth of 40MHz was synthesized by sequential switching between two frequency channels. A single 2MHz frequency channel was recorded at Hobart and Alice Springs.

Observations at Tidbinbilla and Parkes were made at both S and X bands and spanned two 24 hour periods (26 April and 3 May). During the nights of 26 April and 3 May Fleurs was to observe at S band (with BWS) and both Hobart and Alice Springs were to observe at a single S band frequency. No observations were successful at Fleurs on 3 May. The Hobart antenna moved too slowly to observe all the scheduled sources and those observed were spread over less than half of the sky. One additional 12 hour night-time session with all five stations participating at S-band was observed on 28 April. The Parkes maser failed during this time so a Rubidium frequency standard was used. The maser was back in operation on 3 May. Temperature, pressure and humidity readings were taken at regular intervals during the experiment.

The 25 radio sources listed in Table 4.1 were observed. The positions of 17 of these had been determined previously (J. Fanselow, pers. comm. 1982). All of the eight new sources were south of -45° declination. The signals from Circinus X-1 and Vela were too weak and were not

successfully observed. Each radio source was observed for 10 minutes when all sites were observing, or 4 minutes when only Tidbinbilla and Parkes were observing. The time spent slewing between sources was governed by Fleurs, the slowest antenna apart from Hobart. Thus during a 12 hour session about 40 observations were made.

Table 4.1. Approximate positions of the sources observed.

Source	Other name	RA (1950)	dec (1950)	RA (2000)	dec (2000)
		h m s	o ' "	h m s	o ' "
0208-512		2 08 57.0	-51 15 08	2 10 46.2	-51 01 02
0235+164	OD 160	2 35 52.6	16 24 04	2 38 38.9	16 36 59
0430+05	3C 120	4 30 31.6	05 15 00	4 33 11.1	5 21 16
0438-436		4 38 43.2	-43 38 53	4 40 17.2	-43 33 09
0537-441		5 37 21.0	-44 06 45	5 38 50.4	-44 05 09
0605-085		6 05 36.0	-08 34 20	6 07 59.7	-08 34 50
0637-752		6 37 23.3	-75 13 38	6 35 46.5	-75 16 17
0743-673		7 43 22.2	-67 19 08	7 43 31.5	-67 26 26
0835-450	VELA	8 35 39.3	-45 00 11	8 35 20.6	-45 10 37
0851+202	OJ 287	8 51 57.2	20 17 59	8 54 48.9	20 06 31
1104-445		11 04 50.4	-44 32 53	11 07 08.7	-44 49 08
1127-145		11 27 35.7	-14 32 53	11 30 07.1	-14 49 27
1226+023	3C 273	12 26 33.2	02 19 43	12 29 06.7	02 03 09
1253-055	3C 279	12 53 35.8	-05 31 08	12 56 11.2	-05 47 22
1502+106	OR 103	15 02 00.2	10 41 18	15 04 25.0	10 29 39
1510-089		15 10 08.9	-08 54 48	15 12 50.5	-09 06 00
1519-571	CIR X-1	15 19 17.4	-57 06 50	15 23 10.9	-57 17 30
1610-771		16 10 51.5	-77 09 53	16 17 49.3	-77 17 18
1730-130	NRAO 530	17 30 13.6	-13 02 46	17 33 02.7	-13 04 50
1921-293	OV-236	19 21 42.3	-29 20 26	19 24 51.1	-29 14 30
1934-638		19 34 47.5	-63 49 38	19 39 25.0	-63 42 46
2134+004	OX 057	21 34 05.2	00 28 25	21 36 38.6	00 41 54
2251+158	3C 454.3	22 51 29.5	15 52 54	22 53 57.7	16 08 54
2326-477		23 26 33.7	-47 46 51	23 29 17.7	-47 30 19
2345-167	OZ-176	23 45 27.7	-16 47 52	23 48 02.6	-16 31 12

DATA REDUCTION.

After the experiment the video tapes, on which the data were recorded at each station, were brought together for digital cross-correlation on the Mark II VLBI Processor at the California Institute of Technology (Thomas, 1981). The resulting post-correlation computer tapes, containing the highly compressed data were then processed further at JPL by the author. The delay model, phase model, phase tracking and BWS techniques used in the experiment are described by Thomas (1981), and will not be presented in detail here.

To obtain the baseline vectors, the delay and delay rate observables were adjusted by least squares using appropriate models. These models comprise principally a geometric delay, instrumental delays, and transmission media delays. In this experiment uncertainties in the geometric delay due to errors in the earth orientation parameters (polar motion, UT1, precession, and nutation) were small in comparison with other errors as discussed below. That is, these parameters have been obtained with sufficient accuracy by independent measurements so that they could be treated as known quantities. Therefore, only the components of the baselines and the source positions were regarded as unknown (or 'solve for') parameters in the geometric delay.

The instrumental delay can, in the ideal case, be modelled by a series of constant (clock offset, synchronization errors) and linear drift (clock rate difference) terms, but often a more complicated form is necessary to account for frequency oscillator instabilities. In this experiment the clock terms were estimated at all sites except Tidbinbilla.

The transmission media (ionosphere and troposphere) delays could not be reliably estimated from the data. On the short baselines the atmospheric delay at each site is highly correlated, on the long baselines other errors dominate. S and X band data, where available, were used to correct for

the effect of the ionosphere and appropriate models and meteorological data (see below) were used to correct for the troposphere refraction.

A cylindrical reference coordinate system with axes parallel to those of the CTS was adopted in this experiment. In VLBI cylindrical coordinates typically have smaller correlations than Cartesian coordinates. The coordinates of Tidbinbilla were held fixed to define the origin of the reference system and to relate the measurements to the global network of VLBI stations. These coordinates were derived from VLBI measurements to the DSN Goldstone site in California. Any future improvement in the absolute coordinates of Tidbinbilla (DSS 43) could be applied simply and directly as a shift to the coordinates of all the other Australian sites.

Initially, each observation was weighted according to system noise. However this produced residuals which were larger than could reasonably be expected. The original error estimates were then increased using the conventional method (sigcons), outlined in Chapter 2.

The results were obtained in three steps because some of the measurements were at S band only and would thus give distorted results. In the first step the three components of the Tidbinbilla - Parkes baseline, 11 clock parameters, and 45 source coordinates were estimated from 145 delay and 145 delay rate observations. Other variables eg. atmosphere, polar motion and UT, and earth tides were not estimated. The S band Rubidium data acquired on 28 April and observations of Vela (S band only) were not included. The RA of radio source 3C273 was held fixed at $12^h\ 26^m\ 33.2792^s$ (epoch 1950.0) to refer the source positions to the dynamical equinox (Fricke, 1981). The error in the corrected RA origin is about ± 0.005s. This produces errors in the site coordinates which are included with 'other errors' in Figure 4.2. The positions of all other sources were solved for. However those sources whose

positions are given in JPL catalogue 1982D4.BAR (J. Fanselow, priv. comm. 1982) were assigned a weight equivalent to their estimated one sigma accuracy (±0.03"). Covariance terms were ignored.

In the second step the three coordinates of Fleurs and 18 clock parameters were estimated from the 185 delay and 185 delay rate S band (BWS) observations acquired at Tidbinbilla, Parkes and Fleurs on 26 and 28 April. The S band data from Tidbinbilla - Parkes on 26 and 28 April was included to strengthen the solution of Parkes clock parameters. The coordinates of Parkes, the catalogue source positions, and the positions for the new sources, as obtained above, were held fixed.

In the third step the six coordinates of Alice Springs and Hobart and 23 clock parameters were estimated from the 217 delay and 217 delay rate S band (single channel) observations made at Tidbinbilla, Parkes, Hobart and Alice Springs on 26 and 28 April and 3 May. The coordinates of Tidbinbilla, Parkes, the catalogue source positions, and the positions for the new sources, as obtained above, were held fixed.

RESULTS.

The baseline measurements and their formal errors are summarised in Tables 4.2 and 4.3. As expected, the most precise measurement was the distance from Tidbinbilla to Parkes (3cm or 0.1ppm). The remaining distances are all precise to better than 0.7ppm except those to Hobart which are precise to about 4ppm.

The accuracy of the results was estimated by solving for the baselines, the source positions and clock terms from portions of the data, by estimating the effect on the results of errors in the parameters treated as known, and by estimating the effect of subjective aspects of the analysis. These results are presented in Figure 4.2.

Table 4.2. Site coordinates

Site	R, m	λ, deg*	Z, m
T	5205 251.365	148.981 279 10	-3674 748.367
P	5354 918.850 ± .047	148.263 526 19 [± .018]	-3454 035.798 ± .047
F	5302 029.34 ± .19	150.763 759 9 [±.063]	-3533 527.69 ± .14
A	5841 280.8 ± 0.8	133.882 357 [± 0.9]	-2554 104.9 ± 2.0
H	4683 738.3 ± 1.1	147.512 08 [± 1.4]	-4314 838.7 ± 4.5

R - Distance from the Z axis.

λ - Longitude from the Greenwich meridian.

Z - Distance from the equatorial plane.

T - Tidbinbilla, P - Parkes, F - Fleurs, A - Alice Springs, H - Hobart

* The formal precisions in longitude are in metres.

Table 4.3. Baseline Measurements and Comparisons with Survey.

Baseline	VLBI	SURVEY	DIFF.	
	m	m	m	ppm
Tidbin.- Parkes	274 751.784 ± 0.031	274 751.9 ± 0.2	-0.12	-0.4
Tidbin.- Fleurs	236 681.188 ± 0.068	236 681.00 ± 0.13	0.19	0.8
Parkes - Fleurs	251 340.465 ± 0.065	251 340.8 ± 0.2	-0.34	-1.2
Tidbin.- Alice	1938 997.1 ± 1.3	1938 994.7 ± 0.9	2.4	1.2
Tidbin.- Hobart	835 297.0 ± 3.6	835 298.4 ± 0.5	-1.4	-1.6
Parkes - Alice	1733 991.1 ± 1.2	1733 989.6 ± 0.9	1.5	0.9
Parkes - Hobart	1093 516.8 ± 3.7	1093 518.8 ± 0.6	-2.0	-1.8
Hobart - Alice	2445 610.4 ± 3.0*	2445 610.5 ± 1.2	-0.1	0.0
Fleurs - Hobart	1035 709.1 ± 3.7*	1035 710.5 ± 0.6	-1.4	-1.4
Fleurs - Alice	1979 707.5 ± 1.3*	1979 706.5 ± 1.0	1.0	0.5

* These baselines were not observed directly because the SNR was too low.

Degrees of freedom.

In a standard least squares adjustment, with no a priori weights on the parameters, the a posteriori variance factor ($\tilde{\sigma}_o^2$) is found from -

$$\tilde{\sigma}_o^2 = (V^T P V) / \mu \qquad (4.1)$$

where μ is the degree of freedom in the adjustment and equals the number of observations minus the number of

parameters.

In a Bayesian-type least squares adjustment, where a priori weights are assigned to the parameters, $\tilde{\sigma}_0^2$ is found from (Krakiwsky, 1981) -

$$\tilde{\sigma}_0^2 = (V^T P V + \Delta X^T P_x \Delta X) / \mu \qquad (4.2)$$

where μ = number of observations
- number of parameters without a priori weights

This is an approximate formula that works best when μ is large. When μ is small a slight error in μ will cause significant errors in $\tilde{\sigma}_0^2$. For example, when the number of degrees of freedom in a solution is less than 10, an error of one (in the number of degrees of freedom) causes more than 11% error in $\tilde{\sigma}_0^2$. Another problem is the magnitude of the a priori weight of a parameter. If the weight is large (that is small variance), then the parameter estimate is obviously affected by this weight. If the weight is small then it may not have much affect on the solution and would give a misleading value of μ. In such a case the analyst may chose to regard parameters with small weights as not weighted for the purposes of calculating μ and $\tilde{\sigma}_0^2$. Then the problem of determining whether a parameter is significantly weighted or not, arises. Again this problem is not so critical when there are many more observations than parameters, ie μ is large. Bossler (1972) presents a procedure to overcome this problem and give more accurate estimates of μ and of $\tilde{\sigma}_0^2$. The procedure to be used with weighted parameter solutions is outlined below.

1) Compute a value of $\tilde{\sigma}_0^2$ ($\tilde{\sigma}_0^2 f$)from a solution with no weights on the parameters. Using (see page 114) -

$$V = -(A \Delta X + W)$$

$$\Delta X = -(A^T P A)^{-1} A^T P W$$

$$\tilde{\sigma}_{0_f}^2 = V^T P V / (\text{no. of obs.} - \text{no. of parameters}) \qquad (4.3)$$

2) Multiply the VCV of the observation by $\tilde{\sigma}_0^2 f$.

3) Compute ΔX and V from a solution with weighted parameters. (The required formulae are given on page 114.)

4) Compute μ', the number of unweighted parameters, from the following formula.

$$\mu' = tr\{ \frac{1}{\tilde{\sigma}^2_{of}} A^T P A (\frac{1}{\tilde{\sigma}^2_{of}} A^T P A + P_x)^{-1} \} \qquad (4.4)$$

$$= tr\{ A^T P_t A (A^T P_t A + P_x)^{-1} \}$$

where P is the inverse of the original VCV of the observations and P_t is the inverse of the new (by step 2) VCV of the observations. Note that μ' is not necessarily an integer. Therefore the degrees of freedom in the adjustment, which is the number of observations minus μ', is not necessarily an integer.

5) Compute the final $\tilde{\sigma}^2_o$ from -

$$\tilde{\sigma}^2_o = \frac{V^T P_t V + \Delta X^T P_x \Delta X}{\text{number of observations} - \mu'} \qquad (4.5)$$

6) Compute the share of $\tilde{\sigma}^2_o$ due to the VCV of the observations, Ωs, and the share of $\tilde{\sigma}^2_o$ due to the a priori weights of the parameters, Ωp.

$$\Omega s = \mu' / \text{number of parameters} \qquad (4.6)$$

$$\Omega p = 1 - \Omega s$$

This procedure was applied to the analysis of the data obtained in the Australian VLBI experiment. The Tidbinbilla - Parkes solution involved 33 source coordinates with a priori standard deviations of ±0.03", 12 other source coordinates with zero a priori weight, and 14 other parameters with zero a priori weight. There were a total of 59 parameters and 290 observations. The above procedure was followed and it was found that the number of weighted parameters was 33, thus showing that a standard deviation of ±0.03" is a significant weight, in this experiment. It was also found that the share of the $\tilde{\sigma}^2_o$ due to the variances of the observations was 57% and the share due to the weights of the parameters was 43%. Thus the a priori weights of the parameters do have a significant effect on the estimated variance factor.

ACCURACY ESTIMATES.

A number of parameters were held fixed in the solutions so likely errors caused by them have to be considered. The effects of these error sources on the accuracy of the results are considered below. The error estimates are then compared with the precisions as estimated by the least squares adjustment of the data.

Unless stated otherwise, accuracy estimates apply to the first solution, that is the Tidbinbilla - Parkes baseline with S/X data. For the other baselines the systematic errors are small when compared to the large formal errors, as shown in Figure 4.2.

Independent solutions.

To estimate the repeatability of the various solutions the data sets were subdivided and separate solutions obtained. These separate solutions have lower redundancy than the overall solution and so the effects of subjective errors are increased. However the differences from the results given in Table 4.2 do indicate the likely repeatability of the solutions.

The Parkes-Tidbinbilla data were partitioned as follows- 26 April, 3 May, day-time only, and night-time only. The April 26 solution had 53 parameters and 136 observations, the May 3 solution had 50 parameters and 154 observations. The coordinates of Fleurs were also determined on two independent days. The Fleurs data were partitioned into that observed on 26 April and that on 28 April. The Alice Springs and Hobart data were partitioned into that observed on 26 April and 28 April and that gathered on 28 April and 3 May. The results are summarised in Table 4.4. The lengths agree to better than twice their formal error. The site coordinates agree to better than three times their formal error except the Parkes longitude for the day-time solution. Radio source 3C273 could not be observed at day-

time and another source was chosen as the origin of right ascension. This accounts for a significant portion of the latter discrepancy.

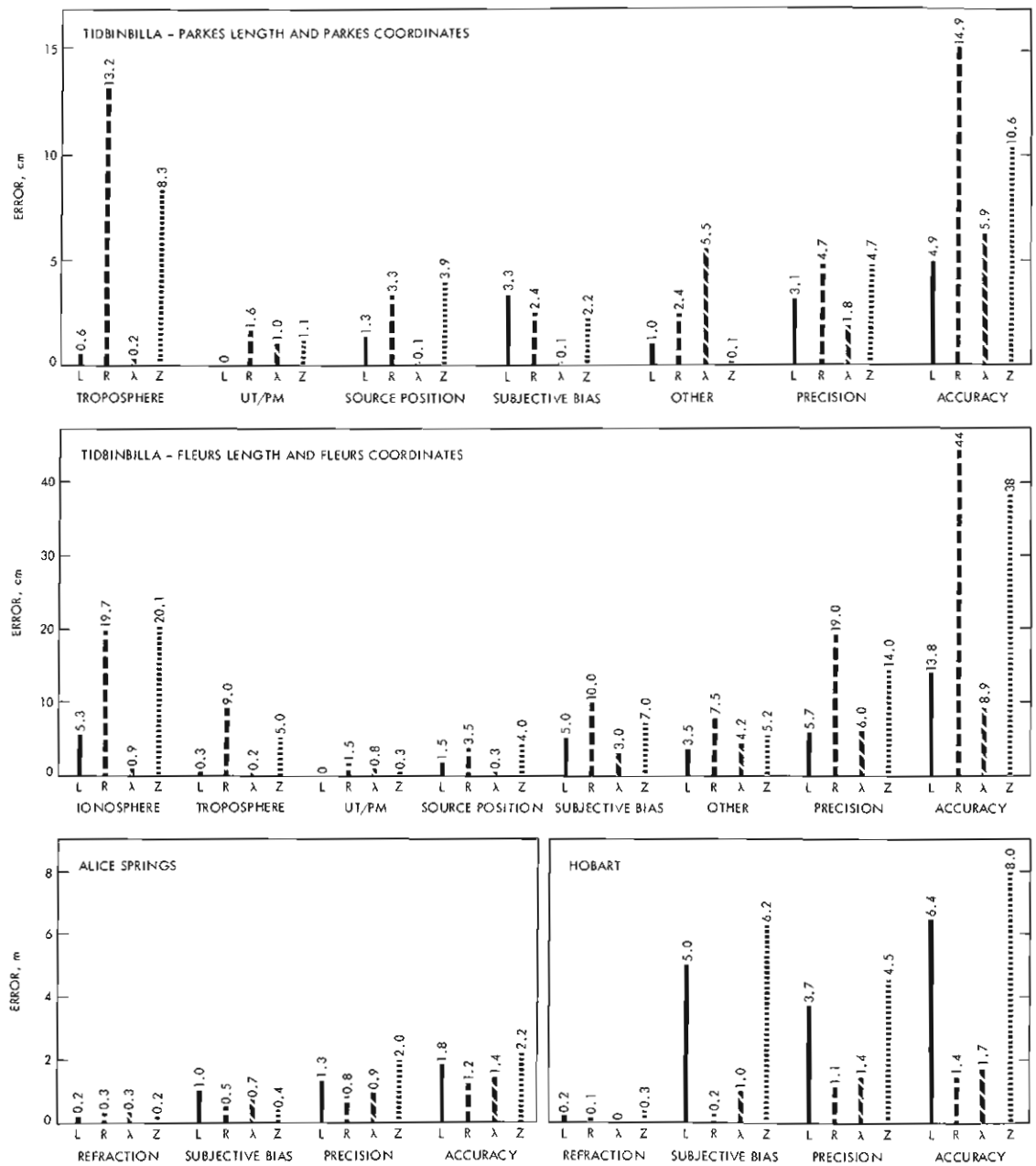

Figure 4.2 Error Budgets for baseline lengths and site coordinates.

(L is the baseline length, R, λ, and Z are the cylindrical site coordinates.)

Table 4.4. Repeatability.
Difference of individual solutions from the results in Tables 4.2 and 4.3.

(a) Lengths (m)					
Baseline	26 April	28 April	3 May	Night	Day
Tidbin. - Parkes	0.038		0.049	0.029	0.009
Tidbin. - Fleurs	0.027	0.035			
Parkes - Fleurs	0.029	0.058			
		26 & 28 April	28 April & 3 May		
Tidbinbilla - Hobart		+1.1	-4.1		
Tidbinbilla - Alice Sp.		0.0	+0.6		
Parkes - Hobart		+1.1	-4.0		
Parkes - Alice Springs		0.0	+0.6		

(b) Coordinates (m)					
	26 April	28 April	3 May	Night	Day*
Parkes R	-0.054		-0.095	0.000	0.137
Parkes λ	0.009		0.017	0.061	0.092
Parkes Z	0.014		0.001	0.018	0.078
Fleurs R	0.37	0.43			
Fleurs λ	0.01	0.02			
Fleurs Z	0.31	0.38			
		26 & 28 April	28 April & 3 May		
Alice Springs R		+1.0	-0.3		
Alice Springs λ		-0.1	-0.4		
Alice Springs Z		-0.8	+0.8		
Hobart R		+1.6	-0.3		
Hobart λ		-1.5	+2.0		
Hobart Z		-2.6	+5.1		

* Most of this discrepancy is due to a change in RA origin.

Ionosphere.

To minimise the effect of the ionosphere, Fleurs, Hobart and Alice Springs only observed at night when the ionospheric effect is much smaller. This procedure reduces the number of observations on these baselines. The baseline from Tidbinbilla to Parkes should not be significantly

affected by ionospheric refraction.

The differences between the results obtained from two Tidbinbilla-Parkes solutions were used to estimate the effect of the ionosphere on the Tidbinbilla-Fleurs and Parkes-Fleurs results. One solution used S/X band night-time observations and the other solution used only S band night-time observations. In both solutions all source positions were held fixed and the same parameters were estimated. As expected the S band solution produced a longer baseline. There was also a significant increase in formal errors and RMS of the residuals in the S band solution. The difference in the Tidbinbilla-Parkes lengths so obtained was 5cm (see Table 4.5a). This difference cannot be applied as a correction to the Fleurs' baselines because of the different orientations of the baselines and the different ionospheric conditions at Fleurs. But the difference does imply that the baselines Tidbinbilla-Fleurs and Parkes-Fleurs are about 5cm too long. The formal errors of the results are also larger than they would be if ionospheric effects could be reduced.

The Tidbinbilla-Parkes solution which used only S/X night-time data was compared with the overall solution (Table 4.5b). So the combined effect of only observing S band and of observing for a shorter time is indicated by the differences between the S band night solution and the overall solution (Table 4.5c).

Table 4.5 Effects of systematic ionospheric errors on the Tidbinbilla - Parkes baseline.

Comparison of solutions	Differences in cm. Length	R	λ	Z
a) Snight-S/Xnight	5.3	19.7	0.9	20.1
b) S/Xnight-S/Xall	2.9	0.0	6.1	1.8
c) Snight-S/Xall	8.2	19.7	5.3	21.9

Earth tides.

The results reported in this chapter were obtained by holding the Love numbers (h and l) and the solid earth tide phase lag fixed at 0.610, 0.085 and 0.0 respectively. Separate attempts were also made to estimate these parameters. In these separate solutions the estimated formal errors of the tidal parameters were larger than the accuracy of their a priori values. A covariance analysis showed that plausible systematic errors of 0.05, 0.03 and 2^{o} in h, l and phase lag respectively, produce errors of less than 1mm in the Tidbinbilla-Parkes baseline length and components.

Neutral atmosphere.

Refraction in the neutral atmosphere was estimated from models and surface meteorological data (pressure, temperature and relative humidity). Typical errors in these measurements would produce less than 1cm error in zenith path delay at each site, if the models are accurate.

Three models Chao (Chao, 1973), Callahan (Callahan, 1973), and Berman D/N (Berman, 1976) were used to estimate the wet delay at each site. During daytime the difference between Chao and Berman in zenith wet delay was less than 1cm, but at night the difference was constantly about 3cm. Chao's model has been used here because it does not produce a step in the wet delay estimates. In this experiment the minimum observed elevation was about 30^{o} because of a construction limit of the Parkes telescope. At 30^{o} the atmospheric delay is about twice the zenith delay, its associated error is also increased.

The results given in Table 4.2 were obtained from a solution which used hourly estimates of the atmospheric delay at each site as input data. The typical scatter of the hourly zenith delays from the mean delay for each day at each site was ±1cm. So an alternative solution which

used the mean atmospheric delays was computed. This solution gave differences of 3mm in length, 1mm, 5mm, and 4mm in R, λ, and Z coordinates at Parkes when compared with the original solution. In another solution an attempt was made to solve for one atmospheric delay per site per day. However the formal errors for the estimated zenith delays were about 48cm and the correlation between the atmospheric delays at the two sites was 0.98. A further solution was attempted where one value of atmospheric delay per day at Parkes was estimated and the a priori values at Tidbinbilla held fixed. The estimated precisions of the tropospheric delays were about 8cm, which is still larger than the estimated accuracy of surface meteorological measurement and model estimates, of about 5cm. So in this experiment it is not possible to estimate the atmospheric corrections from the VLBI data as well as can be determined by surface meteorological measurement and model estimates.

Covariance analysis showed that a 5cm systematic error in atmospheric delay at one site and on one day produced a 4mm error in the Tidbinbilla-Parkes baseline length. However the effect on the baseline components is significant (Figure 4.2). For example, the height of Parkes would be in error by about 10cm but the azimuth from Tidbinbilla to Parkes would not be significantly affected.

Polar motion and UT1.

BIH values of polar motion and UT variations were used as the a priori values in the analysis. The effects of errors in these values on the baseline results were calculated from equations 3.2 and 3.3, but modified to give errors in R and λ instead of in X and Y. Errors in polar motion and UT1 do not affect baseline length, they do however affect baseline orientation and site coordinates. Typical errors of 30cm, 30cm, and 0.001sec in the adopted BIH values for x, y, and UT1 caused errors of less than 2cm in baseline components (Figure 4.2).

Source positions and source structure.

To assess the effect of a priori source position variances on the results given in Table 4.2 three other solutions were computed with different a priori source position variances. The same Tidbinbilla to Parkes S/X data was used in each solution. The differences between the results of these solutions and those in Table 4.1, are given in Table 4.6. In one solution no a priori weights were assigned to the source positions. The baseline length was 32.7cm shorter and the associated formal precision was ±40cm (Table 4.6a). The formal precisions of the Parkes coordinates were also much larger. In another solution the catalogue source positions were held fixed. The differences were all less than the formal precisions quoted in Table 4.2 (Table 4.6b). In the third solution a priori weights inversely proportional to the variances given in the source catalogue were used. Again the results differ by less than their corresponding formal errors (Table 4.6c).

Table 4.6. Effect of source position a priori weights.

	Differences from overall solution in cm.			
Solution	Length	R	λ	Z
a) no apriori weights	32.7	4.8	12.3	41.1
b) all sources fixed	1.3	3.3	0.1	3.9
c) catalogue variances	1.1	2.9	0.1	3.3

Some of the errors in source positions will be absorbed in the estimates of the formal precision of the baseline components because a priori variances were applied to the source positions. If the positions of the sources south of -45° declination were also known to ± 0.03" or better the accuracy and precision of the geodetic results would improve, probably giving a precision of about ± 2cm in length. To obtain better a priori source positions it would be necessary to observe these sources on a longer baseline where the telescopes can observe sources to the south celestial pole.

Since these results were calculated, improved source position data has become available (Morabito et al, 1983). The positions of five of the southern sources have been determined to ± 0.5" accuracy using single channel S band VLBI measurements. These measurements were made on the Parkes - Hartebeesthoek baseline (1980) and on the Tidbinbilla - Hartebeesthoek baseline (1982). The Tidbinbilla - Parkes S/X solution was recomputed using these values as a priori estimates with weights equivalent to a standard deviation of ± 0.5". The baseline length and its formal precision changed by about 1mm. Clearly much tighter constraints on source positions are needed to significantly improve the geodetic results.

A discussion of the source positions and their accuracies (about ± 0.1") determined in this experiment is given by Jauncey et al (1985). The error due to source structure for all baselines is expected to be of the order of a few millimetres or less, in lengths and coordinates.

Subjective effects.

As well as systematic errors due to models there is a certain amount of subjectivity in the analysis. The analyst must decide which points to delete from the solution, which clock parameters to solve for, what a priori weights to assign to some of the parameters, eg. source positions, and what a priori variances to assign to the observations. The magnitude of this subjective error on the Tidbinbilla to Parkes solution is probably of the order of 3-4cm on baseline length and components. The effect of subjective analysis is significant and could be reduced by using more stable clocks which require little or no modelling, increasing the observation rate so that there is more redundancy, and having more reliable estimates of accuracy of the data and source positions.

Summary of accuracy.

Figure 4.2 summarises the estimated effects of various error sources and the accuracy of the baseline results. Other error sources such as those due to instrumental effects and differences in computer programs and models have not been mentioned above but may be of the order of a few centimetres. A better estimate of the accuracy of the results would be obtained if the experiment was repeated many times with different instruments and computer analysis.

Considering the baseline precisions (Table 4.3) and the analysis of accuracy given above, it can be concluded that the accuracy of the baseline lengths is not more than twice their formal errors. Therefore the 275km Tidbinbilla-Parkes baseline length and components have been determined with estimated accuracies of ±6cm and better than ±15cm respectively. The 235km Tidbinbilla - Fleurs and 250km Parkes - Fleurs baseline lengths and components have been determined with estimated accuracies of ±13cm and ±25cm respectively. The Tidbinbilla - Alice Springs and Parkes - Alice Springs baseline lengths and components have been determined with estimated accuracies of ±1.8m and ±2.2m respectively. The Tidbinbilla - Hobart and Parkes - Hobart baseline lengths and components have been measured with estimated accuracies of ±6.4m and ±8m respectively.

COMPARISON WITH GROUND SURVEY.

In addition to the VLBI measurements reported here, the baselines have also been determined by conventional survey techniques. They were computed from coordinates of the 1983 adjustment of the Australian Geodetic Datum, as provided by J. S. Allman (personal communication, 1984). Table 4.3 shows the differences between the VLBI and ground results. The ground survey chord lengths were derived from geodetic latitude, longitude, height above the geoid and geoid-ellipsoid separation at each site. Expected errors in

latitude and longitude would cause an error of about 30cm in the lengths Tidbinbilla - Parkes - Fleurs. And an error of 1m in the height or geoid-ellipsoid separation at one site would cause about 9cm error in the Tidbinbilla -Parkes baseline length.

In contrast to conventional geodetic and satellite techniques VLBI measurements are purely geometric and are not complicated by local gravity field variations. These measurements are therefore of immediate benefit for strengthening the Australian geodetic network and providing a valuable check on terrestrially determined distances.

A comparison of the two sets of baselines (excluding the Hobart baselines which, in the case of VLBI, are of low quality) shows excellent agreement on both the long and the short baselines. Any systematic differences in the baseline lengths are statistically insignificant, while the spread in the observed differences is in complete agreement with the claimed precisions. In no case do the observed differences exceed 1.5 times the calculated precision of the difference. It should be remembered that the ground surveys were not designed to specifically determine these baselines, so the ground data could be improved.

COMMENTS.

The goals of the Australian Geodetic VLBI experiment have been achieved except for the Hobart baselines (the Hobart antenna moved too slowly to observe all scheduled sources). Clearly, the higher accuracies were achieved for the better instrumented sites.

Useful estimates could not be made of polar motion, earth spin, earth tide parameters or the precession constant because of the brief time span of the experiment (1 week) and because the accurate baselines are short (<300km). Conversely errors in the adopted values of these parameters have little effect on the geodetic results.

The data from this experiment is stored in an easily accessible form. When better source positions or better models become available the solutions should be recomputed. Better positions for those sources south of -45^{o} declination could be achieved by observing on a longer baseline. Since Parkes cannot observe at the low elevations necessary for long baseline experiments. The most suitable baseline currently available is from Hartebeesthoek to Tidbinbilla. Such an experiment is being planned.

To obtain improved geodetic results in any future Australian Geodetic VLBI experiment, it is recommended -
1) that Circinus X-1 and Vela not be observed.
2) that the number of observed sources be limited to 15 rather than 25.
3) that consideration be given to observing at most only one out of each of the following pairs because they are close together in the sky: 0438-43 and 0537-44; 0637-75 and 0743-67; and 3C 273 and 3C 279.
4) that the data acquisition rate be substantially increased.
5) that the participating sites be better instrumented. In particular, masers need to be installed at Fleurs, Hobart and Alice Springs so that measurements can be made at X band. Further, BWS equipment is required at both Alice Springs and Hobart for improved delay measurements, and the slew rate of the Hobart antenna needs to be increased.

The single most significant addition to each site would be: Mark III at Tidbinbilla, phase calibration at Parkes, a Hydrogen maser frequency standard at Fleurs, BWS at Alice Springs, and a faster slew rate at Hobart.

CHAPTER 5.

GROUND MEASUREMENTS.

This chapter briefly reviews those aspects of the theory of geodetic networks which are an essential basis for the research reported in this thesis. A detailed coverage of the theory of Geodesy and ground survey measurements is given by Vanicek and Krakiwsky (1982), Torge (1980) and Bomford (1980), to which the reader is referred. A discussion of the survey of the VLBI reference point is included in this chapter because these measurements form part of the ground net and are a likely source of error in combined adjustments of ground and VLBI data.

OBSERVATIONS.

The measurements considered here are horizontal directions, distances, zenith angles (vertical angles), height differences, and astronomic determinations of latitude, longitude, and azimuth. The precisions quoted below depend on appropriate observational procedures being followed.

The directions to stars of known position are observed and the time recorded. These observations are used to determine the direction of the local vertical (ie. astronomic latitude and longitude) and the azimuth of a line. Field instruments achieve precisions of about ±0.3" in latitude and longitude (Bomford, 1980). Corrections are made to the observations for astronomic refraction, precession, nutation, proper motion of the stars, parallax and aberration. The astronomic results refer to the instantaneous rotation axis and are converted to the CTS system by applying corrections for polar motion and UT1. Astronomic observations of azimuth (Laplace azimuths) are used to control orientation within large geodetic networks. However Laplace azimuths are well known to be affected by large systematic errors. They are probably accurate to about ±1.4" (Bomford, 1980).

Horizontal directions are measured by theodolite in the plane perpendicular to the local vertical. A precision of about ±0.7" can be achieved for each direction (Hoar, 1975). Zenith angles are also measured with respect to the local vertical, but they are more severely affected by refraction. Accuracies of about ±2", or worse, are typical. By simultaneously observing zenith angles from each end of a line the effect of refraction can be reduced.

Distances are usually measured by EDM (Electromagnetic Distance Meters) which use either light waves or microwaves. The measured lines are typically 30 - 40km long but may be up to about 150km. Accuracies obtained are about 1 - 2 ppm for light waves and 3 - 5 ppm for microwaves. Distances have to be corrected for refraction. A recent development is to measure a distance with 2 or 3 different wavelengths simultaneously. The dispersion of signals of different frequency will yield different distances, and the correct distance can be computed. An instrument with two lightwaves and a microwave signal, described by Hugget and Slater (1975), can measure 10km with a precision of 0.1ppm (Slater et al., 1983). However, these types of instruments have not been used in Australia.

Since the late 1800's directions have been measured with accuracies of about ±1" or better. This represents a displacement of about 15cm for a typical 30km line. Since the advent of EDM in the 1960's distances have been measured to about 4cm over 30km. Accordingly most recent measurements are distances while older measurements are mainly directions.

The precision of levelling, with 30 - 40 km station spacing, can be about two orders of magnitude better than that obtained by observing zenith angles and distances. However the sum of the staff reading differences for a level run does not equal the height difference between the sites. The height difference obtained depends on the route

followed. A better practice is to measure potential differences between sites by also measuring gravity at sites along the level run. Potential differences are not path dependent. Alternatively ellipsoidal height differences can be obtained by correcting the levelling measurements for the geoid slope. The slope of the geoid may be obtained from measurements of the deflections of the vertical. The effects of many error sources such as refraction can be reduced by appropriate observation techniques. The reader is referred to the geodetic references given at the beginning of this chapter for further explanations of levelling and the many height systems.

Heights in Australia refer to the Australian Height Datum (Granger, 1972). They do not constitute a freely adjusted level network because they have been distorted, by up to about 1m, to fit mean sea level at tide gauges around Australia. Note that mean sea level does not necessarily coincide with the geoid.

The separation of geoid and ellipsoid (geoid height) can be computed from deflections of the vertical, from gravity measurements, or from a combination of satellite positioning and levelling. Deflections of the vertical are obtained from the difference between astronomically and geodetically determined position. Gravimetric data is best used for interpolation between astronomic sites to give local information about the geoid because of inherent systematic errors in the gravimetric data.

Ellipsoidal heights should be used in a ground network which is to be combined with space data. These ellipsoidal heights are the sum of the geoid height and the height above the geoid. To calculate these heights geopotential differences and local gravity values, not those from a normalised gravity field, should be used.

As well as the theoretical limitations there are a number

of important practical limitations affecting the accuracy of ground surveys, such as -

1) Ground surveys across large bodies of water (eg Bass Strait) are of poor quality.
2) For practical reasons horizontal control stations are typically on mountain tops. Levelling networks generally avoid such points.
3) Zenith angles, if observed, are of poor quality.
4) The values of geoid height or its variations along levelling lines, are not usually reliable because of insufficient gravity data.
5) Astronomic observations are not made at every site because they are expensive.

Accuracy deteriorates with distance from a fixed point at a rate of about one ppm, because of the accumulation of errors. Therefore the relative position of nearby points within a geodetic network is more accurate than position with respect to the origin of the network. Additionally the height component is poorly determined because of inadequate knowledge of the geoid heights.

A network of ground data is strengthened over long distances by the inclusion of Doppler data. But the relative accuracy obtainable with Doppler is poor over short distances (<200km). To improve the inner strength of a geodetic network it is therefore important that Doppler stations are widely separated. Bossler (1978) recommends that the minimum spacing be 200km - 300km.

ADJUSTMENT METHODS.

Geodetic surveys were traditionally separated into horizontal and vertical networks because the separate adjustments were easier and more economical to compute. Moreover, the two nets require different observations and are only weakly correlated. Also the horizontal and vertical networks have few points in common, because points suitable for horizontal control are generally unsuitable

for vertical control and vice versa. However 3D networks are becoming more popular.

Ground data in Australia is currently adjusted using the classical method. Observations are reduced to the ellipsoid and adjusted by either the Canadian Section method (Pinch and Peterson, 1974), or the Helmert Block method (Vanicek and Krakiwsky, 1982) which is very similar. The data is split into blocks and each block is then separately adjusted, as a free net. Each adjustment yields coordinates and a variance covariance matrix for points which are common to other blocks. This is called stage 1. In stage 2 the common coordinates and VCV matrices from each block are combined into a single adjustment to yield the final adjusted coordinates of the common points. In stage 3 each block is separately adjusted with the above final coordinates of the common points held fixed. This yields the adjusted coordinates for all remaining points. Doppler, SLR and VLBI data form separate blocks and are combined with the ground data in stage 2.

The 2D adjustment of ground data can use either the classical ellipsoidal or the 3D - height fixed approach (Vincenty, 1980). The 3D - height fixed method does not reduce the measurements to a computational surface and there are no restrictions on the lengths of the lines. In the adjustment each point is restricted to movement in the plane of the astronomic horizon at that point. The heights must be sufficiently accurate or the entire process will have to be iterated. If the network is large the Helmert block procedure can be implemented so that the size of the matrices to be inverted, at any one stage, is reduced.

The classical method of reductions onto the ellipsoid is formally equivalent to three dimensional methods. That is, both methods should give the same results if applied correctly. However there are practical differences. In the classical approach the heights above the geoid are combined with astrogeodetic determinations of the geoid heights to

give ellipsoidal heights. Whilst in the 3D approach zenith distances, with their dependence on vertical refraction, are also used.

Alternative adjustment procedures.

In contrast to the separate adjustment of horizontal and vertical networks, methods of 3D network adjustments have been proposed but have not yet been widely adopted. Three recently proposed methods are - a purely geometric approach (eg Vincenty and Bowring, 1978), an integrated or 'operational' approach (eg Grafarend, 1978 and Hein, 1982), and a combined approach (eg Reilly, 1980). All approaches are affected by data inadequacies, refraction (especially of zenith angles) and sparse astronomic observations of the direction of the vertical. The geodetic information about a point can be described by seven parameters, the three Cartesian coordinates (X Y Z), the direction of the gravity vector (astronomic latitude Θ and longitude λ), the magnitude of the gravity vector (g), and the absolute potential (W).

In the geometric approach five unknowns, X, Y, Z, Θ, and λ, are determined. The main difficulty with this approach is the treatment of orthometric heights which are not a geometrical distance in the vertical direction. Astronomic latitudes and longitudes, whether observed or interpolated, are required at all sites at which directions are observed.

The integrated approach includes an earth gravity model and solves for all seven unknowns. The inclusion of gravity data strengthens the solution for the unknowns Θ, λ, W, and g, and also X, Y, and Z through a possibly small correlation. The height coordinate is significantly improved.

The combined approach uses gravity data within and surrounding the network, not just that at the network sites and on the interconnecting lines. Reilly (1980) suggests

that all this gravity data could be reduced to a set of five curvature parameters, obtained by least squares collocation, of the gravity field at each network site.

ORIGIN CONDITIONS.

The coordinates of the origin (or initial point, or fundamental point) of a terrestrial network are held fixed throughout adjustments of the network. The relation of this point, and therefore of the network, to the CTS, can be described by either, three translations and three rotations or by topocentric coordinates at the initial point. The latter method consists of, for example, geodetic latitude and longitude, a geodetic azimuth to another point, deflections of the local vertical with respect to the ellipsoidal normal in two directions, and geoid height. In another equivalent method the X, Y, and Z coordinates of the initial point, the direction of its local vertical (ie. the astronomic latitude and longitude), and the azimuth of a line from this point, are adopted as the origin conditions. Often the values of azimuth and deflections at the initial point are obtained from a least squares analysis of all such observations across the network.

Regardless of which method is chosen the adopted values are determined by observation. Errors in these observations will cause errors in the orientation and location of the ground network with respect to the CTS, as follows.

1. Errors in astronomic latitude and longitude cause the coordinates of the points of the network to be shifted parallel to the true system by (eg. Stolz, 1972) -

$$\begin{aligned} \Delta X &= -(M+h)\sin\phi\cos\lambda\,\Delta\phi - (N+h)\cos\phi\sin\lambda\,\Delta\lambda \\ \Delta Y &= -(M+h)\sin\phi\sin\lambda\,\Delta\phi + (N+h)\cos\phi\cos\lambda\,\Delta\lambda \\ \Delta Z &= (M+h)\cos\phi\,\Delta\phi \end{aligned} \qquad (5.1)$$

where M is the radius of curvature of the ellipsoid in the meridian and N is the radius of curvature in the direction of the prime vertical.

2. An error in azimuth causes the whole survey network to be rotated through the angle $\Delta\alpha$ about the local vertical at the initial point (x_o, y_o, z_o). The error in the coordinates is given by (eg. Stolz, 1972) -

$$\begin{bmatrix} \Delta X \\ \Delta Y \\ \Delta Z \end{bmatrix} = R \begin{bmatrix} x - x_o \\ y - y_o \\ z - z_o \end{bmatrix} \qquad (5.2)$$

$$\text{where } R = \begin{bmatrix} 0 & \Delta\alpha \sin\phi & -\Delta\alpha \cos\phi\sin\lambda \\ -\Delta\alpha \sin\phi & 0 & \Delta\alpha \cos\phi\cos\lambda \\ \Delta\alpha \cos\phi\sin\lambda & -\Delta\alpha \cos\phi\cos\lambda & 0 \end{bmatrix}$$

A new rotational matrix R is introduced for each site where an azimuth is constrained to an observed value. The overall effect is to produce a series of non-parallel reference frames. That is, a distortion in the coordinates.

The latitude and azimuth may be held fixed at the local astronomic values or some other value so as to obtain better agreement between astronomic and geodetic values throughout the region concerned. If the longitude is held fixed, then the deflection of the vertical in the meridian must be consistent with the azimuth and the Laplace equation.

3. An error in geoid height causes the network to be shifted parallel to the true system by -

$$\begin{aligned} \Delta X &= \cos\phi\cos\lambda \, \Delta H \\ \Delta Y &= \cos\phi\sin\lambda \, \Delta H \\ \Delta Z &= \sin\phi \, \Delta H \end{aligned} \qquad (5.3)$$

A reference ellipsoid is usually adopted as the geodetic datum. This is an ellipsoid of revolution about the minor (Z) axis. The ellipsoid is either centred at the geocentre or offset from it. The centre is chosen so as to closely approximate the geoid for the whole earth or a portion of it, such as a continent. The geoid is the equipotential surface of the earth equivalent to mean sea level. It is not perfectly regular due to anomalies in the gravitational field caused by the earth's non-homogeneous mass

distribution. If the datum closely approximates the geoid then the corrections applied to the observations are small.

The semi-major axis (a), the flattening (f), and the coordinates of the centre of the ellipsoid are chosen so that the ellipsoid closely approximates the geoid for the region concerned. While the coordinates of the centre of the ellipsoid cannot be determined by conventional survey techniques, the direction of the coordinate axes can be made parallel to the reference axes by the use of the Laplace equation (eg. Torge, 1980).

For the Australian Geodetic Datum (AGD) (a = 6 378 160 m, f = 1 / 298.25) the adopted coordinates of the Johnston Origin are -

Geodetic latitude = Ø = -25° 56' 54.5515"

Longitude = λ = 133° 12' 30.0771"

Ellipsoidal height = h = 571.2m

The AGD is aligned with the mean geoid slope across Australia as defined by the mean of the deflections of the vertical at about 150 sites. The ellipsoid is not geocentric.

OTHER SYSTEMATIC ERRORS.

EDM measurements are affected by atmospheric refraction. Within the few kilometres of the atmosphere close to the ground where observations are made, the atmosphere is not stable and the index of refraction varies with time and position. The effects of refraction on distance and direction measurements are systematic and differ throughout a network depending on the equipment used, the time of observation and the observational procedure. The effect of differences between refraction errors on different baselines or regions can be solved for by introducing appropriate parameters into the adjustment. These parameters are then eliminated in a similar way to the orientation unknowns during the adjustment. The technique is described by Vanicek and Krakiwsky (1982). However when

these additional parameters are included care must be taken so that they do not absorb the effects of other parameters or distort the adjustment. A scale error which is constant for the whole network cannot be eliminated in this way.

Systematic errors in scale and orientation in large terrestrial networks are due to poor calibration of EDM instruments, inadequate modelling of atmospheric refraction, systematic differences between lightwave and microwave distance measurements, insufficient determinations of the deflection of the vertical, and inaccurate geoid heights. Scale and orientation errors vary throughout a network because of variations in the above systematic errors, and because in some regions the observations are of better quality and are denser than in other regions. Systematic errors in the refraction corrections or in the EDM instrument calibration will produce 2D scale errors which are discussed in Chapter 7. Systematic errors and their variations can be controlled by inclusion of independent measurements such as VLBI.

Orientation of a ground net is generally determined by the mean of astronomic azimuths across a region. Any systematic error in this mean value of azimuth will not affect the internal accuracy of the network. Astronomic azimuths are also used to control the effect of the accumulation of errors in direction observations on orientation within a large network. However if there are numerous astronomic azimuths and their systematic errors are large and are not uniform, then the network will be distorted. Whether the azimuth observations should be included or not depends on the magnitude of the systematic errors, size of the network, and the distances between adjacent azimuth observations. Astronomic azimuth observations should be spaced at least 200km apart (Torge, 1980). If the whole region in question is less than 400km in extent, then only one azimuth observation should be included. Any error in this observation will cause only a pure rotation of the net.

The accumulation of random and systematic measurement errors in a network depends on the distances covered because the networks consist of a series of line-of-sight observations. Typical rates of accumulation are about 1ppm, although better rates can be obtained for small, high quality networks. Moreover the geometric structure of the network may reduce the accumulation of error.

Adjustments on the ellipsoid require corrections for geoid height, skew normals and deflections of the vertical (eg. Bomford, 1980). Approximations to, or neglect of, these corrections will result in systematic errors in the results. Whilst these errors may be less than the accuracy required for the particular application, they may be significant for crustal movement studies and should not be neglected.

It is well known that errors in heights cause errors in the scale of terrestrial networks. If the height error is constant over a region then the error in scale Δs is -

$$\Delta s = \Delta h / R \qquad (5.4)$$

where Δh is the height error and R is the average geocentric radius of the region. For example if Δh is 6m, Δs is about 1ppm. If the geoid used has been determined from satellite observations it will generally refer to a geocentric ellipsoid. This ellipsoid has to be transformed to the local datum of the ground adjustment. Any errors in this transformation will cause errors in the adopted heights. A geoid height error also causes errors in the estimated translation components as in equation 5.3 above.

SURVEY CONNECTION TO VLBI REFERENCE POINT.

The VLBI reference point, described in Chapter 3, needs to be connected to the ground network so that the two data types can be combined. Clearly, the connection should be as reliable as any other line in the terrestrial network. The connection can be surveyed with an accuracy of a few

millimetres provided instrument calibration, observation procedure, and modelling corrections are to a high standard. However gross errors, such as that reported by Thomas et al (1976), need to be eliminated. A misidentification of the VLBI reference point will not be detected in a ground adjustment, but it will cause errors in a combined adjustment.

Each VLBI site should be surrounded by a ground network of several stations. Repeated observations should be made, to locate the reference point and to monitor local geophysical and structural motions. The whole telescope may move due to the force of gravity or the wind. The sun may heat one side of telescope and cause it to expand more than the other side. Hung et al (1976) estimated that a 40 C temperature change would produce about 9mm movement of the reference point of DSS 14, a 64m antenna. The effect is predominantly to raise or lower the reference point. McGinness et al (1979) estimated the displacements of the reference point of DSS 13, a 26m antenna, due to bearing 'runout', temperature change, and wind loading, to be less than a few millimetres.

To determine the position of the reference point, observations have to be made to determine the centrelines of the axes. These observations should be made with the antenna pointing in different directions to discover whether the reference point is independent of the direction of antenna pointing. The inclination of all axes with respect to the local vertical and the local variations of the local vertical are needed. No axis should be assumed to be in correct alignment, and the axes should not be assumed to intersect.

There are a number of practical difficulties in the survey. Among these are -

1) There is not necessarily any physical component at the reference point.

2) The VLBI reference point is located in the midst of the

structural components of the telescope which obstruct many observations.
3) Usually the reference point, or any nearby point, cannot be conveniently occupied by surveying instruments.
4) The reference point of telescopes surrounded by radomes will be difficult to observe because of the physical obstruction.
5) It is not possible to observe astronomic latitude, longitude or azimuth at a mark below the reference point because the view of the stars is obstructed by the telescope.
6) Observations to elevated targets are more severely affected by dislevelment of the theodolite. The error in direction observations are a function of the dislevelment error and the tangent of the elevation angle. At an elevation angle of 45° this can amount to 3". The error can be reduced by placing observing sites so that the elevations are small, by relevelling the theodolite between each set of observations, and by using striding levels.

The survey observations should be made with a variety of instruments and observers to minimise systematic errors and observation times should be scheduled to minimise the effects of time-dependent atmospheric anomalies. Even without reciprocal observations, corrections for lateral and vertical refraction can be estimated to 1"-2" (Torge, 1980). So, provided proper precautions are taken, the residual error from observations of less than 100m should be less than about 1mm. The direction of the local vertical for all sites within a few hundred metres of the telescope is, generally, adequately determined by interpolation. However this assumption should be checked by making a detailed geoid map of the area by gravimetry.

Three methods of surveying the reference point will be discussed.
1) The conventional method is to establish a mark near ground level and directly beneath the reference point, using for example a vertical collimator. The position of

the reference point is usually determined by accepting that construction is in agreement with the engineering design. Lines of sight through doorways, or through holes bored in the structure, or both, connect the ground mark to the exterior site(s). A number of exterior sites should be used to provide redundancy. However, this is not always done. The horizontal position of the ground mark and the height difference to the reference point are then measured. The measurement of height difference is not necessarily simple or error free especially for large antennas. The desired measurements can be obtained by levelling from nearby stable towers, by observing zenith angles from exterior sites to the reference point, or by hanging a tape from the reference point to a ground mark. However in this last case the tape would often be obstructed by parts of the telescope mount. If zenith angles are observed care must be taken to reduce refraction and theodolite errors. Thus for many telescopes the use of a ground mark directly beneath the reference point may not be the most practical or effective method.

2) Another possibility is to build a temporary tower over the antenna so that a survey instrument could be set up directly above the reference point. Astronomic observations could be made and the height measurements would be less obstructed. Clearly, the tower would need to be stable.

3) A better approach may be to determine the coordinates of the reference point by observing a 3D ground network surrounding the telescope. A target should be placed on each end of the moving axis and the fixed axis. The targets should then be observed, with a theodolite, as the telescope is rotated about this axis. Note that the axis itself should not move. If a target does not move then it is truly on the centreline of the axis. However it is not usually possible to rotate the telescope through 360^{o} about each axis, especially with equatorial mount telescopes.

After the targets have been correctly positioned,

horizontal directions, zenith angles, and distances are observed to each target. These measurements are repeated for a variety of positions of the axes and from a number of sites in the immediate surrounds of the telescope. Each site should observe simultaneously, if possible, to minimise refraction errors and errors due to movement of the telescope. Unfortunately, due to obstructions, the targets may not be visible at many positions. Measurements could be made under different sun and wind exposure conditions. The axis offset, the inclination of each axis, and the position of the reference point with respect to the local geodetic network, are then computed from an adjustment of these observations, which would include many redundancies. However the axis offset, for example, might be determined by direct measurements and would thus strengthen the solution for the position of the reference point. With this method many sites could surround the telescope whereas for method (1) only one or two sites observe because of the common necessity to bore holes into the tower. This method is suitable for locating the reference point of all types of telescope including a transportable antenna.

CHAPTER 6.

COMBINATION OF GROUND AND VLBI DATA - THEORETICAL CONSIDERATIONS.

INTRODUCTION.

This chapter will discuss the theory of combining two sets of data primarily by solving for transformation parameters, though other methods will be considered. The peculiarities of different data and the importance of accurate VCV matrices are also discussed here. A rigorous analytical procedure for combining ground and VLBI networks is developed and appropriate statistical tests are included. Combination models, parameters, and numerical examples are given in the next chapter.

If correct procedures are followed, the combined adjustment of independent data will improve - (i) the accuracy of a network by controlling the systematic errors, and (ii) the precision of the network because additional data is included. If systematic errors in scale and orientation exist within a geodetic network then not only will the adjusted coordinates be incorrect, but their estimated accuracies will be optimistic. Therefore the combination of independent data also produces more realistic accuracy estimates.

Combined adjustments strengthen geodetic networks, relate different geodetic networks together, and improve investigations of crustal dynamic parameters. Generally it is necessary to combine VLBI and ground data to give the best strain analysis over a region. This is because ground measurements are less accurate than VLBI measurements and a VLBI network is not as dense as a ground network. However systematic errors in the coordinates of one of the nets may produce apparent strain in a combined network adjustment. So in strain determinations it is important that all

systematic errors in the observations and their reductions, be allowed for. This will be discussed in Chapter 8.

There are similarities between the block adjustment technique used in photogrammetry and the combination of VLBI results with ground data. However photogrammetric block adjustments produce scale differences and rotation angles that may be large. On the other hand, VLBI and ground networks are at nearly the same scale and are usually oriented to within a few arc seconds of the same CTS frame. Moreover, photogrammetric block adjustments usually have to deal with data sets involving thousands of common points. They thus require special strategies and considerations (Blais, 1979). The problems associated with transformations between networks containing small numbers of common points are investigated in this thesis.

There have also been a number of suggestions for combining ground and Doppler data. However VLBI data is not necessarily best combined in the same way as Doppler and ground data. This is because VLBI is far more accurate than Doppler, especially over short distances, and gives only relative positions while Doppler measurements can relate points to the geocentre. With these exceptions in mind, many of the techniques used in photogrammetric block adjustments and for combining Doppler and ground data can be applied to the combination of VLBI and ground data.

Two main problems arise when combining data from different networks. They are:
1) Finding the most accurate estimates of the external bias parameters (ie. scale, rotation, translation and systematic error terms) between the systems, and
2) Achieving the best internal combination of the different systems, that is to minimise the corrections to the observations.
The solution which provides the best estimates of the bias parameters is not necessarily the solution which provides the best internal combination and vice versa. Among the

questions to be answered are whether a 2D or 3D adjustment model should be used, the type and quantity of bias parameters, modelling of systematic errors, and the assignment of a priori variances and correlations and their influence on the results. These decisions should be made for each particular data set and are generally based on statistical tests as described below.

It is proposed in this thesis to combine the two data types by solving for transformation parameters between the networks. That is, those parameters which transform the coordinates of one net to the scale, location and orientation of the other net. Alternative combination procedures and the reasons why they are not adopted in this thesis are given below (page 104).

The observation equations can be expressed in terms of the VLBI coordinates (or coordinate differences from a base point) and the ground coordinates. For example, a series of rotation, scale and translation matrices could be applied to each net to relate them to the CTS frame. These matrices would represent the differences between reference frames and systematic errors (eg. one of the rotation matrices could represent the error in VLBI source RA's). The elements of these matrices could then be estimated (with or without a priori constraints). However some parameters will be indistinguishable from others. So it may not be possible to solve for them separately. Consequently only single rotation, scale, and translation matrices are estimated. Each of the terms in these matrices represents the sum of all similar parameters.

TRANSFORMATIONS.

There are a number of ways of transforming one data set to another. The most general transformation considered here is the affine transformation. An affine transformation transforms straight lines to straight lines and parallel lines remain parallel. Generally the size, shape, position,

and orientation of lines in a network are changed. The scale factor depends on the orientation of the line but not on its position within the net. Hence the lengths of all lines in a certain direction are multiplied by the same scalar. For a transformation between two large networks with many common points it may be possible to use a projection transformation where the scale factor is also a function of position. However this would not be wise because the VLBI data sets usually contain only a few points thus leading to a solution with few (if any) degrees of freedom. Transformations in which the scale factor does not depend on position within the net, involve fewer parameters but assume that there are no systematic distortions of the networks.

The affine transformation of the coordinates (XYZ) of a point in one system to the coordinates (xyz) of the corresponding point in the other system is given by -

$$\begin{bmatrix} X \\ Y \\ Z \end{bmatrix} = \begin{bmatrix} a & b & c \\ d & e & f \\ g & h & i \end{bmatrix} \begin{bmatrix} x \\ y \\ z \end{bmatrix} + \begin{bmatrix} Tx \\ Ty \\ Tz \end{bmatrix} \qquad (6.1)$$

Thus there are 12 parameters, so at least four common sites are needed. It is conventional, though not essential, to use right-handed Cartesian coordinate systems for both networks, because the algorithms are simpler.

An affine transformation in which the scale factor is the same in all directions is called a conformal or similarity transformation. A conformal transformation preserves shape, so angles are not changed, but the lengths of lines and the position of points may be changed. An orthogonal transformation is a conformal transformation in which the scale factor is unity. The angles and distances within the network are preserved and only position of points changes upon transformation.

The general conformal transformation is given by -

$$\begin{bmatrix} X \\ Y \\ Z \end{bmatrix} = s\ R \begin{bmatrix} x \\ y \\ z \end{bmatrix} + \begin{bmatrix} Tx \\ Ty \\ Tz \end{bmatrix} \qquad (6.2)$$

where s is the scale factor and R is a 3x3 orthogonal rotation matrix. There are seven parameters which are usually associated with three rotation angles, three translation components and one scale factor. The translation terms are the coordinates of the origin of the xyz net in the frame of the XYZ net. Scale factors and rotation matrices are described below.

Although a similarity transformation is a linear transformation of the coordinates it cannot be expressed linearly in terms of the seven parameters (Blais, 1972). However if the rotations are small, as expected, then the equations are approximately linear. A single iteration is then generally sufficient. However if additional iterations are required, because of poor a priori estimates of the parameters, the convergence is usually very rapid.

It is presumptuous to assume that conformal transformations, rather than affine or projection transformations, correctly describe the differences between any two data sets. However in practice little more than the smoothing of these differences can be accomplished. Moreover, using fewer parameters would seem to be safer when there are few common points. Conformal transformations guard against undue deformations in small regions, but using a conformal transformation on a large network may distort local scale and orientation. Hence the important question is whether local distortions in scale and orientation are significant or not. Conformal transformations will tend to smooth them out. Also, because the conformal transformation is linear in the coordinates, it cannot be applied to estimate, or to allow for, any distortions or deformations that are common to the two nets.

In a transformation adjustment the mathematical aspects of the model, statistical analysis, computational errors, and the reliability of the adjustment results that is, the stability of the solution, all have to be considered. In a stable solution small changes in the observations give small changes in the results. Error analysis associated with least squares adjustment requires a priori assumptions or hypotheses which require a posteriori testing. Uncorrelated observations generally lead to correlated residuals because of the geometrical implications in the adjustment. The residuals are also affected by mathematical approximations and computational errors (eg. round off errors).

It is important to realise that any systematic errors in the coordinates alter the geometry of a network and hence should ideally be removed prior to the adjustment. Any remaining errors in either network are considered random. This hypothesis should be tested by a posteriori analysis.

Rotation matrices.

It is well known that the rotation matrices about the x, y, and z axes are given by -

$$Rz(k) = \begin{bmatrix} \cos k & \sin k & 0 \\ -\sin k & \cos k & 0 \\ 0 & 0 & 1 \end{bmatrix} \qquad Ry(\theta) = \begin{bmatrix} \cos\theta & 0 & -\sin\theta \\ 0 & 1 & 0 \\ \sin\theta & 0 & \cos\theta \end{bmatrix}$$

$$Rx(\omega) = \begin{bmatrix} 1 & 0 & 0 \\ 0 & \cos\omega & \sin\omega \\ 0 & -\sin\omega & \cos\omega \end{bmatrix} \qquad (6.3)$$

Successive rotations of a body about fixed axes are not, in general, commutative, so the order of the rotations is important. Moreover the magnitude of each rotation angle depends on the order that the rotations are applied, unless the rotations are small.

There are at least three ways of rotating a network -

1) Cardanian angles (see fig. 6.1).
There are six possibilities, one of which is - Rz(k) Ry(ϑ) Rx(ω). There is no universally adopted convention as to which combination of the three rotation matrices should be adopted, though the example given is the most common.

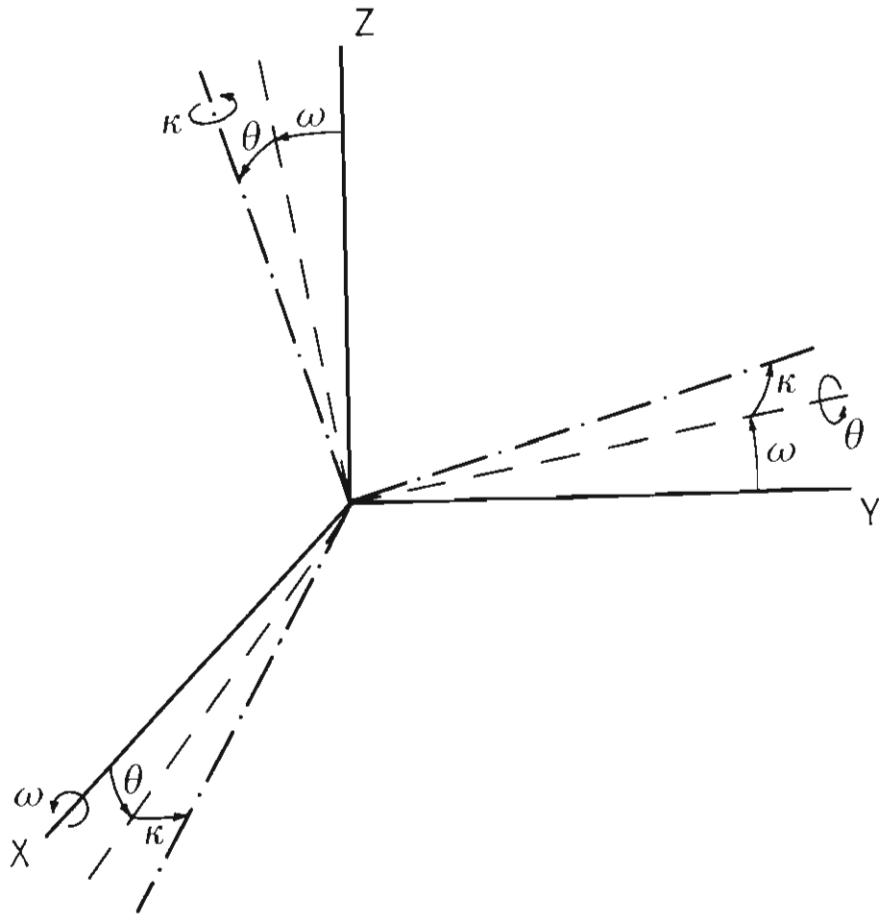

Figure 6.1 Cardan Rotations. (Rx(k) Ry(ϑ) Rz(ω)).

2) Eulerian angles (see fig. 6.2).
Again there are 6 possibilities, one of which is - Rz(γ) Rx(β) Rz(α). Georgiadou and Grafarend (1983) note that if β is zero then γ and α will be indeterminant. Thus when β is very small γ and α will be highly correlated and there may be instabilities in the solution. Since the rotation angles used to transform between VLBI and ground nets will frequently be small this method has not been adopted in this thesis.

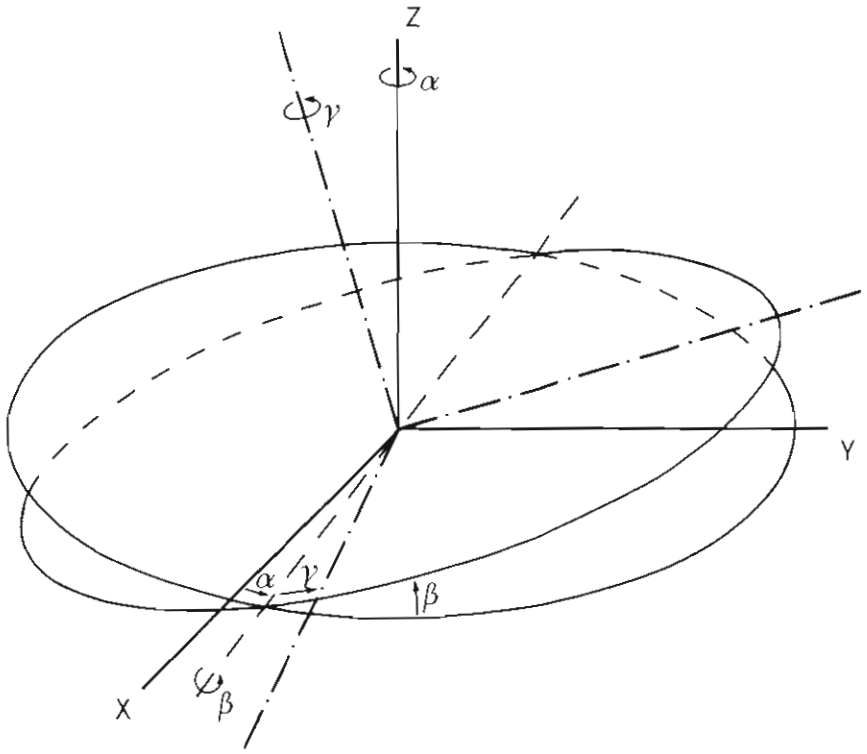

Figure 6.2 Euler Rotations. (Rz(γ) Rx(β) Rz(α)).

3) Euler's Theorem (eg. Thompson, 1969) states that provided one point of a body remains fixed the entire succession of rotations is equivalent to a single rotation about one axis. However this axis (E) does not necessarily coincide with either the x, the y or the z axis (see figure 6.3).

The rotation matrix is (Thompson, 1969) -

$$R_E(\varepsilon) = \begin{bmatrix} l^2+(1-l^2)\cos\varepsilon & lm(1-\cos\varepsilon)-n\sin\varepsilon & ln(1-\cos\varepsilon)+m\sin\varepsilon \\ lm(1-\cos\varepsilon)+n\sin\varepsilon & m^2+(1-m^2)\cos\varepsilon & mn(1-\cos\varepsilon)-l\sin\varepsilon \\ ln(1-\cos\varepsilon)-m\sin\varepsilon & mn(1-\cos\varepsilon)+l\sin\varepsilon & n^2+(1-n^2)\cos\varepsilon \end{bmatrix} \quad (6.4)$$

where l, m, and n are the direction cosines of the E axis, and ε is the magnitude of the rotation angle. The direction of the axis can also be expressed in terms of its latitude and longitude (or declination and hour angle) using -

$$n = \sin(\phi), \quad l = \cos(\phi)\cos(\lambda), \quad m = \cos(\phi)\sin(\lambda)$$

Regardless of the size of l, m, and n, if ε is small then -

$$R_E(\varepsilon) \approx \begin{bmatrix} 1 & -n\varepsilon & m\varepsilon \\ n\varepsilon & 1 & -l\varepsilon \\ -m\varepsilon & l\varepsilon & 1 \end{bmatrix} \quad (6.5)$$

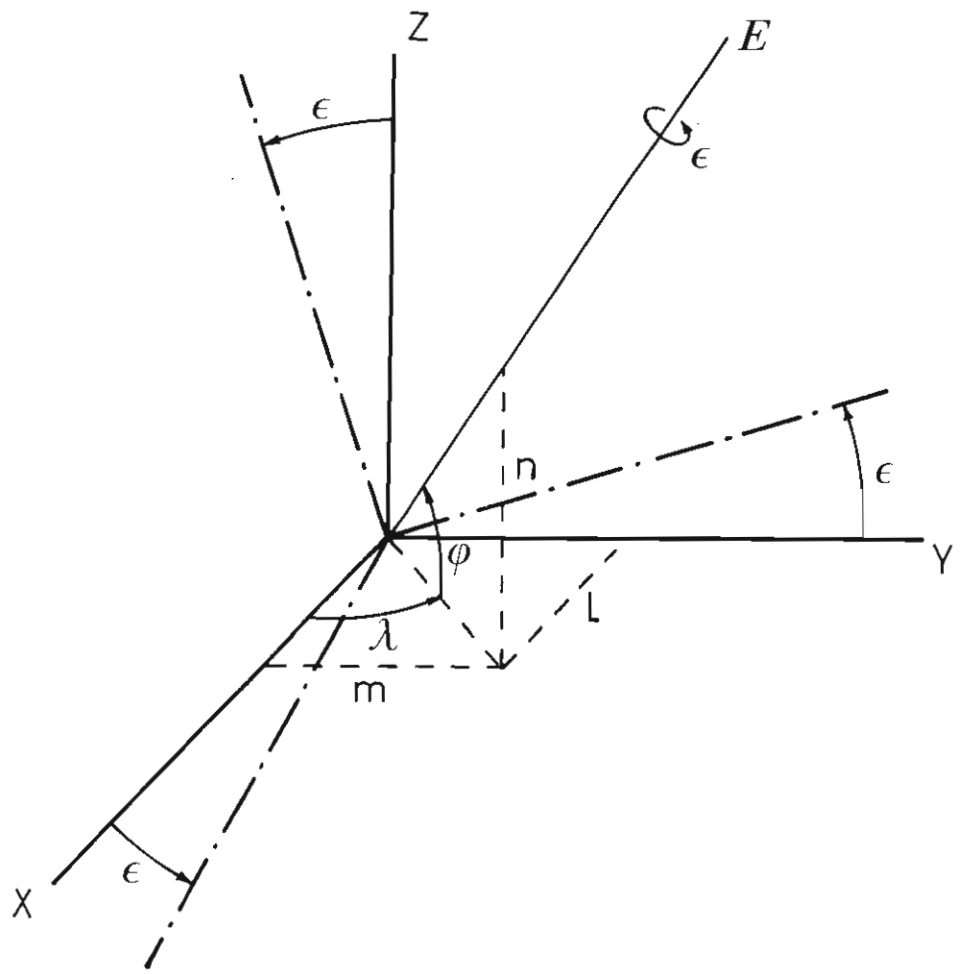

Figure 6.3. Rotation about a single axis, $R_E(\varepsilon)$.

In each of the above cases three parameters are involved. The choice of which form to adopt depends on the particular application. However all the above procedures are related. If one method is used in the adjustment of data then the rotation angles in the other systems can be subsequently determined as follows.

The conversions between ω, Θ, k and α, β, γ are given by (Georgiadou and Grafarend, 1983) -

$$\omega = \arctan(+\tan\beta \cos\alpha)$$

$$\Theta = \arcsin(\sin\beta \sin\alpha)$$

$$k = \arctan\{(\tan\gamma + \cos\beta \tan\alpha)/(1 - \cos\beta \tan\alpha \tan\gamma)\}$$

$$\alpha = \arctan(\tan\Theta / \sin\omega)$$

$$\beta = \arccos(\cos\omega \cos\Theta)$$

$$\gamma = \arctan\{(\tan k - \cot\omega \sin\theta)/(1 + \cot\omega \tan k \sin\theta)\}$$

If ε is small then (Thompson, 1969) -

$$\varepsilon = + \sqrt{(\omega^2 + \theta^2 + k^2)}$$

and

$$\begin{bmatrix} l \\ m \\ n \end{bmatrix} = 1/\varepsilon \begin{bmatrix} \omega \\ \theta \\ k \end{bmatrix}$$

So, for small rotations, the equivalent rotation angle about a single axis and the direction of this axis can be calculated from the rotation angles ω, θ, and k. The direction of the E axis is informative because it may pass through or nearly through the network. In this case the rotation is probably due to a 2D azimuth error in one of the nets.

For small rotations the Cardanian rotation matrix can be approximated by -

$$Rs = \begin{bmatrix} 1 & k & -\theta \\ -k & 1 & \omega \\ \theta & -\omega & 1 \end{bmatrix} \qquad (6.6)$$

where ω, θ, and k are the rotation angles about the x, y, and z axes respectively.

It is important to have some understanding of how small a rotation has to be before the approximation in equation 6.6 is valid. Figure 6.4, gives the error in position, due to adopting Rs, when the three baseline components are equal and the three rotation angles are equal. The figure only gives the maximum error because some baseline components or some rotation angles may be less than the others. The assumption of small angles is thus suitable for rotation angles of up to about 2.5". However considerably larger angles can be tolerated if the lines being rotated are shorter. For example, rotating a 500km baseline with each rotation angle equal to 10" will cause only 1mm error in coordinates if Rs is used instead of R.

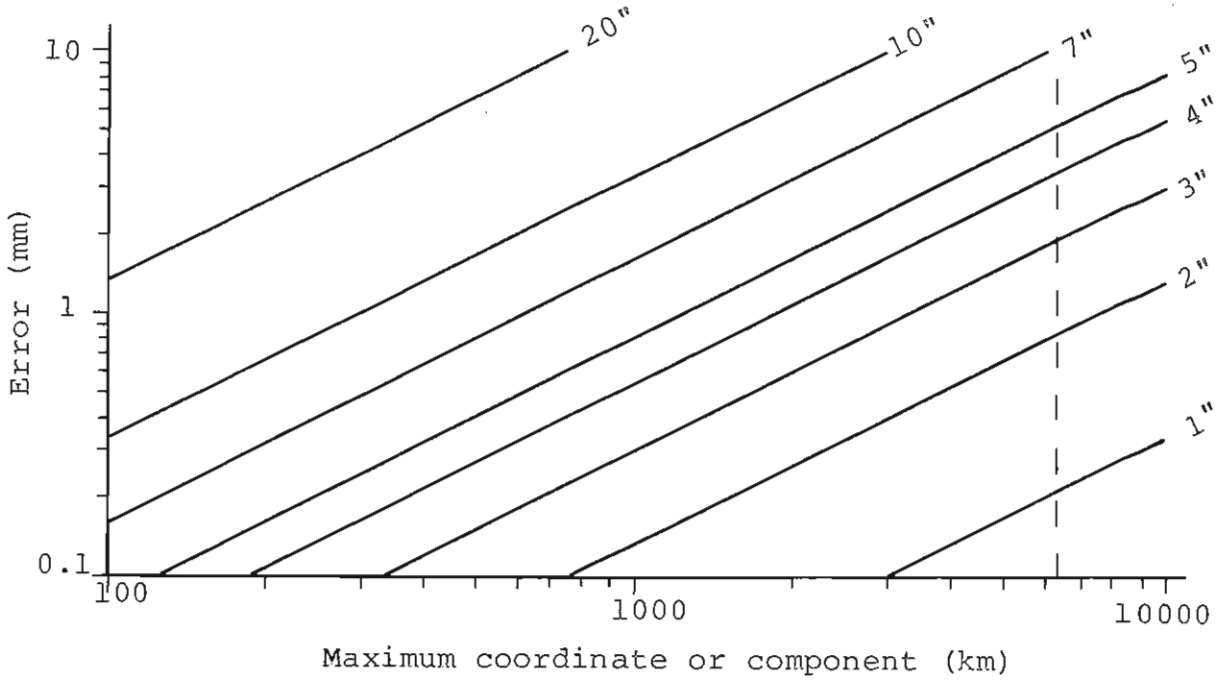

Figure 6.4 Maximum error caused by adopting Rs instead of Rz Ry Rx.

Scale factor.

A 3D scale factor is described here so that the concept of a 2D scale factor applied to a network on a curved surface, can be better understood and distinguished later. A 3D scale factor can be visualised as follows. Imagine a network is drawn on the surface of an inflatable sphere. As the sphere is inflated, the points of the network will be spread apart from each other and from the centre of the sphere. The inflation of the sphere is equivalent to the application of a positive 3D scale factor.

Multiplication of a set of rectangular Cartesian coordinates by a scale factor is identical to multiplying the corresponding baseline lengths by the same scale factor. So, in 3D networks the scale factor can be determined from either the site coordinates or from the baseline lengths. If

$$s = X/x = Y/y = Z/z \quad \text{and} \quad m = L/l$$

where XYZ and L are the coordinates and length in one network, and xyz and l are the corresponding coordinates

and length in the other network, then it can easily be shown that the two scale factors are the same, as follows -

$$m = \frac{Lij}{lij} = \frac{\sqrt{(Xj - Xi)^2 + (Yj - Yi)^2 + (Zj - Zi)^2}}{\sqrt{(xj - xi)^2 + (yj - yi)^2 + (zj - zi)^2}}$$

$$= \frac{\sqrt{(sxj - sxi)^2 + (syj - syi)^2 + (szj - szi)^2}}{\sqrt{(xj - xi)^2 + (yj - yi)^2 + (zj - zi)^2}}$$

$$= s \frac{\sqrt{(xj - xi)^2 + (yj - yi)^2 + (zj - zi)^2}}{\sqrt{(xj - xi)^2 + (yj - yi)^2 + (zj - zi)^2}}$$

$$= s$$

In deriving the above, it was assumed that none of the points are fixed. If one point is held fixed then the change in coordinates at other points will be more complicated. However the change in Cartesian baseline components will be affected as above.

In polar coordinates only the radius coordinate is changed when a scale factor is applied. The latitude and longitude remain the same. In cylindrical coordinates R and Z are changed, but again longitude is not affected. In ellipsoidal coordinates the longitude is not affected but the geodetic latitude is slightly affected. For example, a 1ppm scale change will change geodetic latitude by less than about 0.0007" (2cm). However the effect on ellipsoidal height is significant. For example, a 1ppm scale change will produce a change in height of about 6.4m. The formula for the effect of a scale factor on ellipsoidal coordinates is given in Chapter 7.

The estimate of the scale difference between VLBI and ground data, and its precision, may be more reliable if chord lengths are used instead of coordinates or coordinate differences between sites. This is because generally the estimate of accuracy of a VLBI baseline length is more reliable than that of the baseline components. The covariance terms are also less of a problem when converting the 'precision' VCV to an 'accuracy' VCV.

ANALYSIS PROCEDURES.

There are a number of ways of combining two data sets and some of these are discussed here.

1) A single one-step adjustment involving all data, such as distances and directions and even delays and rates, would need to solve for many parameters. Such an adjustment could not be economically computed for anything except a very small network.

2) Observation equations formed by the adjusted VLBI coordinates (or coordinate differences) can be included in the adjustment of the ground data. This method can quite simply allow for variations in scale and orientation factors across a region. However an adjustment of the ground data must be in progress. This is rarely the case because geodetic network adjustments are expensive and time consuming. Whether the ground adjustment is computed in 2D or 3D is also important and is considered below.

The inclusion of VLBI observation equations in a 3D adjustment of ground observations is equivalent to a transformation provided the rotation, scale and translation parameters are included in the observation equations. The transformation adjustments described above are equivalent to free net adjustments where the VLBI observation equations form one of the Helmert blocks in the ground adjustment.

It is important to adjust each network separately to check for outliers, systematic errors, and to do the statistical tests of the quality of the observations before the data sets are combined. If the VLBI coordinates are directly input into a ground adjustment then these checks are not possible unless separate adjustments of the ground data are computed, one with the VLBI data included and one without. The results of these two solutions then have to be compared.

3) Transformation parameters between the VLBI coordinates and the adjusted ground coordinates of the VLBI sites can be estimated. Only the preadjusted ground and VLBI coordinates of the common sites and their VCV matrices are required as input. This method is simple and the computation is not expensive.

The approach suggested by Krakiwsky and Thomson (1974) and applied in the examples in Chapter 7 is as follows. The terrestrial observations are adjusted in two dimensions (geodetic latitude and longitude), then orthometric heights are combined with the corresponding geoid heights to form triplets of ellipsoidal coordinates. Finally, these coordinates, together with their VCV matrix, are combined with the space (VLBI) coordinates in a 3D transformation adjustment.

4) Vincenty (1982) recommends that the adjustment of the terrestrial observations be first performed in two dimensions up to the stage of forming the least squares normal equations. Either the classical ellipsoidal or the '3D height fixed' approaches (see Chapter 5) can be used. The adjustment of the space data is done separately in 3D also up to the stage of forming the normal equations. Finally, the normal equations from the two systems are then combined.

Wolf (1980) suggests the space data should be a separate Helmert block in the ground adjustment. Thus the terrestrial and the space coordinates and their VCV matrices are not determined. The determination of the ground coordinates and their VCV may require inversion of a large normal equations matrix. This is then reinverted in the combination with space data. This problem arises when Doppler data is to be combined with ground data. However, since there are usually only a few VLBI points, the matrix of normal equations of the common points will not be large and therefore can be inverted without difficulty. Also,

since the adjusted coordinates and VCV of the ground net are probably desired for diagnostic and other purposes, the normal equations of the terrestrial net should be inverted before the VLBI data is added.

5) In a combined adjustment the differences in scale and orientation must be modelled. However, some analysts may suggest that the combined adjustment be computed without estimating the scale, rotation and translation parameters and then investigate the residuals for systematic effects. However if systematic errors are highly correlated with the estimated parameters, they will produce residual patterns that appear to be random. In this case the transformation parameter or systematic error might not be detected but would influence the results. Therefore this procedure has not been adopted in this thesis.

6) Wolf (1980 and 1982) recommends a sequential approach. He states that an internal 2D solution should be computed first, followed by a 3D solution for translation, rotation, and scale. The internal processing is done in 2D by eliminating the heights as unknowns so that height imperfections do not distort the results. One way of achieving this is to convert the VLBI data to ellipsoidal coordinates and ignore the heights. However before the 2D solution can be calculated one of the nets must be shifted, rotated and scaled to the datum of the other net. In order to produce the best external solution, a complete 3D solution using geoid undulations and orthometric elevations should be calculated. A change in these external parameters does not alter the adjusted baseline lengths of the 2D solution.

However, in photogrammetric applications Blais (1979) showed that 3D similarity transformations yield better stability in height with more homogeneity in planimetry (latitude and longitude) than the use of sequential planimetry-height methods. Therefore Wolf's sequential procedure is not adopted in this thesis.

The above discussion has outlined several analysis procedures. Each has been shown to have shortcomings except for the adopted method, that is to solve for the transformation parameters relating the preadjusted VLBI and ground coordinates.

The examples of the combined adjustment of ground and VLBI data given in Chapter 7 include only geometric data. A better approach is to include additional data such as gravity observations at and between the sites. This would improve the results by reducing some of the adverse effect of poor heights in the ground data. The inclusion of gravimetric data in the ground adjustment does not alter the analysis procedure for combining VLBI and ground data by transformation, unless it is also desired to adjust the gravimetric data. A rigorous adjustment technique which also adjusts gravity data is beyond the scope of this thesis.

DATA.

Before combining two nets the analyst must be sure the data in each net does not contain systematic and gross errors. If the nets are combined by a conformal transformation then each system must have uniform scale. Since the data is also combined in a stochastic sense the error estimates (VCV) must be reliable.

So far it has been tacitly assumed that the ground net is fully observed. However the ground net may not contain any azimuth observations or any distance observations. This often arises when only ground observations of the same epoch as the VLBI observations are included. If there are no azimuth observations then a single arbitrary azimuth should be included (it need not be accurate) and the ground data adjusted. In the transformation, the derived rotation parameters will be meaningless, but the internal adjustment and the estimated scale factor will be correct. Similarly, if there are no distances observations, an estimate of the

length of one line should be inserted and the ground data adjusted. The estimated scale factor will be meaningless, but the estimated rotation angles and the adjusted angles between the baselines will be correct. This matter is further discussed in Chapter 8 with regard to deformation analysis.

The origin of VLBI coordinates can be arbitrarily shifted. Hence, it is meaningless to solve for translation components (Tx,Ty,Tz). The VLBI data can be either coordinates or coordinate differences (ie. baseline components). It will be seen later that each will give the same results, the choice being a matter of convenience. If coordinate differences are used only independent baselines are adjusted. The simplest case is to use baselines from the fixed site to each other site. The VCV matrix of the components will then be the VCV matrix of the coordinates with the rows and columns of the fixed site removed.

Since both the ground and VLBI systems are aligned with the instantaneous rotation pole and corrections are applied to align them with the CTS frame, the rotation angles should be near zero. If the VLBI and ground coordinates were truly related to the same reference system, they could be more easily combined. However, even though both VLBI and ground coordinates are supposedly referred to the same CTS frame, there are a number of reasons for actual differences. Among these are:

1) Ground observations are usually made at different epochs to VLBI observations. Thus any errors in the earth rotation parameters or models will introduce rotations differences between the networks when reducing the observations to a common epoch.

2) Ground astronomic observations use a stellar catalogue while VLBI uses a radio source catalogue. The two types of catalogues are not perfectly aligned yet.

Ground data on the Australian Geodetic Datum, the European Datum, and the North American Datum are expected to differ from the CTS frame by translations and rotation angles of less than 200m and 2" respectively (Bomford, 1980).

All ground data must be referred to the same ellipsoid datum with no discontinuities at boundaries (such as between countries). It is quite likely that different parts of a continental geodetic network will have distortions in scale and orientation. If this is so, then it is better to solve for parameters in local and regional areas rather than one set of parameters for the whole of the continent. Moreover, all the VLBI data should refer to the same reference system. This consistency is an important consideration when using VLBI data from separate experiments or measurement campaigns. The VLBI results must thus come from a single solution where only one epoch of earth rotation parameters have been held fixed. Otherwise each VLBI data set will have a different orientation due to the errors in the adopted polar motion and UT at each fixed epoch. Also the same models and constants (eg tide models, precession constant, and speed of light) must be used in the reduction of all VLBI data.

Variance Covariance Matrices of Coordinates.

The stochastic model be correct as well as the mathematical model. As always, there is the problem of "internal" and "external" accuracy. The elements of the VCV matrices of the data may represent precision estimates. It is difficult to change these values to accuracies, especially the off-diagonal terms. The VCV matrices could be multiplied by one or more factors to account for the differences between internal and external accuracies. But how can these factors be determined? If only the diagonal terms are increased, for example by taking the rms of all error sources, or by scaling them, then the correlations will probably be reduced. Alternatively, the diagonal terms can be increased by the quadratic addition of other errors and then the

covariance terms increased so as to maintain the original correlations. There is no guarantee that this is a true representation of the actual VCV matrix but it may be a good approximation. Application of the covariance law (Jacobians) to add the effect of systematic errors to the VCV, is the best method. Unfortunately, it is based on functional relationships between the parameters and the systematic errors. These relationships may not be known.

The VCV matrix can be diagonal, block diagonal, or full. Considerable savings in computer resources can be made if the matrix is sparse. However, in practice the VCV is not diagonal, because the X, Y and Z coordinates of a point are correlated. Furthermore, the VCV is generally not block diagonal, because a coordinate of one point is correlated with coordinates of other points. Therefore full VCV matrices should be allowed for in the computation of transformation parameters. Assuming that the VCV is block diagonal or diagonal when in fact it is not would cause errors in the results and their VCV estimates. An example is given in Chapter 7.

The horizontal terrestrial coordinates, from a conventional 2D ellipsoidal adjustment, are usually combined with ellipsoid heights. It is assumed that these heights are not correlated with the horizontal coordinates. However, a small correlation exists because the deflections of the vertical and the ellipsoidal heights were used to reduce the observations to the ellipsoid before the adjustment of the horizontal network.

The precision of a geodetic network, or of a VLBI network, can be described by any number of VCV matrices which are all equivalent. This is because, in both systems, absolute coordinates have no physical meaning and therefore the variances of the coordinates have no real meaning. Only angles and distances can be determined by either technique and so only the variances of, and correlations between, these angles and distances are physically meaningful.

In both VLBI and ground adjustments the coordinates of one point are conventionally assigned zero variance. If only a portion of the ground net is to be used and it is a considerable distance from the fundamental point then the variances of coordinates of the points within this portion will usually be large. Strang van Hees (1982) gives formulae to convert VCV matrices so that they have minimum trace, or zero variances for some point(s) within the selected portion of the network. While the elements of the VCV of the coordinates change, the variances of the lengths and angles do not. Thus the translation parameters and absolute coordinates estimated from a combined ground - VLBI adjustment are meaningless. An example of the effect of this datum defect within the VCV matrix is given in Chapter 7.

The 3D confidence ellipsoid of the coordinates of a point in a network or the components of a baseline can be determined from the VCV matrix (eg. Vanicek and Krakiwsky, 1982). The lengths and orientations of the axes of the ellipsoid are useful in interpreting the quality of an adjustment.

Network Geometry.

The geometrical formulation of a similarity transformation represents a continuum. Replacing this continuum by a discrete set of common points can cause errors. Moreover, in the presence of observational and computational errors, the accuracy of the estimated parameters may vary considerably. This depends on the spatial distribution of the points used. Hence the implications of the spatial distribution of the points of the network must be studied.

Points should not be colinear because components of rotations about axes parallel to the line of points cannot be determined. For a stable solution it is important that the points are spatially well distributed. For example, a

network with one point which is a considerable distance from the rest of the net would give an unstable solution. An uneven geographical spread of points will cause the solution to be biased towards the areas of high density. Points in areas of low density will be disadvantaged and probably have large corrections to their coordinates. Thus an even geographical distribution of points is desirable.

PARAMETERS.

The minimum number of observations required to solve for the seven parameters of a conformal transformation is seven. This could comprise two common points, with their three coordinates known in each net, and a third point with three coordinates in one net known and one coordinate in the other net known. Three common points, each with their three coordinates known in each net, will yield a redundancy of two. However it is desirable to have at least four common sites because there should be at least four degrees of freedom in a solution for seven parameters.

Removing systematic errors in the observations can be very difficult because either the source of error or its magnitude may be unknown. The effects of systematic errors can be assessed by procedures such as the use of check points as described below.

One check for systematic model deformations is to compare the estimated transformation parameters from an adjustment using all common sites with those from another solution where one site has been eliminated (the check point). If the changes in the adjustment results are acceptable, then the adjustment is stable and reliable. The coordinates of the check point in one net should be transformed by the parameters determined by the second solution. The transformed coordinates should then be compared with the corresponding coordinates in the other net. Check points are a valuable tool but can give misleading information about the solution's stability if they are poorly chosen.

For instance, a check point in a cluster of points checks only the consistency within the cluster itself.

Parameters representing systematic errors can also be added to the basic similarity transformation of coordinates. This will be done in Chapter 7. Such an estimation procedure, where additional unknown parameters are included to account for possible systematic biases in the observations, is self-calibrating.

If the model includes a large number of parameters, the adjustment may lead to a poorly conditioned system of equations. Many parameters will usually fit the data better, that is produce smaller residuals, than a few parameters will. But the estimates of the parameters may not be accurate. Moreover, the degrees of freedom of the adjustment will be reduced and therefore the statistical tests will be less effective. When the rotation and translation components are highly correlated, non existing rotations may absorb part of the translation corrections. This occurs when the network covers only a small portion of the globe. If it is only desired to obtain a good internal adjustment then the high correlations between the parameters and these errors in the adjusted values of the parameters, are of no concern provided the solution is stable.

It should be noted that the scale difference may be due to systematic errors in the fixed terrestrial heights as well as an error in terrestrial distance scale.

One problem that arises with VLBI data is what to do with a net that contains a mix of S/X and S band baselines. It is not recommended that just S band data be used and only solve for a single scale factor. This is because the errors in S band baselines are not well represented by a simple scale factor. These errors depend on the orientation and length of each baseline and on local ionospheric conditions. Only those baselines which have been corrected

for ionospheric error should be used. However the effect of the ionospheric error may be smaller than can be detected in a combined adjustment with ground data. In such a case the error may be ignored provided the VCV of the VLBI data includes an allowance for the additional error due to the ionospheric effects.

LEAST SQUARES ADJUSTMENT.

Least squares adjustment theory is covered in many textbooks (eg. Mikhail, 1976). The particular method adopted here takes into account the a priori estimates of the parameters and their VCV. Both equations which relate observables to each other and equations which relate observables to the parameters to be estimated are incorporated. The notation of Krakiwsky (1981) has been adopted throughout this thesis.

The linearized mathematical model is -

$$A\Delta X + Bv + W = 0 \qquad (6.8)$$

and the results of adjustment are obtained from -

$$\Delta X = -(A^T(BQB^T)^{-1}A + Q_x^{-1})^{-1}\, A^T(BQB^T)^{-1}\, W \qquad (6.9)$$

$$v = -\, QB^T(BQB^T)^{-1}\, (A\Delta X + W) \qquad (6.10)$$

$$\tilde{\sigma}_o^2 = (v^T Q^{-1} v + \Delta X^T Q_x^{-1} \Delta X) \,/\, (n-u+u_x) \qquad (6.11)$$

$$Q_{x'} = \sigma_o^2 (A^T(BQB^T)^{-1}A + Q_x^{-1})^{-1} \qquad (6.12)$$

$$Q_{l'} = \sigma_o^2 \{Q + QB^T(BQB^T)^{-1}A(Q_{x'}/\sigma_o^2)A^T(BQB^T)^{-1}BQ - QB^T(BQB^T)^{-1}BQ\} \qquad (6.13)$$

where
- X are the a priori parameters
- X' are the adjusted parameters
- L are the observations
- L' are the adjusted observations
- $v = L' - L$ are the residuals
- $\Delta X = X' - X$ are the corrections to parameters
- $A = \partial F/\partial X$ at (X,L)
- $B = \partial F/\partial L$ at (X,L)
- $W = F(X,L)$
- Q = VCV matrix of observations

Qx = VCV matrix of a priori parameters

Ql' = VCV matrix of adjusted observations

Qx' = VCV matrix of adjusted parameters

n = number of observation equations (3 times the number of common points)

u = number of parameters

u_x = number of weighted parameters

It is well known that a least squares adjustment in phases is equivalent to a single step adjustment, provided that the VCV matrices are propagated correctly. However, for practical convenience, the observables (coordinates) are often assumed to be uncorrelated at various phases of the complete adjustment.

The normal equations form a symmetric positive definite coefficient matrix. Moreover, when the unknown parameters are properly ordered the matrix has a band structure. These properties can be exploited for greater computer efficiency, however the benefits only accrue when there are many observations. Since VLBI does not provide many points the special techniques to achieve greater efficiency are not discussed here.

The adjustment yields the optimum values of the parameters and adjusted observables only when all relevant information has been included. Thus auxiliary information, such as constraints between parameters or between the observables, and independent estimates of the parameters, should be included. This can improve the stability of the solution and reliability of the results. The use of a priori estimates of the parameters, or the a priori transformation of the coordinates of one net can also save the expense of extra adjustment iterations.

The whole process can only be partly automated. The analyst must decide which parameters to hold fixed, whether to accept the results of statistical tests, and which data to delete. He must also make judgements on the stability of

the solution and reliability of the results.

Computation errors.

A well-conditioned computational procedure gives numerically stable results. That is, the results do not change drastically when the initial conditions are slightly changed. So if an adjustment is stable the addition or removal of a few observations, or the presence of small errors in the observations, should not significantly affect the results. An ill-conditioned procedure is not stable. The calculation of the condition number provides a common test of whether a matrix, such as the coefficient matrix of the normal equations, is ill-conditioned. The condition number of a matrix can be defined as the largest eigenvalue divided by the smallest eigenvalue.

The effect of rounding errors in the computations may not be negligible. However, if the dimensions of the normal equations matrix are small then the effects of rounding errors should not be serious. One test for the effect of rounding and truncation errors is to repeat the computations using different internal precisions (in the computer program). The results are then compared. Changing the order of a long series of computations may also reveal magnitude of the effects of these errors.

A computer program may invert a nearly singular matrix and not give the analyst any indication that his solution is ill-conditioned. Therefore checks that determine if the matrix to be inverted is singular should be applied. One useful method is to calculate the condition number. This should be less than the number of significant digits carried by the computer. If the matrix is singular the rank defect should be investigated. Special computational techniques are also necessary if the range of variances in one of the VCV matrices is very large and the computer has a small dynamic range.

STATISTICAL TESTS.

The application of statistical tests can be a demanding task, especially when the data sets are large. Moreover, most tests require the full VCV matrices, which may be very large. However, because there are only several parameters in a transformation adjustment and there are usually only a few VLBI points, none of the following tasks are too demanding and should all be carried out.

Several statistical tests are discussed below. These tests assume that the observations and their residuals are normally distributed. So before the tests can be applied it is necessary to check that the residuals normally are distributed. If they are not normally distributed then the results of the adjustment are biased by systematic errors.

To test for normal distribution, U_x, the x th moment, is calculated from (Hoar, 1975) -

$$U_x = \frac{1}{n-1} \sum \left(\frac{v_i}{\sigma_i} \right)^x \qquad (6.14)$$

where v_i is the residual of the ith observation, σ_i is its standard deviation, n is the sample size. For a normal distribution -

$$U_1 = \text{Mean} = 0,\ U_2 = \text{Variance} = 1,\ U_3 = 0,\ U_4 = 3.$$

Skewness (γ_1) and kurtosis (γ_2) are calculated from (Kendall and Stuart, 1958) -

$$\gamma_1 = U_3 \ / \ U_2^3 \qquad (6.15)$$

$$\gamma_2 = \{U_4 \ / \ U_2^2\} - 3 \qquad (6.16)$$

For a symmetrical distribution, γ_1 will be zero. If γ_2 is greater than zero then the distribution is more sharply peaked than a normal distribution. If γ_2 is less than zero then the distribution is less sharply peaked than a normal distribution.

Altering the significance level of statistical tests may alter the outcome of the test. If a particular test is not satisfied it implies that either one, or a combination, of the mathematical model, statistical weights, and systematic

error corrections are questionable. If the results are sensitive to the weights of the observations, then a higher significance level than usual should be used. If the results are relatively insensitive to the weights, then the solution is stochastically stable and one can have more confidence in the results.

Tests of the a posteriori variance factor.

The F test is applied when there are two estimates, s_1^2 and s_2^2, of σ_1^2 and σ_2^2 and it is desired to know if these estimates indicate a significant difference between σ_1^2 and σ_2^2. Let s_1^2 be the larger of $\tilde{\sigma}_0^2$ and σ_0^2, and s_2^2 the smaller. Then

$$F = s_1^2 / s_2^2$$

The hypothesis that $s_1^2 > s_2^2$ should be rejected if $F > F_{\alpha,f1,f2}$, where f1 and f2 are the degrees of freedom in s_1^2 and s_2^2 respectively. If $\sigma_0^2 = 1$, and comes from an infinite population then a useful two-tail rejection test is as follows. Reject the hypothesis that $\tilde{\sigma}_0^2 = \sigma_0^2$ if

$$\tilde{\sigma}_0^2 < \frac{\chi^2_{1-\alpha/2,r}}{r} \quad \text{or} \quad \tilde{\sigma}_0^2 > \frac{\chi^2_{\alpha/2,r}}{r} \qquad (6.17)$$

If the test fails and $\tilde{\sigma}_0^2 < \sigma_0^2$, then the a priori estimates of the elements in the VCV matrix are too pessimistic. Similarly, if the test fails and $\tilde{\sigma}_0^2 > \sigma_0^2$ then the a priori estimates of the elements in the VCV matrix are too optimistic. These test are not valid if the models used in the adjustment are inaccurate.

A procedure which gives more accurate estimates of the degrees of freedom and the a posteriori variance factor ($\tilde{\sigma}_0^2$) was described in Chapter 4. Accurate estimates of these values are important because $\tilde{\sigma}_0^2$ is sometimes used to scale the variances of the results, and is used in the statistical tests. An example of the effects of errors in these values is given in Chapter 7. These considerations are even more important for strain analysis because there are more parameters and thus less degrees of freedom.

Tests of residual outliers.

After the adjustment the coordinates of each point should be tested for outliers. Even though the coordinates are obtained from previously tested adjustments they may still contain unknown systematic errors such as, local scale errors in the ground survey, and misidentification of the VLBI reference point during the ground survey.

When the residuals are correlated, it is inappropriate to use a simple rejection criterion based on 2.5 or 3 times the standard deviation of the residuals. Nevertheless this criteria is often applied because of its simplicity. More elaborate methods are given by Pope (1976) and Vanicek and Krakiwsky (1982).

Tests of the estimated parameters.

To determine whether the estimate of a parameter or group of parameters is significant the following multivariate tests should be applied. Calculate t from (Vanicek and Krakiwsky, 1982) -

$$t = (U-X)^T C_x^{-1} (U-X) \qquad (6.18)$$

where X is the vector of parameter estimates being tested, U is the vector of a priori values against which each Xi is being compared (often the null vector), and Cx is the estimated VCV of the parameters being tested. The vectors X and U may contain either all the parameters or some subset of them. If a subset is being tested then the corresponding portion of the VCV matrix of the parameters must be used. If only a single parameter is being tested, then it is obvious that

$$t = (u-x)^2 / \sigma_x^2 \qquad (6.19)$$

The hypothesis that $X_i \neq U_i$ should be rejected if -

$$t < \chi^2_{k,\alpha} \qquad (6.20)$$

where k is the number of parameters being tested and α is

the significance level. If X_i is not significantly different to U_i at the α level then the analyst can be $1-\alpha\%$ sure that the estimate(s) can be ignored and a readjustment safely computed holding the tested parameters fixed at the U_i values. For the test of a single parameter at the 95% confidence level, the parameter estimate is insignificant if its difference from the test value (u) is less than 1.96 times its standard deviation.

The above procedure tests the parameters simultaneously and is rigorous. All variances and covariances are taken into account. However, in the test (6.20) it is assumed that the a priori variance factor is known. If the a priori variance factor is not known, then the following test should be used (Mikhail, 1976) -

$$t' = (U-X)^T C_x^{-1} (U-X) / k \qquad (6.21)$$

where Cx is the estimated VCV matrix of the parameters, or the relevant portion of it, multiplied by the a posteriori estimate of the variance factor.

The hypothesis that $X_i \neq U_i$ should be rejected if -

$$t' < F_{k,r,\alpha} \qquad (6.22)$$

where r is the number of degrees of freedom in the adjustment. If a reliable VCV was used with the input data, then the a priori variance factor is known (=1). The estimated variance factor is then used only as a check (as in test 6.17). Otherwise test 6.22 should be used. The value of t' required to reject the hypothesis will be much larger than the value of t required in test 6.20, unless r is very large.

Effect of holding parameters fixed.

If some parameter estimates do not differ significantly from zero, it is advisable to recompute the adjustment with these parameters fixed at zero. The effect, of holding these parameters fixed, on the estimates of the other parameters, the adjusted coordinates, and the adjusted lengths should also be studied.

Knowledge of the effect of holding certain parameters fixed on the adjustment results is useful for studying error propagation in combinated adjustments of networks. One method to calculate the effects is simply to recompute the solution holding the relevant parameters fixed and then to compare the results of the two solutions. Since the number of common points will usually be small the recomputation should not be a problem.

If this method is undesirable, then covariance analysis can be used (see Chapter 3). To determine the changes to the adjusted observables, the covariances between the adjusted parameters and the adjusted observables are needed. The VCV matrix which relates the adjusted observables and the adjusted parameters is given by (Mikhail, 1976) -

$$Qxl = Qlx^T = -(A^T(BQB^T)^{-1}+Qx^{-1})^{-1}A^T(BQB^T)^{-1}BQ \qquad (6.23)$$

From this equation it is possible to calculate the effect of holding one or more parameters fixed on one or more coordinates. However this procedure calculates the covariances between the coordinates in the type used in the particular combination model eg. Cartesian or ellipsoidal. If the covariances between the parameters and the adjusted coordinates in a type different from that used in the model, or if the covariances between the parameters and the adjusted baseline lengths are required, then further computation is necessary.

The covariance law may be used to determine the covariances and correlations between the coordinates, of any type, and the parameters as follows.

$$\begin{bmatrix} Qc'c' & Qc'x \\ Qxc' & Qxx \end{bmatrix} = \begin{bmatrix} R & 0 \\ 0 & I \end{bmatrix} \begin{bmatrix} Qcc & Qcx \\ Qxc & Qxx \end{bmatrix} \begin{bmatrix} R & 0 \\ 0 & I \end{bmatrix} \qquad (6.24)$$

where Qc'c' is the VCV of the desired coordinates, Qcc is the VCV of the internal coordinates, Qxx is the VCV of the parameters and R is the matrix of derivatives of desired coordinates with respect to the internal coordinates (see Appendix A). Thus -

$$Qc'x = R\ Qcx \qquad (6.25)$$

R is also needed to convert the VCV of the coordinates from one coordinate type to another.

The covariance law may also be applied to determine the covariances and correlations between the baseline lengths and parameters as follows.

$$Qlx = S\ Qcx \qquad (6.26)$$

where S is the matrix of derivatives of baseline lengths with respect to the Cartesian coordinates. The matrix required to convert rectangular Cartesian coordinates to baseline lengths is given in Appendix A. S is also used for computing the VCV and correlations of the lengths.

These cross covariances yield cross correlations which are useful for interpreting the adjustment results. As well as being needed for the above calculations they reveal the dependency of the parameters on the lengths and coordinates, and the sensitivity of each parameter to errors in the lengths and coordinates.

CHAPTER 7.

COMBINATION MODELS.

In the previous chapter theoretical aspects of the combination of two data sets, specifically VLBI and ground data, were considered. This chapter presents several models suitable for combining and comparing the data sets. Geodetic networks normally cover only small portions of the globe. Thus some of the transformation parameters will be poorly determined. A number of techniques have been developed to improve the determination of these parameters, and will be mentioned below. For many applications, the internal adjustment of the network is also of interest. Each of the models given below is examined to determine their effect on the internal adjustment and on the estimated transformation parameters.

A computer program was written to compute the least squares adjustment of a number of the transformation models described in this chapter and the strain models described in Chapter 8. The transform and strain (TAS) program is described in Appendix B.

DATA.

The coordinates of the points of both nets are treated as observations and are adjusted. The transformation parameters are treated as quasi observables, so any a priori knowledge about them can be used. The a priori parameter estimates can be assigned appropriate variances. They can be held fixed or estimated as free parameters, by using very small or very large a priori variances respectively. It is not necessary to hold the coordinates of any point fixed. However this can be done if desired. None of the a priori variances should be exactly zero as that will cause singular matrices in the adjustment. If a point is to be held fixed its coordinates are assigned a very small variance, say $(0.1\text{mm})^2$, and all the covariances related to this point are set equal to zero.

To distinguish the two networks which are combined, one will be called the A network and the other the B network. The A network when transformed by the parameters yields the B network. In most models either the VLBI data or the ground data can be the A net and the other the B net. If the A and B nets are swapped the transformation is reversed. The adjusted coordinates and lengths will be the same. However the estimated rotation angles and translations will be of the same magnitude but of opposite sign to those obtained from the reverse transformation. The scale factor will be the reciprocal of that obtained from the reverse transformation.

Generally two data sets were used in the numerical examples given below. The first data set contained the results of the Australian VLBI experiment and the corresponding ground measurements. The VLBI data consisted of the results given in Chapter 4 and the associated precision VCV, which is known to be optimistic. The latitudes and longitudes of points in the ground net, and their VCV, were taken from GMA82 (see Chapter 4). The estimate of the variance, $(\pm\ 4m)^2$, of the ellipsoidal heights is probably conservative. These heights were assumed to be uncorrelated with the latitudes and longitudes.

The second data set was a simulated data set of five points which spanned a region of about 300km (see fig. 7.1). A program was written to create these simulated coordinates with full VCV matrices. Random noise was added to the site coordinates with zero mean and standard deviation equal to the corresponding standard deviation contained in the VCV matrix. The results of the simulation are given in Table 7.1.

Table 7.1 Simulated data set.

(a) Ground coordinates. (Ellipsoidal)

Latitude	Longitude	h(m)	Site
-35°37'35.368" ± 0.004"	148°57'12.862" ± 0.005"	946. ± 2.	Orroral
-35 24 14.366 ± 0.004	148 58 48.132 ± 0.005	680. ± 2.	Tidbinbilla
-33 51 38.927 ± 0.005	150 45 45.248 ± 0.004	59. ± 2.	Fleurs
-32 59 59.870 ± 0.006	148 15 44.293 ± 0.007	407. ± 2.	Parkes
-23 45 37.606 ± 0.012	133 52 51.884 ± 0.013	572. ± 2.	Alice Sp.
-29 2 51.874 ± 0.008	115 20 43.098 ± 0.010	283. ± 2.	Yarragadee
-42 50 44.934 ± 0.012	147 30 38.521 ± 0.017	20. ± 2.	Hobart
-34 0 0.000 ± 0.012	149 10 0.000 ± 0.017	200. ± 2.	MP
-12 30 0.000 ± 0.012	131 0 0.000 ± 0.017	50. ± 2.	Darwin
-12 0 0.000 ± 0.012	143 0 0.000 ± 0.017	50. ± 2.	Cape York
-35 10 0.000 ± 0.012	150 20 0.000 ± 0.017	5. ± 2.	BB
-35 0 0.000 ± 0.012	138 30 0.000 ± 0.017	50. ± 2.	Adelaide

(b) VLBI coordinates. (Cylindrical)

R(m)	Longitude (degs.)	Z(m)
5190936.492 ± 0.192	148.95235898 ± 0.0000007	-3695289.980 ± 0.138
5205063.127 ± 0.000	148.97882590 ± 0.0000000	-3675039.621 ± 0.000
5301841.406 ± 0.047	150.76140697 ± 0.0000002	-3533824.488 ± 0.047
5354740.543 ± 0.047	148.26111250 ± 0.0000002	-3454332.709 ± 0.047
5841168.838 ± 0.047	133.87982117 ± 0.0000002	-2554410.775 ± 0.047
5580513.802 ± 0.047	115.34388187 ± 0.0000002	-3078819.137 ± 0.047
4683550.357 ± 0.047	147.50934300 ± 0.0000002	-4315124.647 ± 0.047
5293343.857 ± 0.047	149.16548057 ± 0.0000002	-3546713.414 ± 0.047
6227945.728 ± 0.047	130.99880942 ± 0.0000002	-1371624.635 ± 0.047
6239657.136 ± 0.047	142.99890365 ± 0.0000002	-1317572.275 ± 0.047
5219720.200 ± 0.047	150.33215182 ± 0.0000002	-3653155.280 ± 0.047
5230407.821 ± 0.047	138.49864651 ± 0.0000002	-3638050.529 ± 0.047

(c) Approximate transformation parameters

Scale difference	-3.0 ppm		
Rotation about X axis	0.8"	Translation along X axis	110. m
Rotation about Y axis	1.0"	Translation along Y axis	60. m
Rotation about Z axis	0.2"	Translation along Z axis	-120. m

matrices which are closer to diagonal in one system than in the other. This would lead to advantages in converting the precision VCV to an accurate VCV, and computer savings if only diagonal terms are needed instead of the full VCV. The use of baseline components or just the baseline lengths instead of site coordinates are considered below.

Bursa-Wolf model.

This model, presented by Bursa (1965) and Wolf (1963), solves for a 7 parameter transformation - a scale factor, 3 rotation angles, and 3 translation components.

$$0 = F = s\,R \begin{bmatrix} x_A \\ y_A \\ z_A \end{bmatrix} + \begin{bmatrix} Tx \\ Ty \\ Tz \end{bmatrix} - \begin{bmatrix} x_B \\ y_B \\ z_B \end{bmatrix}$$

where R (= Rz(k) Ry(θ) Rx(ω)) is the rotation matrix about the axes of the xyz_A system, x_A, y_A, and z_A are the coordinates of points in the A net, x_B, y_B, and z_B are the coordinates of points in the B net, s is the scale factor, and Tx, Ty, and Tz are the translations, that is, the coordinates of the origin of the xyz_A system in the xyz_B system (see figure 7.2).

Allowing for rotation angles of any size, the design matrices of the least squares adjustment are, (Mikhail, 1976) -

$$Ai = \begin{bmatrix} \frac{\partial F}{\partial s} & \frac{\partial F}{\partial \omega} & \frac{\partial F}{\partial \theta} & \frac{\partial F}{\partial k} & \frac{\partial F}{\partial Tx} & \frac{\partial F}{\partial Ty} & \frac{\partial F}{\partial Tz} \end{bmatrix}$$

where $\partial F/\partial s = R\,x$

$$\frac{\partial F}{\partial \omega} = s\,R \begin{bmatrix} 0 & 0 & 0 \\ 0 & 0 & 1 \\ 0 & -1 & 0 \end{bmatrix} \begin{bmatrix} x_A \\ y_A \\ z_A \end{bmatrix}$$

$$\frac{\partial F}{\partial \theta} = s \begin{bmatrix} 0 & 0 & -\cos k \\ 0 & 0 & \sin k \\ \cos k & -\sin k & 0 \end{bmatrix} R \begin{bmatrix} x_A \\ y_A \\ z_A \end{bmatrix}$$

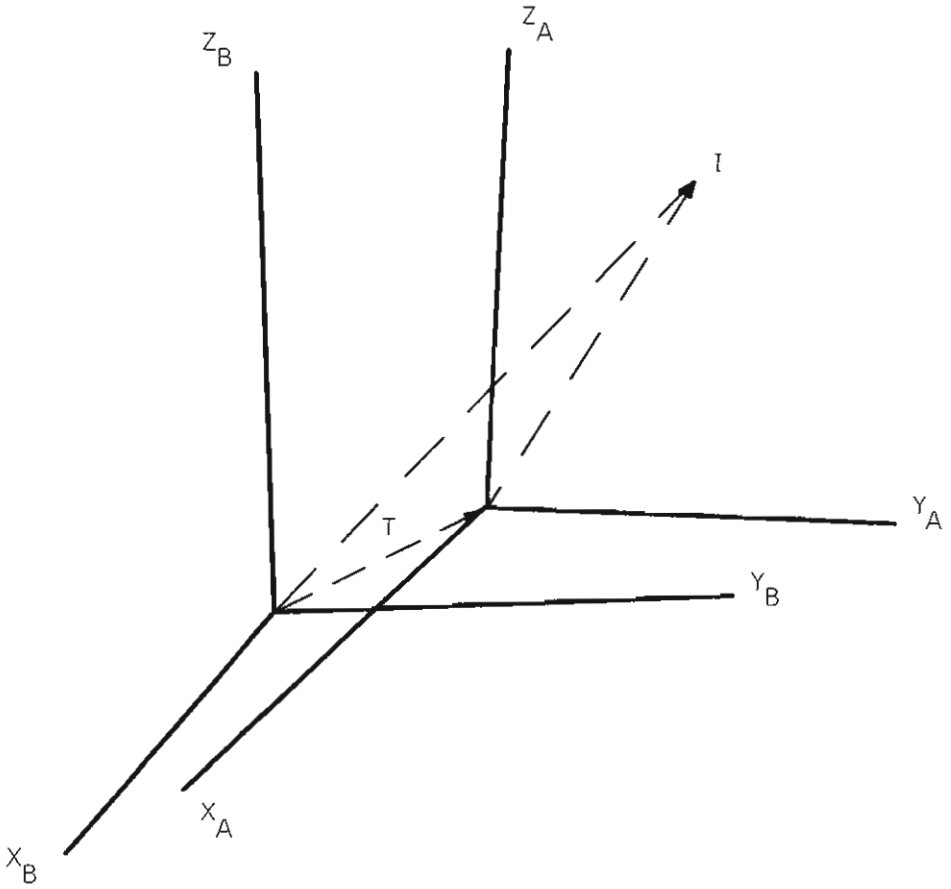

Figure 7.2 Bursa - Wolf model.

$$\frac{\partial F}{\partial k} = s \begin{bmatrix} 0 & 1 & 0 \\ -1 & 0 & 0 \\ 0 & 0 & 0 \end{bmatrix} R \begin{bmatrix} x_A \\ y_A \\ z_A \end{bmatrix}$$

$$\begin{bmatrix} \frac{\partial F}{\partial Tx} & \frac{\partial F}{\partial Ty} & \frac{\partial F}{\partial Tz} \end{bmatrix} = \begin{bmatrix} 1 & 0 & 0 \\ 0 & 1 & 0 \\ 0 & 0 & 1 \end{bmatrix}$$

Ai is a 3 x 7 matrix, and $A = [\, A_1 \; A_2 \; A_3 \; . \; . \; . \; A_n \,]^T$

$$Bi = \begin{bmatrix} \frac{\partial F}{\partial x_A} & \frac{\partial F}{\partial y_A} & \frac{\partial F}{\partial z_A} & \frac{\partial F}{\partial x_B} & \frac{\partial F}{\partial y_B} & \frac{\partial F}{\partial z_B} \end{bmatrix}$$

where

$$\begin{bmatrix} \frac{\partial F}{\partial x_A} & \frac{\partial F}{\partial y_A} & \frac{\partial F}{\partial z_A} \end{bmatrix} = s\, R$$

$$\begin{bmatrix} \frac{\partial F}{\partial x_B} & \frac{\partial F}{\partial y_B} & \frac{\partial F}{\partial z_B} \end{bmatrix} = \begin{bmatrix} -1 & 0 & 0 \\ 0 & -1 & 0 \\ 0 & 0 & -1 \end{bmatrix}$$

Bi is a 3 x 6 matrix and

$$B = \begin{bmatrix} B_1 & 0 & 0 & 0 & \cdots \\ 0 & B_2 & 0 & 0 & \cdots \\ 0 & 0 & B_3 & 0 & \cdots \\ \cdots & & & & B_n \end{bmatrix}$$

The observation vector is -

$$L = (x_{A1}\ y_{A1}\ z_{A1}\ x_{B1}\ y_{B1}\ z_{B1}\ x_{A2}\ y_{A2}\ z_{A2}\ x_{B2}\ y_{B2}\ z_{B2}\ \ldots)^T$$

Thus the residual vector is of the form -

$$V = (vx_{A1}\ vy_{A1}\ vz_{A1}\ vx_{B1}\ vy_{B1}\ vz_{B1}\ vx_{A2}\ vy_{A2}\ vz_{A2}\ vx_{B2}\ \ldots)^T$$

and the VCV matrix of the observations, both a priori and a posteriori is of the form -

$$Q = \begin{bmatrix} QxA1 & 0 & QxA1xA2 & 0 & QxA1xA3 & \cdots \\ 0 & QxB1 & 0 & QxB1xB2 & 0 & \cdots \\ & 0 & QxA2 & 0 & QxA2xA3 & \cdots \\ & & 0 & QxB2 & 0 & \cdots \\ sym. & & \cdots & & & etc \end{bmatrix}$$

where, for example,

$$QxA1 = \begin{bmatrix} \sigma^2_{xA1} & \sigma_{xA1yA1} & \sigma_{xA1zA1} \\ \sigma_{xA1yA1} & \sigma^2_{yA1} & \sigma_{yA1zA1} \\ \sigma_{xA1zA1} & \sigma_{yA1zA1} & \sigma^2_{zA1} \end{bmatrix}$$

and

$$QxA1xA2 = \begin{bmatrix} \sigma_{xA1xA2} & \sigma_{xA1yA2} & \sigma_{xA1zA2} \\ \sigma_{yA1xA2} & \sigma_{yA1yA2} & \sigma_{yA1zA2} \\ \sigma_{zA1xA2} & \sigma_{zA1yA2} & \sigma_{zA1zA2} \end{bmatrix}$$

The terms Q_{xiXj} are assumed to equal zero, that is, the correlations between the measurements of the two networks are assumed to be zero. This is valid when two independent measurement techniques are used. However correlations between the two data sets could be allowed for if the two data sets are not independent. The largest matrix to be inverted when using this model is 6n x 6n, where n is the number of common points.

Initially an analyst should solve for all seven parameters and then test their estimates using statistical test 6.20 or 6.22. If a subset of parameters is found to be insignificantly different to zero then another solution could be calculated with those parameters held fixed at

zero.

One well known problem is that generally the adjusted parameters are very highly correlated because the data covers only a small portion of the globe. Kumar (1972) points out that the scale factor can be determined from the chord lengths independently from the other parameters. Therefore the scale and its precision can be determined and then used as a priori constraints in the calculation of the other parameters. Such a solution was calculated and the adjusted lengths did not differ from those obtained from the usual procedure but the estimates of the translation parameters did improve.

Examples.

All seven parameters were estimated from the real data. The results are given in Tables 7.2, 7.3 and 7.4.

The rotations were highly correlated (~0.9) with the translations but the other correlations were not large. The $\tilde{\sigma}_0^2$ was 1.09 and passed test 6.17 at the 95% confidence level. This was surprising considering the known inadequacies of the a priori VCV matrices. The corrections to all coordinates and baseline lengths were in statistical agreement with their a priori variances. So no erroneous observations were detected. The condition number of N+Px, ie the normal equations, was 2.7×10^5. There were no weighted parameters and eight degrees of freedom. The statistical moments of the residuals were -

u1 = -0.1, u2 = 1.4, skewness = -0.5, kurtosis = 23.

The parameter estimates were individually statistically tested using eqn. 6.19, at the 95% confidence level. The estimates of scale factor, and rotations about the Y and Z axes were found to be insignificantly different from zero. According to this individual test the rotation about the X axis was significant, as were the three translation terms. The multivariable test (eqn. 6.22) which considers the

Table 7.2. Adjusted parameters obtained from the combination of the Australian VLBI and ground data (Bursa-Wolf model).

(a) Adjusted transformation parameters.

Parameter	Adjusted value
Scale factor (s)	0.303 ± 0.448 ppm
Rotation about X axis (ω)	-0.790 ± 0.315 secs
Rotation about Y axis (θ)	-1.078 ± 0.659 secs
Rotation about Z axis (k)	-0.142 ± 0.613 secs
Translation along X axis	-109.111 ± 18.428 m
Translation along Y axis	-64.439 ± 16.627 m
Translation along Z axis	118.734 ± 15.767 m

(b) Correlations between adjusted parameters.

	s	ω	θ	k	Tx	Ty	Tz
s	1.000						
ω	-0.109	1.000					
θ	0.320	0.139	1.000				
k	0.340	-0.447	0.795	1.000			
Tx	-0.293	0.118	-0.958	-0.929	1.000		
Ty	-0.346	0.685	-0.603	-0.957	0.790	1.000	
Tz	0.314	0.398	0.961	0.612	-0.847	-0.375	1.000

correlations between parameter estimates, was also applied. The s, θ, k subset of parameters was again found to be insignificantly different to the null vector at 95% confidence. However the subset s, ω, θ, k was also found to be insignificant. This conflicts with the individual parameter test for ω. So a transformation solution was computed with s, θ, and k constrained to zero. This solution gave an estimate of ω which was not significant at the 95% confidence level. This agrees with the multivariable test above. So a final solution was computed constraining the scale difference and all rotation angles to zero, thus estimating only the three translation terms. The $\tilde{\sigma}_0^2$ still passed its statistical test.

Table 7.3. Baseline lengths obtained from the combination of the Australian VLBI and ground data. (Bursa-Wolf model).

Baseline	A priori lengths (m) Ground	A priori lengths (m) VLBI	Adjusted lengths (m) Ground	Adjusted lengths (m) VLBI
T-P	274 751.885 ± 0.206	274 751.785 ± 0.032	274 751.711 ± 0.125	274 751.795 ± 0.031
T-F	236 680.956 ± 0.131	236 681.144 ± 0.069	236 681.021 ± 0.101	236 681.092 ± 0.060
P-F	251 341.008 ± 0.195	251 340.717 ± 0.068	251 340.679 ± 0.121	251 340.755 ± 0.062
T-A	1938 994.754 ± 0.943	1938 997.083 ± 1.259	1938 995.419 ± 0.743	1938 996.007 ± 0.813
P-A	1733 989.558 ± 0.869	1733 991.057 ± 1.194	1733 989.573 ± 0.692	1733 990.098 ± 0.777
F-A	1979 706.741 ± 0.956	1979 707.776 ± 1.164	1979 706.319 ± 0.746	1979 706.919 ± 0.767
T-H	835 298.387 ± 0.532	835 297.046 ± 3.516	835 298.695 ± 0.484	835 298.948 ± 0.556
P-H	1093 518.802 ± 0.628	1093 516.798 ± 3.634	1093 518.542 ± 0.527	1093 518.874 ± 0.576
F-H	1035 710.354 ± 0.601	1035 708.950 ± 3.432	1035 710.265 ± 0.518	1035 710.579 ± 0.572
A-H	2445 610.458 ± 1.193	2445 610.440 ± 3.847	2445 610.901 ± 1.042	2445 611.642 ± 1.323

T = Tidbinbilla, P = Parkes, F = Fleurs, A = Alice Springs, H = Hobart.
The adjusted σ have not been multiplied by $\tilde{\sigma}_o^2$ (=1.09).

Table 7.4 Adjusted coordinates obtained from the combination of the Australian VLBI and ground data. (Bursa-Wolf model).

(a) Adjusted ground coordinates. (AGD ellipsoidal)

Site	Latitude	Δ	Longitude	Δ	Ellipsoidal Height	Δ
					m	m m
T	-35°24'14".3678	± 0".0039 (-".0014)	148°58'48".1321	± 0".0047 (0".0002)	683.64	± 1.99 (3.43)
P	-32 59 59.8774	± 0.0046 (-.0071)	148 15 44.2980	± 0.0046 (0.0053)	405.08	± 2.07 (-2.33)
F	-33 51 38.9259	± 0.0036 (0.0007)	150 45 45.2484	± 0.0037 (0.0000)	55.17	± 2.42 (-3.35)
A	-23 45 37.6038	± 0.0118 (0.0026)	133 52 51.8844	± 0.0128 (0.0007)	572.78	± 3.66 (0.48)
H	-42 50 44.9337	± 0.0117 (0.0002)	147 30 38.5177	± 0.0167 (-.0036)	21.79	± 3.28 (1.78)

(b) Adjusted VLBI coordinates. (Cylindrical)

	R (m)	Δ	Longitude	Δ	Z (m)	Δ
T	5205 251.365	± 0.000 (0.000)	148°58'52".6048	± 0".0000 (0".0000)	-3674 748.367	± 0.000 (0.000)
P	5354 918.852	± 0.047 (0.002)	148 15 48.6942	± 0.0007 (-.0001)	-3454 035.788	± 0.047 (0.010)
F	5302 029.193	± 0.191 (-.034)	150 45 49.5427	± 0.0022 (0.0002)	-3533 527.963	± 0.136 (-0.067)
A	5841 280.822	± 0.810 (0.052)	133 52 56.4811	± 0.0253 (-.0041)	-2554 106.901	± 1.411 (-2.041)
H	4683 737.914	± 1.094 (-.395)	147 30 43.5540	± 0.0257 (0.0541)	-4314 841.103	± 1.146 (-2.418)

T = Tidbinbilla, P = Parkes, F = Fleurs, A = Alice Springs, H = Hobart.

Δ = Change from apriori coordinates.

A procedure which gives more accurate estimates of the degrees of freedom and of the a posteriori variance factor (was described in Chapter 4). As an example a solution was calculated with the real data set with a priori standard deviations on the scale, 3 rotation and 3 translation parameters of 5ppm, 5", and 15m respectively. In this solution there were 9.24 degrees of freedom and 1.24 weighted parameters compared with eight degrees of freedom and zero weighted parameters in an adjustment with no a priori constraints on the parameters. The share of the variance factor due to the parameter weights was 18%.
It would be difficult to estimate the effect of the a priori weights of the parameters on the degrees of freedom, the variance factor, and the estimated precisions of the adjusted parameters, without using the above mentioned procedure. If the conventional approximate formula was used then assuming the a priori weights were having no effect would yield 8 degrees of freedom, and assuming all seven weights were having a significant effect would yield 15 degrees of freedom.

Another solution was computed using only the block diagonal portion of the VCV matrices. Correlations between the coordinates of one point were present, but there were no correlations with the coordinates of other points. This solution, when compared with the corresponding solution which used the full VCV matrices, gave a smaller variance factor (0.84 compared to 1.1), small changes in the adjusted values of coordinates ($\sigma/4$), lengths and transformation parameters and small changes in their precisions. Similarly, a solution using only the diagonal elements of the VCV matrices was computed. This gave an even smaller variance factor (0.73), and differences in adjusted values of the order of half of their precision. It therefore appears that the use of reduced VCV matrices does not cause large errors in the results for this data set.

A seven parameter solution was again computed, but with the Hobart data deleted. The estimates of the scale and

rotation parameters were not statistically significant. Another solution, in which both Hobart and Alice Springs coordinates were deleted, yielded statistically insignificant estimates of all seven parameters. This is because the baselines used were shorter and the precisions of the estimated parameters poorer.

As an example of the effect of the datum defect within the VCV matrix the VCV of the ground net of the real data, which is relative to the Johnston origin, was converted so that the coordinates of Tidbinbilla had zero variances. The VCV was converted by using Jacobian matrices based on a direct translation of origin from Johnston to Tidbinbilla. Other procedures such as allowing for rotation and scale, a shift of origin to the simple (not weighted) barycentre of the network, or the minimum trace conversion method, could also have been applied (Strang van Hees, 1982). A seven parameter Bursa-Wolf transformation was then computed and the results compared with those in Tables 7.2, 7.3 and 7.4. It was found that the adjusted (and a priori) lengths and their precisions were the same. The adjusted scale and rotation parameters and their precisions and correlations, and the adjusted VLBI coordinates and their VCV were also the same. However the adjusted translation parameters, their precisions, and the adjusted ground coordinates and their VCV were slightly different. This is further evidence that the resultant translation parameters and absolute coordinates are physically meaningless in a combined ground - VLBI adjustment.

Molodensky-Badekas model.

This model (Badekas, 1969), which removes the high correlation between parameters by relating them to the centroid (m) of the network, is represented by -

$$O = F = \begin{bmatrix} xm \\ ym \\ zm \end{bmatrix} + \begin{bmatrix} Tx \\ Ty \\ Tz \end{bmatrix} + s\,R \begin{bmatrix} x_A - xm \\ y_A - ym \\ z_A - zm \end{bmatrix} - \begin{bmatrix} x_B \\ y_B \\ z_B \end{bmatrix}$$

where $xm = \sum x_{Ai}/n$, $ym = \sum y_{Ai}/n$, $zm = \sum z_{Ai}/n$.

Alternatively m can represent the initial point of the terrestrial network.

This model gives the same answers as the Bursa-Wolf model for the internal adjustment, and the scale and rotation parameters. However the translation parameters are different and have smaller a posteriori precisions. This can be readily seen if the equation is rewritten as-

$$F = P + Q$$

where
$$P = \begin{bmatrix} xm \\ ym \\ zm \end{bmatrix} - s\,R \begin{bmatrix} xm \\ ym \\ zm \end{bmatrix}$$

and
$$Q = \begin{bmatrix} Tx \\ Ty \\ Tz \end{bmatrix} + s\,R \begin{bmatrix} x_A \\ y_A \\ z_A \end{bmatrix} - \begin{bmatrix} x_B \\ y_B \\ z_B \end{bmatrix}$$

Q is the standard Bursa-Wolf model. P is a constant term, that is, it is the same for all points, and obviously affects the translation terms. The derived values of s and R are determined by Q and thus equal those from the Bursa-Wolf model. If s and R are approximately equal to unity and the identity matrix respectively, then the model is very similar to the Bursa-Wolf model. Clearly the difference in the translation terms obtained from the two models is due to the scaling and rotating of the point m.

The least squares design matrices are -

$$Ai = \begin{bmatrix} \frac{\partial F}{\partial s} & \frac{\partial F}{\partial \omega} & \frac{\partial F}{\partial \theta} & \frac{\partial F}{\partial k} & \frac{\partial F}{\partial Tx} & \frac{\partial F}{\partial Ty} & \frac{\partial F}{\partial Tz} \end{bmatrix}$$

$$\frac{\partial F}{\partial s} = R \begin{bmatrix} x_A - xm \\ y_A - ym \\ z_A - zm \end{bmatrix}$$

$$\frac{\partial F}{\partial \omega} = s\,R \begin{bmatrix} 0 & 0 & 0 \\ 0 & 0 & 1 \\ 0 & -1 & 0 \end{bmatrix} \begin{bmatrix} x_A - xm \\ y_A - ym \\ z_A - zm \end{bmatrix}$$

$$\frac{\partial F}{\partial \theta} = s \begin{bmatrix} 0 & 0 & -\cos k \\ 0 & 0 & \sin k \\ \cos k & -\sin k & 0 \end{bmatrix} R \begin{bmatrix} x_A - xm \\ y_A - ym \\ z_A - zm \end{bmatrix}$$

$$\frac{\partial F}{\partial k} = s \begin{bmatrix} 0 & 1 & 0 \\ -1 & 0 & 0 \\ 0 & 0 & 0 \end{bmatrix} R \begin{bmatrix} x_A - xm \\ y_A - ym \\ z_A - zm \end{bmatrix}$$

$$\begin{bmatrix} \frac{\partial F}{\partial Tx} & \frac{\partial F}{\partial Ty} & \frac{\partial F}{\partial Tz} \end{bmatrix} = \begin{bmatrix} 1 & 0 & 0 \\ 0 & 1 & 0 \\ 0 & 0 & 1 \end{bmatrix}$$

$$Bi = [\ \partial F/\partial x \ \ \partial F/\partial X\ ]$$

where $\partial F/\partial x_A = s\ R$ and $\partial F/\partial x_B = \begin{bmatrix} -1 & 0 & 0 \\ 0 & -1 & 0 \\ 0 & 0 & -1 \end{bmatrix}$

The adjusted coordinates, baseline lengths, scale factor and rotation angles, their VCV matrices and the variance factor computed from this model are the same as those from a corresponding Bursa-Wolf solution. However the translations are different and their precisions are generally an order of magnitude smaller.

Ellipsoidal model.

The model given here is a combination of that given by Wolf (1963) and equation A.10. However it is rewritten in matrix form with different notation. The ellipsoidal model of Zhou (1983) makes approximations about the M, N and h terms and is less rigorous.

$$F = 0 = \begin{bmatrix} \phi \\ \lambda \\ h \end{bmatrix} - \begin{bmatrix} \phi_t \\ \lambda_t \\ h_t \end{bmatrix} + Cs + D \begin{bmatrix} \omega \\ \theta \\ k \end{bmatrix} + E \begin{bmatrix} Tx \\ Ty \\ Tz \end{bmatrix}$$

where $$C = \begin{bmatrix} -Ne^2 \sin\phi\cos\phi/(M+h) \\ 0 \\ N(1-e^2\sin^2\phi)+h \end{bmatrix}$$

$$D = \begin{bmatrix} -\sin\lambda\{N(1-e^2\sin^2\phi)+h\}/(M+h) & \cos\lambda\{N(1-e^2\sin^2\phi)+h\}/(M+h) & 0 \\ \{(1-e^2)N+h\}\tan\phi\cos\lambda/(N+h) & \{(1-e^2)N+h\}\tan\phi\sin\lambda/(N+h) & -1 \\ -Ne^2\sin\phi\cos\phi\sin\lambda & Ne^2\sin\phi\cos\phi\cos\lambda & 0 \end{bmatrix}$$

$$E = \begin{bmatrix} \frac{-\sin\phi\cos\lambda}{(M+h)} & \frac{-\sin\phi\sin\lambda}{(M+h)} & \frac{\cos\phi}{(M+h)} \\ \frac{-\sin\lambda}{(N+h)\cos\phi} & \frac{\cos\lambda}{(N+h)\cos\phi} & 0 \\ \cos\phi\cos\lambda & \cos\phi\sin\lambda & \sin\phi \end{bmatrix}$$

where $N = \dfrac{a}{\sqrt{1-e^2\sin^2\phi}}$ and $M = \dfrac{a(1-e^2)}{(1-e^2\sin^2\phi)^{3/2}}$

and ϕ_t is the geodetic latitude, λ_t is the longitude and h_t is the ellipsoidal height in the B net. ϕ, λ, and h are the corresponding coordinates in the A net.

This model assumes that the coordinates of points in both networks are based on ellipsoids with the same parameters, a and e^2. If they are not, one network should have its coordinates and VCV matrix converted so as to refer to the ellipsoid of the other net, or the model should be extended to cater for different shaped ellipsoids as in Vanicek and Krakiwsky (1982).

The least squares design matrices are -

$$Ai = \begin{bmatrix} \frac{\partial F}{\partial s} & \frac{\partial F}{\partial \omega} & \frac{\partial F}{\partial \theta} & \frac{\partial F}{\partial k} & \frac{\partial F}{\partial Tx} & \frac{\partial F}{\partial Ty} & \frac{\partial F}{\partial Tz} \end{bmatrix}$$

$$= [\ C\ D\ E\ ]$$

$$Bi = \begin{bmatrix} \frac{\partial F}{\partial \phi} & \frac{\partial F}{\partial \lambda} & \frac{\partial F}{\partial h} & \frac{\partial F}{\partial \phi_t} & \frac{\partial F}{\partial \lambda_t} & \frac{\partial F}{\partial h_t} \end{bmatrix}$$

$$\frac{\partial F}{\partial \phi} = \begin{bmatrix} 1 - D1(\cos\lambda\ Tx + \sin\phi\ Ty) + D2Tz + D3(\theta\cos\lambda - \omega\sin\lambda) - e^2sD4 \\ -D5(\sin\lambda\ Tx - \cos\lambda\ Ty) - D6(\omega\cos\lambda + \theta\sin\lambda) \\ -\sin\phi(\cos\lambda\ Tx + \sin\lambda\ Ty) + \cos\phi Tz + D7e^2(\theta\cos\lambda - \omega\sin\lambda) - sD8 \end{bmatrix}$$

where

$D1 = \cos\phi/(M+h) - \sin\phi(\partial M/\partial\phi)/(M+h)^2$

$D2 = -\sin\phi/(M+h) - \cos\phi(\partial M/\partial\phi)/(M+h)^2$

$D3 = \{(\partial N/\partial\phi) - 2e^2\sin\phi\cos\phi\}/(M+h) + (\partial M/\partial\phi)(e^2\sin^2\phi - N - h)/(M+h)^2$

$D4 = D7/(M+h) - \{N\sin\phi\cos\phi(\partial M\partial\phi)\}/(M+h)^2$

$D5 = \{(N+h)\sin\phi - \cos\phi(\partial N\partial\phi)\}/\{(N+h)\cos\phi\}^2$

$D6 = \{(1-e^2)(N\sec^2\phi + \tan\phi\partial N/\partial\phi) + h\sec^2\phi\}/(N+h)$
$\quad - \{(1-e^2)N+h\}\tan\phi(\partial N/\partial\phi)/(N+h)^2$

$D7 = \sin\phi\cos\phi(\partial N/\partial\phi) + N\cos^2\phi - N\sin^2\phi$

$D8 = -Ne^2\sin\phi\cos\phi$

$$\text{and} \quad \partial N/\partial \phi = Ne^2 \sin\phi\cos\phi/(1-e^2\sin^2\phi)$$

$$\partial M/\partial \phi = 3Me^2 \sin\phi\cos\phi/(1-e^2\sin^2\phi)$$

$$\frac{\partial F}{\partial \lambda} = \begin{bmatrix} \{\sin\phi(\sin\lambda\ Tx - \cos\lambda\ Ty) - [N(1-e^2\sin^2\phi)+h](\omega\cos\lambda+\theta\sin\lambda)\}/(M+h) \\ 1-(Tx\cos B+Ty\sin\lambda)/\{(N+h)\cos\phi\}-\{(1-e^2)N+h\}\tan\phi(\omega\sin\lambda-\theta\cos\lambda)/(N+h) \\ -\cos\phi(\sin\lambda\ Tx - \cos\lambda\ Ty) - Ne^2\sin\phi\cos\phi(\omega\cos\lambda + \theta\sin\lambda) \end{bmatrix}$$

$$\frac{\partial F}{\partial h} = \begin{bmatrix} \sin\phi(\cos\lambda\ Tx + \sin\lambda\ Ty) - \cos\phi\ Tz + sNe^2\sin\phi\cos\phi/(M+h)^2 \\ \quad + [N(1-e^2\sin^2\phi)M](\omega\sin\lambda - \theta\cos\lambda) \\ \{\sin\lambda\ Tx - \cos\lambda\ Ty + Ne^2\sin\phi(\omega\cos\lambda + \theta\sin\lambda)\}/\cos\phi(N+h)^2 \\ 1 + s \end{bmatrix}$$

$$\begin{bmatrix} \frac{\partial F}{\partial \phi_t} & \frac{\partial F}{\partial \lambda_t} & \frac{\partial F}{\partial h_t} \end{bmatrix} = \begin{bmatrix} -1 & 0 & 0 \\ 0 & -1 & 0 \\ 0 & 0 & -1 \end{bmatrix}$$

The ellipsoidal method should produce the same results as a Bursa-Wolf solution because the same parameters are being estimated, and the Cartesian and ellipsoidal coordinates can be related. So the two models can be used as a check of the programming, the formulae of both models, and the conversion of VCV matrices and coordinates from the input data type to either ellipsoidal or Cartesian.

However, a question of whether the ellipsoidal model or one of the Cartesian models (eg Bursa-Wolf or Molodensky-Badekas) is preferable may arise. The least squares adjustment procedure linearises the models by using the first partial derivatives. If higher order partial derivatives of the Cartesian or ellipsoidal models, or both, are significant then the least squares adjustment will not give accurate answers for the adjusted observations and parameters. The differences between the results and the observation residuals obtained from each method can be statistically tested (see eg Fubara, 1972) and the better method chosen. In solutions obtained with real data and the simulated data, the differences between the results from each of the above models have been less than 1mm for adjusted lengths and coordinates and may therefore be ignored. The differences in the parameters were also found to be insignificant.

Cartesian baseline components.

The model is -

$$0 = F = s\,R \begin{bmatrix} \Delta x_A \\ \Delta y_A \\ \Delta z_A \end{bmatrix} - \begin{bmatrix} \Delta x_B \\ \Delta y_B \\ \Delta z_B \end{bmatrix}$$

where R is as above and Δx_A Δy_A Δz_A are the baseline components of the A net and Δx_B Δy_B Δz_B are the components of the B net.

The least squares design matrices are the same as those for the Bursa-Wolf model except -

$$Ai = \begin{bmatrix} \frac{\partial F}{\partial s} & \frac{\partial F}{\partial \omega} & \frac{\partial F}{\partial \theta} & \frac{\partial F}{\partial k} \end{bmatrix}$$

where $\partial F/\partial s = R\,\Delta x_A$

$$\frac{\partial F}{\partial \omega} = s\,R \begin{bmatrix} 0 & 0 & 0 \\ 0 & 0 & 1 \\ 0 & -1 & 0 \end{bmatrix} \begin{bmatrix} \Delta x_A \\ \Delta y_A \\ \Delta z_A \end{bmatrix}$$

$$\frac{\partial F}{\partial \theta} = s \begin{bmatrix} 0 & 0 & -\cos k \\ 0 & 0 & \sin k \\ \cos k & -\sin k & 0 \end{bmatrix} R \begin{bmatrix} \Delta x_A \\ \Delta y_A \\ \Delta z_A \end{bmatrix}$$

$$\frac{\partial F}{\partial k} = s \begin{bmatrix} 0 & 1 & 0 \\ -1 & 0 & 0 \\ 0 & 0 & 0 \end{bmatrix} R \begin{bmatrix} \Delta x_A \\ \Delta y_A \\ \Delta z_A \end{bmatrix}$$

Only independent baselines, such as all baselines radiating from one point, should be used. An important advantage of this method is that smaller matrices need to be inverted. This is because there are a maximum of four parameters to estimate and since for n sites there are n(n-1)/2 baselines of which n-1 are independent. The largest matrix to be inverted is therefore 6n-6 x 6n-6 rather than 6n x 6n.

Adjusted lengths, angles, scale and rotation parameters and their VCV matrices are identical to those from an equivalent Bursa-Wolf solution. However this model does not yield adjusted coordinates or estimate translation parameters.

Baseline lengths in a 2D adjustment.

Although this is not a transformation it is the simplest method for combining the two data types. The VLBI baseline lengths are included in the 2D ground adjustment just as if they were measured by EDM. This method should be applied when there is only one VLBI baseline, though it could be used for any number of baselines. A scale factor is the only parameter though it may be held fixed at unity. All baseline lengths and their variances are included, not just those baselines radiating from one point. Either the 3D-height fixed or the classical methods can be used. The main problem with this method is that the high quality VLBI vectors are constrained to agree with the often poorly determined ground network ellipsoidal heights. Errors in the fixed ellipsoidal ground heights will distort the results. Moreover the conversion of long (greater than 2000km) VLBI chord lengths to spheroidal lengths may not be accurate (see eg. Bomford, 1980) unless conversion formulae such as those of Vincenty (1975) are applied.

Other models and methods.

Veis (1960) used 3D coordinates in one network and components from an initial point in the other network. This approach is similar to the Molodensky-Badekas model but uses a rotation matrix about the three axes of the local topocentric coordinate system at the initial point, with components in azimuth and two vertical angles instead of rotation angles about the x, y, and z axes.

Hotine (1969) estimates two sets of rotation parameters. These are the ω, Θ, and k rotation angles relating the two nets and two additional rotations, azimuth and zenith distance from a central site, to represent systematic errors within the terrestrial network - a total of nine parameters. Krakiwsky and Thomson (1974) solve for ten parameters - the interstation vectors are rotated, added to

the initial point vector and then rotated, scaled and translated as in the Bursa-Wolf model. Vanicek and Wells (1974) solve for eight parameters - ω, Θ, k, scale, a rotation about the ellipsoidal normal at the initial point, and translation of origin.

These models separate the rotations into components due to systematic measurement errors and reference frame differences. Many of these rotations are highly correlated. The solutions are therefore not as stable and special estimation procedures may be required to overcome the stability problems. If the solution is stable then the internal adjustment and strain parameters are not affected by separation of the total rotation into its components. Therefore these methods have not been further investigated here.

Another technique is based on the experience in England when combining satellite and ground data (Ashkenazi, 1981). The X-Z plane passes through the networks there, so two parameters, k and Ty, have almost identical effects and only one of them has to be determined. If k is less than 3.7" then the error in the coordinates is less than 1mm when Ty is used instead of k. This reduces the number of parameters and increases the degrees of freedom. This is especially suitable when there are only a few data points.

A number of possibilities to extend this concept exist.
1) Rotate both nets onto the X-Z plane, so that k is similar to Ty if the network is small (few hundred km).
2) Rotate both nets onto the Y-Z plane so that k is similar to Tx.
3) Rotate both nets onto the intersection of the equator and the 0° meridian (or similarly 90°, 180°, or 270°). In this case k is similar to Ty and Θ is similar to Tz so that it is only necessary to solve for five parameters such as scale, ω, Tx, Ty, and Tz. However in each of the above cases the VCV matrices associated with the coordinates will have to be altered to conform with the new coordinates.

There are less parameters to estimate and the internal adjustment of lengths and angles should be more stable. However, the adjusted coordinates and most of the adjusted parameters do not have any physical meaning.

SCALE FACTOR RESIDUALS.

As well as combining the two data sets using one of the above models the analyst can and should investigate the scale factor as determined from each baseline. A scale factor can be determined for each baseline using -

$$s = L_t/L_f$$

where L_t is length in one frame and L_f the corresponding length in the other frame. These scale factors, and possibly also the estimate of scale factor from one of the transformation models, can then be plotted. Generally the scale difference, which is the scale factor minus one, would be plotted as in the hypothetical example in figure 7.3 below.

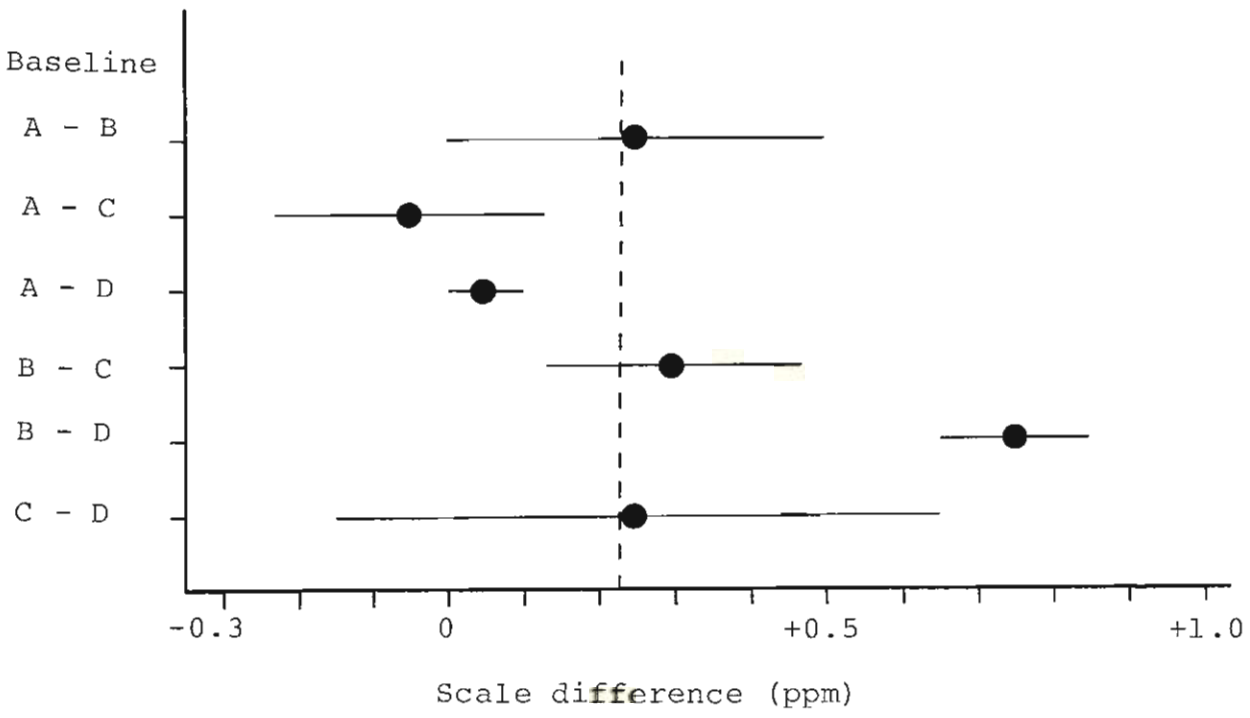

Figure 7.3 Individual baseline scale factors (hypothetical example).

The one sigma error bars are calculated as follows.

$$\sigma^2 s = \begin{bmatrix} \frac{\partial s}{\partial Lt} & \frac{\partial s}{\partial Lf} \end{bmatrix} \begin{bmatrix} \sigma^2_{Lt} & 0 \\ 0 & \sigma^2_{Lf} \end{bmatrix} \begin{bmatrix} \frac{\partial s}{\partial Lt} \\ \frac{\partial s}{\partial Lf} \end{bmatrix}$$

$$= \sigma^2_{Lt} / Lf^2 + Lt^2 \sigma^2_{Lf} / LfR$$

$$\cong (\sigma^2_{Lt} + \sigma^2_{Lf}) / Lf^2$$

Note that scale factor, if determined from a single baseline, is not as precise as the baseline lengths. For example if the baseline is measured to 0.10ppm in both nets the derived scale factor will have a precision of 0.14ppm. It should also be noted that the longest lines do not necessarily give the best determinations of scale factor. The lines with the best fractional (ppm) accuracies give the most precise estimates of scale factor. That is a very accurate short baseline may have more effect on an estimated scale factor than a poor quality long line. In this way the analyst can determine which baselines are having the most effect on the overall scale factor as determined by a least squares solution of one of the models.

This procedure does not consider the correlations between baseline lengths (which are usually small) but it is useful for finding inconsistencies or outliers in the data and the relative power of each baseline to the overall scale factor. The analyst should look for the following.

1) Single baselines being inconsistent with the overall network, such as line B-D in figure 7.3. Standard statistical tests for detecting outliers should be applied.
2) All baselines from one site being inconsistent with the rest.
3) All baselines in one direction (eg East-West) being inconsistent.
4) If there are many baselines so that the data can reasonably be separated into regions, then all baselines in a region being inconsistent with the overall network.

MODELLING OF SYSTEMATIC ERRORS.

This section adds terms to the basic similarity transformation models given above. However if the data does not contain significant contributions from the systematic error parameters as added, then using these additional parameters will give smaller residuals but not necessarily a more accurate solution. The parameters added here solve for 2D scale and azimuth errors in the ground net and tropospheric bias errors in the VLBI net. These systematic errors have been discussed in Chapters 5 and 3 respectively. It was shown in Chapter 3 that many of the systematic errors in VLBI can be represented by the scale, rotation and translation terms and do not need to be further modelled because even though they affect the estimated parameters they do not affect the internal adjustment. Of those VLBI systematic errors which cannot be represented by scale, rotation and translation terms, the tropospheric bias error may be the largest error source and so it is modelled below.

Chapter 5 showed that errors in the origin conditions of a ground net and a constant error in heights affect the scale, rotation and translation terms. Zhou (1983) proposed two additional parameters to cater for some of the other systematic errors in the ground survey. These are a 2D scale factor representing errors in measured distances (caused by, for example, miscalibration of EDM and incorrect refraction corrections), and a 2D azimuth error at the origin of the network.

2D scale and azimuth errors.

A 2D scale factor is different to a 3D scale factor (see page 102). It can be thought of as follows.

If a ball has a network drawn on it and in this network one point is held fixed and if the size of the ball is not

altered then increasing the lengths of all the lines joining the points of the network will move the points along the surface of the ball and further from the fixed point. Note that if the ball is a sphere then the points of the network will not be further from the centre of the ball. If a network is on, or referred to, the surface of an ellipsoid then a 3D scale factor will have a much greater effect on the heights of points than on the latitudes or longitudes. However a 2D scale factor will have much more affect on the latitudes and longitudes of points than on the heights.

For a region of less than a few thousand kilometres, a 3D scale factor can be approximated by a 2D scale factor and a constant height error, and vice versa. Now a constant height error can be approximated by an appropriate component of the total translation vector. So if a 2D scale error or constant height error or both are present and are not solved for then the adjusted lengths and angles should not be severely affected, but the estimates of the 3D scale factor and translation components will be affected. The effects of such errors on strain parameters will be discussed in Chapter 8.

The model and least squares design matrices for these additional parameters are an extension of those given in the ellipsoidal model above.

$$F' = F - mt \begin{bmatrix} a_{11} \\ a_{21} \\ 0 \end{bmatrix} - \Delta a \begin{bmatrix} a_{12} \\ a_{22} \\ 0 \end{bmatrix}$$

where mt is the 2D scale factor and Δa is the origin azimuth error, F is the ellipsoidal model, and (Zhou, 1983)-

$$a_{11} = \phi - \phi_o - 1.5\tan\phi\eta^2(\phi-\phi_o)^2 - 0.5\cos\phi\sin\phi(1+\eta^2)(\lambda-\lambda_o)^2 - \cos^2\phi(\phi-\phi_o)(\lambda-\lambda_o)^2/3$$

$$a_{12} = -\cos\phi(1+\eta^2)(\lambda-\lambda_o) + 3\sin\phi\eta^2(\phi-\phi_o)(\lambda-\lambda_o) + \cos\phi(\lambda-\lambda_o)^3/6$$

$$a_{21} = 1 + \tan\phi(1-\eta^2)(\phi-\phi_o)(\lambda-\lambda_o) + (2+3\tan^2\phi)(\phi-\phi_o)^2(\lambda-\lambda_o)/3 - \sin^2\phi(\lambda-\lambda_o)^3/6$$

$$a_{22} = \{(1-\eta^2+\eta^4)(\phi-\phi o) + \tan\phi(1-\eta^2/2)(\phi-\phi o)^2\}/\cos\phi - \sin\phi(\lambda-\lambda o)^2/2 - (\phi-\phi o)(\lambda-\lambda o)^2/2\cos\phi + (1+3\tan^2\phi)(\phi-\phi o)^3/3\cos\phi$$

where $\eta^2 = e^2\cos^2\phi/(1-e^2)$

$$A'i = \left[\frac{\partial F}{\partial s} \quad \frac{\partial F'}{\partial mt} \quad \frac{\partial F'}{\partial \Delta a} \quad \frac{\partial F}{\partial \omega} \quad \frac{\partial F}{\partial \theta} \quad \frac{\partial F}{\partial k} \quad \frac{\partial F}{\partial Tx} \quad \frac{\partial F}{\partial Ty} \quad \frac{\partial F}{\partial Tz} \right]$$

$$\frac{\partial F'}{\partial mt} = \begin{bmatrix} -a_{11} \\ -a_{21} \\ 0 \end{bmatrix} \quad \text{and} \quad \frac{\partial F'}{\partial \Delta a} = \begin{bmatrix} -a_{12} \\ -a_{22} \\ 0 \end{bmatrix}$$

$$B'i = \left[\frac{\partial F'}{\partial \phi} \quad \frac{\partial F'}{\partial \lambda} \quad \frac{\partial F}{\partial h} \quad \frac{\partial F}{\partial \phi_t} \quad \frac{\partial F}{\partial \lambda_t} \quad \frac{\partial F}{\partial h_t} \right]$$

$$\frac{\partial F'}{\partial \phi} = \frac{\partial F}{\partial \phi} + \begin{bmatrix} -mt\ (\partial a11/\partial\phi) - \Delta a\ (\partial a12/\partial\phi) \\ -mt\ (\partial a21/\partial\phi) - \Delta a\ (\partial a22/\partial\phi) \\ 0 \end{bmatrix}$$

$$\frac{\partial F'}{\partial \lambda} = \frac{\partial F}{\partial \lambda} + \begin{bmatrix} -mt\ (\partial a11/\partial\lambda) - \Delta a\ (\partial a12/\partial\lambda) \\ -mt\ (\partial a21/\partial\lambda) - \Delta a\ (\partial a22/\partial\lambda) \\ 0 \end{bmatrix}$$

If the ground adjustment is a conventional 2D adjustment then the rotation, Δa, about the fundamental point is not the same as a rotation of the points in the network about the axis through the fundamental point. This is because the points are constrained to remain at the same height above the ellipsoid. If this model is computed with mt and dAt held fixed at zero then the results will be identical to those obtained from a normal seven parameter transformation solution. These parameters, mt and Δa, were estimated in two solutions, one using the real data and the other the simulated 300km data set. In both cases the 3D scale factor and 2D scale factor were highly correlated. However the larger net (~2000km) gave a slight improvement in the correlation between the two factors, from 0.86 to 0.7, compared to the smaller net. Also, the estimated precisions of the scale and azimuth rotation parameters were smaller in the larger net, that is the estimates of these two systematic error parameters improved with an increase in the size of the network. Both these results were expected. It is also of interest to note that for the real data used here, the estimates of the 2D scale and azimuth errors were not statistically significant at the 95% level. So for this

data a conventional combination model is suitable.

VLBI tropospheric bias.

The effect of tropospheric biases on VLBI results was discussed in detail in Chapter 3. In principle, the tropospheric biases at each site can be determined if the VLBI results are combined with an independent determination of the site coordinates, such as by geodetic survey. Whether these parameters are highly correlated with other parameters, and the mechanics of solving for them when combining various data sets are discussed below.

The combination models are modified to allow for this systematic error as follows.

$$\mathbf{F'} = \mathbf{F} + \Delta\mathbf{X}$$

where $\Delta\mathbf{X}$ is as in equation 2.8 or 2.9. However if the fixed VLBI site is included in the combination, then three rows of zeros must be inserted into K since ΔX for the fixed site is zero. The TBi are then treated as 'solve for' parameters in the adjustment, though after statistical tests, or analyst choice, the TB_i may be held fixed at zero in which case the model will be identical to its original form. This method can be used to extend either the Cartesian models (eg Bursa-Wolf) or the ellipsoidal model. If the VLBI data is to be included in a Cartesian model then it is desirable to have the output VLBI results in Cartesian coordinates. If the output coordinates of the VLBI software are not Cartesian, or ellipsoidal for use in the ellipsoidal model, then they need to be converted (as in Chapter 6). But this is an undesirable complication. There is one additional parameter per site, so if these parameters are added to a conformal transformation at least 4 common points are necessary.

The least squares design matrices (partials) are quite simple. The Ai matrices are simply appended by the relevant terms of K or L. The Bi' matrices are the same as Bi, because the terms in K and L do not vary significantly with

small changes in the site coordinates.

Will these bias corrections behave like scale, rotation, or translation parameters? On a network of short baselines (<1000km) the effect of a troposphere bias can be modelled as follows. If there are only two or three sites then the errors can be well approximated by rotations of the network. If there are four or more sites then the errors cannot be modelled by rotations and they will cause a vertical strain of the net. Moreover if only a single scale factor is estimated, rather than strain parameters, then it may be in error.

Generally the TB_i will be poorly determined if VLBI data is combined with ground data which has poor heights. Moreover the biases will be highly correlated with the other parameters when there are only a few sites. Although it varies from experiment to experiment the error in the ellipsoidal height of an estimated site due to a tropospheric bias is approximately -

$$\Delta h = 1.9 * TB$$

where Δh and TB are both in centimetres. The actual amplification factor depends on the elevation cut off in the VLBI experiment. A higher elevation cut off means Δh is less sensitive to TB. If the tropospheric bias at a site is to be estimated to better than ±5cm, then the heights in the ground network will have to be accurate to better than about ±10cm. This is rarely the case with existing ground networks. Even if this method does not produce estimates of the TB_i more accurate than ±5cm, it is still useful for determining the sensitivity of the results of the combined solution to tropospheric bias errors.

If the tropospheric bias terms are poorly determined then the terms in the VCV of the VLBI data should be increased so that it is more representative of the accuracy of the coordinates, and the combination adjustment computed without estimating tropospheric bias parameters. The variances of the heights will be the only terms

significantly affected so (if necessary) the VCV should be converted to its equivalent for ellipsoidal coordinates (see Appendix A). Estimates of the errors due to tropospheric bias are then added to the variances of the heights.

INTERPRETATION OF RESULTS.

When the rotations are small the models are almost linear, so one iteration is usually sufficient, provided the a priori estimates of the parameters are reasonably correct. Though a second iteration does check convergence of both the results and their VCV matrices. In the Australian data examples the results of the second iteration did not differ by significant amounts to those of the first, except when the a priori translations were in error by several hundred metres.

The results of an adjustment are two sets of adjusted coordinates which differ by the adjusted parameters. Even though the two coordinate sets as observed are generally not correlated the adjusted coordinate sets will be slightly correlated. Though the magnitudes of the correlations depend on the data. An example is given in Table 7.6.

The adjusted coordinates corresponding to the A network have the same weighted scale, orientation and location as the a priori A network. Similarly for the B network. The overall scale, location and orientation of each network remains unchanged. Only the individual coordinates, angles and lengths are changed. In other words, the movements of points within a network are small but the overall net does not change. If a transformation adjustment is computed between the a priori and adjusted versions of a net, it will be found that the estimated rotation angles, scale difference, and translations will all equal zero.

Table 7.6. Correlations between the adjusted Cartesian coordinates of the Australian VLBI and ground nets.

		T			P			F			AS			H		
		x	y	z	x	y	z	x	y	z	x	y	z	x	y	z
	x	0.00	0.00	0.00												
T	y	0.00	0.00	0.00												
	z	0.00	0.00	0.00												
	x	-.01	0.01	-.01	0.02	-.02	0.02									
P	y	0.00	-.01	0.01	-.01	0.02	-.01									
	z	-.01	0.00	-.01	0.01	-.01	0.03									
	x	-.02	0.02	-.02	-.04	0.04	-.03	0.06	-.06	0.06						
F	y	0.04	-.05	0.04	0.06	-.08	0.07	-.01	0.01	-.01						
	z	-.03	0.04	-.04	-.01	-.01	-.02	0.07	-.07	0.07						
	x	0.02	-.02	0.03	-.10	0.07	-.10	-.04	0.04	-.04	-.11	0.13	-.11			
AS	y	0.03	-.03	0.05	-.07	0.03	-.06	-.09	0.09	-.09	-.13	0.16	-.14			
	z	0.21	-.25	0.22	0.32	-.30	0.26	0.46	-.46	0.46	-.33	0.35	-.28			
	x	-.18	0.17	-.18	-.12	0.11	-.12	-.12	0.12	-.12	0.07	-.06	0.06	0.22	-.16	0.19
H	y	-.00	-.05	-.01	-.10	0.11	-.13	-.18	0.17	-.17	0.14	-.15	0.14	0.07	0.05	0.03
	z	-.16	0.16	-.18	-.19	0.20	-.19	-.19	0.19	-.19	-.05	0.06	-.05	0.38	-.39	0.46

The results of this type of adjustment are convenient for Surveyors because the coordinates of points of a network do not change by large transformation parameters. The coordinates of points change by small amounts (of the order of the standard deviations of the observations). Any large change in coordinates of a survey control network necessitates recomputation and design of surveys and construction work based on the control network, and is therefore undesirable. The coordinates of the fundamental point of the ground net (eg Johnston in Australia) will not change if its a priori variances equal zero, or are very small, even if the point is not included in the transformation calculations. This is also of importance for Surveying applications.

The precision of the adjusted length of a line is a function of the a priori VCV matrix of the observations (which is usually different for each net), the lengths of the baselines, and the precision of the adjusted scale factor (which is not zero unless the scale factor is held fixed). Therefore the precision of an adjusted baseline length will generally be different in the two networks. They will be the same only when the a priori VCV of the observables of each net is the same or when the scale factor is held fixed (not necessarily at unity). Since an adjusted length in the B network, L_B, equals the corresponding adjusted length in the A net, L_A, times the scale factor, s, it can be shown that -

$$\sigma^2_{LB} = s^2\ \sigma^2_{LA} + 2\ s\ LA\ \sigma_{sLA} + LA^2\ \sigma^2_s$$

Obviously σ^2_{LB} equals σ^2_{LA} if σ^2_s or σ_{sLA} equal zero, that is when the scale factor is fixed. Note that if s is not held fixed then generally σ_{sLA} will not equal zero because of correlations introduced in the least squares adjustment. Also note that σ_{sLA} may be negative and thus allows σ_{LB} to be less than σ_{LA}. If s is held fixed at some value other than unity then σ_{LB} does not exactly equal σ_{LA}. However since s rarely differs from unity by more than a few ppm the difference will be insignificant.

The internal network adjustment (ie the precisions of the adjusted baseline lengths) improves when the a priori scale factor is fixed or assigned a small variance. As a typical example, three separate solutions were obtained with the real data described above. The results for the Tidbinbilla - Fleurs baseline are given here. The a priori precision of this length in the VLBI net was ±6.9cm and in the ground net it was ±13.1cm. In the first transformation solution the scale factor was estimated without a priori constraint. The estimated precision of the adjusted length in the VLBI net was ±5.9cm and it was ±10.2cm in the ground net. A second transformation solution constrained the scale difference to 0.303 ± 0.468 ppm, ie the values determined in the first solution. The estimated precisions of the adjusted lengths improved to ±5.7cm in the VLBI net and ±8.2cm in the ground net. A third solution with the scale factor held fixed at unity gave the estimated precision of the adjusted length as ±5.7cm in both nets.

Which adjusted net should be adopted?

If it is desired to adopt the VLBI scale, orientation and location, then the adjusted VLBI coordinates are adopted. However as it may be desirable to adopt the VLBI scale and orientation and the ground (or Doppler) location further calculations are necessary. This would involve shifting the adjusted VLBI coordinates by the adjusted estimates of translation parameters and changing the VCV matrix of the coordinates by the law of propagation of variances (see eg. Mikhail, 1976 and Strang van Hees, 1982). Generally the VLBI data will be more accurate and so the adjusted VLBI net will be adopted if the net with the best internal adjustment is desired. However if the adjusted coordinates of the VLBI net are adopted and some of the measurements of the ground net are more precise, then the adopted coordinates in the vicinity of these measurements will not be as precise as if the adjusted coordinates of the ground net had been adopted. In such a case the initial quality of

the observations would not be fully utilised.

Again if the best internal adjustment is required and if the two adjusted nets are of similar quality then that net with the smallest trace of the VCV of the adjusted lengths should be adopted. If there are many points in the adjustment and the internal adjustment of data in a certain region is of prime interest, then the traces of the VCV of the adjusted lengths of only the baselines in that region should be compared. The traces of the VCV of the adjusted coordinates should not be used for this test because 1) the adjusted coordinates are usually more highly correlated than the adjusted lengths and this method ignores the correlations, and 2) because the VCV of coordinates may contain large components due to a network's datum defects and its distance from the fixed point.

APPLICATION OF RESULTS.

The results of a combined adjustment can be applied to deformation and strain analysis as discussed in the next chapter. Four other applications are discussed below.

1) Geodetic network adjustment.

The adjusted network of common points can be used as control to adjust the remainder of the geodetic network. The adjusted ground latitudes and longitudes could also be used to determine new values of ellipsoid-geoid separation and the ground adjustment recomputed. Then the whole process could be iterated with these improved heights. However the slope of the geoid is typically less than 1'. So that a change in coordinates of say 3m, which is larger than expected, would cause a change in height of less than 1mm, which is insignificant.

In an adjustment, the ground heights will change by large amounts, because of their poor a priori precisions. If the adjusted ground coordinates are then adopted in a 2D ground

adjustment of points intermediate to the common sites an analyst has the following choices with regard to the ground heights - use the new heights at the common sites, leave heights as before the combination, change heights only at the common sites, or change heights at intermediate sites by, for example, linear interpolation. Which ever choice is made there will be little effect on the adjusted latitudes and longitudes of the intermediate sites provided the changes to the heights are less than several metres. It is expected that after combining a ground network with a perimeter of more accurate VLBI measurements that generally the accuracy of the coordinates of points in the adjusted ground network will decrease (the variances will become larger) from the perimeter to the centre of the network.

2) Transforming coordinates.

Another application of combining ground and VLBI via transformation is to determine parameters which could be used to transform the known ground coordinates of points that may be prospective VLBI sites into the VLBI coordinate frame. This would provide useful a priori positions for experiment scheduling and correlation. However it must be remembered that a transformation is essentially an interpolation procedure. So the results may be unreliable if the adjusted parameters are used to transform the coordinates of a point outside the region spanned by the common points.

As an example the following procedure should be used to convert the ground coordinates of a prospective VLBI site, with geodetic latitude and longitude obtained from the 1983 adjustment of the Australian Geodetic Network and AHD height plus geoid height, to VLBI coordinates which are consistent with those used in the experiment described in Chapter 4. Convert the latitude, longitude and height to Cartesian coordinates using equation A.5. Then the Cartesian coordinates in the VLBI frame are approximately -

X = x - 1.E-6 y + 4.8E-6 z - 110.
Y = 1.E-6 x + y - 3.9E-6 z - 63. (units are metres)
Z = -4.8E-6 x + 3.9E-6 y + z + 119.

These coordinates would have an error in position of about ±5m, but would be useful for experiment planning and as a priori positions in the processing and adjustment of VLBI data.

3) Ground link.

The transformation parameters are also useful for converting a ground survey link to the VLBI system for comparisons between VLBI, SLR, and GPS measurements. The ground link is needed to compare the baseline measurements for independent checks of these space techniques because the space techniques cannot generally co-locate sites. It has been common in the past, when comparing two space systems via a ground connection, to use the ground Cartesian components and assume the orientations of the reference axes are the same. Since the ground orientation can be a few arc seconds, or more, different to that used by VLBI, the maximum length of connection using this assumption is limited. For example a 2" orientation difference subtends 1cm at 1km.

A network of common sites is needed to solve for the differences in orientation. However a ground connection may be more accurate if reduced as a small regional network than to be constrained by the whole ground network. Ideally there should be a micro net around the connection. That is, at least three or four VLBI sites within a kilometre or two. These would each be connected to the ground net which also includes the SLR or GPS site(s). The orientation and scale differences between the local VLBI and local ground nets are determined. The ground net, including the SLR or GPS site(s), is thus transformed into the VLBI frame. Naturally this may not be practical, unless a transportable VLBI antenna is available, and so orientation differences from a much larger net must also be assumed to apply to the

local net.

The error in the link would be due to errors in the ground observations and in the transformation parameters used. The VCV of the transformed ground link can be determined by applying the law of propagation of variances, as follows. Since

$$\begin{bmatrix} \Delta X \\ \Delta Y \\ \Delta Z \end{bmatrix} = s \begin{bmatrix} 1 & k & -\theta \\ -k & 1 & \omega \\ \theta & -\omega & 1 \end{bmatrix} \begin{bmatrix} \Delta x \\ \Delta y \\ \Delta z \end{bmatrix}$$

then the

$$VCV_{\Delta X \Delta Y \Delta Z} = J \begin{bmatrix} VCV_{\Delta x \Delta y \Delta z} & 0 \\ 0 & VCV_{s\omega\theta k} \end{bmatrix} J^T$$

where

$$J = \begin{bmatrix} s & sk & -s\theta & \Delta x + k\Delta y - \theta\Delta z & -s\Delta z & s\Delta y & 0 \\ -sk & s & s\omega & \Delta y - k\Delta x + \omega\Delta z & 0 & -s\Delta x & s\Delta z \\ s\theta & -s\omega & s & \theta\Delta x - \omega\Delta y + \Delta z & s\Delta x & 0 & -s\Delta y \end{bmatrix}$$

The ground survey connecting Tidbinbilla to the SLR site at Orroral was used as an example. Such a connection would be necessary if the VLBI and SLR measurements of the very long baselines connecting Canberra and, for example, California were to be compared. The ground survey chord length was 24807.528 ± 0.072m, which could be improved. However even if the survey was error free, the VCV of the scale factor and rotation angles as determined from a Tidbinbilla - Parkes - Fleurs combination of VLBI and ground data would produce an error ellipse for the connection with semi-axis lengths of 44.0cm, 1.4cm, and 1.3cm. Obviously this is not good enough and it assumes that these transformation parameters are representative of those for the line connecting Tidbinbilla and Orroral. The main contribution to the size of the error ellipse is the precisions of the rotation angles which were about ±3".

An improvement to the link could be made by conducting a VLBI experiment with a mobile VLBI telescope within a few hundred metres of the Orroral site. The connection would then be much shorter and the effects of errors in the scale and rotation terms far less. Alternatively the precisions

of the rotation angles and scale factor could be improved by using a larger net. However this is valid only if the larger net is representative of the scale and orientation of the two data sets in the region of the link.

Another alternative method is to estimate the likely error in the scale and orientation of the VLBI and of the ground nets from some ideal reference frame. The likely differences in the scale and orientation of the two nets can then be estimated and used as estimates of the accuracy of the conversion of the link with no actual conversion being calculated. However this method depends on the quality of the analyst's knowledge of the errors in scale and orientation in each net.

4) Precision of scale factor.

Before strain can be studied at the 0.1ppm level using combined VLBI and ground data, the analyst must be sure that the scale difference between the VLBI net and the ground net is less than 0.1ppm.

Simulation studies were computed to determine how accurately the scale factor could be determined using different precisions of data, with three sites, Tidbinbilla, Parkes, and Fleurs. It was found that improvements in the VLBI have little effect on the precision of the scale factor. However an improvement in the horizontal and especially height accuracies of the ground data was very significant. With present accuracies scale cannot be determined to better than 0.3ppm around the Tidbinbilla - Parkes - Fleurs triangle. This places a limit on the crustal strain that can be reliably detected over this area. If VLBI data was not available and two epochs of ground data were available at present accuracies the scale difference between the two epochs could be determined to only ±0.7ppm. Thus it would take about twice as long to detect any geophysical strain. If two epochs of VLBI data, with baseline length precisions of about ±3cm were combined

the scale factor could be determined to about ± 0.10ppm. If two additional nearby sites (see Fig. 7.1) with similar precisions were added the scale factor would be precise to about ±0.09ppm.

Simulations were also calculated to determine how well scale differences could be determined if data from sites spread over the whole of Australia were used. The sites considered were near each of Canberra, Hobart, Alice Springs, Adelaide, Perth, Darwin, and Cairns (see figure 7.4). The baseline lengths ranged from 830km to 3700km and their a priori precisions from 2cm to 5cm, in both nets. The estimated precision of the scale factor was found to be ±0.007ppm. Thus if this network was measured at two epochs one year apart the strain rate that could be detected at the one sigma level is about 0.007μstrains/year.

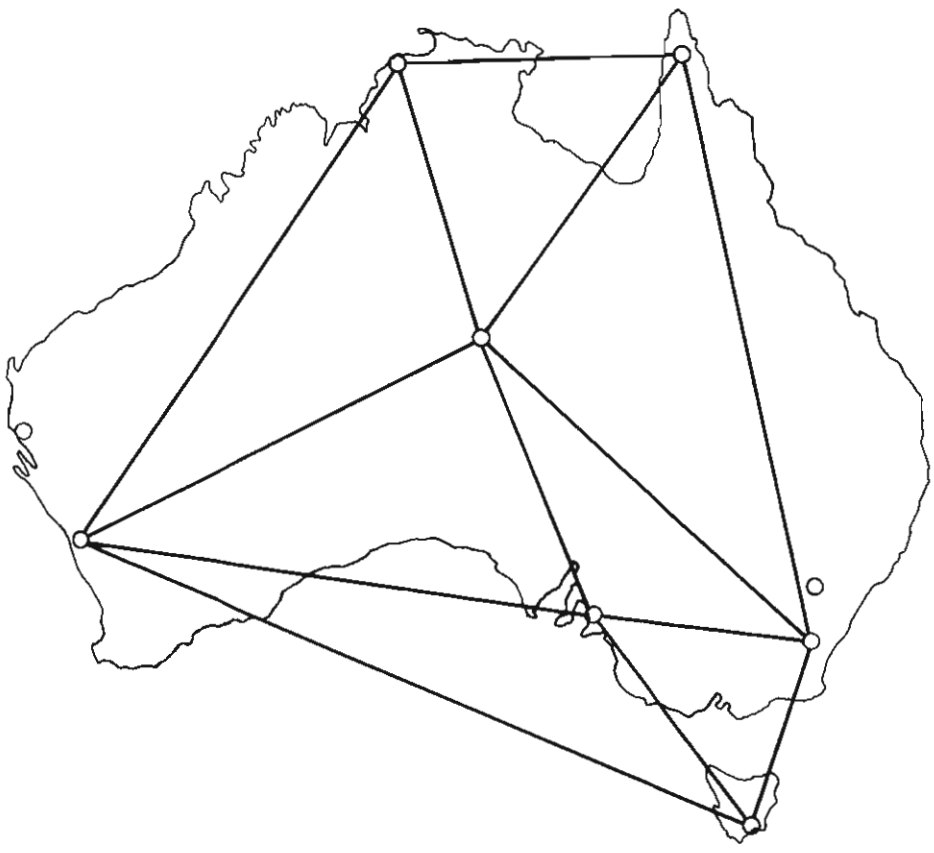

Figure 7.4 Simulated network across Australia.

CHAPTER 8.

REGIONAL DEFORMATION AND STRAIN.

INTRODUCTION.

The method proposed here to determine the strain parameters is similar to the method of determining the transformation and systematic error parameters given in Chapters 6 and 7. That is adjusted ground and adjusted VLBI coordinates are used as input data, not the direction, distance or delay observations. While Chapters 6 and 7 combined two networks this chapter will frequently call them two epochs referring to the fact that the two sets of observations are often measured at different times. However the two epochs may be two networks measured separately but at the same time. Each net should be subjected to statistical and other tests before solving for the strain parameters.

As well as determining strain parameters for geophysical applications, the strain parameters are also required for some geodetic network adjustments. If sites are moving it is not valid to include data observed over a long period of time into a single network adjustment, because systematic errors will occur. Moreover, in areas that are very unstable, a control network adjustment made several years ago may not be suitable as control for recent surveys. So either continual readjustments of networks would be needed or a 4D network would need to be established. Therefore, when combining new data with old data, allowance may have to be made for any network deformations occurring between observing epochs. This can be done by hypothesising certain properties of the displacement field, for example that horizontal movements are linear with time, that all motion is in a certain direction, or that motion is a function of distance from some feature (eg. fault line). Observations, and their analysis, are needed to determine unstable regions and the magnitude of the instability.

STRAIN.

A body, or a network on the surface of the body, deforms when stress is applied to it. If the earth's crust fractures because of an applied stress, there will be a relative displacement of points in the network (on both sides of the fault). If fracture does not occur the network will be translated or deformed or both. The translation component cannot be detected, unless there are some observations of absolute position. So neither conventional geodetic or VLBI observations can detect translation, but they can detect deformation.

Instead of regarding the displacement at each observing site as an individual measurement of Earth movement, the points are treated as part of a continuum of the Earth's strained surface. The displacements of individual sites are therefore correlated. A finite element approach may be adopted where the continuum of the deformation is replaced by a collection of small elements, eg triangles, which are connected. Ideally the data should be dense, uniformly distributed across a region, and continuous in time. However, it has not been possible in the past to measure dense networks over large areas at frequent intervals. It is also difficult to make sufficiently accurate measurements of vertical movements and many old measurements are of varying and uncertain accuracies.

If the displacement of points in a network corresponds to translation and rotation as a rigid body there is no strain. There are basically two measures of strain, first the change in length of a line (extension) and, second the change in angle between two lines (shear). The extension of a line is -

$$e = (l' - l) / l$$

where l is the initial length and l' is the length after straining. This is the same as a scale change between the two epochs. If two perpendicular lines pass through a point then the shear strain at this point is -

$$Y = \tan(\psi)$$

where ψ is the change in angle between the two lines. In three dimensions, shear strain is similarly defined with ψ equal to the change in angle between a line and a plane which were initially perpendicular.

The formulae for 3D strain analysis have been known for many years (Love (1944) gives a detailed description of the history of their development). If $(\alpha_1, \alpha_2, \alpha_3)$ are orthogonal coordinates then the elements e_{ij} of the strain tensor S, and the components ω_{ij} of the rotation matrix R, can be written as (Love, 1944; Bibby, 1973) -

$$e_{ij} = \frac{1}{2}\left[\frac{g_i}{g_j}\frac{\partial(\Delta\alpha_i)}{\partial\alpha_j} + \frac{g_j}{g_i}\frac{\partial(\Delta\alpha_j)}{\partial\alpha_i} \right] + \frac{\delta_{ij}}{g_i}\sum_{k=1}^{3}\Delta\alpha_k\frac{\partial g_i}{\partial\alpha_k} \qquad (8.1)$$

$$\omega_{ij} = \frac{1}{2g_ig_j}\left[\frac{\partial(g_i^2\,\Delta\alpha_i)}{\partial\alpha_j} - \frac{\partial(g_j^2\,\Delta\alpha_j)}{\partial\alpha_i} \right] \qquad (8.2)$$

where δ_{ij} is the Kronecker delta which equals one if i equals j, otherwise it is zero. g_i are the metric coefficients.

In homogeneous (linear or uniform) strain all straight lines remain straight and all lines originally parallel remain parallel, although their orientation may be altered. Moreover, the change (displacement) of an observation is independent of its position within the network. Finite or total strain relates the current configuration to the original configuration. Infinitesimal or incremental strain relates the displacements to the current network configuration and ignores the second order terms of total strain. Infinitesimal strain theory can be applied in virtually all geodetic applications because the displacements are much smaller than the size of the network. The magnitude of the error caused by ignoring second order terms can be computed from theory developed by Novozhilov (1953). If the extensional strain parameters are less than 10μstrains and the shear strains and rotations are less than 5μrads (10"), then the magnitudes of the second order terms are less than 0.003μstrains and

0.004μrads. However the strain associated with the vertical coordinate may not be as small as 10μstrain or 10" and in that case the second order terms cannot be neglected.

There are higher orders of strain than that given by equation 8.1. The bending (heterogeneous) strain of a network is an example of higher order strain. However, to reliably estimate the extra parameters associated with higher order strain, more data points are required than VLBI is expected to supply. Therefore these higher order strains are not considered in this thesis.

ADJUSTMENT METHODS.

A number of methods have been developed for studying regional strain or deformation. These existing methods and their weaknesses and the proposed method are discussed here.

Deformation, or strain, can be calculated directly from differences between repeated observations, such as the difference between two measurements of the same distance or angle (Frank, 1966). However only the observations common to both epochs can be used. Moreover, this method does not properly account for conditions imposed by the network geometry, such as closure, and cannot directly treat heterogeneous data (eg direction observations in epoch 1 and distance observations in epoch 2). Due regard should be taken of the precision of each individual observation. However, in Frank's method, all observations are usually assumed to have equal precision.

Often more information about the deformation is available than can be obtained from the analysis of repeated observations alone. This is because closure constraints and the unrepeated observations strengthen the solution giving smaller standard deviations for the results. A more widely adopted approach is to calculate strain from differences in adjusted coordinates of the points in each network. This

approach is particularly suitable when using different measurement techniques such as geodetic surveys and VLBI. For each epoch, the station coordinates are adjusted and the displacement vectors between epoch coordinates, for common stations, are determined. The components of the strain tensor (which are used to describe the deformation) are then determined from the displacement vectors. Movement can be detected by changes in coordinates of a point determined from separate observations, only if the coordinate systems (eg origin of reference frames) are the same for each epoch or network. It is not necessary for a particular site to be common to both networks. Sites that are in only one epoch can be included to strengthen the solution.

Any constraint introduced into a network can disguise the true deformations. For example, because angles and distances are only relative measurements, it may be necessary to hold some point and the azimuth of a line fixed. However this would imply that there was zero deformation at this point. Another approach is to constrain the solution so that the sum of squares of all displacements is a minimum (free net adjustment). Free net solutions such as the inner coordinate solution have been devised to overcome the problems of datum defects (Brunner, 1979). There probably are no geophysical justifications for these assumptions. Solving for displacements directly, suffers from the same datum problems as solutions which use coordinates. If it is found that three or more points within a network have not moved with respect to each other then the displacements of the other points can be calculated with respect to these reference points.

A better approach is to solve for the strain parameters directly because strain depends on the derivatives of displacement (strain = displacement/length) not on the absolute value of displacement. Although the displacements obtained depend on whether the adjustments use a free net or a fixed origin, the strain parameters and their VCV

components do not. So if only the strain terms and not the displacements are desired then any point can be held fixed without affecting the strain results (Bibby, 1982). Bibby (1982) suggests that all data be analysed simultaneously to solve for strain components which are unbiased, and the station coordinates at one epoch. However because the displacements are not determined, statistical tests on the conformity of all displacements cannot be applied.

The method proposed here determines the strain parameters in a transformation adjustment. The adjusted ground coordinates and adjusted VLBI coordinates and their VCV matrices are used as input data, not the direction, distance or delay observations. It is important to adjust each network separately and to check for outliers and systematic errors by applying statistical tests, before combining data sets in a strain analysis. If the VLBI and ground observations (eg distances and angles) are directly combined in the same adjustment then these checks are not possible. Otherwise measurement errors may be interpreted as deformation phenomena. Once each net has been adjusted and its coordinates and VCV determined the strain computations, by transformation adjustments, can be repeated with many variations in parameters and using different subsets of the data. This is a simpler (and more efficient) process than to repeat the 'simultaneous' procedure recommended by Bibby (1982).

Homogeneous strain analysis assumes uniform strain. In an area such as a fault zone this would probably be an invalid assumption. Provided there are sufficient data points, the strain field can be tested for homogeneity by dividing the data into subsets. If each subset yields strain components which are insignificantly different then the strain is homogeneous. The reverse may not be true due to systematic observation and model errors or to instability of the solutions. Apart from assuming that the whole region is subject to homogeneous strain, it is possible to use a priori data from analysis of seismic data and direct

measurements of fault displacements to model the strain field. The application of models of non-homogeneous strain, other than dividing the region into homogeneous subsets, is beyond the scope of this thesis. For an introduction to 2D finite element strain analysis the reader is referred to Welsch (1983) and Chen (1983). Chen (1983) also discusses how to decide which strain model best describes the deformation of a region.

Most strain and deformation investigations in the past have studied vertical movements or 2D horizontal movements. This could lead to a misinterpretation of the real (3D) strain situation. In the adjustment methods described below it is not necessary to only solve for homogeneous strain, because constraints for geophysical features such as fault zones can be included. Extensions can also be made to the methods for multi-epoch analysis. If more than two epochs of observations exist and the strain rate is thought to be constant over the entire period, then all observations can be included in one adjustment to solve for strain rate parameters. These strain rate parameters are the strain tensor terms divided by the time interval between the epochs of the measurements. However geophysical constraint models and multi-epoch analysis are beyond the scope of this thesis.

If two, or more, epochs of VLBI observations are used to solve for strain or displacements, then only the coordinates of the sites common to both epochs can be used in the strain calculations. However the observations from all sites should be included in each VLBI adjustment so that the coordinates of the common sites are more accurate. Then the determination of displacements and strain parameters is also more accurate.

In strain analysis there are two ways in which the VLBI data can be combined with ground data, provided that the two data types can be combined without causing artificial strain. 1) The VLBI sites are part of the strain field, and

2) All deformation is well inside the VLBI network, so the VLBI sites do not move. If it can be assumed that all deformation lies within a control network, such as is common in mining site and dam wall deformation studies, then the control sites can be held fixed and used to control both epochs of observations. So if geological and geophysical evidence indicates that the strain lies well within a VLBI network, or repeated measurements of the VLBI net confirm their stability, then the VLBI observations can be used to control both the old ground data and any recent measurements. The displacements of points within the strain field could then be determined with respect to these VLBI coordinates and would thus not be affected by the usual datum defects of location and orientation. If the VLBI sites are part of the strain field then they can only be used to control the ground observations taken at the same epoch as the VLBI measurements.

3D MODELS FOR DETERMINING STRAIN.

3D Geocentric Strain.

Strain analysis using 3D rectangular Cartesian coordinates is investigated here. The coordinates are usually referred to the CTS frame and so this type of analysis will be called geocentric strain.

In rectangular Cartesian coordinates the space metric is -

$$ds^2 = g_1^2\, dx^2 + g_2^2\, dy^2 + g_3^2\, dz^2$$

where the metric coefficients g_1, g_2, and g_3 all equal unity. From equations 8.1 and 8.2 -

$$e_{xx} = \partial\Delta x/\partial x \qquad e_{yy} = \partial\Delta y/\partial y \qquad e_{zz} = \partial\Delta z/\partial z \qquad (8.3)$$

$$e_{xy} = (\partial\Delta x/\partial y + \partial\Delta y/\partial x)/2 \qquad e_{xz} = (\partial\Delta x/\partial z + \partial\Delta z/\partial x)/2$$

$$e_{yz} = (\partial\Delta y/\partial z + \partial\Delta z/\partial y)/2$$

$$\omega_{11} = \omega_{22} = \omega_{33} = 0$$

$$\omega_{13} = \theta = (\partial\Delta x/\partial x - \partial\Delta z/\partial z)/2$$

$$\omega_{12} = k = (\partial\Delta x/\partial x - \partial\Delta y/\partial y)/2$$

$$\omega_{23} = \omega = (\partial\Delta y/\partial y - \partial\Delta z/\partial z)/2$$

If X_A are the coordinates of epoch 1 and X_B are the coordinates of epoch 2, then the affine transformation describing the homogeneous strain is -

$$X_B = (S+R)\ X_A + T \qquad (8.4)$$

where S is the strain tensor and R is the rigid body rotation assuming that the rotation angles are small, and

$$S = \begin{bmatrix} e_{xx} & e_{xy} & e_{xz} \\ e_{xy} & e_{yy} & e_{yz} \\ e_{xz} & e_{yz} & e_{zz} \end{bmatrix} \qquad R = \begin{bmatrix} 1 & +k & -\theta \\ -k & 1 & +\omega \\ +\theta & -\omega & 1 \end{bmatrix}$$

where ω, θ, and k are rotations about the x, y, and z axes respectively. The diagonals of the rotation matrix are unity instead of zero so that the diagonal strain components are very small and in the usual sense of fractional change rather than being close to unity and representing a scale factor. The strain elements e_{xx}, e_{yy}, and e_{zz} are the extension of an element initially parallel to the x, y, and z axes respectively. A positive value is an extension and a negative is a contraction. Common units for the diagonal terms of the strain matrix are μstrains (similar to ppm), and for the off-diagonal terms are μradians. The principal strains are the eigenvalues of the S matrix. A detailed review and description of these terms is given by Chen (1983).

The observation equations are -

$$F = (S+R) \begin{bmatrix} x_A \\ y_A \\ z_A \end{bmatrix} + \begin{bmatrix} Tx \\ Ty \\ Tz \end{bmatrix} - \begin{bmatrix} x_B \\ y_B \\ z_B \end{bmatrix} \qquad (8.5)$$

$$= \left(\begin{bmatrix} e_{xx} & e_{xy} & e_{xz} \\ e_{xy} & e_{yy} & e_{yz} \\ e_{xz} & e_{yz} & e_{zz} \end{bmatrix} + \begin{bmatrix} 1 & +k & -\theta \\ -k & 1 & +\omega \\ +\theta & -\omega & 1 \end{bmatrix} \right) \begin{bmatrix} x_A \\ y_A \\ z_A \end{bmatrix} + \begin{bmatrix} Tx \\ Ty \\ Tz \end{bmatrix} - \begin{bmatrix} x_B \\ y_B \\ z_B \end{bmatrix}$$

The partial derivatives are -

$$Ai = \begin{bmatrix} \frac{\partial F}{\partial e_{xx}} & \frac{\partial F}{\partial e_{yy}} & \frac{\partial F}{\partial e_{zz}} & \frac{\partial F}{\partial e_{xy}} & \frac{\partial F}{\partial e_{xz}} & \frac{\partial F}{\partial e_{yz}} & \frac{\partial F}{\partial k} & \frac{\partial F}{\partial \theta} & \frac{\partial F}{\partial \omega} & \frac{\partial F}{\partial Tx} & \frac{\partial F}{\partial Ty} & \frac{\partial F}{\partial Tz} \end{bmatrix}$$

$$= \begin{bmatrix} x_A & 0 & 0 & y_A & z_A & 0 & y_A & -z_A & 0 & 1 & 0 & 0 \\ 0 & y_A & 0 & x_A & 0 & z_A & -x_A & 0 & z_A & 0 & 1 & 0 \\ 0 & 0 & z_A & 0 & x_A & y_A & 0 & x_A & -y_A & 0 & 0 & 1 \end{bmatrix}$$

$$Bi = \begin{bmatrix} \frac{\partial F}{\partial x_A} & \frac{\partial F}{\partial y_A} & \frac{\partial F}{\partial z_A} & \frac{\partial F}{\partial x_B} & \frac{\partial F}{\partial y_B} & \frac{\partial F}{\partial z_B} \end{bmatrix}$$

$$= \begin{bmatrix} 1+e_{xx} & e_{xy}+k & e_{xz}-\theta & -1 & 0 & 0 \\ e_{xy}-k & 1+e_{yy} & e_{yz}+\omega & 0 & -1 & 0 \\ e_{xz}+\theta & e_{yz}-\omega & 1+e_{zz} & 0 & 0 & -1 \end{bmatrix}$$

Statistical tests.

The statistical tests of parameters, given in Chapter 6, can be applied to determine if there is any significant strain. If there is no significant strain then the data sets can be combined with perhaps a single scale factor using the methods of Chapter 7. Noting the similarity between the Bursa-Wolf model and equation 8.5, it can be seen that s is replaced by either SP or S where

$$SP = \begin{bmatrix} e_1 & 0 & 0 \\ 0 & e_2 & 0 \\ 0 & 0 & e_3 \end{bmatrix} \quad \text{and} \quad S = \begin{bmatrix} e_{xx} & e_{xy} & e_{xz} \\ e_{xy} & e_{yy} & e_{yz} \\ e_{xz} & e_{yz} & e_{zz} \end{bmatrix}$$

where e_1, e_2, and e_3 are the principal strains of the strain matrix S. If there is no significant difference between e_1, e_2 and e_3 then a simple scale factor could be applied. The VCV of e_1, e_2 and e_3 must be known in order to correctly test any difference between them. The computation of this VCV is rather involved. Note however that if a single scale factor was appropriate it would equal $(e_{xx} + e_{yy} + e_{zz}) / 3$. Therefore a suitable test would use equation 6.21 and test the X vector $(e_{xx}, e_{yy}, e_{zz}, e_{xy}, e_{xz}, e_{yz})^T$ against the U vector $(\Delta/3, \Delta/3, \Delta/3, 0, 0, 0)^T$. If X is found to be not significantly different to U then a simple scale factor would suffice. Otherwise at least some of the strain parameters are significant and must be estimated.

Numerical examples.

In all examples in this chapter the precision estimates of the adjusted parameters have not been scaled by the a posteriori variance factor because there are only a few degrees of freedom in each adjustment. And, for comparison purposes, more digits have been quoted than would normally be warranted.

Table 8.1. 3D Geocentric Strain determined from the observed data of the Australian VLBI network.

Parameter	Estimate
e_{xx}	-28. ± 49. μstrain
e_{yy}	-14. ± 28. μstrain
e_{zz}	-33. ± 38. μstrain
e_{xy}	21. ± 39. μradians
e_{xz}	-32. ± 43. μradians
e_{yz}	23. ± 33. μradians
ω	-1.0 ± 1.1 secs
θ	1.0 ± 1.5 secs
k	2.2 ± 2.2 secs
Tx	-210. ± 527. m
Ty	200. ± 313. m
Tz	-470. ± 405. m
3D dilatation	-75.3 ± 115.
Principal strains	0.9, 1.5, and -77.7
	$\tilde{\sigma}_o^2 = 0.38$

The example in Table 8.1 is for the real network which approximately spans a triangle with sides 1000km, 2000km, 2500km. All parameter estimates are statistically insignificant at the 95% level. The results in Table 8.2 were obtained from a simulated network which spans about 300km (see figure 7.1). The a priori baseline length precisions of the VLBI net ranged from 1.8cm to 4.4cm, though typically 3cm. Variances of, and correlations between, coordinates were similar to those for Tidbinbilla - Parkes baseline in the real VLBI data. The simulated

ground network had a priori baseline length precisions of 9.4cm to 51.9cm, though typically 30cm. Variances of, and correlations between, coordinates were similar to those for Tidbinbilla - Parkes - Fleurs baselines in the real ground data.

Table 8.2. 3D Geocentric Strain determined from the simulated data.

Parameter	Estimate
e_{xx}	-41.1 ± 539. μstrain
e_{yy}	27.8 ± 208. μstrain
e_{zz}	29.5 ± 338. μstrain
e_{xy}	-7.9 ± 317. μradians
e_{xz}	0.1 ± 412. μradians
e_{yz}	-26.8 ± 254. μradians
ω	-2.1 ± 17. secs
θ	5.9 ± 23. secs
k	6.6 ± 23. secs
Tx	-495. ± 4812. m
Ty	-431. ± 3153. m
Tz	423. ± 3842. m
3D dilatation	16.3 ± 1027.
Principal strains	-42.2, 2.6, and 55.8
	$\tilde{\sigma}_o^2$ = 0.62

In the solution the normal equations matrix (N+Px) had a virtual rank defect of one in the real data example and three in the simulated data example. The virtual rank defect is identified by one or more eigenvalues of the matrix being significantly smaller (about 10^{12}) than the rest of the eigenvalues. The translation terms were poorly determined in both examples. The Singular Value Decomposition (SVD) (Lawson and Hanson, 1974) method was used to solve the normal equations. However the results were considerably different to those from the conventional matrix inversion solution. This will be further discussed below.

3D Topocentric Strain.

If a network covers a small portion of the Earth's surface it can be approximated by a plane. At 150km from a tangent point a plane is about 1.8km above the Earth. Therefore the height difference of points, in a 300km region, from a plane is likely to be a few kilometres, but local topography also has to be considered. This approach, while still being three dimensional, computes the strain components in the plane and a component normal to the plane.

In this method both nets are translated and rotated to frames with origin at the centroid of the common points (see figure 8.1).

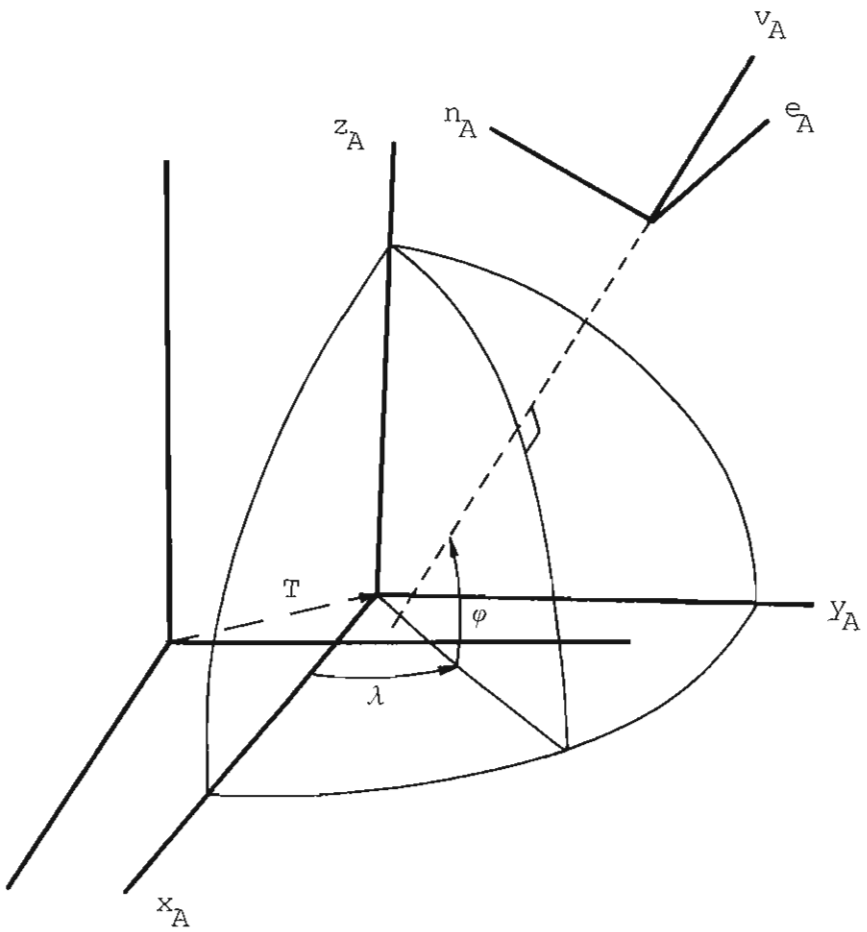

Figure 8.1 Topocentric Reference Frame.

The centroid of each system is -

$$xc_A = (\Sigma x_{Ai}) / N \qquad xc_B = (\Sigma x_{Bi}) / N$$
$$yc_A = (\Sigma y_{Ai}) / N \qquad yc_B = (\Sigma y_{Bi}) / N \qquad (8.6)$$
$$zc_A = (\Sigma z_{Ai}) / N \qquad zc_B = (\Sigma z_{Bi}) / N$$

where N is the number of points. The z axis is normal to the plane containing or approximating the points which are common to both nets, the x axis points east, and the y axis points north to complete a right hand triad. However, if strain analysis of more than two epochs, or data sets, is attempted and there are large displacements or if some points are not observed in every network, or epoch, then the centroids and direction of the vertical will be different when combining different pairs of epochs. In this case it would be preferable to select an arbitrary position near the centre of the network as the datum point and the direction of the z axes for all epochs. Otherwise the computed strains between different epoch pairs will refer to different planes, thus making comparisons difficult.

There are many different ways to define the orientation of the plane. The direction of the normal to the plane can be defined by the geocentric latitude and longitude, or by the geodetic latitude and longitude, of the centroid. Alternatively the analyst may select a plane parallel to a plane passing through three chosen points of the net. Another approach, not pursued here, is to use the best fitting plane through all points of the net.

The directions of the z axes (ie latitude and longitude) can be obtained as follows -

1) Geocentric

$$\sin\phi c = zc / \sqrt{(xc^2 + yc^2 + zc^2)}$$
$$\cos\phi c = \sqrt{(xc^2 + yc^2)} / (xc^2 + yc^2 + zc^2)$$
$$\sin\lambda c = yc / \sqrt{(xc^2 + yc^2)}$$
$$\cos\lambda c = xc / \sqrt{(xc^2 + yc^2)}$$

2) Geodetic

$$\sin\lambda c = yc / \sqrt{(xc^2 + yc^2)}$$
$$\cos\lambda c = xc / \sqrt{(xc^2 + yc^2)}$$

$$\left.\begin{aligned} v &= R / \sqrt{(1-e^2\sin^2\phi)} \\ \phi c &= \arctan\{(zc + e^2 v \sin\phi c) / \sqrt{(xc^2 + yc^2)}\} \end{aligned}\right\} \text{Iterate to find } \phi c$$

3) Through three points (x1, y1, z1), (x2, y2, z2), and (x3, y3, z3)

$$\sin\phi c = C/\sqrt{(A^2 + B^2 + C^2)}$$

$$\cos\phi c = \sqrt{(A^2 + B^2 / A^2 + B^2 + C^2)}$$

$$\sin\lambda c = B/\sqrt{(A^2 + B^2)}$$

$$\cos\lambda c = A/\sqrt{(A^2 + B^2)}$$

where
$$A = (y2-y1)*(z3-z1) - (z2-z1)*(y3-y1)$$
$$B = (z2-z1)*(x3-x1) - (x2-x1)*(z3-z1)$$
$$C = (x2-x1)*(y3-y1) - (y2-y1)*(x3-x1)$$

The coordinates are rotated and translated into the topocentric system by-

$$(e_A, n_A, v_A)^T = Rx(\pi-\phi c)\ Rz(\pi+\lambda c)\ \ (x_A-xc, y_A-yc, z_A-zc)^T$$

$$= \begin{bmatrix} -\sin\lambda_A & \cos\lambda_A & 0 \\ -\sin\phi_A\cos\lambda_A & -\sin\phi_A\sin\lambda_A & \cos\phi_A \\ \cos\phi_A\cos\lambda_A & \cos\phi_A\sin\lambda_A & \sin\phi_A \end{bmatrix} \begin{bmatrix} x_A-xc \\ y_A-yc \\ z_A-zc \end{bmatrix}$$

and similarly for e_B, n_B, v_B.

The model is-

$$F = \left(\begin{bmatrix} e_{ee} & e_{en} & e_{ev} \\ e_{en} & e_{nn} & e_{nv} \\ e_{ev} & e_{nv} & e_{vv} \end{bmatrix} + \begin{bmatrix} 1 & +\omega_v & -\omega_n \\ -\omega_v & 1 & +\omega_e \\ +\omega_n & -\omega_e & 1 \end{bmatrix} \right) \begin{bmatrix} e_A \\ n_A \\ v_A \end{bmatrix} + \begin{bmatrix} Te \\ Tn \\ Tv \end{bmatrix} - \begin{bmatrix} e_B \\ n_B \\ v_B \end{bmatrix} \quad (8.7)$$

Although the coordinates of the centroid are subtracted the translation terms still have to be estimated because only a simple (not weighted) centroid is subtracted. Since the simple centroid is normally close to the weighted centroid the translation terms will be small. The solution could possibly be iterated with different origins for each transformed net and eventually there would be no need to solve for the translation terms. This is possible because the translation terms are functionally independent of the strain parameters. However they may be correlated due to the geometry and quality of the observations.

The equations for the least squares adjustment are-

$$Ai = \begin{bmatrix} \frac{\partial F}{\partial e_{ee}} & \frac{\partial F}{\partial e_{nn}} & \frac{\partial F}{\partial e_{vv}} & \frac{\partial F}{\partial e_{en}} & \frac{\partial F}{\partial e_{ev}} & \frac{\partial F}{\partial e_{nv}} & \frac{\partial F}{\partial \omega_v} & \frac{\partial F}{\partial \omega_n} & \frac{\partial F}{\partial \omega_e} & \frac{\partial F}{\partial Te} & \frac{\partial F}{\partial Tn} & \frac{\partial F}{\partial Tv} \end{bmatrix}$$

$$= \begin{bmatrix} P & 0 & 0 & Q & R & 0 & Q & -R & 0 & 1 & 0 & 0 \\ 0 & Q & 0 & P & 0 & R & -P & 0 & R & 0 & 1 & 0 \\ 0 & 0 & R & 0 & P & Q & 0 & P & -Q & 0 & 0 & 1 \end{bmatrix}$$

where $P = -\sin\lambda_A(x_A - xc_A) + \cos\lambda_A(y_A - yc_A)$

$Q = -\sin\phi_A\cos\lambda_A(x_A - xc_A) - \sin\phi_A\sin\lambda_A(y_A - yc_A) + \cos\phi_A(z_A - zc_A)$

$R = \cos\phi_A\cos\lambda_A(x_A - xc_A) + \cos\phi_A\sin\lambda_A(y_A - yc_A) + \sin\phi_A(z_A - zc_A)$

$$Bi = \begin{bmatrix} \frac{\partial F}{\partial x_A} & \frac{\partial F}{\partial y_A} & \frac{\partial F}{\partial z_A} & \frac{\partial F}{\partial x_B} & \frac{\partial F}{\partial y_B} & \frac{\partial F}{\partial z_B} \end{bmatrix}$$

$$\frac{\partial F}{\partial x_A} = \begin{bmatrix} -\sin\lambda_A(1+e_{ee}) - \sin\phi_A\cos\lambda_A(e_{en}+\omega_v) + \cos\phi_A\cos\lambda_A(e_{ev}-\omega_n) \\ -\sin\lambda_A(e_{en}-\omega_v) - \sin\phi_A\cos\lambda_A(1+e_{en}) + \cos\phi_A\cos\lambda_A(e_{nv}+\omega_e) \\ -\sin\lambda_A(e_{ev}+\omega_n) - \sin\phi_A\cos\lambda_A(e_{nv}-\omega_e) + \cos\phi_A\cos\lambda_A(1+e_{vv}) \end{bmatrix}$$

$$\frac{\partial F}{\partial y_A} = \begin{bmatrix} \cos\lambda_A(1+e_{ee}) - \sin\phi_A\sin\lambda_A(e_{en}+\omega_v) + \cos\phi_A\sin\lambda_A(e_{ev}-\omega_n) \\ \cos\lambda_A(e_{en}-\omega_v) - \sin\phi_A\sin\lambda_A(1+e_{en}) + \cos\phi_A\sin\lambda_A(e_{nv}+\omega_e) \\ \cos\lambda_A(e_{ev}+\omega_n) - \sin\phi_A\sin\lambda_A(e_{nv}-\omega_e) + \cos\phi_A\sin\lambda_A(1+e_{vv}) \end{bmatrix}$$

$$\frac{\partial F}{\partial z_A} = \begin{bmatrix} \cos\phi_A(e_{en}+\omega_v) + \sin\phi_A(e_{ev}-\omega_n) \\ \cos\phi_A(1+e_{en}) + \sin\phi_A(e_{nv}+\omega_e) \\ \cos\phi_A(e_{nv}-\omega_e) + \sin\phi_A(1+e_{vv}) \end{bmatrix}$$

$$\begin{bmatrix} \frac{\partial F}{\partial x_B} & \frac{\partial F}{\partial y_B} & \frac{\partial F}{\partial z_B} \end{bmatrix} = \begin{bmatrix} \sin\lambda_B & -\cos\lambda_B & 0 \\ \sin\phi_B\cos\lambda_B & \sin\phi_B\sin\lambda_B & -\cos\phi_B \\ -\cos\phi_B\cos\lambda_B & -\cos\phi_B\sin\lambda_B & -\sin\phi_B \end{bmatrix}$$

There are two ways to compute the topocentric strain components: either by applying the above model, or by pre-conversion of the coordinates and applying the geocentric model. Though care must be taken with the converted data so as to avoid the effects of rounding errors. The TAS program was checked by comparing the results from both procedures. The same answers were obtained from the topocentric strain and geocentric strain models.

The effect of choice of plane on topocentric strain parameters.

The change of plane can be thought of as a change of reference axes of the strain ellipsoid. No matter what plane is chosen the adjusted lengths and coordinates are the same. The overall strain, that is the 3D dilatation and the principal strains, is also identical. The differences in the strain parameters are caused by the different orientations of the reference axes, but all represent the same total strain conic. In fact given one set of parameters a simple transformation will convert these to any other frame. Chen (1983) gives this transformation as -

$$E' = A\ E\ A'$$

that is -

$$\begin{bmatrix} e'_{xx} & e'_{xy} & e'_{xz} \\ e'_{xy} & e'_{yy} & e'_{yz} \\ e'_{xz} & e'_{xz} & e'_{zz} \end{bmatrix} = \begin{bmatrix} lx & mx & nx \\ ly & my & ny \\ lz & mz & nz \end{bmatrix} \begin{bmatrix} e_{xx} & e_{xy} & e_{xz} \\ e_{xy} & e_{yy} & e_{yz} \\ e_{xz} & e_{xz} & e_{zz} \end{bmatrix} \begin{bmatrix} lx & mx & nx \\ ly & my & ny \\ lz & mz & nz \end{bmatrix}$$

where the rows of A are the direction cosines of the x y and z axes of the new reference frame with respect to the old reference frame.

If the reference frames differ by small rotations, ω_x, ω_y, and ω_z about the x, y, and z axes respectively, then it follows that -

$$E' = \begin{bmatrix} 1 & \omega_z & -\omega_y \\ -\omega_z & 1 & \omega_x \\ \omega_y & -\omega_x & 1 \end{bmatrix} E \begin{bmatrix} 1 & -\omega_z & \omega_y \\ \omega_z & 1 & -\omega_x \\ -\omega_y & \omega_x & 1 \end{bmatrix}$$

If the e_{ij} terms are less than 100 μstrain and the change in any e_{ij} is desired to be less than 0.1 μstrain then the sum of the rotation angles would have to be less than about 100". Clearly a change in orientation of the reference plane of a few minutes of arc could cause significant changes in the strain parameters. The difference between geodetic and geocentric latitude at a point is a maximum of about 11.5' at a latitude of $\pm 45^{\circ}$ and decreases to zero at the equator and poles. Generally the smaller the net the less the difference between the various three-point planes.

That is the ωx, ωy, and ωz are smaller. This in turn leads to smaller differences between the e_{ij} referred to different planes.

Numerical examples of the effect of choice of plane are given in Tables 8.3 and 8.4. In both examples the adjusted lengths and coordinates and the weighted sum of the residuals are the same from each solution with a differently oriented plane. Solutions using the geodetic normal to orientate the plane also give slightly different estimates of the parameters, but exactly the same adjusted lengths and coordinates.

Table 8.3. 3D Topocentric Strain determined from the observed data of the Australian VLBI network.

	Plane defined by	
Parameter	Geocentric Ø	3 pt (FHA)
e_{ee}	0.874 ± 1.27	0.203 ± 1.18
e_{nn}	-0.005 ± 0.679	0.336 ± 0.723
e_{vv}	-76.2 ± 116.	-75.8 ± 116.
e_{en}	-0.300 ± 0.39	0.844 ± 0.723
e_{ev}	1.44 ± 6.04	-7.25 ± 9.63
e_{nv}	10.72 ± 4.82	9.44 ± 4.26
ωe	5.26 ± 1.10	1.8 ± 1.0
ωn	-1.26 ± 2.63	1.6 ± 2.7
ωv	2.48 ± 0.10	0.57 ± 0.17
Te	-0.084 ± 0.341	-0.083 ± 0.400
Tn	0.113 ± 0.484	0.118 ± 0.485
Tv	-0.073 ± 1.84	-0.065 ± 1.82
2D dilat	0.869 ± 1.285	0.539 ± 1.336
3D dilatation	-75.3 ± 115.	75.3 ± 115.
Principal	-77.67	-77.67
strains	1.49	1.49
	0.88	0.88
	$\tilde{\sigma}_0^2 = 0.38$	

The dependence of the strain parameters on the orientation

of the plane is especially important if it is desired to constrain the strain normal to the plane to zero.

Table 8.4. 3D Topocentric Strain determined from the simulated data set.

Parameter	Geocentric Ø	Plane defined by 3 pt (TPF)	3 pt (TPBB)
e_{ee}	-3.12 ± 0.80	-2.93 ± 0.58	-3.34 ± 1.43
e_{nn}	-2.35 ± 0.68	-2.45 ± 0.57	-2.52 ± 0.69
e_{vv}	-13.39 ± 1353.	-13.47 ± 1360.	-12.99 ± 1360.
e_{en}	-0.02 ± 0.49	-0.04 ± 0.40	0.23 ± 0.72
e_{ev}	41.1 ± 138.	41.2 ± 138.	41.1 ± 138.
e_{nv}	26.5 ± 114.	26.4 ± 114.	-26.6 ± 114.
ωe	9.67 ± 23.5	5.28 ± 23.5	-5.32 ± 23.6
ωn	-11.72 ± 28.5	-8.25 ± 28.4	-8.25 ± 28.4
ωv	2.19 ± 0.12	-0.19 ± 0.10	0.17 ± 0.15
Te	-0.101 ± 0.106	-0.102 ± 0.106	0.101 ± 0.106
Tn	-0.082 ± 0.113	-0.082 ± 0.113	-0.082 ± 0.114
Tv	0.000 ± 0.895	0.000 ± 0.895	0.001 ± 0.895
2D dilat.	-5.47 ± 1.01	-5.38 ± 0.82	-5.87 ± 1.62
3D dilat.	-18.9 ± 1358.	-18.9 ± 1358.	-18.9 ± 1358.
Principal	41.0	41.0	41.0
strains	-2.6	-2.6	-2.6
	-57.3	-57.3	-57.3
	$\tilde{\sigma}_o^2 = 0.61$		

Comparison of Geocentric and Topocentric Strain.

When using the geocentric strain model on the simulated data the normal equations were found to have a rank defect of three. However when the local topocentric approach was applied there were no rank defects. Moreover the two horizontal components were far more precisely determined than the strain along the vertical axis, as Table 8.4 shows.

The adjusted lengths and their precisions, the a posteriori variance factor, and the adjusted coordinates and their

VCV, are virtually the same in both the topocentric solutions and in the geocentric matrix inversion solution. However the geocentric SVD solution gives different, presumably incorrect, answers for the adjusted lengths, coordinates and variances. As expected the 3D dilatation and the magnitudes of the principal strains as determined by the geocentric and topocentric solutions are the same in each example.

In the numerical examples given above the strain in any one direction is not statistically different from the strain in any other direction. Therefore the data sets could be combined with a single scale factor, that is, using a similarity transformation (see Chapters 6 and 7). In the topocentric system some components are far better determined (smaller precisions) than others. Moreover, all parameters are far less correlated in the topocentric solution than they are in the geocentric solution.

In the topocentric model the translations and rotations represent differences after shift of centroids. The rotations in the geocentric model are about global xyz axes, while in the topocentric model they are about the local north, east, and vertical axes.

3D Ellipsoidal Strain.

If the range of heights in a network is small, then the precision of the estimated vertical strain should be poor and the correlations with the horizontal strain components small. Ellipsoidal strain is investigated here because the points of a network may be closer to an ellipsoidal reference surface than to a plane. However the topography may have a significant effect on the range of heights unless the net spans thousands of kilometres. The precision of the 'horizontal' strain components should be similar in both ellipsoidal and plane strain approaches because the arc lengths and chord lengths between points are similar.

Now, for 3D strain in ellipsoidal coordinates -

$$ds^2 = g_1^2\, d\phi^2 + g_2^2\, d\lambda^2 + g_3^2\, dh^2$$

$$\text{where } g_1 = (1-e^2)N/(1-e^2\sin^2\phi) + h = M + h$$

$$g_2 = (N + h)\cos\phi$$

$$g_3 = 1.$$

The displacements are given by -

$$\begin{bmatrix} \Delta\phi \\ \Delta\lambda \\ \Delta h \end{bmatrix} = \begin{bmatrix} \frac{\partial\Delta\phi}{\partial\phi} & \frac{\partial\Delta\phi}{\partial\lambda} & \frac{\partial\Delta\phi}{\partial h} \\ \frac{\partial\Delta\lambda}{\partial\phi} & \frac{\partial\Delta\lambda}{\partial\lambda} & \frac{\partial\Delta\lambda}{\partial h} \\ \frac{\partial\Delta h}{\partial\phi} & \frac{\partial\Delta h}{\partial\lambda} & \frac{\partial\Delta h}{\partial h} \end{bmatrix} \begin{bmatrix} \phi \\ \lambda \\ h \end{bmatrix} = \begin{bmatrix} sa & sb & sc \\ sd & se & sf \\ sg & sh & si \end{bmatrix} \begin{bmatrix} \phi \\ \lambda \\ h \end{bmatrix} \qquad (8.8)$$

where the nine terms, $\partial\Delta\phi/\partial\phi$ etc, are assumed to be constant across the field. This means that the linear relation between the displacements at a point and the coordinates of the point is constant. However the strain is not uniform or homogeneous across the field in the manner of rectangular Cartesian strain. In general, straight lines do not remain straight and lines originally parallel do not remain parallel, and the change of an angle or distance is dependent on its position within the network. Now

$$\begin{bmatrix} \phi_B \\ \lambda_B \\ h_B \end{bmatrix} = \begin{bmatrix} \Delta\phi \\ \Delta\lambda \\ \Delta h \end{bmatrix} + \begin{bmatrix} \phi \\ \lambda \\ h \end{bmatrix} + \begin{bmatrix} \text{translation} \\ \text{terms} \end{bmatrix}$$

where ϕ, λ, h are the coordinates in data set A, and ϕ_B, λ_B, h_B are the corresponding coordinates in data set B.

The Least Squares Design matrices are -

$$F = 0 = \begin{bmatrix} 1+sa & sb & sc \\ sd & 1+se & sf \\ sg & sh & 1+si \end{bmatrix} \begin{bmatrix} \phi \\ \lambda \\ h \end{bmatrix} - \begin{bmatrix} \phi_B \\ \lambda_B \\ h_B \end{bmatrix} \qquad (8.9)$$

$$+ \begin{bmatrix} \frac{-\sin\phi\cos\lambda}{(M+h)} & \frac{-\sin\phi\sin\lambda}{(M+h)} & \frac{\cos\phi}{(M+h)} \\ \frac{-\sin\lambda}{(N+h)\cos\phi} & \frac{\cos\lambda}{(N+h)\cos\phi} & 0 \\ \cos\phi\cos\lambda & \cos\phi\sin\lambda & \sin\phi \end{bmatrix} \begin{bmatrix} Tx \\ Ty \\ Tz \end{bmatrix}$$

$$Ai = \begin{bmatrix} \frac{\partial F}{\partial sa} & \frac{\partial F}{\partial sb} & \frac{\partial F}{\partial sc} & \frac{\partial F}{\partial sd} & \frac{\partial F}{\partial se} & \frac{\partial F}{\partial sf} & \frac{\partial F}{\partial sg} & \frac{\partial F}{\partial sh} & \frac{\partial F}{\partial si} & \frac{\partial F}{\partial Tx} & \frac{\partial F}{\partial Ty} & \frac{\partial F}{\partial Tz} \end{bmatrix}$$

$$= \begin{bmatrix} \phi & \lambda & h & 0 & 0 & 0 & 0 & 0 & 0 & \frac{-\sin\phi\cos\lambda}{(M+h)} & \frac{-\sin\phi\sin\lambda}{(M+h)} & \frac{\cos\phi}{(M+h)} \\ 0 & 0 & 0 & \phi & \lambda & h & 0 & 0 & 0 & \frac{-\sin\lambda}{(N+h)\cos\phi} & \frac{\cos\lambda}{(N+h)\cos\phi} & 0 \\ 0 & 0 & 0 & 0 & 0 & 0 & \phi & \lambda & h & \cos\phi\cos\lambda & \cos\phi\sin\lambda & \sin\phi \end{bmatrix}$$

$$Bi = \begin{bmatrix} \frac{\partial F}{\partial \phi} & \frac{\partial F}{\partial \lambda} & \frac{\partial F}{\partial h} & \frac{\partial F}{\partial \phi_B} & \frac{\partial F}{\partial \lambda_B} & \frac{\partial F}{\partial h_B} \end{bmatrix}$$

$$\frac{\partial F}{\partial \phi} = \begin{bmatrix} 1 + sa - D1(\cos\lambda\ Tx + \sin\phi\ Ty) + D2\ Tz \\ sd - D5(\sin\lambda\ Tx - \cos\lambda\ Ty) \\ sg - \sin\phi(\cos\lambda\ Tx + \sin\lambda\ Ty) + \cos\phi\ Tz \end{bmatrix}$$

where D1, D2, and D5 are as in Chapter 7.

$$\frac{\partial F}{\partial \lambda} = \begin{bmatrix} sb + \sin\phi(\sin\lambda\ Tx - \cos\lambda\ Ty) / (M+h) \\ 1 + se - (\cos\lambda\ Tx + \sin\lambda\ Ty) / (N+h)\cos\phi \\ sh - \cos\phi(\sin\lambda\ Tx - \cos\lambda\ Ty) \end{bmatrix}$$

$$\frac{\partial F}{\partial h} = \begin{bmatrix} sc + (\sin\phi\cos\lambda\ Tx + \sin\phi\sin\lambda\ Ty - \cos\phi\ Tz)/(M+h)^2 \\ sf + (\sin\lambda\ Tx - \cos\lambda\ Ty) / \cos\phi(N+h)^2 \\ 1 + si \end{bmatrix}$$

$$\begin{bmatrix} \frac{\partial F}{\partial \phi_B} & \frac{\partial F}{\partial \lambda_B} & \frac{\partial F}{\partial h_B} \end{bmatrix} = \begin{bmatrix} -1 & 0 & 0 \\ 0 & -1 & 0 \\ 0 & 0 & -1 \end{bmatrix}$$

The procedure is to solve for the nine components of displacement (sa - si), and convert these to strain components, e_{ij}, using equations according to Bibby (1973) -

$$e_{\phi\phi} = \frac{\partial \Delta\phi}{\partial \phi} + \frac{\Delta\phi}{g_1}\frac{\partial M}{\partial \phi} + \frac{\Delta h}{g_1}$$

$$e_{\lambda\lambda} = \frac{\partial \Delta\lambda}{\partial \lambda} - g_1 \frac{\sin\phi}{g_2}\Delta\phi + \frac{\cos\phi\ \Delta h}{g_2} \qquad (8.10)$$

$$e_{hh} = \frac{\partial \Delta h}{\partial h}$$

$$e_{\phi\lambda} = \frac{1}{2}\left[\frac{g_1}{g_2}\frac{\partial \Delta\phi}{\partial \lambda} + \frac{g_2}{g_1}\frac{\partial \Delta\lambda}{\partial \phi}\right] = e_{\lambda\phi}$$

$$e_{\lambda h} = \frac{1}{2}\left[g_2 \frac{\partial \Delta\lambda}{\partial h} + \frac{1}{g_2}\frac{\partial \Delta h}{\partial \lambda}\right] = e_{h\lambda}$$

$$e_{\phi h} = \frac{1}{2}\left[g_1 \frac{\partial \Delta\phi}{\partial h} + \frac{1}{g_1}\frac{\partial \Delta h}{\partial \phi}\right] = e_{h\phi}$$

$$\omega_h = \frac{1}{2}\left[\frac{g_1}{g_2}\frac{\partial \Delta\phi}{\partial \lambda} - \frac{g_2}{g_1}\frac{\partial \Delta\lambda}{\partial \phi}\right] + \sin\phi\ \Delta\lambda$$

$$\omega_\phi = \frac{1}{2}\left[g_2 \frac{\partial \Delta\lambda}{\partial h} - \frac{1}{g_2}\frac{\partial \Delta h}{\partial \lambda}\right] + \cos\phi\ \Delta\lambda$$

$$\omega_\lambda = \frac{1}{2}\left[-g_1 \frac{\partial \Delta\phi}{\partial h} + \frac{1}{g_1}\frac{\partial \Delta h}{\partial \phi}\right] - \Delta\phi$$

$$\text{Dilatation} = e_{\phi\phi} + e_{\lambda\lambda} + e_{hh}$$

where, from (8.8) above, -

$$\Delta\lambda = \frac{\partial \Delta\lambda}{\partial \phi}\phi + \frac{\partial \Delta\lambda}{\partial \lambda}\lambda + \frac{\partial \Delta\lambda}{\partial h}h$$

$$\Delta\phi = \frac{\partial \Delta\phi}{\partial \phi}\phi + \frac{\partial \Delta\phi}{\partial \lambda}\lambda + \frac{\partial \Delta\phi}{\partial h}h$$

$$\Delta h = \frac{\partial \Delta h}{\partial \phi}\phi + \frac{\partial \Delta h}{\partial \lambda}\lambda + \frac{\partial \Delta h}{\partial h}h$$

At each point of computation,

$e_{\phi\phi}$ is the extension of an element in the direction of the parallel of latitude at that point,

$e_{\lambda\lambda}$ is the extension of an element in the direction of the meridian of longitude at that point,

e_{hh} is the extension of an element in the direction of the ellipsoidal normal at that point,

$e_{\phi h}$, $e_{\lambda h}$, and $e_{\phi\lambda}$ are the shear strains,

ω_h is the rotation about the ellipsoidal normal at that point,

ω_ϕ is the rotation about the tangent to the parallel of latitude at that point, and

ω_λ is the rotation about the tangent to the meridian of

longitude at that point.

So it can be seen that even in a homogeneous field, the e_{ij} (except for e_{hh}) and ω_{ij} vary from point to point. With typical displacements the strain parameters at each point will not differ by more than 0.01μstrain for points within a region of a few kilometres. Over regions of a few hundred kilometres the strain parameters could vary considerably (see Tables 8.5 and 8.6).

Table 8.5. 3D Ellipsoidal Strain determined from the observed data of the Australian VLBI net.

	Site where parameters evaluated	
	Tidbinbilla	Parkes
$e_{\phi\phi}$	-2.65 ± 2.24	-3.70 ± 2.31
$e_{\lambda\lambda}$	3.37 ± 1.49	2.53 ± 1.38
e_{hh}	10492. ± 8430.	10492. ± 8430.
$e_{\phi\lambda}$	-1.15 ± 1.41	-1.02 ± 1.37
$e_{\lambda h}$	538. ± 319.	554. ± 328.
$e_{\phi h}$	-1112. ± 660.	-1112. ± 660.
ω_h	-0.74 ± 0.33	-0.76 ± 0.33
ω_ϕ	110.9 ± 65.5	114. ± 67.
ω_λ	227.8 ± 137.	227.7 ± 136.
Tx	-124.99 ± 7.56	same at all points
Ty	-68.7 ± 22.9	
Tz	210.5 ± 41.7	
3D dilat	10493. ± 8430.	10491. ± 8430.
$\tilde{\sigma}_o^2 = 3.41$		

The VCV of the derived strain parameters is calculated as follows -

$$\text{VCV } e_{ij} = J \text{ VCV } s_i \, J^T$$

where e_{ij} are in the order $e_{\phi\phi}$, $e_{\lambda\lambda}$, e_{hh}, $e_{\phi\lambda}$, $e_{\lambda h}$, $e_{\phi h}$, and the s_i are in the order sa, sb, sc, sd, se, sf, sg, sh, si. The Jacobian matrix J is given by -

$$
\begin{bmatrix}
1+\frac{\phi}{g_1}\cdot\frac{\partial M}{\partial \phi} & \frac{\lambda}{g_1}\cdot\frac{\partial M}{\partial \phi} & \frac{h}{g_1}\cdot\frac{\partial M}{\partial \phi} & 0 & 0 & 0 & \frac{\phi}{g_1} & \frac{\lambda}{g_1} & \frac{h}{g_1} \\
\frac{-\phi g_1 \sin\phi}{g_2} & \frac{-\lambda g_1 \sin\phi}{g_2} & \frac{-h g_1 \sin\phi}{g_2} & 0 & 0 & 0 & \frac{\phi\cos\phi}{g_2} & \frac{\lambda\cos\phi}{g_2} & \frac{h\cos\phi}{g_2} \\
0 & 0 & 0 & 0 & 0 & 0 & 0 & 0 & 1 \\
0 & \frac{g_1}{2g_2} & 0 & \frac{g_2}{2g_1} & 0 & 0 & 0 & 0 & 0 \\
0 & 0 & 0 & 0 & 0 & \frac{g_2}{2} & 0 & \frac{1}{2g_2} & 0 \\
0 & 0 & \frac{g_1}{2} & 0 & 0 & 0 & \frac{1}{2g_1} & 0 & 0 \\
0 & \frac{g_1}{2g_2} & 0 & \phi\sin\phi-\frac{g_2}{2g_1} & \lambda\sin\phi & h\sin\phi & 0 & 0 & 0 \\
0 & 0 & 0 & \phi\cos\phi & \lambda\cos\phi & h\cos\phi+\frac{g_2}{2} & 0 & \frac{-1}{2g_2} & 0 \\
-\phi & -\lambda & -h-\frac{g_1}{2} & 0 & 0 & 0 & \frac{1}{2g_1} & 0 & 0
\end{bmatrix}
$$

Table 8.6. 3D Ellipsoidal Strain determined from using the simulated data set.

	Site where parameters evaluated	
	Tidbinbilla	Parkes
$e_{\phi\phi}$	-3.91 ± 1.51	-3.75 ± 1.53
$e_{\lambda\lambda}$	-5.75 ± 2.57	-5.43 ± 2.48
e_{hh}	-99. ± 6760.	-99. ± 6760.
$e_{\phi\lambda}$	-1.90 ± 1.43	-1.92 ± 1.46
$e_{\lambda h}$	-579. ± 544.	-595. ± 559.
$e_{\phi h}$	-472. ± 451.	-472. ± 450.
ω_h	0.19 ± 0.29	0.21 ± 0.28
ω_ϕ	-119. ± 112.	-123. ± 115.
ω_λ	98.7 ± 92.8	98.7 ± 92.8
Tx	119.2 ± 32.6	same at all points
Ty	53.6 ± 101.	
Tz	-141.9 ± 129.	
3D dilat	-108.7 ± 6760.	-108.2 ± 6760.
$\tilde{\sigma}_o^2$ = 0.01		

Comparison of Ellipsoidal and Topocentric Strain.

The real and simulated examples given above do not prove that the ellipsoidal strain model is any better than topocentric strain model. The ellipsoidal model fits the data better, that is, it produces smaller residuals in the one example but is worse in the other example. The adjusted lengths and coordinates from each model are different. However the topocentric approach is computationally simpler.

The horizontal strain components determined by both models have similar precisions since the precision depends on the displacement divided by the length and the length along an arc is approximately the same as the length along its tangent. The precision of vertical strain in the ellipsoidal model should be poorer than the equivalent strain in the topocentric model because the range of heights is generally less (though this depends on the topography). Similarly the precision of the estimated 3D dilatation, which is usually dominated by the precision of the vertical or height strain, is poorer in the ellipsoidal model than the topocentric model.

If the network and its displacements were very small the topocentric and ellipsoidal strain parameters would be equivalent. However with typical displacements the differences between topocentric and ellipsoidal strain parameters is significant, even for networks of a few kilometres extent.

2D MODELS FOR DETERMINING STRAIN.

The methods considered here are plane, ellipsoidal displacements, ellipsoidal coordinates, TM projection and the plane of maximum strain. The first four of these are discussed in more detail below. The plane - of - maximum - strain method could be applied as follows. Compute the eigenvalues and eigenvectors of the strain tensor from a 3D

analysis. This will give the plane that has the maximum strain, its direction and the magnitude of the strain. Then solve for the 2D strain in this plane. However this result is not useful because even though the strain in a particular direction may be numerically large it may also be statistically insignificant. For example say the two horizontal directions have strains of about 0.3 ± 0.1 μstrains and the vertical direction 70 ± 100 μstrains. The plane of maximum strain would be nearly vertical and is obviously not the most significant direction of strain.

2D Strain analysis on a plane.

This is the conventional method in which strain is computed between points which lie on a plane. This chosen plane could be the same as the plane described above in the 3D topocentric model. If there are only three points common to both nets then the plane through these points should be chosen.

Now, for 2D strain in Cartesian coordinates (x y) -

$$ds^2 = dx^2 + dy^2 \text{ and so -}$$

$$S = \begin{bmatrix} e_{xx} & e_{xy} \\ e_{xy} & e_{yy} \end{bmatrix} \quad \text{and} \quad R = \begin{bmatrix} 0 & \omega \\ -\omega & 0 \end{bmatrix}$$

(Some authors use engineering strain units which are twice the value of the tensor strains given here.) From the strain terms e_{xx}, e_{xy}, and e_{yy}, and their VCV (VCV_e) further strain parameters can be derived (see for example Welsch, 1983) -

$$\text{Pure shear} = \gamma 1 = e_{xx} - e_{yy}$$

$$\text{Engineering shear} = \gamma 2 = 2e_{xy}$$

$$\text{Total shear (or maximum shear strain)} = \gamma = / (\gamma 1^2 + \gamma 2^2)$$

$$\text{Maximum principal strain} = e1 = (\Delta + \gamma)/2$$

$$\text{Minimum principal strain} = e2 = (\Delta - \gamma)/2$$

$$\text{Dilatation} = \Delta = e_{xx} + e_{yy} = e_1 + e_2$$

$$\text{Bearing of e1} = \Theta = \arctan(2e_{xy}/e_{yy}-e_{xx})/2$$

$$\text{Bearing of maximum shear} = \Psi = \Theta + \pi/4$$

Let $e = (e_{xx}, e_{xy}, e_{yy})^T$ and $p = (\gamma 1, \gamma 2, \Delta)^T$ then

$$VCV_p = \begin{bmatrix} 1 & 0 & -1 \\ 0 & 2 & 0 \\ 1 & 0 & 1 \end{bmatrix} VCV_e \begin{bmatrix} 1 & 0 & 1 \\ 0 & 2 & 0 \\ -1 & 0 & 1 \end{bmatrix}$$

Let $q = (\gamma, e1, e2, \Theta, \Psi)^T$ then -

$$VCV_q = \begin{bmatrix} \gamma1/\gamma & \gamma2/\gamma & 0 \\ \gamma1/2\gamma & \gamma2/2\gamma & 1/2 \\ -\gamma1/2\gamma & -\gamma2/2\gamma & 1/2 \\ -\gamma2/2\gamma2 & \gamma1/2\gamma2 & 0 \end{bmatrix} VCV_p \begin{bmatrix} \gamma1/\gamma & \gamma1/2\gamma & -\gamma1/2\gamma & -\gamma2/2\gamma2 \\ \gamma2/\gamma & \gamma2/2\gamma & -\gamma2/2\gamma & \gamma1/2\gamma2 \\ 0 & 1/2 & 1/2 & 0 \end{bmatrix}$$

The diagonal components of S are the scale changes along each of the axes and the off-diagonal terms are the orientation (or shearing strain) of the axes. These extensional and shearing strains are therefore dependent on the direction of these axes. Dilatation is the change in area (size) of a network under deformation, positive for an increase. γ is the shear across the direction of maximum strain. $\gamma1$ is the shear across any line parallel to the y (north) axis. $\gamma2$ is the shear across any line parallel to the x (east) axis. Note that $\gamma1$, $\gamma2$, Δ, γ, e_1, and e_2 are independent of a rotation or translation in the reference frame of either or both networks. However Θ and Ψ, and the e_{ij} are dependent on the reference frame.

This method of 2D strain analysis on a plane tacitly assumes that both nets are on the same plane. However two VLBI nets or a VLBI and ground net contain coordinates that are probably not referred to the same plane. So this method should not be applied unless additional parameters are included to allow for the different orientation (tilts) of the two reference planes. This is why different answers will generally be obtained if 2D is compared with 3D strain with the vertical strain fixed at zero.

Numerical examples of this model and comparisons with other strain models are given in Tables 8.7 and 8.8. In both tables the strains refer to the same plane for each of the methods of computation. The precisions of the strain components in both data sets are better for the 3D Topocentric strain with the vertical strain fixed at zero, than for the other methods.

Table 8.7. 2D Strain determined from the observed data of the Australian VLBI net.

	Model		
	2D plane	3D topocentric	3D topocentric
e_{ee}	2.005 ± 0.887	0.874 ± 1.269	-0.218 ± 0.602
e_{nn}	-1.283 ± 0.648	-0.005 ± 0.679	-0.328 ± 0.579
e_{vv}	-- --	-76.175 ± 116.0	0.000 fixed
e_{en}	-0.443 ± 0.431	-0.300 ± 0.393	-0.458 ± 0.345
e_{ev}	-- --	1.441 ± 6.04	0.000 fixed
e_{nv}	-- --	10.718 ± 4.82	0.000 fixed
ωe	-- --	5.262 ± 1.098	4.110 ± 0.686
ωn	-- --	-1.260 ± 2.631	-3.829 ± 0.799
ωv	2.539 ± 0.124	2.483 ± 0.102	2.470 ± 0.082
Te	-0.116 ± 0.290	-0.084 ± 0.341	-0.342 ± 0.259
Tn	1.990 ± 0.256	0.113 ± 0.484	0.929 ± 0.295
Tv	-- --	-0.073 ± 1.840	-0.569 ± 1.816
2D dilat	0.722 ± 0.997	0.868 ± 1.285	-0.546 ± 0.900
$\tilde{\sigma}_o^2$	5.50	0.379	1.14

Table 8.8. 2D Strain determined from the simulated data set.

	Model		
	2D plane	3D topocentric	3D topocentric
e_{ee}	2.922 ± 0.805	3.120 ± 0.803	2.950 ± 0.571
e_{nn}	2.474 ± 0.797	2.345 ± 0.678	2.437 ± 0.562
e_{vv}	-- --	13.39 ± 1353.	0.000 fixed
e_{en}	0.037 ± 0.566	0.019 ± 0.490	0.038 ± 0.393
e_{ev}	-- --	-41.14 ± 138.	0.000 fixed
e_{nv}	-- --	-26.47 ± 114.	0.000 fixed
ωe	-- --	-9.67 ± 23.5	-4.233 ± 1.973
ωn	-- --	11.72 ± 28.5	3.262 ± 2.288
ωv	-2.154 ± 0.140	-2.186 ± 0.122	-2.161 ± 0.100
Te	0.116 ± 0.140	0.101 ± 0.106	0.113 ± 0.099
Tn	0.090 ± 0.155	0.082 ± 0.113	0.088 ± 1.109
Tv	-- --	0.000 ± 0.895	0.000 ± 0.894
2D dilat	5.396 ± 1.150	5.465 ± 1.007	5.387 ± 0.796
$\tilde{\sigma}_o^2$	0.51	0.61	0.33

Ellipsoidal Displacements.

In this method the changes in coordinates (ie displacements) between epochs are computed in terms of the changes in the geodetic latitude, longitude and ellipsoid height at each site. These changes are converted to changes in north, east, and vertical by multiplication by the appropriate radius of curvature. The displacements are therefore referred to the geodetic normal at each site. This is an inconsistent system because the geodetic normals of the sites are not parallel. Over a few hundred kilometres they deviate by a few degrees. However this will have an insignificant effect on the expected displacements due to crustal movements, of less than 30cm. (2^{o} in 30cm changes displacements by 0.2mm and strains by less than 0.001 μstrains.) So the procedure when combining two or more epochs of data is to hold the same point fixed throughout, and compute the displacements between coordinates in each epoch. The strain terms are then determined from these displacements. The method is suitable only when displacements are small (about 30cm). If rotations of a few arcseconds (2" at the Earth radius equals about 60m displacement) or large translations exist between the epochs to be combined, then the displacements will be large. So this method is not further investigated here.

2D Strain analysis on a Transverse Mercator projection.

Dermanis et al. (1983) discuss the strain caused by mapping latitude and longitude onto the common mapping surfaces. They show that the conformal map projections (eg. Transverse Mercator (TM)) do not cause a shear strain but do cause dilatation. Other map projections cause both dilatation and shear strain. So if the coordinates are projected onto a conformal map projection, commonly TM, before strain analysis then it must be remembered that the transformation onto the map surface has caused a dilatation that may amount to hundreds of ustrains, but no shear

strain. Since both epochs are transformed onto the map surface the error in the displacements will be negligible (0.01%) and the effect on the computed strain terms will also be insignificant. Bibby (1973) has also shown that the computation of horizontal strain on such a projection will result in negligible error provided the extent of the network is much smaller than the Earth's radius.

The above discussion assumes that the latitudes and longitudes of each point are similar in both epochs, or nets. No problems arise when the translations or rotations between the two epochs or networks are small. However there may be translations of a few hundred metres between ground coordinates on a non geocentric datum and VLBI coordinates which are referred to a geocentric coordinate system. In the TM projection the scale factor is a function of the distance of a point from the central meridian. Accordingly, if one network has all its points shifted further east (say) of the central meridian than the other network, then the two networks will be distorted, upon projection, in different ways. This difference caused by the projection will produce apparent strains and will mask or at least contaminate estimates of geophysical strain. Tables 8.9 and 8.10 illustrate this problem with a hypothetical numerical example. Since all angles and all distances are the same in each network no strain should be present when the two networks are combined.

Table 8.9. Initial Coordinates of triangular network.

From net	Latitude	Longitude	To net	Latitude	Longitude
A	-33°	149°	a	-33°	149° 00' 02"
B	-35°	149°	b	-35°	149° 00' 02"
C	-34°	149° 50'	c	-34°	149° 50' 02"

The coordinates of the points in Table 8.9 were projected on to a TM projection with central meridian 149°, central scale factor 0.9994, and a 2° zone width. The resultant

coordinates are given in Table 8.10. The baseline lengths are no longer the same. The transformation onto the map grid has introduced a large strain in the east-west direction. Both dilatation and shear terms are affected.

Table 8.10 TM projection of triangular net.

(a) Projection coordinates (metres)		
	N	E
A	-3652 541.546	0.000
B	-3763 135.607	76 994.375
C	-3874 373.875	0.000
a	-3652 541.546	51.916
b	-3763 135.190	77 035.332
c	-3874 373.875	50.713

(b) Grid distances between projected points (metres)	
A - C	221 832.329
a - c	221 832.329
A - B	134 756.002
a - b	134 749.399
B - C	135 285.203
b - c	135 279.993

It is therefore important that if strain is to be determined on a map projection surface then the two epochs or networks should be translated and rotated to a common datum before projection and subsequent strain analysis. This problem only arises when strain is determined from coordinate differences. If the strain is determined from differences in the observables (eg angles and distances) no errors would be introduced by transforming the observables onto the projection surface prior to solving for strain components provided that, the displacements are small (less than a metre or so), that the extent of the network is much less than an Earth radius (Bibby, 1973), and that identical trial coordinates of the points are used for the reductions of the observations of each epoch or network.

2D ellipsoidal strain.

Bibby (1973) considers a form of ellipsoidal strain where all vertical displacements are zero (ie Δh, $\partial\Delta h/\partial\phi$, $\partial\Delta h/\partial\lambda$, and $\partial\Delta h/\partial h$ all equal zero). However this technique does not allow for displacements due to rotations. It is assumed that both data sets refer to the same ellipsoidal surface or to the surfaces of ellipsoids that have parallel axes. This is analogous to assuming that both data sets lie on the same (or parallel) plane and not allowing for tilts between the planes. In earlier chapters it has been shown that there is good reason to believe that significant rotations between the reference frames of the two data sets may exist.

The following procedure is recommended to constrain vertical strain to zero but still allow for vertical displacements due to rotations. (It should be noted that the equivalent procedure in the topocentric Cartesian model is simpler because the vertical strain can be held fixed at zero and the 3D rotations solved for without altering the model.)

For zero vertical strain -

$$e_{hh} = e_{h\phi} = e_{h\lambda} = 0.$$

It follows from (8.10) that -

$$\text{If } e_{hh} = 0 \quad \text{then } \partial\Delta h/\partial h = 0,$$

$$\text{if } e_{\phi h} = 0 \quad \text{then } \partial\Delta\phi/\partial h = \frac{-1}{g_1^{\,2}}\,\frac{\partial\Delta h}{\partial\phi}$$

$$\text{and if } e_{\lambda h} = 0 \quad \text{then } \partial\Delta\lambda/\partial h = \frac{-1}{g_2^{\,2}}\,\frac{\partial\Delta h}{\partial\lambda}$$

so

$$\begin{bmatrix} \Delta\phi \\ \Delta\lambda \\ \Delta h \end{bmatrix} = \begin{bmatrix} \frac{\partial\Delta\phi}{\partial\phi} & \frac{\partial\Delta\phi}{\partial\lambda} & \frac{-1}{g_1^{\,2}}\frac{\partial\Delta h}{\partial\phi} \\ \frac{\partial\Delta\lambda}{\partial\phi} & \frac{\partial\Delta\lambda}{\partial\lambda} & \frac{-1}{g_2^{\,2}}\frac{\partial\Delta\lambda}{\partial h} \\ \frac{\partial\Delta h}{\partial\phi} & \frac{\partial\Delta h}{\partial\lambda} & 0 \end{bmatrix} \begin{bmatrix} \phi \\ \lambda \\ h \end{bmatrix} = \begin{bmatrix} sa & sb & \frac{-sg}{g_1^{\,2}} \\ sd & se & \frac{-sh}{g_2^{\,2}} \\ sg & sh & 0 \end{bmatrix} \begin{bmatrix} \phi \\ \lambda \\ h \end{bmatrix} \quad (8.11)$$

The Least Squares Design matrices are -

$$F = 0 = \begin{bmatrix} 1+sa & sb & \frac{-sg}{g_1^2} \\ sd & 1+se & \frac{-sh}{g_2^2} \\ sg & sh & 1 \end{bmatrix} \begin{bmatrix} \phi \\ \lambda \\ h \end{bmatrix} - \begin{bmatrix} \phi_B \\ \lambda_B \\ h_B \end{bmatrix} \qquad (8.12)$$

$$+ \begin{bmatrix} \frac{-\sin\phi\cos\lambda}{(M+h)} & \frac{-\sin\phi\sin\lambda}{(M+h)} & \frac{\cos\phi}{(M+h)} \\ \frac{-\sin\lambda}{(N+h)\cos\phi} & \frac{\cos\lambda}{(N+h)\cos\phi} & 0 \\ \cos\phi\cos\lambda & \cos\phi\sin\lambda & \sin\phi \end{bmatrix} \begin{bmatrix} Tx \\ Ty \\ Tz \end{bmatrix}$$

$$Ai = \begin{bmatrix} \frac{\partial F}{\partial sa} & \frac{\partial F}{\partial sb} & \frac{\partial F}{\partial sc} & \frac{\partial F}{\partial sd} & \frac{\partial F}{\partial se} & \frac{\partial F}{\partial sg} & \frac{\partial F}{\partial sh} & \frac{\partial F}{\partial Tx} & \frac{\partial F}{\partial Ty} & \frac{\partial F}{\partial Tz} \end{bmatrix}$$

$$= \begin{bmatrix} \phi & \lambda & 0 & 0 & \frac{-h}{g_1^2} & 0 & \frac{-\sin\phi\cos\lambda}{(M+h)} & \frac{-\sin\phi\sin\lambda}{(M+h)} & \frac{\cos\phi}{(M+h)} \\ 0 & 0 & \phi & \lambda & 0 & \frac{-h}{g_2^2} & \frac{-\sin\lambda}{(N+h)\cos\phi} & \frac{\cos\lambda}{(N+h)\cos\phi} & 0 \\ 0 & 0 & 0 & 0 & \phi & \lambda & \cos\phi\cos\lambda & \cos\phi\sin\lambda & \sin\phi \end{bmatrix}$$

$$Bi = \begin{bmatrix} \frac{\partial F}{\partial \phi} & \frac{\partial F}{\partial \lambda} & \frac{\partial F}{\partial h} & \frac{\partial F}{\partial \phi_B} & \frac{\partial F}{\partial \lambda_B} & \frac{\partial F}{\partial h_B} \end{bmatrix}$$

$$\frac{\partial F}{\partial \phi} = \begin{bmatrix} 1 + sa - D1(\cos\lambda\ Tx + \sin\phi\ Ty) + D2\ Tz + 2sgh\ \partial M/\partial\phi\ /\ (M+h)^3 \\ sd - D5(\sin\lambda\ Tx - \cos\lambda\ Ty) - 2shh(M+h)\sin\phi\ /\ \{(N+h)\cos\phi\}^3 \\ sg - \sin\phi(\cos\lambda\ Tx + \sin\lambda\ Ty) + \cos\phi\ Tz \end{bmatrix}$$

where D1, D2, and D5 are as in Chapter 7.

$$\frac{\partial F}{\partial \lambda} = \begin{bmatrix} sb + \sin\phi(\sin\lambda\ Tx - \cos\lambda\ Ty)\ /\ (M+h) \\ 1 + se - (\cos\lambda\ Tx + \sin\lambda\ Ty)\ /\ (N+h)\cos\phi \\ sh - \cos\phi(\sin\lambda\ Tx - \cos\lambda\ Ty) \end{bmatrix}$$

$$\frac{\partial F}{\partial h} = \begin{bmatrix} -sg/g_1^2 + (\sin\phi\cos\lambda Tx + \sin\phi\sin\lambda Ty - \cos\phi Tz)/(M+h)^2 + 2hsg/g_1^3 \\ -sh/g_2^2 + (\sin\lambda Tx - \cos\lambda Ty)/\cos\phi(N+h)^2 + 2hsh\cos\phi\ /\ g_2^3 \\ 1 \end{bmatrix}$$

$$\begin{bmatrix} \frac{\partial F}{\partial \phi_B} & \frac{\partial F}{\partial \lambda_B} & \frac{\partial F}{\partial h_B} \end{bmatrix} = \begin{bmatrix} -1 & 0 & 0 \\ 0 & -1 & 0 \\ 0 & 0 & -1 \end{bmatrix}$$

The procedure is to solve for the six components of displacement (sa - sh), and convert these to strain components, e_{ij}, as follows -

$$e_{\phi\phi} = \frac{\partial \Delta\phi}{\partial \phi} + \frac{\Delta\phi}{g_1}\frac{\partial M}{\partial \phi} + \frac{\Delta h}{g_1}$$

$$e_{\lambda\lambda} = \frac{\partial \Delta\lambda}{\partial \lambda} - g_1 \frac{\sin\phi}{g_2}\Delta\phi + \frac{\cos\phi\ \Delta h}{g_2} \qquad (8.13)$$

$$e_{\phi\lambda} = \frac{1}{2}\left[\frac{g_1}{g_2}\frac{\partial \Delta\phi}{\partial \lambda} + \frac{g_2}{g_1}\frac{\partial \Delta\lambda}{\partial \phi}\right] = e_{\lambda\phi}$$

$$\omega_h = \frac{1}{2}\left[\frac{g_1}{g_2}\frac{\partial \Delta\phi}{\partial \lambda} - \frac{g_2}{g_1}\frac{\partial \Delta\lambda}{\partial \phi}\right] + \sin\phi\ \Delta\lambda$$

$$\omega_\phi = \frac{-1}{g_2}\frac{\partial \Delta h}{\partial \lambda} + \cos\phi\ \Delta\lambda$$

$$\omega_\lambda = \frac{1}{g_1}\frac{\partial \Delta h}{\partial \phi} - \Delta\phi$$

$$\text{Dilatation} = e_{\phi\phi} + e_{\lambda\lambda}$$

where

$$\Delta\lambda = \frac{\partial \Delta\lambda}{\partial \phi}\phi + \frac{\partial \Delta\lambda}{\partial \lambda}\lambda - \frac{1}{g_2^2}\frac{\partial \Delta h}{\partial \lambda}h$$

$$\Delta\phi = \frac{\partial \Delta\phi}{\partial \phi}\phi + \frac{\partial \Delta\phi}{\partial \lambda}\lambda - \frac{1}{g_1^2}\frac{\partial \Delta h}{\partial \phi}h$$

$$\Delta h = \frac{\partial \Delta h}{\partial \phi}\phi + \frac{\partial \Delta h}{\partial \lambda}\lambda$$

Note that the e_{ij} and ω_{ij} vary from point to point. The VCV of the strain parameters is calculated as follows

$$\text{VCV } e_{ij} = J\ \text{VCV } s_i\ J^T$$

where e_{ij} are in the order eØØ, eλλ, eØλ and the s_i are in the order sa, sb, sd, se, sg, sh. The Jacobian matrix J is-

$$\begin{bmatrix}
1+\frac{\phi}{g_1}\frac{\partial M}{\partial \phi} & \frac{\lambda}{g_1}\frac{\partial M}{\partial \phi} & 0 & 0 & \frac{-h}{g_1^3}\frac{\partial M}{\partial \phi} + \frac{\phi}{g_1} & \frac{\lambda}{g_1} \\
\frac{-\phi g_1 \sin\phi}{g_2} & \frac{-\lambda g_1 \sin\phi}{g_2} & 0 & 1 & \frac{h\sin\phi}{g_2 g_1} + \frac{\phi\cos\phi}{g_2} & \frac{\lambda\cos\phi}{g_2} \\
0 & \frac{g_1}{2g_2} & \frac{g_2}{2g_1} & 0 & 0 & 0 \\
0 & \frac{g_1}{2g_2} & \frac{\phi\sin\phi - g_2}{2g_1} & \lambda\sin\phi & 0 & \frac{-h\sin\phi}{g_2^2} \\
0 & 0 & \phi\cos\phi & \lambda\cos\phi & 0 & \frac{-1}{g_2} - \frac{h\cos\phi}{g_2^2} \\
-\phi & -\lambda & 0 & 0 & \frac{1}{g_1} - \frac{h}{g_1^2} & 0
\end{bmatrix}$$

Numerical examples of this model are given in Tables 8.11 and 8.12.

Table 8.11 2D Ellipsoidal strain determined from the observed data of the Australian VLBI net.

	Site where parameters evaluated	
	Tidbinbilla	Parkes
$e_{\phi\phi}$	0.39 ± 0.59	0.05 ± 0.56
$e_{\lambda\lambda}$	0.76 ± 0.57	0.39 ± 0.59
$e_{\phi\lambda}$	0.24 ± 0.34	0.24 ± 0.35
ω_h	-0.11 ± 0.09	-0.10 ± 0.09
ω_ϕ	0.77 ± 0.98	0.76 ± 0.97
ω_λ	-1.95 ± 0.63	-1.96 ± 0.65
Tx	-126.8 ± 6.8	same at all sites
Ty	-47.6 ± 20.9	
Tz	147.1 ± 27.1	
2D dilat	1.15 ± 0.82	0.44 ± 0.82
	$\tilde{\sigma}_o^2$ = 1.31	

Table 8.12 2D ellipsoidal strain determined from the simulated data set.

	Site where parameters evaluated	
	Tidbinbilla	Parkes
$e_{\phi\phi}$	-2.55 ± 0.60	-2.25 ± 0.63
$e_{\lambda\lambda}$	-3.16 ± 0.62	-2.91 ± 0.58
$e_{\phi\lambda}$	0.03 ± 0.39	0.01 ± 0.41
ω_h	0.23 ± 0.11	0.23 ± 0.12
ω_ϕ	-0.23 ± 2.30	-0.24 ± 2.29
ω_λ	1.30 ± 1.68	1.30 ± 1.74
Tx	128.3 ± 17.8	same at all points
Ty	46.7 ± 56.9	
Tz	-159.9 ± 73.5	
2D dilat	-5.72 ± 0.86	-5.16 ± 0.86
	$\tilde{\sigma}_o^2$ = 0.34	

Comparison of 2D strain models.

Ellipsoidal strain parameters always refer to the same reference surface but Cartesian strain parameters depend on

the orientation of the chosen plane. The 2D plane method which uses only x and y coordinates does not allow for 3D rotations (tilts of the plane) which may exist between the 2D networks. This is especially important when both VLBI and ground data are used. The 3D topocentric method with the vertical strain components (e_{vv}, e_{nv}, e_{ev}) fixed at zero is better because it solves for the 3D rotations. The 2D ellipsoidal strain model, as presented in this thesis, also solves for the 3D rotations. The ellipsoidal displacement and mapping projection methods have been shown to be inappropriate for use with combined VLBI and ground data.

Therefore the recommended methods of 2D strain analysis are the 2D ellipsoidal model and the 3D topocentric model with the vertical strain fixed at zero. Of these two methods neither fits the data better (ie smaller residuals) than the other in all cases. The internal adjustments from the two methods are different and the estimated parameters cannot be directly compared. The ellipsoidal model represents homogeneous ellipsoidal displacements but not homogeneous strain parameters while the Cartesian model does represent homogeneous strain parameters. The two methods are thus intrinsically different. The choice of which model best represents the strain field in a particular region is subject to geophysical hypothesis. For example, the tectonic plates may be better represented by ellipsoidal shells than flat plates, especially over large regions.

EFFECT OF SYSTEMATIC ERRORS ON STRAIN.

Height errors.

A numerical example is given here to indicate some of the effects of non-systematic height errors on strain results. The five station simulated 300km network, described elsewhere, was used. The ellipsoidal heights of the ground coordinates were altered by +0.5, -0.2, +1.0, -0.4, -0.3

metres. The strain results are given in Table 8.13 below.

Table 8.13 shows that the changes in the 2D strain components caused by height errors are only slight. As expected, an error in the vertical coordinates has virtually no effect on 2D strain. The adjusted VLBI baseline lengths from each solution did not differ significantly. However the adjusted ground coordinates changed by about a centimetre from one solution to another. The 3D and 2D approaches are both similarly affected by height errors.

Table 8.13 Effect of height errors on strain parameters.

	(1)		(2)		(3)		(4)	
e_{ee}	3.124 ±	0.803	3.133 ±	0.805	2.953 ±	0.571	2.948 ±	0.571
e_{nn}	2.343	0.675	2.415	0.675	2.434	0.563	2.496	0.563
e_{vv}	13.50	1360.	-453.	1360.	0.000	fixed	0.000	fixed
e_{en}	0.021	0.490	-0.022	0.489	0.038	0.394	0.005	0.394
e_{ev}	-41.11	138.	-40.06	138.	0.000	fixed	0.000	fixed
e_{nv}	-26.51	114.	-29.58	114.	0.000	fixed	0.000	fixed
ωe	-9.68	23.5	-10.40	23.6	-4.23	1.98	-4.34	1.98
ωn	11.71	28.4	10.58	28.4	3.26	2.29	2.32	2.29
ωv	-2.19	0.122	-2.19	0.122	-2.16	0.10	-2.16	0.10
Te	0.102	0.106	0.101	0.106	0.113	0.100	0.113	0.100
Tn	0.082	0.113	0.080	0.113	0.089	0.111	0.087	0.111
Tv	0.000	0.895	0.000	0.895	0.000	0.895	0.000	0.895
2D dil.	5.467	1.008	5.548	1.007	5.387	0.797	5.445	0.797
3D dil.	18.96	1358.	-447.4	1358.	5.387	0.797	5.445	0.797

Column (1) is the reference solution with the simulated data set,
(2) is the solution obtained with erroneous height data,
(3) is the solution obtained with the vertical strain held fixed at zero,
(4) is the solution obtained with the vertical strain held fixed at zero and erroneous height data.

3D scale error.

Two data sets spanning a 300km net were simulated so that the only difference between them was a pure (and large) 3D scale factor. A 3D topocentric strain analysis was then performed. The strain in each direction was found to be equal to the scale factor, and the 3D dilatation equalled three times the scale factor, as expected. The adjusted lengths and coordinates were the same as those that were obtained by a simple Bursa-Wolf transformation. Next, a topocentric strain solution was obtained with the vertical strain (e_{vv}, e_{nv}, and e_{ev}) held fixed at zero. It was found that the strains on the plane were the same as those computed with the full 3D approach. Although there were slight differences in the adjusted lengths and coordinates none of these differences were significant. So in this data set the presence of a 3D scale factor on a 2D strain solution causes no significant errors in the solution. This result would also apply to other networks with small (few km) vertical relief.

3D OR 2D STRAIN ANALYSIS?

Since geodetic observations are measured near the surface of the Earth, often all 3D components of strain can not be well determined, unless the network covers a large portion of the Earth's surface. One way in which this problem can be overcome is to solve for horizontal and vertical displacements separately and then combine the results to determine 3D strains. However, estimates of vertical strains are still of much lower precision than the horizontal strains. This is because the vertical relief is often much smaller than the horizontal extent of the network. Another reason for not solving for vertical strain is that vertical motion, as determined by conventional techniques, is severely dependent on gravity field changes, which may be due to density redistributions within the crust without surface changes. For example, withdrawal of

water near a gravity observing site can cause a change in the gravity reading. This is not a reflection of crustal movement. Also, vertical displacements determined from VLBI measurements are severely affected by errors in the atmospheric refraction corrections.

In 3D strain analysis there are 6 strain, 3 rotation, and 3 translation parameters so at least 12 common coordinates are needed (eg. 4 common points each with their 3 components known). If there are many common points the net should be separated into portions containing at least 4 points. The difference between the strain parameters determined from each portion indicates how homogeneous the whole area is. A stable solution for all the components of 3D strain is possible only if the four, or more, points are not coplanar or nearly coplanar. In a 2D strain adjustment there are 3 strain, 1 rotation, and 2 translation parameters, so at least 6 common coordinates are needed (eg. 3 common points each with two components known). For redundancy an additional common point with at least one component known is desirable.

In a small region (<300km) all points on the Earth's surface are usually within a few kilometres of a plane. Also the mean height of the Earth's surface above sea level is about 700m (King, 1962) and it is therefore unlikely that the difference in ellipsoidal height between two points in a net will be more than 2km. Moreover, in both ground and VLBI networks the vertical component is usually poorly determined. So often only a 2D analysis is viable.

The recommended approach to strain analysis follows. Initially a 3D strain analysis should be computed by an affine transformation of coordinates. If for example, statistical tests indicate that the height component of strain differs insignificantly from zero then strain should be computed with a 2D model. If 2D strain is to be determined it is important, especially when using both VLBI and ground data, to include parameters for the 3D

rotations. Finally, if the 2D strain is still statistically insignificant then it is suggested that one of the similarity transformation models in Chapter 7 be adopted. If the strain is statistically significant in the combination of VLBI and ground data then the models in Chapter 7 which include estimates of systematic errors should be applied. Estimates of these systematic errors could then be compared with the strain parameter estimates to assist interpretation of the strain as being of geophysical or geodetic (ie systematic error) origin. The net should also be subdivided, if possible, to investigate regional homogeneity of the estimated parameters.

DATA DEFICIENCIES.

Whilst each VLBI observation epoch will yield a full set of coordinates with no rank defect other than the usual datum defect, an epoch of ground observations may not form a full or complete network. Recent geodetic networks often include some of the stations of an old survey but the same directions and distances have not necessarily been observed. This may be because some of the old marks are lost, different equipment is used (eg EDM as well as theodolite), different observation techniques are used (eg traverse instead of triangulation), or gross errors are discovered causing some observations to be deleted. Moreover because many geodetic observations have not been made primarily for deformation analysis, not all observations of earlier networks have been repeated in later measurement campaigns. These are practical limitations of the technique proposed here. However while a partial ground net can be used to study strain for portions of a region the VLBI data could not be included unless the ground net connected the VLBI sites to each other. That is, there must not be isolated sections (islands) of ground observations. There must be at least a unique solution in both networks for all common points.

The data deficiencies that may exist and the way in which

they may be overcome in practice are as follows.

1) Neither VLBI or ground observations can determine absolute coordinates. Arbitrary geocentric coordinates are therefore usually assigned to one point and this point is held fixed. The fixed point need not be common to both networks or epochs. The derived estimates of translation will be physically meaningless but other estimates of the strain parameters will not be biased by the assumption of approximate absolute coordinates. Moreover, as already mentioned the displacements will not be physically meaningful.

An example using the real data network (see Chapter 7) was computed with the Tidbinbilla coordinates held fixed in the ground network instead of the Johnston origin. The estimated strain parameters and their VCV were the same as when using the normal ground data set. The adjusted VLBI coordinates and all the adjusted lengths and VCV were also the same. However, as expected the estimates of the translation components and the ground coordinates were different.

2) Some ground networks do not contain distance measurements because the reliable measurement of long (up to 30km) distances has only been possible in the last 20 years. If only angle or direction observations are available only shear components can be determined. So generally only the shear components can be determined unless both epochs of observation are recent. If only direction observations are available then exx and eyy can not be separately determined because the scale of the network is unknown. Instead the difference exx-eyy is determined. Distance measurements are also necessary to determine the dilatation component. An arbitrary (approximate) distance can therefore be assigned to one line and the coordinates of sites computed. If two epochs of ground data are being combined and neither contains distance measurements then an arbitrary distance can be

inserted into each network. In both these cases (ie one or both networks lack distance measurements) the derived estimates of dilatation and of the diagonal components of the strain tensor are physically meaningless but the other parameters are not affected. The displacements will also be meaningless. Similarly if a scale error is present in one or both of the networks then the dilatation and diagonal components of the strain tensor will be in error but the shear strain terms will be unaffected.

3) If a ground network does not contain any azimuth measurements then one line is assigned an arbitrary azimuth. The estimates of the rotation terms will be physically meaningless but the estimates of the other parameters will not be affected.

If a ground network contains distance measurements and at least one azimuth measurement, but no angle or direction measurements there will be no data deficiencies. No artificial observations need to be inserted and all parameter estimates will be valid.

COMMENTS ON THE APPLICATION OF STRAIN ANALYSIS.

It is possible to calculate the minimum strain that can be detected for a network, if the type of observations and their accuracies are known.

Systematic errors in the data can produce similar effects to geophysical strain and their presence has to be checked. The inclusion of VLBI data may strain a network. So in a strain analysis it will not be known what part of the resultant strain is due to scale differences and what part is due to geophysical effects. If the scale differences, or differences in systematic errors, can be determined then the geophysical portion can be separated. There have been a number of examples of misinterpretation of geodetic data, assuming that distortions in the measurements are due to geophysical causes, see for example Strange (1981) and

Coleman and Lambeck (1983).

For strain analysis, measurement repeatability and not absolute accuracy is important. So if the repeat surveys are carried out under identical conditions and reduction models (eg deflections of the vertical, geoid heights, or datum parameters) then the strain determined will be unaffected. But if the repeat surveys consist of a different type of measurement then reduction errors are very important because they could introduce systematic errors and thus artificial strain. When estimating strain parameters, rather than determining relative positions (as in Chapters 6 and 7) it is satisfactory to leave known systematic errors in the observations provided the error is identical in each epoch. For example, errors in geoid heights will have no effect if they are common to both networks. However care must be taken with refraction errors. Consider for example, two VLBI experiments where only S-band was observed. The difference between the two measurements of the same baseline will be the result of both deformation and the difference in the ionospheric effect between the two epochs. It is very important to remove systematic errors that vary from one epoch to the next, or between networks of different measurement type, otherwise they may cause apparent deformation.

It is important that if a region is being studied then only data from this region should be included in the calculations. If for example, the whole continent's data is included then the strain in the region of interest may be distorted by errors in other regions.

The study of geodetic data and its changes in time is not only useful for Earth deformation studies but also for detecting significant distortions of geodetic networks due to errors in measurements. These studies can also be used to detect an erroneous observation or group of observations. This follows the concept used by Vanicek et al (1981) and Thapa (1980) for ground nets. Strain

transformations are calculated between two data sets, with the suspect observation(s) included in one solution and excluded in an other. The results of the two solutions are then compared. If there are significant differences then the particular observation(s) are affecting the solution. Similarly strain analysis can be used to determine systematic differences between the ground and VLBI measurements by computing a strain analysis where both sets of data are measured at the same epoch. Any resulting strain is not of geophysical origin and reveals the strain due to systematic error.

When strain is computed from ground and VLBI data measured at the same epoch any resulting strain is due to systematic error and is not of geophysical origin, even if the network straddles a fault. If two different epochs of data are combined and yield significant estimates of strain it will not be clear whether this strain is due to ground movements or to systematic errors. However if each epoch of data is separately combined with a network of measurements observed at the same epoch by an independent technique, and no significant strain is detected, then the strain detected between the two epochs is due to geophysical causes and not systematic errors. Therefore VLBI and ground data should be combined at each epoch and then the strain between these epochs determined.

SUMMARY AND RECOMMENDATIONS.

The main applications of combined adjustments are crustal deformation analysis, comparisons between space techniques, and the strengthening of geodetic networks. It is better to perform crustal deformation analysis with combined data than with only one data type. This is because VLBI data is generally more accurate and cheaper than repeated ground measurements. The VLBI data can also be observed in a much shorter time span. But the ground data spans many more years and has a much denser network. A combined adjustment can also better identify regions which are stable and thus suitable for the siting of major dams, nuclear power generating stations and other critical facilities. Even if ground geodetic networks are completely replaced by GPS, there will still be a need to combine the VLBI data with the many years of old ground data for strain and crustal deformation analysis.

The combined adjustment of independent data will improve the accuracy of a network by controlling the systematic errors, provided correct procedures are followed. The precision of the network will also be improved because more data is used. The combination of different and independent data types also produces more realistic accuracy estimates. The consideration of systematic errors is particularly important because their effects may be misinterpreted as evidence of tectonic motions.

VLBI data is processed in two basic phases - the determination of delay and delay rate, and the estimation of geodetic parameters. This two step procedure is valid only if the full VCV matrix of the delays and delay rates (of all baselines) is carried through to the computation of the geodetic parameters. Current practice is to apply the sigcons method which ignores the VCV matrix. However the sigcons method does not account for the correlations between the observations and the effect of errors in the atmospheric corrections. Corrections for atmospheric

refraction are often incorrectly assumed to be error free. The errors in these corrections were found to have a significant effect on both the variances of, and correlations between, the observations. Better methods of determining the VCV matrix of the delay and delay rate observations were suggested but further research is needed. Further research is also needed on the effects of using the full VCV matrix instead of sigcons, on the baseline results of different experiments.

It is recommended that if the sigcons method is used, then a global set of sigcon values should be applied to all similar experiments.

The effect of many of the systematic errors on VLBI results depends on the experiment schedule. Thus the preparation of schedules was briefly reviewed and the design of an optimum schedule was considered. Apart from recommending simulation studies of several different schedules for each experiment, no improvement over current procedures was found. Further research in this area is needed.

Any differences between the reference frame to which the VLBI results refer and the ground reference frame must be considered when combining the two data types.

In order to correctly combine two data types it is essential that the VCV of the data be reliable and all systematic errors be considered. The systematic errors in VLBI were classified into two categories, those that propagate into the baseline results in a way dependent on the schedule, and those that are independent of the schedule. It was shown that the schedule-independent errors can be represented by scale, rotation and translation parameters. Errors in RA origin, source catalogue declination pole, earth rotation data, reference clock epoch and rate, and the coordinates of the fixed site, were considered.

On the other hand, the schedule-dependent errors cannot be so simply represented. Errors in axis offset corrections, catalogue positions of individual sources, source structure, and tropospheric and ionospheric refraction, were investigated. Two methods were proposed to analyse the effects of these errors on the results. Improvements to existing axis offset correction models to cater for inclinations of axes and refractive bending of the source direction have been recommended. However the overall effect on baseline results is expected to be small.

Particular attention was paid to the effect of a bias in the tropospheric corrections on baseline results because it is expected to cause the largest systematic errors in the VLBI results. The proposed method produces a more accurate representation of the effect of a bias in the tropospheric corrections on baseline results, than simply doubling the bias to produce the change to the local vertical coordinates.

The results of the first geodetic VLBI experiment within Australia were presented and their accuracies estimated. The baselines ranged from 250km to 2500km. This VLBI data and the corresponding ground data of the Australian Geodetic Network gave independent determinations of the ten baselines. The differences between the two measurements of each baseline were within bounds consistent with their estimated accuracies.

The accuracies of the VLBI lengths were shown to be probably no more than twice their formal errors. Therefore the 275km Tidbinbilla - Parkes baseline length and components have been determined with estimated accuracies of ±6cm and ±15cm respectively. The 235km Tidbinbilla - Fleurs and 250km Parkes - Fleurs baseline lengths and components have been determined with estimated accuracies of ±13cm and ±25cm respectively. The Tidbinbilla - Alice Springs and Parkes - Alice Springs baseline lengths and components have been determined with estimated accuracies

of ±1.8m and ±2.2m respectively. The Tidbinbilla - Hobart and Parkes - Hobart baseline lengths and components have been measured with estimated accuracies of ±6.4m and ±8m respectively. The results of this experiment have been applied to strengthen the Australian geodetic network.

The data from this experiment is stored in an easily accessible form. When either better source positions or better models become available the solutions should be recomputed. Better positions for those sources south of -45° declination could be achieved by observing on a longer baseline, such as Hartebeesthoek to Tidbinbilla. Such an experiment is being planned.

To obtain better geodetic results in any future geodetic VLBI experiment in Australia, it is recommended -
1) that Circinus X-1 and Vela not be observed.
2) that the number of observed sources be limited to 15 rather than 25.
3) that consideration be given to observing at most only one out of each of the following pairs because they are close together in the sky: 0438-43 and 0537-44; 0637-75 and 0743-67; and 3C 273 and 3C 279.
4) that the data acquisition rate be substantially increased, ie. more observations per day.
5) that participating sites be better instrumented. In particular, masers need to be installed at Fleurs, Hobart and Alice Springs, BWS equipment is required at both Alice Springs and Hobart, and the slew rate of the Hobart antenna needs to be increased.

Constraints placed on the coordinates and observations of the fundamental point of the ground net were shown to cause rotations and translations of the net. Refraction and calibration errors in the ground distance measurements cause 2D scale errors. Constant height errors cause 3D scale errors and translations of the net, and astronomic azimuth errors can distort the network. Therefore a scale difference between VLBI and ground data may be due to

systematic errors in the fixed terrestrial heights as well as an error in terrestrial distance scale.

An important source of systematic error in a ground net is the connection of the net to the VLBI reference point. If the reference point is misidentified then no error will be detected in the ground net adjustment. However a combined adjustment with VLBI data will be incorrect. Thus it is essential that the survey connection be of at least as high a quality as the rest of the geodetic network and that it contain redundant measurements to guard against gross errors. It is recommended that each VLBI site be surrounded by a network of several stations. Repeated observations should be made to locate the reference point and to monitor local geophysical and structural motions. The orientations and any eccentricities of the various telescope axes should also be determined.

The terrestrial observations may be adjusted in two dimensions (ie. geodetic latitude and longitude). Orthometric heights may then be combined with geoid heights to form triplets of ellipsoidal coordinates. Alternatively, the adjustment may be computed in three dimensions. In either case it is recommended that the VLBI and ground data be combined by solving for the 3D transformation parameters relating the coordinates of the points of each network.

This transformation method is preferred to alternative methods such as including the VLBI data, via suitable observation equations, in a ground adjustment, or combining the normal equations of the two data types. It is important to compute separate adjustments of each network to check for outliers, systematic errors, and to do statistical tests of the quality of the observations before the data sets are combined.

It is recommended that a conformal or affine (strain) transformation be applied because there are not expected to be enough VLBI points to warrant a more general

transformation, such as where the scale factor varies with geographical location. If the scale factor does vary with location, or it is suspected that it might, then the data should be separated into homogeneous regions.

The inclusion of gravity observations in a ground adjustment would improve the accuracies of the heights in the ground data. The inclusion of gravimetric data in the ground adjustment does not alter these combination methods, unless it is also desired to adjust the gravimetric data.

The minimum number of common points required to solve for the seven parameters of a conformal transformation is three. Two of the points should have their three coordinates known in each system, and the third point should have its three coordinates in one system known and one coordinate in the other system known. However, it is desirable to have at least four common sites.

The Cardanian method of describing the rotation angles is recommended in preference to the Eulerian approach because it is more stable when the rotation angles are small. The equivalent rotation angle about a single axis, and the direction of this axis, should also be calculated because its direction may be informative. Approximate formulae for use with small rotation angles were also investigated.

A 3D scale error will have a much greater effect on the heights of points than on their latitudes or longitudes. Conversely a 2D scale error will have much more effect on the latitudes and longitudes of points than on their heights. If a 2D scale error or constant height error or both are present in a network and they are not solved for in a combined adjustment, then the estimates of the 3D scale factor and translation components will be incorrect. However if the network spans a region of less than a few thousand kilometres, the errors in the adjusted lengths and angles should be small.

It is quite likely that a continental geodetic network will have local distortions in scale and orientation. If this is so then it is better to solve for the transformation, strain or systematic error parameters in local and regional areas rather than one set of parameters for the whole of the continent. All ground data should be on the same ellipsoid datum and VLBI data from separate experiments should refer to the same reference system.

Several combination models were investigated and compared. The investigations have considered both the internal adjustment (the adjusted observations, especially the baseline lengths) and the scale, strain and systematic error parameters. The Molodensky-Badekas model was shown to give the same answers as the Bursa-Wolf model for the internal adjustment, and the scale and rotation parameters. However the translation parameters are different and have smaller a posteriori precisions. VLBI is not sensitive to the translation terms so this difference is of no practical concern.

Theoretically the ellipsoidal model should produce the same results as the Bursa-Wolf model. However the least squares adjustment procedure linearizes the models. If the higher order partial derivatives of the Cartesian or ellipsoidal models, or both, are significant then the adjusted observations and parameters will not be accurate. In the examples examined the differences between the results from each of the models were found to be insignificant when compared to measurement precisions.

An important advantage of the Cartesian baseline component method is that the matrices which have to be inverted are smaller than the corresponding matrices for other models. The adjusted lengths, angles, scale and rotation parameters and their VCV matrices are identical to those from an equivalent Bursa-Wolf solution. However this model does not yield adjusted coordinates, nor does it estimate translation parameters.

The VLBI baseline lengths may be included in a 2D ground adjustment. This is the simplest method for combining the two data types and should be applied when there is only one VLBI baseline, though it could be used for any number of baselines. The main problem with this method is that the high quality VLBI vectors are constrained to agree with the often poorly determined ground network ellipsoidal heights. Errors in these fixed ground heights will distort the results.

Other models decompose the rotation matrix into parts which represent systematic measurement errors and reference frame differences. However, if the solution is stable, the internal adjustment and strain parameters are not affected by the decomposition of the rotation matrix.

Another technique is to rotate the networks' coordinates (and appropriately change their VCV matrices) before combination so that at least one of the XY, XZ, or YZ planes passes through the networks. Some of the parameters will then have almost identical effects on the network coordinates. Consequently not all of the parameters need to be determined. Thus there are less parameters to estimate and the internal adjustment of lengths and angles will be more stable. However, the adjusted coordinates and most of the adjusted parameters are meaningless.

As well as combining the two data sets by using one of the given models the analyst should calculate the scale factor, and its precision, for each baseline. He can then determine which baselines have the most effect on the overall scale factor and investigate possible inconsistencies or outliers in the data. The lines with the best fractional (ppm) accuracies give the most precise estimates of scale factor. These are not necessarily the longest baselines.

The implications of the spatial distribution of the points of the network were considered. It is important that the

points are not close to co-linear. An uneven geographical distribution of points is also undesirable because areas of high density will bias the solution. The coordinates of points in areas of low density may then have undeservedly large residuals. The shape of a network has no effect on the derived scale factor or its accuracy, but does affect the accuracies of some of the strain parameters.

If the model contains a large number of parameters then the adjustment may lead to a poorly conditioned system of equations. This is especially the case when the network under consideration covers only a small part of the Earth's surface. An adjustment with a model which contains many parameters will usually produce smaller residuals than an adjustment with a model which contains only a few parameters. However adjustments for many parameters may not produce realistic estimates of the parameters because some parameters may absorb part of the effects of other parameters. Moreover, the degrees of freedom of the adjustment will be reduced and therefore the statistical tests will be less effective. If an accurate internal transformation is the main concern, then the high correlations between the parameters and the fact that the adjusted values of the parameters may not represent real physical quantities are of no concern. This is, of course, provided the solution is stable.

Even though the coordinates come from previously tested adjustments they may contain unknown systematic errors (eg. local scale errors in the ground survey, and mis-identification of the VLBI reference point by the ground survey). A number of appropriate statistical tests to investigate these errors were presented. None of these statistical tests are too demanding and they should all be carried out.

For the correct combination of data it is essential that the data does not contain errors and the VCV must be reliable. The variances of the data will generally be

underestimated because not all error sources have been considered. The systematic errors should be parameterised and included in the combined adjustment. Alternatively the VCV of the coordinates of each net could be altered to allow for the biases. However it is difficult to correctly change a VCV matrix. The recommended procedure is to leave the VCV matrices, as estimated by the VLBI program and by the geodetic network adjustment, unaltered and to model the systematic effects in the combined adjustment. Of course, if the sum of the systematic biases is insignificantly small compared to the precision of the baseline parameters then the baseline estimates and their VCV need not be altered or bias terms considered.

Considerable savings in computer resources can be made when the VCV is not a full matrix. However this situation does not often arise in practice. Assuming that the VCV is block diagonal or diagonal when in fact it is not, would cause errors in the results. Therefore it is recommended that the full VCV matrices be used in the computation of transformation parameters.

Additional parameters were included in the combination model to account for possible systematic biases. These biases were - 2D scale and azimuth errors in the ground net and tropospheric bias errors in the VLBI net. Either the Cartesian models (eg Bursa-Wolf) or the ellipsoidal model can be extended. Though an ellipsoidal model can be more simply extended to model systematic errors which primarily effect the height component, than the other models. Moreover, it is still possible to solve for the scale, rotation and translation parameters. However, in all cases, there are additional parameters so more common points are necessary.

Those systematic errors which can be accounted for by rotation and translation terms do not need to be further modelled. Even though they affect the estimated parameters they do not affect the internal adjustment. The influence

of the remaining systematic errors can be assessed by the use of check points. If a point is given zero statistical weight and the changes in the adjustment results are acceptable, then the adjustment is stable and reliable. However such a check point in a cluster of points examines the consistency only within the cluster itself.

In the case of only two or three sites forming a network of short baselines (<1000km), the effect of tropospheric bias errors can be well approximated by rotations of the network. For four or more sites these errors cannot be modelled by rotations. If VLBI data is combined with ground data which has poor heights then the tropospheric bias parameters will generally be poorly determined. Moreover they will be highly correlated with the other parameters when there are only a few sites. However the proposed method of including tropospheric bias parameters in the transformation, is useful for determining the sensitivity of the results of the combined solution to tropospheric bias errors.

If the estimates of any of the parameters do not differ significantly from zero, then the solution should be recomputed with these parameters held fixed at zero. This solution will have more degrees of freedom, which is important when adjusting small data sets. Appropriate multivariate statistical tests were reviewed and shown to be preferable to commonly applied univariate tests. The analyst should also study the effect of holding these parameters fixed, on the estimates of the other parameters, adjusted coordinates, and adjusted lengths, by using one of the methods given in Chapter 6. This is useful for studying error propagation in the combined networks. It also reveals the sensitivity of the observations to the various parameters and the sensitivities between various subsets of the parameters.

The products of a combined adjustment are two sets of adjusted coordinates which differ by the adjusted

parameters and are slightly correlated. The changes to the coordinates of the points in a network are small (of the order of the standard deviations of the observations) but the overall scale, orientation and location of each net does not change from its original state. This is convenient for Surveying applications. It was shown that the precision of an adjusted baseline length is generally different in the two networks. Moreover, these precisions improve when the scale factor is held fixed or assigned a small a priori variance.

If it is desired to adopt the scale, orientation and location of the VLBI net, then the adjusted VLBI coordinates should be adopted. However if it is desired to adopt the VLBI scale and orientation and the ground location the adjusted VLBI coordinates should be shifted by the estimates of translation parameters and the VCV matrix of the coordinates changed appropriately. Generally the VLBI data will be more accurate and so it should be adopted if the net with the best internal adjustment is desired. However, if the two nets are of similar quality and the best internal adjustment is required then that net with the smallest trace of the VCV of the adjusted lengths should be adopted.

The estimated transformation parameters can be used to transform the known ground coordinates of prospective VLBI sites into the VLBI coordinate frame. This would provide useful a priori positions for experiment scheduling and correlation. However it must be remembered that a transformation is essentially an interpolation procedure. Therefore the results might be unreliable if the adjusted parameters were used to transform the coordinates of a point outside the region spanned by the common points.

The transformation parameters are also useful for converting a ground survey link to the VLBI system for comparisons between VLBI, SLR, and GPS measurements. Common

practice, when comparing two space systems via a ground connection, is to use the ground Cartesian components and assume that the orientations of the reference axes are the same. The orientation of the ground reference frame may differ from that used by VLBI by a few arc seconds. Therefore the maximum length of connection using this assumption is limited to about 1km. Ideally at least three or four VLBI sites should be established within a kilometre or two of the connection. These sites, and the SLR or GPS site(s), should be connected to the ground net and the orientation and scale differences between the local VLBI and local ground nets determined. This may not be practical, unless a transportable VLBI antenna is available, so orientation differences obtained from a larger net must be assumed to also apply to the local net. Although the precisions of the rotation angles and scale factor could be improved by using a larger net, this is valid only if the larger net is representative of the local net.

Improvements in the accuracy of the VLBI coordinates have little effect on the precision of the scale factor obtained from a combined adjustment. However, an improvement in the accuracy of the ground data, especially heights, is very significant. With accuracies presently available the scale factor obtained from the Tidbinbilla -Parkes - Fleurs triangle cannot be determined to better than ±0.3ppm. This places a limit on the crustal strain that can be reliably detected over this area. If two epochs of ground data, at present accuracies, were combined the scale difference could be determined to only ±0.7ppm. Hence it would take about twice as long to detect any geophysical strain. If two epochs of VLBI data, with baseline length precisions of about ±3cm, were combined the scale factor could be determined to about ±0.1ppm.

It is recommended that strain be calculated from a transformation adjustment of the coordinates of the points in each network. This approach is particularly suitable

when using different measurement techniques such as geodetic surveys and VLBI. Once each net has been separately adjusted and the coordinates and VCV determined, it is better to repeat strain computations, perhaps determining different selections of parameters, than to repeat the 'simultaneous' strain computations recommended by Bibby (1982). If only strain and not displacements are desired then any point can be held fixed. The strain results and the internal adjustment will not be affected.

Data deficiencies can be overcome in practice by inserting artificial observations. These artificial observations cause some, but not all of the results, to be meaningless.

If a network covers only a small portion of the Earth's surface it can be approximated by a plane. However there is a choice of how to define the orientation of the plane. In the 3D topocentric model the strain components (in the chosen plane and a component normal to the plane) are computed. The adjusted lengths and coordinates and the sum of the residuals are independent of which plane is chosen. The overall strain, that is the 3D dilatation and the principal strains, is also identical. However a change in orientation of the reference plane of a few minutes of arc could cause significant changes in the strain parameters. Therefore it is recommended that if strain analysis of more than two epochs or data sets is attempted, then the same plane should be used throughout. The dependence of the strain parameters on the orientation of the plane is especially important if it is desired to constrain the strain normal to the plane to zero.

The 3D topocentric model was shown to be preferable to the geocentric strain model. Even though the internal adjustments are identical, the estimated parameters are more meaningful and less correlated. Moreover, the geocentric solution is often unstable.

In the 3D ellipsoidal strain model the linear relation

between the displacements at a point and the point's coordinates is uniform across the network. However, the rotation terms and all the strain components except the strain in the vertical direction, vary from point to point. This is different to rectangular Cartesian strain where the rotation and strain terms are uniform across the field. For points within a region of a few kilometres with typical displacements, the strain parameters at each point will not differ by more than 0.01μstrain. Over regions of a few hundred kilometres the strain parameters could vary considerably. In any case the differences between topocentric and ellipsoidal strain parameters are usually significant, even for networks of a few kilometres extent.

Several methods of 2D strain analysis were considered. They were - plane, ellipsoidal displacements, ellipsoidal coordinates, TM projection and the plane of maximum strain. When analysing data for 2D strain it is important that all data, from every epoch, refer to the same datum.

The 2D plane model which uses only x and y coordinates ignores 3D rotations (tilts of the plane) which may exist between the 2D networks, especially when VLBI and ground data are used. The ellipsoidal displacement and mapping projection methods were also shown to be inappropriate for use with combined VLBI and ground data. The 3D topocentric model, with the vertical strain components fixed at zero, and the 2D ellipsoidal strain model both constrain the vertical strain components to zero and solve for 3D rotations. They are therefore the best 2D models. The 2D ellipsoidal model is an improvement on the ellipsoidal model suggested by Bibby (1973). In his model all vertical displacements are constrained to zero. Therefore it does not allow for displacements due to rotations. It should be noted that the topocentric Cartesian model is simpler to apply because the vertical strain can be held fixed at zero and the 3D rotations solved for without altering the 3D model.

If the range of heights in a net is small then the precision of the estimated vertical strain will be poor and the correlations with the horizontal strain components small. Thus 3D strain, with the vertical strain held fixed at zero, would be more appropriate when the range of heights is small than where there is a large range of heights. If an ellipsoidal surface gives a smaller range of heights than a plane surface then 2D ellipsoidal strain is better. However neither the 2D ellipsoidal model or the 3D topocentric model, with vertical strain fixed at zero, produces smaller residuals than the other in all cases.

The precision of the 'horizontal' strain components should be similar in both ellipsoidal and plane strain approaches because the arc lengths and chord lengths between points are similar. However the topocentric model is computationally simpler than the ellipsoidal models.

Ellipsoidal strain parameters always refer to the same reference surface but Cartesian strain parameters depend on the orientation of the chosen plane. The internal adjustment results from the two methods are different and the estimated parameters cannot be directly compared. The ellipsoidal model yields homogeneous ellipsoidal displacements but not homogeneous strain parameters. However the Cartesian model does produce homogeneous strain parameters. The choice of which model best represents the strain field in a particular region is subject to geophysical hypothesis. For instance, the tectonic plates may be better represented by ellipsoidal shells than flat plates, especially over large regions.

In the past most strain investigations have been into vertical movements or into 2D horizontal movements. This could lead to a misinterpretation of the real (3D) strain situation. Thus the recommended approach to strain analysis is to initially compute a 3D strain analysis.

It is well known that strain in the vertical direction

often has a low precision. This is caused by the small range in heights (generally less than 2km) in a network compared to the extent of the network in the other directions (typically tens to hundreds of kilometres). If statistical tests indicate that the vertical components of strain are insignificant then, and only then, an analyst should compute strain with a 2D model.

The decision of whether to apply 2D or 3D strain analysis depends on the statistical significance of the vertical strain estimate and not on the size of the precision of the vertical strain estimate. When 2D strain is determined it is important to include parameters for the 3D rotations, especially when using VLBI and ground data.

Finally, if the 2D strain is statistically insignificant then it is recommended that one of the conformal transformation models which include parameters for systematic errors, be adopted. The estimates of these systematic errors should also be tested for statistical significance. If possible, the net should be subdivided to investigate regional homogeneity of the estimated parameters.

The results of the Australian VLBI experiment and the corresponding ground measurements were combined and no erroneous observations were detected. The estimates of the parameters were statistically tested by the multivariable test which considers the correlations between parameter estimates. The estimates of the 2D scale and 2D azimuth errors were not statistically significant at the 95% confidence level. The strain was not significantly different in any one direction to another. Therefore the data sets could be combined with a single scale factor. In the conformal transformation the estimates of scale and the rotation angles were found to be insignificantly different to the null vector at the 95% confidence level. It was also found that the use of reduced VCV matrices (ie diagonal or block diagonal) did not cause large errors in the results.

Strain analysis of geodetic networks is not only useful for Earth deformation studies but also for detecting significant distortions of the networks due to errors in the measurements. If the data are not tested for the presence of systematic errors then it will not be known what part of any estimated strain is due to systematic error and what part is due to geophysical strain. However those systematic errors which cause only rotations or translations of a network do not strain a network.

The effects of non-systematic height errors on a strain adjustment cannot be simply generalised. However an error in the vertical coordinates has virtually no effect on 2D strain. The effects of height errors in the data on both the 3D and 2D strain models are similar. Moreover, a 3D scale error generally causes similar errors in 2D and 3D strain solutions.

The VLBI sites are either part of, or are outside the strain field. In the latter case the VLBI sites can be held fixed and used to control the observations of all epochs. The displacements of points within the strain field could then be determined with respect to these VLBI coordinates and would thus not be affected by the usual datum defects of location and orientation. If the VLBI sites are part of the strain field then they can only be used to control the ground observations taken at the same epoch as the VLBI measurements. However it is essential in both cases that the ground and VLBI data be combined without causing artificial strain.

When strain is computed from ground and VLBI data measured at the same epoch, any resulting strain is due to systematic error and is not of geophysical origin, even if the network straddles a fault. If two different epochs of data are combined and yield significant estimates of strain it will not be clear whether this strain is due to ground movements or to systematic errors. It is strongly

recommended that VLBI and ground data be combined at each epoch. If no significant strain is detected, then the analyst can be confident that strain detected between two different epochs is due to geophysical causes and not systematic errors.

REFERENCES.

Adam, J., F. Halmos, and M. Varga (1982) On the concepts of combination of Doppler satellite and Terrestrial Geodetic Networks, Acta Geodaet., Geophys. et Montanist. Acad.Sci.Hung Vol. 17(2) pp 147-170.

Ashkenazi, V. (1981) Models for controlling national and continental networks, Bull. Geod. 55(1981) pp 49-58.

Badekas, J. (1969) Investigations related to the establishment of a World Geodetic System, Department of Geodetic Science, Ohio State University, Rpt. 124.

Berman, A.L. (1976) The Prediction of Zenith Range Refraction From Surface Measurements of Meteorological Parameters, JPL Tech. Rpt. 32-1602.

Bibby, H.M. (1973) The reduction of Geodetic Survey Data for the detection of Earth deformation, Geophys. Divn. Department of Scientific and Industrial Research, New Zealand. Rpt. 84. 34p.

Bibby, H.M. (1982) Unbiased estimate of strain from triangulation data using the method of simultaneous reduction, Tectonophysics 82 pp 161-174.

Blais, J.A.R. (1972) Three-dimensional Similarity, Canadian Surv. pp 71-76.

Blais, J.A.R. (1979) Least-Squares Block Adjustment of Stereoscopic Models and Error Analysis, Divn. Surv. Eng. Uni. Calgary No. 30001, 208p.

Bock, Y. (1980) A VLBI Variance - Covariance Analysis Interactive Computer Program, Department of Geodetic Science, Ohio State University, Rpt. 298.

Bock, Y. (1982) The use of baseline measurements and

geophysical models for the estimation of crustal deformations and the terrestrial reference system, Department of Geodetic Science and Surveying, Ohio State University, Rpt. 337.

Bock, Y. (1983) On the time delay weight matrix in VLBI geodetic parameter estimation, Department of Geodetic Science and Surveying, Ohio State University, Rpt. 348.

Bomford, G. (1980) Geodesy, 4th Ed., Oxford University Press.

Bossler, J.D. (1972) Bayesian inference in Geodesy, Ph.D. Thesis, Department of Geodetic Science, Ohio State University.

Bossler, J.D. (1978) Status of the New Adjustment in the United States, Proc. of the 2nd Int. Symp. on Problems related to the Redefinition of the North American Geodetic Networks, Arlington, Va.

Brunner, F.K. (1979) On the analysis of geodetic networks for the determination of the incremental strain tensor, Survey Review, XXV, 192.

Bursa, M. (1966) Fundamentals of the theory of geometric satellite geodesy, Travaux de l'institut Geophysique de l'academie Teheco-slovaque des Sciences, No. 241.

Callahan, P.S. (1973) Prediction of Tropospheric Wet-Component Range Error from Surface Measurements, JPL Tech. Rpt. 32-1526. Vol. XVIII, pp 41-46.

Cannon, W.H. (1978) The classical analysis of the response of a long baseline radio interferometer, Geophys. J.R.astr. Soc. Vol. 53 pp 503-530.

Carter, W.E., D.S. Robertson, J.E. Pettey, B.D. Tapley, B.E. Shultz, R.J. Eanes, and Miao Lufeng (1984)

Variations in the Rotation of the Earth, Science Vol. 224, pp 957-961.

Carter, W.E. and D.S. Robertson (1984) IRIS Earth Rotation and Polar Motion Results, Presented at Int. Symp. on Space Techniques for Geodesy, Sopron, Hungary, July, 1984.

Chao, C.C. (1973) A New Method to Predict Wet Zenith Range Correction From Surface Measurements, JPL Tech. Rpt. 32-1526, Vol. XIV pp 33-41.

Chen, Y. (1983) Analysis of Deformation Surveys - A Generalized Method, Dept.Surv.Eng. UNB Canada, Tech. Rpt. No. 94, 262P.

Clark, B.G. (1973) The NRAO Tape Recorder Interferometer System, Proc. IEEE Vol. 61, pp 1242-1248.

Coleman, R. and K. Lambeck (1983) Crustal Motion in South East Australia - is there Evidence for it?, Aust. J. Geod.Photo.Surv. No. 39, pp 1-26.

Crane, R.K. (1976) Refraction effects in the Neutral Atmosphere, In Methods of Experimental Physics, Vol. 12B, Academic Press.

Denham, D., L.G. Alexander, and G. Worotnicki (1979) Stresses in the Australian crust; evidence for earthquakes and in situ stress measurements, B.M.R. J. Aust. Geol. Geophys., 4, pp 289-295.

Dermanis, A. and Grafarend, E. (1980) Estimability analysis of Geodetic, Astrometric and Geodynamical quantities in VLBI, Geophys.J.R.Astr.Soc. (1981) Vol. 64, pp 31-56.

Dermanis, A. and E. Livieratos (1983) Applications of Deformation Analysis in Geodesy and Geophysics, Rev.

of Geop. and Sp. Phys. Vol. 21 No. 1, pp 41-50.

Dermanis, A., E. Livieratos, and S. Pertsinidou (1983) Deformation Analysis of Geoid to Ellipsoid Mappings, Quaterniones Geodaesiae, 4, 3, pp 225-240.

Dermanis, A., E. Livieratos, and I. Paraschakis (1983) Applications of Strain criteria in Cartography, Bull. Geod. 57 pp 215-225.

Dermanis, A. and Mueller, I.I (1978) Earth Rotation and Network Geometry Optimisation for Very Long Baseline Interferometers, Bull. Geod. Vol. 52 pp 131-158.

de Vegt, C. and U.K. Gehlich (1978) Precise Optical Positions of Radio Sources in the FK 4-System, Astron. Astrophys. Vol 67, pp 65-71.

Dickey, J.O., X X Newhall, and J.G. Williams (1984) Earth Orientation from Lunar Laser Ranging and an Error Analysis of Polar Motion Services, JPL Geodesy and Geophysics Preprint No. 114, Submitted to J. Geophys. Res.

Fanselow, J.L. (1983) Observation model and parameter partials for the JPL VLBI parameter estimation software "Masterfit-V1.0", JPL Publ. 83-39, 54p.

Frank, C.F. (1966) Deduction of earth strains from survey data, Bull. Seismol. Soc. Am., 56, pp 35-42.

Fubara, D.M.J. (1972) Three-dimensional geodesy for terrestrial network adjustment, J. Geophys. Res. Vol. 77 No. 5, pp 796-807.

Georgiadou, Y. and E.W. Grafarend (1983) The small scale structure of geometry and gravity space I, Bull. di Geod. e Sci. Aff. Anno XLII No. 2,

Grafarend, E.W. (1978) Operational Geodesy, In:

Approximation Methods in Geodesy, Eds. Moritz and Sunkel, Herbert Wichmann Verlag, pp 235-284.

Grafarend, E. and B. Schaffrin (1980) An Introduction to the Variance - Covariance - Component Estimation of Helmert Type, ZfV 4/1980 pp 161-180.

Gubbay, J.S., A.J. Legg, D.S. Robertson, G.D. Nicolson, A.T. Moffet, and D.B. Schaffer (1977) Variations in the intensities and sizes of compact radio sources at 13cm wavelength, Astrop. J. 215 pp 20-35.

Gubbay, J.S. (1978) Radio Source Positions from Southern and Trans - equatorial Very Long Baseline Interferometers, Astron. J. 83(7) pp 697-703.

Guinot, B. (1980) Comments on the terrestrial pole of reference, the origin of the longitudes, and on the definition of UT1, In Reference Coordinate Systems for Earth Dynamics, Eds. E.M. Gaposhkin and B. Kolaczek, pp 125-134, D. Reidel.

Harvey, B.R. and A. Stolz (1982) The Australian Geodetic VLBI Experiment (AGE), Aust.J.Geod.Photo.Surv. No. 36, pp 31-46.

Harvey, B.R., A. Stolz, D.L. Jauncey, A.E. Niell, D.D. Morabito, and R.A. Preston (1983) Results of the Australian Geodetic VLBI Experiment, Aust.J.Geod.Photo.Surv. No. 38, pp 39-51. Also publ. in TDA Progress Report 42-75 Jul-Sept 1983 pp 140-146.

Hein, G.W. (1982) A contribution to 3D-operational geodesy, Part I: Principle and observation equations of terrestrial type, Deutsche Geodatische Kommission, Reihe B, Nr. 258/VII, pp 31-64.

Hinteregger, H.F. (1979) The Mark III wideband digital recorder in perspective, In Radio Interferometry: Techniques for Geodesy, NASA CP 2115, 1980, pp

305-316.

Hoar, G.J. (1975) The Analysis, Precision and Optimisation of Control Surveys, UNISURV S-13, School of Surveying, University NSW.

Hotine, M. (1969) Mathematical Geodesy, ESSA Mono. 2, US Dept. of Commerce, Washington D.C., 416p.

Hung, N.T., H. Phillips, and R. Zanteson (1976) Magnitude of 64m Elevation Axis Movements Due to Alidade Temperature Changes, JPL DSN Prog. Rpt. 42-36, pp 41-44.

Jauncey, D.L., R.A. Preston, A.E. Niell, B.R. Harvey, D.L. Meier, D.D. Morabito, M.A. Slade, and A. Tzjoumis (1984) Accurate Radio Source Positions for Six Southern Radio sources, In preparation.

Johnston, K.J. and J.S. Ulvestad (1982) Radio Source Reference Frames, In Proc. of Symp. No. 5: Geodetic Applications of Radio Interferometry, NOAA Tech. Rpt. NOS 95 NGS 24, pp 7-18.

Kellerman, K.I. (1982) Extragalactic Radio Sources as Geodetic Targets: Structure, Proper Motions, Lifetimes, In Proc. of Symp. No. 5: Geodetic Applications of Radio Interferometry, NOAA Tech. Rpt. NOS 95 NGS 24, pp 1-6.

Kendall, M.G. and A. Stuart (1958) The Advanced Theory of Statistics, Vol. 1, Charles Griffin and Co. Ltd, London.

King, C.A.M (1962) Oceanography for Geographers, Arnold, London.

Kisslinger, C. (1984) Practical Approaches to Earthquake Prediction and Warning, Meeting Report, EOS

Transactions AGU, June 12, 1984.

Krakiwsky, E.J. and D.B. Thomson (1974) Mathematical Models for the Combination of Terrestrial and Satellite Networks, Canadian Surveyor Vol. 28 No. 5.

Krakiwsky, E.J. (1981) A Synthesis of recent advances in the method of Least Squares, Dept.Surv.Eng. Uni. of Calgary Canada, Publ. 10003

Kumar, M. (1972) Coordinate transformation by minimizing correlations between parameters, Department of Geodetic Science, Ohio State University, Rpt.184.

Lambeck, K. (1980) Some Geodetic Aspects of the Plate Tectonics Hypothesis, In - Reference Coordinate Systems for Earth Dynamics, E.M. Gaposhkin and B. Kolaczek (Eds), 1981, pp 87-101. D. Reidel.

Lanyi, G. (1984) Tropospheric Calibration in Radio Interferometry, JPL Geodesy and Geophysics Preprint No. 119, 12p.

Lawson, C.L., and R.J. Hanson (1974) Solving Least Squares Problems, 340p, Prentice-Hall Inc., Englewood Cliffs, New Jersey.

Love, A.E.H. (1944) A Treatise on the Mathematical Theory of Elasticity, 4th Edition, Dover Publications.

Ma, C. (1978) VLBI applied to Polar Motion, Relativity and Geodesy, Ph.D. Thesis NASA Tech.Mem. 79582.

Mather, R.S. and J.G. Fryer (1970) Orientation of the Australian Geodetic Datum, Aust. Surv. pp 5-14.

McGinness, H., G. Gale, and R. Levy (1979) Estimated Displacements for the VLBI reference point of the DSS 13 26m Antenna, DSN Prog. Rpt. 42-50 pp 36-51.

Mikhail, E.M. (1976) Observations and Least Squares, IEP, Harper & Row, 497p.

Morabito, D.D., R.A. Preston, M.A. Slade, D.L. Jauncey, and G.D. Nicholson (1983) Arcsecond positions for milli-arcsecond VLBI nuclei of extragalactic radio sources. II 207 sources, Astron.J. Vol. 88, No. 8, pp 1138-1145.

Musman, S. (1982) Statistical Tests of ARIES Data, J. Geophys. Res. Vol. 87 No. B7 pp 5553-5562.

Novozhilov, V.V. (1953) Foundations of the nonlinear theory of elasticity, Graylock Press.

Panel on Crustal Movement Measurements, Committee on Geodesy/Committee on Seismology, Assembly of Mathematical and Physical Sciences, National Research Council, USA (1981) Geodetic Monitoring of Tectonic Deformation - Toward a Strategy, National Academy Press, 109p.

Pinch, M. and A.E. Petersen (1974) Adjustment of Survey Networks by Sections, Canadian Surveyor, Vol.28, No.1.

Pope, A.J. (1976) The statistics of residuals and the detection of outliers, NOAA Tech. Rpt. NOS 65 NGS 1.

Reilly, W.I. (1980) Three-Dimensional Adjustment of Geodetic Networks with incoporation of Gravity Field Data, Rpt. 160 Geophys. Divn. Dept. of Scientific and Industrial Research, New Zealand. 54p.

Robertson, D.S. (1975) Geodetic and Astrometric measurements with VLBI, Ph.D. Thesis Massachusetts Institute of Techology, Publ. by NASA Goddard Space Flight Center, Document X-922-77-228.

Rogers, A.E.E. (1970) VLBI with large effective bandwidth for phase delay measurements, Radio Science Vol. 5 pp

1239-1247.

Rogers, A.E.E., R.J. Cappallo, H.F. Hinteregger, J.I. Levine, E.F. Nesman, J.C. Webber, A.R. Whitney, T.A. Clark, C. Ma, J. Ryan, B.E. Corey, C.C. Counselman, T.A. Herring, I.I. Shapiro, C.A. Knight, D.B. Shaffer, N.R. Vandenberg, R. Lacasse, R. Mauzy, B. Rayhrer, B.R. Schupler, and J.C. Pigg (1983) VLBI: The MKIII system for Geodesy, Astrometry and Aperture Synthesis, Science Vol. 219 pp51-54.

Saastamoinen, J. (1972) Atmospheric Correction for Troposphere and Stratosphere in Radio Ranging of Satellites, A.G.U. Geophysical Monograph Series No. 15, pp 247-251.

Savage, J.C., W.H. Prescott, M. Lisowski, and N.E. King (1978) Strain in southern California: measured uniaxial north-south regional contraction, Science Vol. 202, pp 883-885.

Schaffrin, B. (1981) Best invariant covariance component estimators and its application to the generalised multivariate adjustment of heterogeneous deformation observations, Bull. Geod. 55 pp 73-85.

Scherneck, H-G. (1983) Crustal loading affecting VLBI sites, Uni. of Uppsala Dept. of Geodesy Rpt. No. 20, 64p.

Shapiro, I.I. (1976) Estimation of Astrometric and Geodetic Parameters, In Methods of Experimental Physics Vol. 12C.

Shapiro, I.I. (1978) Principles of VLBI, In Department of Geodetic Science, Ohio State University, Rpt. No. 280.

Shapiro, I.I. (1983) Use of space techniques for Geodesy, In Proc. of the Int. School of Physics "Enrico Fermi", Course LXXXV, Earthquakes: Observation, Theory and

Interpretation, pp 530-568, North-Holland.

Slater, L.E., A. McGarr, J.O. Langbein, and M.F. Linker (1983) Multiwavelength EDM measurements in Southern California, Tectonophysics, 97 (1983) 39.

Stolz, A. (1972) Three-D Cartesian co-ordinates of part of the Australian Geodetic network by use of local astronomic vector systems, UNISURV S-8, School of Surveying, University NSW.

Stolz, A., B.R. Harvey, D.L. Jauncey, A.E. Niell, D.D. Morabito, R.A. Preston, B. Greene, K. Lambeck, A. Tzioumis, A. Watkinson, G.W.R. Royle, and D. Johnston (1983) Geodetic Surveying with Quasar Radio Interferometry, Australian Surveyor Vol.31 No.5, pp 305-314.

Stolz, A., B.R. Harvey, D.L. Jauncey, A.E. Niell, D.D. Morabito, and R.A. Preston, (1983) Australian baselines measured by Radio Interferometry, Australian Surveyor Vol.31 No.8, pp 563-566.

Strang van hees, G. L. (1982) Variance - Covariance transformations of geodetic networks, Manus. Geod. Vol 7 pp 1-20.

Strange, W. (1981) The impact of refraction correction on leveling interpretations in southern California, J. Geophys. Res. 86, pp 2809-2824.

Thapa, K. (1980) Strain as a diagnostic tool to identify inconsistent observations and constraints in horizontal geodetic networks, Dept.Surv.Eng. UNB Canada Tech.Rpt.No. 68, 160p.

Thomas, J.B. (1973) An Analysis of Long Baseline Radio Interferometry, Pt. III, JPL Tech.Rpt. 32-1526 Vol. XVI pp 47-64.

Thomas, J.B., J.L. Fanselow, P.F. MacDoran, L.J. Skjerve, D.J. Spitzmesser, and H.F. Fliegel (1976) A Demonstration of an Independent-Station Radio Interferomtry System with 4cm Precision on a 16km Baseline. J. Geophys. Res. Vol.81 No. 5 pp 995-1005.

Thomas, J.B. (1981) An analysis of radio interferometry with the Block 0 system, JPL Publication 81-49.

Thompson, E.H. (1969) An introduction to the algebra of matrices with some applications, Hilger.

Torge, W. (1980) Geodesy, Trans. by C. Jekeli, W. De Gruyter, 254p.

Vanicek, P., K. Thapa, and D. Schneider (1981) The Use of Strain to Identify Incompatible Observations and Constraints in Horizontal Geodetic Networks, Manus. Geod. Vol.6 pp 257-281.

Vanicek, P. and E.J. Krakiwsky (1982) Geodesy: The Concepts, North-Holland, 691p.

Veis, G. (1960) Geodetic Uses of Artificial Satellites, Smithsonian Contributions to Astrophysics, Vol. 3 No. 9, Smithsonian Institution, Washington D.C.

Vincenty, T. (1975) Direct and inverse solutions of geodesics on the ellipsoid with application of nested equations, Survey Review XXII, 176, pp 88-93.

Vincenty, T. and B.R. Bowring (1978) Application of three-dimensional geodesy to adjustment of horizontal networks, NOAA Tech. Mem. NOS NGS-13.

Vincenty, T. (1980) Height-controlled three-dimensional adjustment of horizontal networks, Bull. Geod. (54) pp 37-43.

Vincenty, T. (1982) Methods of adjusting space systems data and terrestrial measurements, Bull. Geod. (56) pp 231-241.

Welsch, W. (1981) Estimation of variances and covariances of geodetic observations, Aust.J.Geod.Photo.Surv. No. 34, pp 1-14.

Welsch, W.M. (1983) Finite element analysis of strain patterns from geodetic observations across a plate margin, Tectonop. (97) pp 57-71.

Whitney, A. (1974) Precision Geodesy and Astrometry via VLBI, Ph.D. Thesis, Massachusetts Institute of Technology.

Wolf, H. (1963) Geometric connection and re-orientation of three-dimensional triangulation nets, Bull. Geod. (68) pp 165-169.

Wolf, H. (1980) Scale and orientation in combined Doppler and triangulation nets, Bull. Geod. Vol. 54 pp 45-53.

Wolf, H. (1982) Stochastic aspects in combined Doppler and triangulation nets, Bull. Geod. Vol. 56 pp 63-69.

Zhou, Z. (1983) Untersuchung der mathematischen modelle zur kombination eines terrestrischen netzes mit einem satellitennetz, Deutsche Geodatische Kommission, Reihe c, Heft Nr. 274. 94p In German.

APPENDIX A.

CONVERSION OF VCV MATRICES.

The theory of conversion of Variance Covariance (VCV) matrices and the propagation of variances is clearly presented by Mikhail (1976) and others. This procedure does not depend on the density function of the population of the data.

If $Y = F(X)$ then,

$$VCV_Y = J\ VCV_X\ J^T$$

where J is the Jacobian matrix -

$$J = \partial Y/\partial X = \begin{bmatrix} \partial y_1/\partial x_1 & \partial y_1/\partial x_2 & \partial y_1/\partial x_3 & . & . & . \\ \partial y_2/\partial x_1 & \partial y_2/\partial x_2 & \partial y_2/\partial x_3 & . & . & . \\ \partial y_3/\partial x_1 & \partial y_3/\partial x_2 & \partial y_3/\partial x_3 & . & . & . \\ . & . & . & . & . & . \end{bmatrix} \qquad (A.1)$$

If the function F is not linear then the above derivatives are calculated at the corresponding values of the coordinates. The Jacobian matrices given below are used to transform the VCV of a single point. For conversion of the VCV of more than one point the full Jacobian matrix is -

$$J = \begin{bmatrix} J_1 & 0 & 0 & 0 & . & . \\ 0 & J_2 & 0 & 0 & . & . \\ 0 & 0 & J_3 & 0 & . & . \\ . & . & . & . & . & . \\ . & . & . & . & . & J_n \end{bmatrix} \qquad (A.2)$$

The equations for several coordinate transformations and the Jacobian matrices required to transform the VCV follow.

1) Given cylindrical coordinates (R, λ, Z) and their VCV, find the corresponding Cartesian coordinates (X, Y, Z) and their VCV.

$$X = R\cos\lambda \qquad Y = R\sin\lambda \qquad (A.3)$$

$$J = \begin{bmatrix} \cos\lambda & -R\sin\lambda & 0 \\ \sin\lambda & R\cos\lambda & 0 \\ 0 & 0 & 1 \end{bmatrix} \qquad (A.4)$$

2) Given Cartesian coordinates (X, Y, Z) and their VCV, find the corresponding cylindrical coordinates (R, λ, Z) and their VCV.

$$R = \sqrt{X^2 + Y^2} \qquad \lambda = \arctan(Y/X) \tag{A.5}$$

$$J = \begin{bmatrix} X/\sqrt{X^2+Y^2} & Y/\sqrt{X^2+Y^2} & 0 \\ -Y/(X^2+Y^2) & X/(X^2+Y^2) & 0 \\ 0 & 0 & 1 \end{bmatrix} \tag{A.6}$$

3) Given cylindrical coordinates (R, λ, Z) and their VCV, find the corresponding baseline components (ΔX, ΔY, ΔZ) and their VCV.

$$\begin{aligned} \Delta X &= R_j\cos\lambda_j - R_i\cos\lambda_i \\ \Delta Y &= R_j\sin\lambda_j - R_i\sin\lambda_i \\ \Delta Z &= Z_j - Z_i \end{aligned} \tag{A.7}$$

$$J = \begin{bmatrix} \cos\lambda_j & -\cos\lambda_i & -R_j\sin\lambda_j & R_i\sin\lambda_i & 0 & 0 \\ \sin\lambda_j & -\sin\lambda_i & R_j\cos\lambda_j & -R_i\cos\lambda_i & 0 & 0 \\ 0 & 0 & 0 & 0 & 1 & -1 \end{bmatrix} \tag{A.8}$$

4) Given ellipsoidal coordinates (Ø, λ, h) and their VCV, find the corresponding Cartesian coordinates and their VCV.

$$\begin{aligned} X &= (v+h)\cos\phi\cos\lambda \\ Y &= (v+h)\cos\phi\sin\lambda \\ Z &= \{(1-e^2)v+h\}\sin\phi \end{aligned} \tag{A.10}$$

where $v = a/\sqrt{1-e^2\sin^2\phi}$ and $e^2 = 2f - f^2$

[For the Australian National Ellipsoid, a = 6378160. and f = 1/298.25]

$$J = \begin{bmatrix} \dfrac{ve^2\sin\phi\cos^2\phi\cos\lambda}{(1-e^2\sin^2\phi)} - (v+h)\cos\lambda\sin\phi & -(v+h)\cos\phi\sin\lambda & \cos\phi\cos\lambda \\ \dfrac{ve^2\sin\phi\cos^2\phi\sin\lambda}{(1-e^2\sin^2\phi)} - (v+h)\sin\lambda\sin\phi & (v+h)\cos\phi\cos\lambda & \cos\phi\sin\lambda \\ \dfrac{\{ve^2\sin^2\phi\cos\phi + v\cos\phi\}(1-e^2)}{(1-e^2\sin^2\phi)} + h\cos\phi & 0 & \sin\phi \end{bmatrix} \tag{A.11}$$

5) Given Cartesian coordinates and their VCV, find the corresponding ellipsoidal coordinates and their VCV.

$$\begin{aligned} \phi &= \arctan\{(Z + e^2v\sin\phi)/R\} \quad \text{[iterate]} \\ \lambda &= \arctan(Y/X) \\ h &= R/\cos\phi - v \end{aligned} \tag{A.12}$$

where $R = \sqrt{(X^2 + Y^2)}$ as above

$$
\begin{aligned}
J(1,1) &\approx X\tan\phi \;/\; R^2(e^2 - \sec^2\phi) \\
J(2,1) &= -Y \;/\; R^2 \\
J(3,1) &= \{X/R\cos\phi\} + J(1,1)\{R\sin\phi/\cos^2\phi \\
&\qquad - ve^2\sin\phi\cos\phi/(1-e^2\sin^2\phi)\} \\
J(1,2) &= Y\,J(1,1) \;/\; X \\
J(2,2) &= X \;/\; R^2 \\
J(3,2) &= \{Y/R\cos\phi\} + J(1,2)\{(R\sin\phi/\cos^2\phi) \\
&\qquad - (ve^2\sin\phi\cos\phi/(1-e^2\sin^2\phi))\} \\
J(1,3) &\approx 1/\{R\sec^2\phi - e^2v\cos\phi\} \\
J(2,3) &= 0 \\
J(3,3) &= J(1,3)\;\{(R\sin\phi/\cos^2\phi) - ve^2\sin\phi\cos\phi \;/\; (1-e^2\sin^2\phi)\}
\end{aligned}
\tag{A.13}
$$

6) Given Cartesian coordinates and their VCV, find the baseline lengths and their VCV.

$$L = \sqrt{\{(X_j-X_i)^2 + (Y_j-Y_i)^2 + (Z_j-Z_i)^2\}} \tag{A.14}$$

$$J = \begin{bmatrix} \frac{X_i-X_j}{L} & \frac{Y_i-Y_j}{L} & \frac{Z_i-Z_j}{L} & \frac{X_j-X_i}{L} & \frac{Y_j-Y_i}{L} & \frac{Z_j-Z_i}{L} \end{bmatrix} \tag{A.15}$$

7) Given Cartesian coordinates and their VCV, find the Cartesian baseline components (ΔX, ΔY, ΔZ) of each point with respect to the first point and the associated VCV.

$$
\begin{aligned}
\Delta X_i &= X_{i+1} - X_1 \\
\Delta Y_i &= Y_{i+1} - Y_1 \\
\Delta Z_i &= Z_{i+1} - Z_1
\end{aligned}
\tag{A.16}
$$

$$
J = \begin{bmatrix}
-1 & 0 & 0 & 1 & 0 & 0 & 0 & 0 & 0 & 0 & 0 & \cdots \\
0 & -1 & 0 & 0 & 1 & 0 & 0 & 0 & 0 & 0 & 0 & \cdots \\
0 & 0 & -1 & 0 & 0 & 1 & 0 & 0 & 0 & 0 & 0 & \cdots \\
-1 & 0 & 0 & 0 & 0 & 0 & 1 & 0 & 0 & 0 & 0 & \cdots \\
0 & -1 & 0 & 0 & 0 & 0 & 0 & 1 & 0 & 0 & 0 & \cdots \\
0 & 0 & -1 & 0 & 0 & 0 & 0 & 0 & 1 & 0 & 0 & \cdots \\
-1 & 0 & 0 & 0 & 0 & 0 & 0 & 0 & 0 & 1 & 0 & \cdots \\
 & & & \text{etc} & & & & & & & & \cdots
\end{bmatrix}
\tag{A.17}
$$

APPENDIX B.

TAS PROGRAM

The program computes the least squares adjustment of the transformation models described in Chapter 7 and the strain models described in Chapter 8. The following models are included: Bursa-Wolf, Molodensky-Badekas, Cartesian components, ellipsoidal, topocentric strain, geocentric strain, 3D ellipsoidal strain, and 2D ellipsoidal strain. Approximations which assume small rotation angles are made in all models except Bursa-Wolf, Molodensky-Badekas, and Cartesian components.

The program reads the coordinates of the points comprising each net and their VCV matrix, and apriori estimates of the parameters and their VCV matrix. The data sets can be input or output in Cartesian, ellipsoidal, or cylindrical coordinates. If necessary the input data and VCV matrix are converted to their equivalents in Cartesian coordinates, except for the ellipsoidal models where the data and VCV are converted to ellipsoidal coordinates, if necessary. The formulae given in Appendix A are used for these conversions. The apriori and adjusted baseline lengths and their precisions are also computed.

A least squares adjustment is computed and the results of each iteration are printed out. They include the adjusted coordinates, their standard deviations and correlation matrix, the corrections to the coordinates, the adjusted parameters their standard deviations and their correlation matrix, and the statistical moments of the residuals.

The program has been written in Fortran for use under the VAX/VMS operating system. A listing of the program can be obtained from the author.